REFRAME:
Fundamentals of a Reference Frame Alignment Method Towards Kinematic Phenotyping of Total Knee Arthroplasty Patients Based on Mobile Gait Analysis

VORGELEGT VON

ARIANA ORTIGAS-VÁSQUEZ

AUS

LIMA, PERÚ

JAHR

2025

Erstes Gutachten:	Prof. Dr. Thomas Grupp
Zweites Gutachten:	Prof. Dr. Steffen Peldschus
Drittes Gutachten:	Priv. Doz. Dr. Max Wühr
Weiteres Gutachten:	Prof. Dr. William R. Taylor
Dekan:	Prof. Dr. med. Thomas Gudermann
Tag der mündlichen Prüfung:	26.06.2025

REFRAME:
Fundamentals of a Reference Frame Alignment Method Towards Kinematic Phenotyping of Total Knee Arthroplasty Patients Based on Mobile Gait Analysis

ABSTRACT (ENGLISH)

Research studies surveying satisfaction rates of osteoarthritis patients after total knee arthroplasty have continually found that up to one in five individuals are not fully satisfied with their surgical outcomes. Under the hypothesis that the problem stems from a need for more personalised treatment approaches, experts in the field of orthopaedics have explored the use of different implant geometries, surgical techniques, and alignment methods. The widespread adoption of a fully personalised knee replacement approach with custom, individually made implants for every patient faces a multitude of barriers and is thus not realistically feasible given existing resources and infrastructure, especially for high-volume clinics. Patient phenotyping, on the other hand, holds the potential for improved surgical outcomes by guiding clinicians to opt for targeted treatment approaches that incorporate patient-specific characteristics without demanding a fully customised implant be designed and manufactured for every single patient. Functional gait phenotyping thus relies on clustering osteoarthritis patients into subgroups or "phenotypes" according to clinically meaningful differences between their joint motion patterns. Advocates of such a phenotyping approach expect that ongoing research will establish relationships between different phenotypes and patient satisfaction rates after treatment with e.g. a specific implant geometry to address specific kinematic patterns and knee instability. By identifying the functional phenotype to which each patient belongs, clinicians could therefore make better-informed decisions regarding which treatment approaches to favour (or which to avoid), and thus maximise chances of patient satisfaction.

The development and practical adoption of a functional phenotyping approach to total knee replacement in osteoarthritis patients require the fulfilment of two key objectives. First, a motion capture system that is capable of objectively quantifying joint movement patterns *in vivo*, and that can easily and conveniently be incorporated into the existing clinical workflow that osteoarthritis patients follow, must be readily available. Second, we should be able to reliably identify differences between joint motion patterns based on the data collected by such a system. While motion capture systems to analyse gait *in vivo* are commercially available, the market is dominated by optoelectronic systems, often employing retroreflective markers. Frequently considered the "gold standard" despite known susceptibility to errors associated with soft tissue artefact, optical marker systems are not only difficult to use and time-consuming, but also cumbersome and expensive. One of the underlying goals of this thesis therefore focused on the research and development of alternative technologies to optical motion capture. A mobile gait analysis system for the assessment of tibiofemoral kinematics was designed using two low-cost inertial measurement units. The prototype system involved attaching the mobile sensors to the thigh and shank, and measuring angular velocity and linear acceleration during a movement. A sensor fusion algorithm based on Rauch-Tung-Striebel smoothing was then implemented and adapted to estimate the rotational kinematics of the tibiofemoral joint from the raw inertial values. The system was methodically validated using a six degrees-of-freedom robotic joint simulator, relying on real tibiofemoral kinematics that had originally been captured *in vivo* using moving videofluoroscopy as ground truth data.

Even though a first cursory assessment of results obtained from validation tests indicated the prototype system performed with promising accuracy, a deeper analysis considered the magnitude of any remaining differences between the IMU-based and simulated ground truth kinematics. This exploration revealed important insights into previously misunderstood (sometimes even altogether disregarded) effects of differences in local segment reference frame orientations (and positions) that can result from the lack of consensus regarding joint axes and coordinate system origin definitions. Notably, this work demonstrated that in order for the comparison of two (or more) sets of kinematic signals to be considered robust, researchers must first ensure that possible discrepancies in local reference frame definitions have been properly addressed. To this end, a Frame Orientation Optimisation Method (FOOM) was both developed and tested as part of this dissertation, as a computational approach that allows researchers to harmonise the orientation of joint axes in all three dimensions and thus ensure robust comparisons of kinematic signals (even where these stem from different sources). FOOM was thoroughly validated by relying once again on moving videofluoroscopy data of a tibiofemoral joint during gait.

Application of the developed FOOM approach to re-assess the findings of two representative phenotyping studies demonstrated that FOOM had implications beyond ensuring a reliable assessment of accuracy in IMU-based joint kinematic estimates. Insights from the analysis with FOOM were found to critically impact the identification of clinically meaningful functional gait phenotypes of the knee. Importantly, two phenotypes could not be considered different functionally until FOOM had excluded the possibility that signal differences came from frame inconsistencies (rather than distinct joint movement patterns). Considering that the tibiofemoral joint in fact possesses six degrees-of-freedom, and that the relevant segments can not only rotate but also translate relative to each other, FOOM was further expanded and developed into the REference FRame Alignment MEthod (REFRAME). A comprehensive, flexible, yet robust and repeatable framework, REFRAME allows researchers to postprocess previously collected kinematic data to ensure local segment reference frames are consistent in both orientation *and* position across datasets, thereby unifying the comparison of joint rotations *and* translations. Developed into and released as an openly accessible tool, REFRAME will now allow the wider biomechanics community to compare joint kinematics across subjects, trials, motion capture systems and even institutions.

In conclusion, the scientific outcomes of this dissertation have implications that extend far beyond its initial scope of developing a mobile motion capture for the identification of functional phenotypes among osteoarthritis patients. This dissertation fundamentally challenges a shockingly common assumption in biomechanics research, which misguidedly assumes that the presence of differences between sets of kinematic signals inherently implies there are differences between the underlying movement patterns. In addition to identifying and explaining this critical problem, this thesis lays the foundation of a computational framework that can be used to address it: REFRAME. The unmistakable convergence of local reference frames (and of kinematic signals stemming from the same movement) after REFRAME implementation provided solid evidence of the method's potential to ensure a consistent and reproducible evaluation of joint motion. This doctoral dissertation therefore represents a valuable step forward, extending past the practical development and validation of a mobile gait analysis tool for functional gait phenotyping in osteoarthritis patients, and evolving into a critical inquiry and re-conceptualisation of the fundamental principles behind the comparison of joint kinematics in the field of biomechanics.

Zusammenfassung (Deutsch)

Verschiedene Studien, in denen die Zufriedenheit von Arthrose-Patienten nach einer Knie-Totalendoprothese untersucht wurde, haben ergeben, dass bis zu jeder fünfte Patient mit dem Ergebnis seiner Operation nicht vollständig zufrieden ist. Unter der Hypothese, dass dieses Problem auf den Bedarf an individuelleren Behandlungsansätzen zurückzuführen ist, haben Experten auf dem Gebiet der Orthopädie die Verwendung verschiedener Implantatgeometrien, Operationstechniken und Ausrichtungsmethoden getestet. Die flächendeckende Einführung eines vollständig personalisierten Behandlungsansatzes für den Kniegelenkersatz mit individuell angefertigten Implantaten für jeden Patienten stößt auf eine Vielzahl von Hindernissen und ist angesichts der vorhandenen Ressourcen und Infrastruktur nicht realistisch umsetzbar, insbesondere nicht für Kliniken mit hohem Patientenaufkommen. Die Phänotypisierung von Patienten bietet hingegen das Potenzial für bessere chirurgische Ergebnisse, indem sie Ärzte unterstützt, gezielte Behandlungsansätze zu wählen, bei denen patientenspezifische Merkmale berücksichtigt werden, ohne dass für jeden einzelnen Patienten ein vollständig maßgeschneidertes Implantat entwickelt und hergestellt werden muss. Die funktionelle Gangphänotypisierung beruht daher auf der Einteilung von Arthrose-Patienten in Untergruppen oder "Phänotypen" anhand klinisch bedeutsamer Unterschiede zwischen ihren Gelenkbewegungsmustern. Die Befürworter eines solchen Phänotypisierungsansatzes erwarten, dass die aktuelle und zukünftige Forschung Beziehungen zwischen verschiedenen Phänotypen und der Patientenzufriedenheit nach der Behandlung mit z. B. einer bestimmten Implantatgeometrie, um patientenspezifische Kinematik und Knieinstabilität zu adressieren, herstellen wird. Durch die Identifizierung des funktionellen Phänotyps jedes Patienten könnten Ärzte daher besser informierte Entscheidungen hinsichtlich der zu bevorzugenden (oder zu vermeidenden) Behandlungsansätze treffen und so die Chancen auf Patientenzufriedenheit maximieren.

Die Entwicklung und praktische Anwendung eines funktionellen Phänotypisierungsansatzes für die Knie-Totalendoprothesenimplantation bei Arthrose-Patienten erfordern die Erfüllung von zwei zentralen Zielen. Erstens muss ein Bewegungserfassungssystem zur Verfügung stehen, das objektiv die Bewegungsmuster *in vivo* quantifizieren kann. Zweitens sollten wir die Möglichkeit haben, auf Grundlage der von einem solchen System erfassten Daten zuverlässig Unterschiede zwischen den Bewegungsmustern der Gelenke zu erkennen. Obwohl Systeme zur Bewegungserfassung zur Analyse des Gangs *in vivo* kommerziell verfügbar sind, wird der Markt von optoelektronischen Systemen - oft mit retroreflektierenden Markern - dominiert. Optische Markersysteme - die trotz der bekannten Anfälligkeit für Fehler im Zusammenhang mit Weichteilartefakten häufig als "Goldstandard" genannt werden - sind nicht nur komplex und zeitaufwendig in der Anwendung, sondern auch umständlich und teuer. Eines der grundlegenden Ziele dieser Arbeit war daher die Erforschung und Entwicklung von alternativen Technologien zur optischen Bewegungserfassung. Es wurde ein mobiles Ganganalysesystem für die Bewertung der tibiofemoralen Kinematik entwickelt, das zwei kostengünstige inertiale Messeinheiten (engl. *inertial measurement units*, IMUs) verwendet. Bei dem Prototypsystem wurden die mobilen Sensoren am Oberschenkel und am Unterschenkel befestigt und die Winkelgeschwindigkeit sowie die lineare Beschleunigung während einer Bewegung gemessen. Anschließend wurde ein Sensordatenfusionsalgorithmus basierend auf der Rauch-Tung-Striebel Glättung implementiert und angepasst, um die Rotationskinematik des tibiofemoralen Gelenks aus den Rohdaten der Inertialmessung abzuleiten. Das System wurde methodisch mit einem robotischen Gelenksimulator mit sechs Freiheitsgraden validiert, der sich auf reale tibiofemorale Kinematik stützte, die ursprünglich *in vivo* mit dynamischer Videofluoroskopie als Basisdaten erfasst worden war.

Auch wenn eine erste vorläufige Bewertung der Ergebnisse aus den Validierungstests darauf hindeutete, dass das Prototypsystem mit einer vielversprechenden Genauigkeit funktioniert, wurde bei einer tiefergehenden Analyse das Ausmaß der verbleibenden Unterschiede zwischen der IMU-basierten

und der simulierten Ground-Truth-Kinematik untersucht. Diese Untersuchung brachte wichtige Erkenntnisse über bisher unverstandene (manchmal sogar außer Acht gelassene) Auswirkungen von Unterschieden in den Ausrichtungen (und Positionen) lokaler Segmentkoordinatensysteme zutage, die sich aus dem fehlenden Konsens über die Definitionen der Gelenkachsen und des Koordinatensystemursprungs ergeben können. Diese Arbeit hat insbesondere gezeigt, dass der Vergleich zweier (oder mehrerer) Datensätze kinematischer Signale nur dann als robust angesehen werden kann, wenn die Forscher zunächst sicherstellen, dass mögliche Diskrepanzen in den Definitionen lokaler Koordinatensysteme ausreichend berücksichtigt wurden. Zu diesem Zweck wurde im Rahmen dieser Dissertation eine Optimierungsmethode für die Ausrichtung von Koordinatensystemen (engl. *Frame Orientation Optimisation Method*, FOOM) entwickelt und getestet. Dabei handelt es sich um einen mathematischen Ansatz, der es Forschern ermöglicht, die Orientierung der Gelenkachsen in allen drei Dimensionen zu harmonisieren und so einen robusten Vergleich kinematischer Signale zu gewährleisten (selbst wenn diese aus unterschiedlichen Quellen stammen). FOOM wurde gründlich validiert, indem erneut dynamische Videofluoroskopiedaten des Tibiofemoralgelenks beim Gehen herangezogen wurden.

Die Anwendung des entwickelten FOOM-Ansatzes zur Neubeurteilung der Ergebnisse von zwei repräsentativen Phänotypisierungsstudien zeigte, dass FOOM über die Gewährleistung einer zuverlässigen Bewertung der Genauigkeit von IMU-basierten kinematischen Gelenkschätzungen hinausgeht. Es wurde festgestellt, dass die Erkenntnisse aus der FOOM-Analyse einen entscheidenden Einfluss auf die Identifizierung von klinisch bedeutsamen funktionellen Gangphänotypen des Knies haben. Insbesondere konnten zwei Phänotypen erst dann als funktionell unterschiedlich angesehen werden, wenn FOOM die Möglichkeit ausgeschlossen hatte, dass die Signalunterschiede auf Inkonsistenzen im Koordinatensystem (und nicht auf unterschiedliche Gelenkbewegungsmuster) zurückzuführen waren. In Anbetracht der Tatsache, dass das tibiofemorale Gelenk tatsächlich über sechs Freiheitsgrade verfügt und dass die Segmente sich nicht nur relativ zueinander drehen, sondern auch verschieben können, wurde FOOM weiter ausgebaut und weiterentwickelt zur REference FRame Alignment MEthod (REFRAME). REFRAME ist ein umfassendes, flexibles, aber dennoch robustes und wiederholbares Framework, das es Forschern ermöglicht, zuvor gesammelte kinematische Daten nachzubearbeiten, um sicherzustellen, dass die lokalen Segmentkoordinatensysteme sowohl in der Ausrichtung als auch in der Position über alle Datensätze hinweg konsistent sind, wodurch der Vergleich von Rotationen und Translationen der Gelenke vereinheitlicht wird. REFRAME wurde zu einem frei zugänglichen Tool entwickelt und bereitgestellt und es ermöglicht nun Forschungsgruppen in der Biomechanik, Gelenkkinematiken über Probanden, Studien, Motion Capture Systeme und sogar Institutionen hinweg zu vergleichen.

Zusammenfassend lässt sich sagen, dass die wissenschaftlichen Ergebnisse dieser Dissertation weit über die Entwicklung einer mobilen Bewegungserfassungsmethode zur Identifizierung von funktionellen Phänotypen bei Arthrose-Patienten hinausgehen. Diese Dissertation stellt eine häufige vorkommende Annahme in der Biomechanik-Forschung grundlegend in Frage, die fälschlicherweise davon ausgeht, dass das Vorhandensein von Unterschieden zwischen kinematischen Signalen automatisch Unterschiede zwischen den zugrunde liegenden Bewegungsmustern impliziert. Diese Arbeit identifiziert und erklärt nicht nur dieses kritische Problem, sondern legt auch den Grundstein für ein computergestütztes Verfahren, das zur Lösung dieses Problems eingesetzt werden kann: REFRAME. Die unverkennbare Konvergenz der lokalen Koordinatensysteme (und der kinematischen Signale, die aus derselben Bewegung stammen) nach der Implementierung von REFRAME lieferte einen soliden Beweis für das Potenzial der Methode, eine konsistente und reproduzierbare Bewertung der Gelenkbewegung zu gewährleisten. Diese Dissertation stellt daher einen wertvollen Schritt in die Zukunft dar, der über die praktische Entwicklung und Validierung eines mobilen Ganganalysetools für die funktionelle Gangphänotypisierung bei Arthrose-Patienten hinausgeht und zu einer kritischen Analyse und

Neukonzeptionierung der grundlegenden Prinzipien beim Vergleich von Gelenkkinematiken im Bereich der Biomechanik führt.
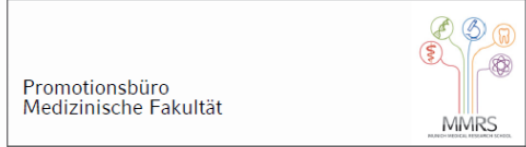
Table of Contents

Affidavit

Ortigas Vásquez, Ariana

_____

Surname, first name

_____

Street

_____

Zip code, town, country

I hereby declare, that the submitted thesis entitled:

REFRAME: Fundamentals of a Reference Frame Alignment Method Towards Kinematic Phenotyping of Total Knee Arthroplasty Patients Based on Mobile Gait Analysis

is my own work. I have only used the sources indicated and have not made unauthorised use of services of a third party. Where the work of others has been quoted or reproduced, the source is always given.
I further declare that the dissertation presented here has not been submitted in the same or similar form to any other institution for the purpose of obtaining an academic degree.

Konstanz, July 10th, 2025   Ariana Ortigas Vásquez

_____   _____

place, date   Signature doctoral candidate

Abbreviations

2D	Two dimensions
3D	Three dimensions
AP	Anteroposterior
BMI	Body mass index
CA	Cylindrical axis
CR	Cruciate retaining
CS	Cruciate sacrificing
DOF	Degree of freedom
FFA	Functional flexion axis
FOOM	Frame orientation optimisation method
IMU	Inertial measurement unit
ISB	International Society of Biomechanics
JCS	Joint coordinate system
LS	Lateral-stabilised
ML	Mediolateral
MS	Medio-stabilised
OA	Osteoarthritis
OMC	Optical motion capture
PC	Personal computer
PD	Proximodistal
PS	Posterior-stabilised
REFRAME	Reference frame alignment method
RMS	Root-mean-square
RMSE	Root-mean-square error
ROM	Range of motion
SARA	Symmetrical axis of rotation approach
SD	Standard deviation
STA	Soft tissue artefact
TEA	Transepicondylar axis
TKA	Total knee arthroplasty
UC	Ultra-congruent

List of Research Outputs

I. Journal publications

*Shared first authorship.

II. Conference works

- **Ortigas-Vásquez, A.**, Maas, A., Taylor, W.R., Grupp, T.M., Validation of an inertial-based gait analysis system using a six degrees-of-freedom joint simulator (**Podium presentation**) *27ᵗʰ Congress of the European Society of Biomechanics (ESB), Jun 26-29, 2022, Porto, Portugal.*

- Sauer, A., **Ortigas-Vásquez, A.**, Maas, A., Grupp, T.M., Einfluss der Achsenausrichtung auf Kinematikdaten – Auswirkungen und ein Ansatz zur Standardisierung (**Podium presentation**) *12. Kongress der Deutsche Gesellschaft für Biomechanik (DGfB), Sep 28-30, 2022, Köln, Deutschland.*

- **Ortigas-Vásquez, A.**, Sauer, A., Maas, A., Taylor, W.R., Grupp, T.M., Standardising frame alignments to allow for consistent kinematic interpretation: Part I (**Poster**) *18th International Symposium on Computer Methods in Biomechanics and Biomedical Engineering (CMBBE), May 3-5, 2023, Paris, France.*

- <u>Sauer, A.</u>, **Ortigas-Vásquez, A.**, Maas, A., Taylor, W.R., Grupp, T.M., Standardising frame alignments to allow for consistent kinematic interpretation: Part II (**Poster**) *18th International Symposium on Computer Methods in Biomechanics and Biomedical Engineering (CMBBE), May 3-5, 2023, Paris, France.*

- **Ortigas-Vásquez, A.**, Taylor, W.R., Maas, A., Woiczinski, M., Grupp, T.M., Sauer, A., A frame orientation optimisation method to enable valid kinematic comparisons: Assessing IMU-based knee kinematics (**Podium presentation**) *28th Congress of the European Society of Biomechanics (ESB), Jul 9-12, 2023, Maastricht, Netherlands.*

- **Ortigas-Vásquez, A.**, Taylor, W.R., Postolka, B., Schütz, P., Maas, A., Woiczinski, M., Grupp, T.M., Sauer, A., A unifying approach for the standardisation of kinematic signals (**Podium presentation**) *28th Congress of the European Society of Biomechanics (ESB), Jul 9-12, 2023, Maastricht, Netherlands.*

- <u>Sauer, A.</u>, **Ortigas-Vásquez, A.**, Postolka, B., Schütz, P., Maas, A., Woiczinski, M., Grupp, T.M., Taylor, W.R., Application of different optimisation criteria to standardise kinematic signals (**Podium presentation**) *28th Congress of the European Society of Biomechanics (ESB), Jul 9-12, 2023, Maastricht, Netherlands.*

- **Ortigas-Vásquez, A.**, Taylor, W.R., Postolka, B., Schütz, P., Maas, A., Utz, M., Woiczinski, M., Grupp, T.M., Sauer, A., A segment frame optimisation method to standardise kinematic signals (**Podium presentation**) *XXIX Congress of the International Society of Biomechanics (ISB), Jul 30 - Aug 3, 2023, Fukuoka, Japan.*

- Sauer, A., **Ortigas-Vásquez, A.**, Postolka, B., Schütz, P., Maas, A., <u>Utz, M.</u>, Woiczinski, M., Grupp, T.M., Taylor, W.R., Aligning local segment frames based on different optimisation criteria to standardise kinematic signals (**Poster**) *XXIX Congress of the International Society of Biomechanics (ISB), Jul 30 - Aug 3, 2023, Fukuoka, Japan.*

- **Ortigas-Vásquez, A.**, Taylor, W.R., Postolka, B., Schütz, P., Maas, A., Utz, M., Woiczinski, M., Grupp, T.M., Sauer, A., A reference frame alignment method for the consistent interpretation of kinematic signals (**Podium presentation**) *32nd Annual Meeting of the European Society for Movement Analysis in Adults and Children (ESMAC), Sep 18-23, 2023, Athens, Greece.*

- Sauer, A., **Ortigas-Vásquez, A.**, <u>Utz, M.</u>, Maas, A., Taylor, W.R., Grupp, T.M., Woiczinski, M., Relating functional kinematics to implant design in total knee arthroplasty based on the location of standardised joint segment frames: An application of REFRAME (**Short talk**) *34th Congress of the International Society for Technology in Arthroplasty (ISTA), Sep 27-30, 2023, New York City, USA.*

- Jakubowitz, E., Budde, L., **Ortigas-Vásquez, A.**, Sauer, A., Utz, M., Einfeldt, A.K., MiKneeSoTA - Minimizing knee soft-tissue artefacts during kinematic analytics (**Poster**) *70th Annual Meeting of the Orthopaedic Research Society (ORS), Feb 2-6, 2024, Long Beach, CA, USA.*

- Antognini, C., **Ortigas-Vásquez, A.**, Knowlton, C. Utz, M., Sauer, A., Wimmer, M.A., Do markerless and marker-based motion analyses provide identical joint kinematics? (**Podium**

presentation) *13. Kongress der Deutsche Gesellschaft für Biomechanik (DGfB), Apr 24-26, 2024, Heidelberg, Deutschland.*

- Sauer, A., **Ortigas-Vásquez, A.**, Thorwaechter, C., Maas, A., Grupp, T.M., Taylor, W.R., <u>Woiczinski, M.</u>, Grundlagen eines REFRAME-basierten Ansatzes für kinematische Phänotypen: Interpretation der Ursprungsposition des femoralen Referenzrahmens bei verschiedenen Implantatdesigns für Knie-Totalendoprothesen (**Podium presentation**) *13. Kongress der Deutsche Gesellschaft für Biomechanik (DGfB), Apr 24-26, 2024, Heidelberg, Deutschland.*

- **<u>Ortigas-Vásquez, A.</u>**, Sauer, A., Postolka, B., Schütz, P., Utz, M., Maas, A., Grupp, T.M., Taylor, W.R., Anatomical pose of functional joint coordinate systems reveals key subject differences (**Podium presentation**) *29th Congress of the European Society of Biomechanics (ESB), Jun 30 - Jul 3, 2024, Edinburgh, Scotland.*

- Sauer, A., **Ortigas-Vásquez, A.**, Thorwaechter, C., Maas, A., Grupp, T.M., Taylor, W.R., <u>Woiczinski, M.</u>, Foundations of a REFRAME-based approach to kinematic phenotypes: Interpreting differences in femoral reference frame origin position across total knee arthroplasty implant designs (**Poster**) *29th Congress of the European Society of Biomechanics (ESB), Jun 30 - Jul 3, 2024, Edinburgh, Scotland.*

Note: Speaker <u>underlined</u>. Doctoral candidate in **bold**.

III. Other

- Guest talks:

    a. Delivered on June 1st, 2023, alongside W.R. Taylor at ETH Zurich, Laboratory for Movement Biomechanics, upon invitation by Prof. William. R. Taylor.

    b. Delivered on February 7th, 2023, alongside A. Sauer and M. Utz at FAU Erlangen, Department of Artificial Intelligence in Biomedical Engineering, upon invitation by Prof. Thomas Seel.

    c. Delivered on November 20th, 2023, alongside A. Sauer and M. Utz at University Hospital Basel, Department of Orthopaedics and Traumatology, upon invitation by Prof. Annegret Mündermann.

    d. Delivered on February 12th, 2024, at Rush University in Chicago, Department of Orthopaedic Surgery, upon invitation by Prof. Markus A. Wimmer.

- Collaborations initiated from PhD work:

    a. Prof. Thomas Seel, Dr. Ive Weygers and Simon Bachhuber, Department of Artificial Intelligence in Biomedical Engineering, FAU Erlangen.

    b. Prof. Markus Wimmer and Camilla Antognini, Department of Orthopaedic Surgery, Rush University Medical Centre.

    c. Dr. Eike Jakubowitz and Ann-Kathrin Einfeldt, Laboratory for Biomechanics and Biomaterials, Department of Orthopaedic Surgery, Hannover Medical School (MHH).

- Courses:

    a. *REFRAME – Interpreting joint motion patterns,* delivered on June 30th, 2024, as a pre-course (2.5 hours) alongside A. Sauer and W.R. Taylor at the 29th Congress of the European Society of Biomechanics (ESB) in Edinburgh.

- Intellectual property:

    a. Invention disclosure 2021ID00199 DE (i.e. Generierung von IMU-Daten) submitted by Utz, M., Maas, A., Dupraz, I., Vazquez Urena D.A., and **Ortigas-Vásquez, A.**

    b. Patent family 2021PF00199 (i.e. Generierung von IMU-Daten) submitted by Utz, M., Maas, A., Dupraz, I., Vazquez Urena D.A., and **Ortigas-Vásquez, A.**

    c. Invention disclosure 2022ID00079 DE (i.e. Verfahren zur Standardisierung von biomechanischen Kinematikdaten) submitted by **Ortigas-Vásquez, A.**, Sauer, A., and Maas, A.

    d. Patent family 2022PF00079 (i.e. Verfahren zur Standardisierung von biomechanischen Kinematikdaten) submitted by **Ortigas-Vásquez, A.**, Utz, M., Sauer, A., Maas, A., and Taylor, W.R.

    e. Invention disclosure 2023ID00126 DE (i.e. REFRAME Application) submitted by Utz, M., Sauer, A., **Ortigas-Vásquez, A.**, and Taylor, W.R.

    f. Invention disclosure 2023ID00127 DE (i.e. REFRAME Phenotyping) submitted by Utz, M., Sauer, A., **Ortigas-Vásquez, A.**, and Taylor, W.R.

Note: Doctoral candidate in **bold**.

Author's Contribution

1. Journal Publication I

The author of this dissertation (AOV) led the formulation and development of the overarching research goals of this publication. She prepared the data for, organised and participated in all joint simulator trials, including preliminary testing. She managed and analysed the collected data, as well as developed and ran the necessary custom MATLAB scripts for data processing. AOV was responsible for the formal analysis of the study results (including all statistical tests) and drafted the full manuscript for journal publication, including preparation of the supplementary material and figures. She played a primary role in the review and editing of the manuscript.

2. Journal Publication II

For the second publication, AOV shared a leading role in the conceptualisation of the study with the article's last author (AS). AOV performed the formal analysis and data processing, based on foundational methods developed by AS. AOV created several of the necessary MATLAB scripts, while also supporting AS in the development (especially validation) of several other scripts. AOV prepared the data for visualisation and took on a leading role in the drafting of the full manuscript for journal publication, including the supplementary material and figures. She played a primary role in the review and editing of the manuscript.

3. Journal Publication III

Within the third publication, AOV and AS were jointly responsible for the concept formulation and study design. AOV supported with software development, under the leadership of AS. AOV performed the formal analysis of the data and associated statistical tests. She reviewed all MATLAB scripts, editing, adapting and commenting them for ease of use of any potential external users. AOV was responsible for the design, development and testing of the executable MATLAB tool that was openly released for non-commercial use, as well as the main author of the accompanying user guide. She prepared manuscript figures, including those in the supplementary material. AOV had a leading role in writing the full manuscript for journal publication, and was also in charge of the review and editing process.

4. Journal Publication IV

AOV took on a leading role in formulating the study concept and design for the fourth publication of this dissertation. Software was developed jointly by AOV and AS. AOV led and executed formal analysis of the dataset, including statistical tests, additionally creating, reviewing and adapting any necessary MATLAB scripts for data processing. AOV drafted the first full version of the manuscript and

generated the associated figures. AOV was responsible for collecting and incorporating other authors' feedback to prepare it for publication, as well as responding to reviewer comments and making revisions during the peer-review process.

5. Journal Publication V

AOV conceived the research question and designed the analysis approach. AOV oversaw as well as participated first-hand in the collection of experimental data. AOV guided and assisted the publication's first author, SS, in the processing of numerical data and interpretation of results. AOV drafted the manuscript alongside SS. Finally, AOV supervised and significantly contributed to manuscript editing and review.

6. Journal Publication VI

First authorship for this publication is shared between AOV and JGW. AOV was responsible for the study design; she conceived and planned the experiments. AOV trained JGW to perform the data collection. AOV steered and supported JGW in the numerical analysis of the collected data. Supported by JGW, AOV spearheaded the interpretation of results and drafting of a first manuscript. AOV supervised JGW throughout manuscript editing and review in preparation for publication.

I. Overview

1. Introduction

Back in 1974, the development and implantation of the first total condylar prosthesis by Walker, Ranawat and Insall [1] represented a major breakthrough in the history of total knee arthroplasty (TKA) [2]. Since then, orthopaedic surgery has evolved past the indiscriminate use of a generic implant design and neutral mechanical alignment technique to more tailored practices aiming to address the individual needs of different patients. Clinicians have the possibility to adapt their TKA approach by choosing, for example, between different types of bearing mobility (e.g. fixed bearing vs. mobile bearing), implant designs (e.g. medial pivot, cruciate retaining, posterior stabilised, etc.), fixation methods (e.g. cemented vs. uncemented), patellar management strategies (e.g. whether or not to resurface), and limb alignment techniques (e.g. mechanic vs. kinematic alignment) [3, 4].

Despite the numerous options available to orthopaedic surgeons within TKA procedures, longitudinal cohort studies have repeatedly found up to a fifth of patients are not fully satisfied with their surgical outcomes [5-7]. These findings therefore seemingly indicate that the mere availability of options to enable more individualised surgical interventions for patients suffering from knee osteoarthritis (OA) is not in itself sufficient to guarantee patient satisfaction. Importantly, surgeons additionally need to have an evidence-based understanding of how choosing between the aforementioned options will impact patient function and surgical outcome, which in turn requires an objective quantification of joint movement patterns.

It has been previously argued that kinematic signals obtained as part of gait analysis studies have the potential to be of value as a quantifiable outcome measure of OA treatment [8]. Naturally, it follows that comparison of joint kinematics before and after TKA, especially considering the use of different implant geometries and surgical techniques, could reveal valuable insight into how different clinical choices empirically affect patients' movement patterns, and numerous studies have in fact begun to explore that hypothesis [9]. Some researchers have gone a step further and proposed that the underlying goal of TKA should be to leverage the knowledge being gained from the availability of kinematic data to target the reproduction of so-called "native" or "normal" knee kinematics post-operatively [10]. This theory is often justified by a presumed avoidance of pain by ensuring the reproduction of more physiologic soft tissue laxities and ligament strains [11-14].

Under the assumption that the overarching aim of TKA should indeed be restoration of pre-operative (or rather pre-pathology) joint kinematics, some experts have proposed using personalised implant geometries [10, 15]. Importantly, however, while custom, individually made prostheses could prevent issues of e.g. implant mismatch with the bony anatomy compared to conventional, off-the-shelf designs, anatomical accuracy of fit is but one aspect influencing TKA outcome [16]. Additional factors contributing to TKA success could potentially also be tackled in a more time- and cost-efficient manner by relying on a comprehensive and flexible implant platform [17, 18]. Such a platform could offer

sufficient size gradations to avoid under- or over-dimensioning, ample compatibility between sizes (and designs) to extend intra-operative flexibility, and even (if necessary) asymmetrical components to ensure a balanced flexion gap. Moreover, such implants could easily undergo more extensive biomechanical testing than customised components, ensuring safety in terms of wear, fatigue and failure modes. In combination with an evidence-based patient-specific alignment strategy, an extensively accommodating implant platform such as the one described could realistically lead to the long-sought improvement in arthroplasty outcomes without demanding excessive workflow times, complexity, or expense. Ultimately, regardless of limiting factors restricting the widespread adoption of such alternative frameworks, opting for the default, yet outdated, "one-design-fits-all" approach to joint arthroplasty that largely ignores individual patient needs is clearly not the optimal solution.

2.   Functional Gait Phenotyping

There is a clear need for an approach to TKA that better recognises the individual needs of different patients without demanding the development of single-use, custom-made implant geometries for every patient. One possible framework that has been recently proposed and is being explored relies on *phenotyping* – that is, the identification of clinically relevant patient subgroups or clusters [19]. An understanding of functional phenotypes both within healthy populations and among individuals affected by knee OA is believed by some to be essential to the successful improvement of treatment outcomes [20].

A phenotype-based approach to patient-specific OA treatment could potentially enhance clinical decision-making by relying on empirical evidence to establish relationships between e.g. the use of a certain implant design and key characteristics in the resulting post-operative kinematic patterns. The identification of such quantifiable associations between surgical strategy and joint function could then be leveraged to design a simple framework with which TKA could easily be tailored to address the needs of individual patients. For example, patients could be classified into one of a handful of functional OA subgroups, where additional research may have determined one of these groups as being especially well-suited for and responding positively to implantation with a posterior-stabilised (PS) implant design, but experiencing pain when implanted with an ultra-congruent (UC) cruciate sacrificing (CS) design instead. Although probably an oversimplification of how phenotyping could be leveraged to improve TKA outcomes, this illustrative case serves to highlight how phenotyping could provide clinicians with the flexibility to incorporate their expert intuition, judgement, and experience into the decision-making process, while still establishing a structural framework that ensures these decisions are guided by robust scientific evidence and at the very least veered away from choices that may lead to patient discomfort. Notably, in order for an evidence-based phenotyping approach to be successful, the objective quantification of patient function (and thus, joint motion) is crucial to reliably classify patients into clinically meaningful subgroups. Consequently, we must circle back once more to the use of gait analysis for the collection of kinematic signals and consider the feasibility of its potential routine implementation in day-to-day clinical workflows.

Despite numerous experts having voiced their conviction that gait analysis could considerably improve the outcomes of orthopaedic treatment and substantially enhance clinical decision-making [21-23], a ubiquitous use of gait analysis, e.g. in all patients both pre- and post-TKA, has been historically restricted by the high costs of these systems and the long time required for data collection, and subsequently data processing, and interpretation. For instance, considered by many to be the "gold standard" [24-27], optical motion capture systems can easily cost as much as 300,000 EUR [28, 29], and often additionally demand dedicated laboratory space, software, hardware, and trained staff. These

combined requirements therefore represent a substantial barrier that critically restricts the widespread use of motion capture and gait analysis in clinical settings (especially as part of routine clinical patient pathways), and by extension, the adoption of a functional phenotype-based approach to TKA.

3.   Mobile Gait Analysis

There is a palpable demand for cheaper, simpler, more mobile alternatives to traditional gait analysis, especially to systems relying on optical motion capture. Several systematic reviews have been published in recent years surveying potential alternative technologies, such as instrumented insoles, electromyography sensors, electrogoniometry sensors and pressure sensors [28, 30, 31]. A particularly promising and popular category of solutions relies on the use of inertial measurement units (IMUs). Such systems are not only mobile and easy to use, but they are also much more affordable than most optical motion capture systems [32, 33]. Although there are certainly numerous advantages associated with IMU-based gait analysis, there are also multiple challenges involved in their use to accurately capture joint kinematics. Some of these key issues include sensitivity to ferromagnetic disturbances, a tendency of inertial measurements to drift over time, and difficulties with sensor-to-segment calibration [34].

Preliminary work for this dissertation involved an informal survey of existing algorithms designed to estimate knee joint angles in three dimensions (3D) from accelerometer and gyroscope measurements, as well as the selection of a particularly promising approach [35-37] seemingly capable of successfully tackling several of the key challenges we identified. This initial exploration of current state-of-the-art methodologies was followed by a first-hand adaptation of the specified chosen algorithm to estimate tibiofemoral flexion/extension, ab/adduction and int/external rotation during gait activities, as well as a subsequent in-depth assessment of the accuracy of these estimates against a reference system.

Previous work has been published on the validation of IMU-based knee joint angles, but most of these studies have tested directly *in vivo*. While testing in realistic conditions is definitely important, we chose to approach the validation of our prototype IMU system in stages instead. We divided the problem into three fundamental layers:

(1) *The factory calibration layer* – This first layer affects the accuracy of the raw data values obtained directly from the IMU sensors. This includes the accuracy of both the inertial measurements (i.e. linear acceleration and angular velocity), as well as of the corresponding time stamps. This layer of error also includes differences in the alignment of the internal accelerometer and gyroscope axes *versus* those of the outer sensor casing. From a product development perspective, we have little influence over this layer of error, as it is performed under controlled laboratory conditions during the sensor manufacturing process, and reported as a fixed range in the device's technical documentation.

(2) *The sensor fusion algorithm layer* – The second layer affects the inherent ability of the chosen algorithm to accurately estimate knee joint angles from inertial data (i.e. linear acceleration and angular velocity) rather than from 3D coordinates (as is usually done in optical motion capture). The errors affecting the system at this stage will mostly be associated with sensor drift, sensor-to-segment calibration, and the use of idealised models and approximations that do not fully represent the complex reality of the joint.

(3) *The soft tissue artefact (STA) layer* – The third layer of error is specific to *in vivo* applications of the IMU system, which involve fixating the IMU sensors to the subject's skin (e.g. with adhesive or elastic straps). This inevitably introduces another layer of uncertainty on our estimates, caused by non-rigid movements of the skin relative to the underlying bones, namely, soft tissue artefact.

Regardless of how well the first and second layers of errors can be addressed, as long as the IMU sensors are attached to subject's skin (and no additional computations are performed aiming specifically to quantify and compensate for the movement of soft tissue relative to the underlying bones), this layer of error will always be introduced to some degree.

Consequently, while determining the approximate magnitude of the total error affecting our finalised system in a real-world scenario is certainly necessary down the line, in a first stage of development, it can instead be more informative to first isolate and evaluate the magnitude and characteristics of the errors that are inherent to the specific sensor fusion algorithm *in the absence of STA*. Subsequent adaptations of the algorithm to reduce sensor-fusion-algorithm-layer errors can then be much more deliberate and targeted than without any indication of how much of the errors can be attributed to the IMU algorithm layer *versus* the STA layer. This first concrete objective was tackled by developing and testing a comprehensive framework for the analytical validation of inertial-sensor-based knee kinematics using a six-degrees-of-freedom (6 DOFs) joint simulator guided by *in vivo* kinematics collected using moving videofluoroscopy [38]. A corresponding research article documenting this part of our investigation was prepared and published in the scientific journal *Sensors* (5-year Impact Factor of 3.7 as of 2023) and has been reproduced in this document as Journal Publication I: *A framework for analytical validation of inertial-sensor-based knee kinematics using a six-degrees-of-freedom joint simulator*.

4. Comparing Joint Kinematics: The Effects of Reference Frame Definition

The results of Journal Publication I were promising; An initial review found that the prototype system achieved excellent accuracy in the IMU-based estimates of the knee joint angles during level walking (root-mean-square error $\leq 0.9°$, maximum absolute error $\leq 3.2°$), although errors were higher for both stair descent and sit-to-stand. Nevertheless, upon further consideration, a potential *fourth layer of error* was identified.

Assessing the accuracy of an estimate using, e.g., root-mean-square error (RMSE) involves quantifying the difference between the estimated values and a "ground truth" reference signal. Conceptually, the goal in Journal Publication I was to evaluate the degree to which the underlying joint motion captured by the IMU sensors differed from the actual fluoroscopy-based kinematics (originally of six patients who had undergone TKA), which the simulator was known to have replicated. In other words, assessing the accuracy of the system at this stage of the development process was akin to determining the extent to which two kinematic signal sets (one originating from the joint simulator; the other, from the IMU-based system) represented fundamentally similar or different underlying joint motion. The ability to successfully tackle the task of establishing whether sets of kinematic signals characterise similar or different movement patterns is not only vital to properly validate our prototype mobile gait analysis system, but also to identify and establish robust functional phenotypes down the line. The foundation of a treatment approach based on the identification of functional phenotypes evidently requires that the corresponding phenotypes reliably represent groups of patients that have objectively different movement patterns (where these differences are large enough to be considered clinically relevant).

Referring to an overwhelming majority of published work investigating potential significant differences between kinematic signal sets (comparing e.g. natural vs. replaced knees [39], mild vs. severe OA [40], fixed- vs. mobile-bearing implants [41]; merely a few of countless other examples), the initial conclusions reached regarding the accuracy of our prototype system in Journal Publication I would

easily hold and warrant no further consideration. After all, the previously mentioned examples, among many others, all evidently operate under the simple premise that *the presence of differences between sets of kinematic signals inherently implies there are differences in the underlying movement patterns that those signals represent*. Nevertheless, we decided to re-evaluate this notion by reconsidering the fundamental theory behind 3D kinematics as a representation of the relative motion between two rigid bodies.

The description and interpretation of the relative rotations of two reference frames (where each frame is represented by a Cartesian coordinate system whose axes are defined by three orthonormal base vectors) is not always straightforward. Simply specifying that rotations have been parametrised as Cardan angles (rather than as axis-angle, quaternions, etc.) is not sufficient to properly convey how the angles of a given joint have been calculated. In addition to the three orthonormal base vectors defining each coordinate system, and assuming they are both known to be, e.g., right-handed, other relevant specifications include:

(1)   the coordinate system acting as reference,
(2)   the use of *passive* or *active* rotations,
(3)   the use of an *intrinsic* or *extrinsic* rotation sequence, and
(4)   the actual rotation sequence.

For example, in the case of the common Joint Coordinate System convention described by Grood and Suntay [42], after accounting for minor differences (e.g. in the sign assigned to certain parameters; see [43, 44] for details), we are essentially referring to an intrinsic extension-adduction-internal rotation (XYZ given the axes directions shown in Figure 1) sequence of the distal relative to the proximal segment frame (for the tibiofemoral joint, of the *tibial* relative to the *femoral* local reference frame,) using active rotations with respect to the local coordinate system. This particular joint angle convention was employed not only for the original fluoroscopy-based reference dataset, but also to guide the joint simulator and to calculate the IMU-based angles. Consequently, any of the visible differences remaining between the IMU kinematics and the simulator ground truth (Figure 2) could not, at this point, reasonably be attributed to differences in angle representation. Nonetheless, before definitively concluding that these differences could be entirely attributed to the sensor fusion algorithm layer of error, yet another possible source of disagreement had to be considered.
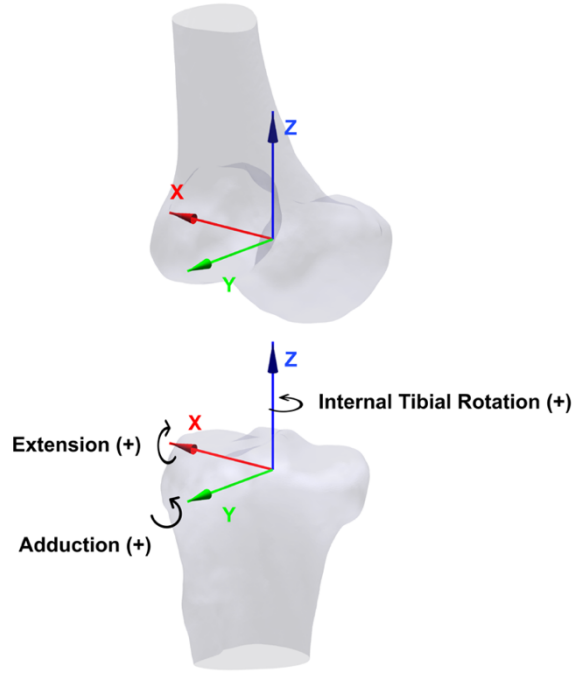
Figure 1. Local femoral (top) and tibial (bottom) coordinate systems for a right knee. Reproduced and adapted from [45]. Note: Unless specifically stated otherwise, the axis directions and rotation conventions shown here can be assumed throughout Section I of this dissertation.
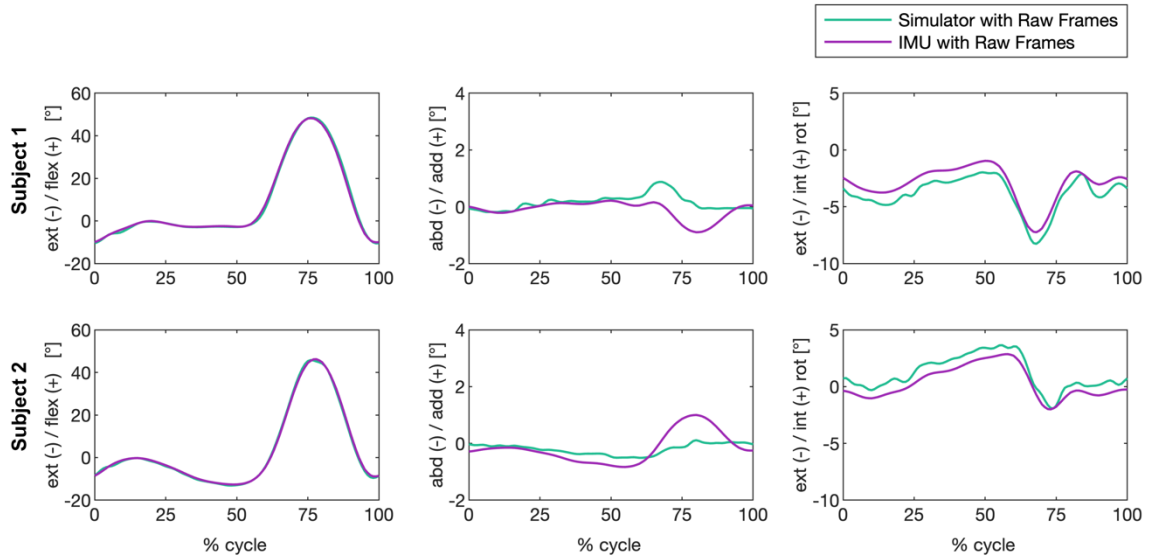
Figure 2. Knee joint angles over one complete exemplary gait cycle (expressed as a percentage) for two sample subjects. The solid green lines illustrate the simulator kinematics, while the solid purple lines illustrate the IMU-based kinematics (prior to any correction in frame alignments in both cases). Simulator and IMU-based kinematic signals are not in perfect agreement, as can be observed from the visible differences between the green and purple lines in ab/adduction and int/external rotation. Reproduced and adapted from [46] for the reader's convenience. Note: Here, knee flexion was purposefully depicted as positive to match common clinical convention.

Even though the same rotation convention was used in both datasets (fluoroscopy/simulator vs. IMU), the availability of different types of data associated with each motion capture modality inevitably demanded that the exact directions of the 3D axes defining each segment's local reference frame were estimated using different joint axis approaches. On one hand, the fluoroscopy-based data that was used to guide the joint simulator leveraged the availability of sequential radiographic images of the joint throughout the gait cycle (Figure 3), as well as access to 3D models of the knee prosthesis components each patient had had implanted, to ultimately employ a cylindrical-axis-based approach [47-49] for the definition of the joint's flexion/extension axis (Figure 4a). On the other hand, the IMU-based dataset relied entirely on inertial measurements. The lack of direct information regarding the position of the IMU sensors, let alone of the underlying bone segments the sensors were meant to represent, made it arguably impossible to implement anything other than a functional-based approach [50] (Figure 4b) to define the flexion/extension axis from the IMU-based system.
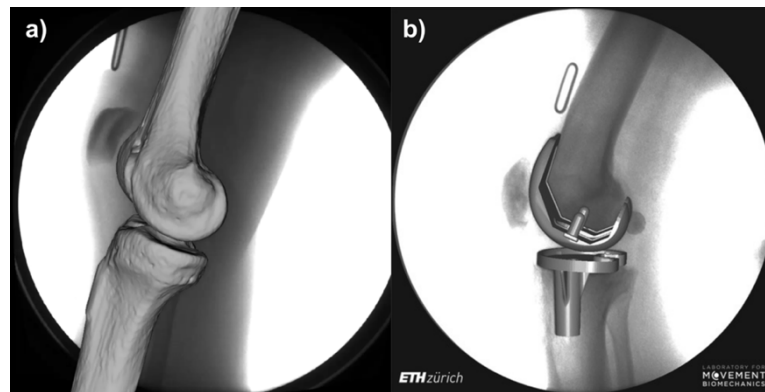
Figure 3. Fluoroscopic images of a) a natural knee, and b) a total knee replacement, with registered bone/implant geometries. Reproduced and adapted with permission from [51, 52].
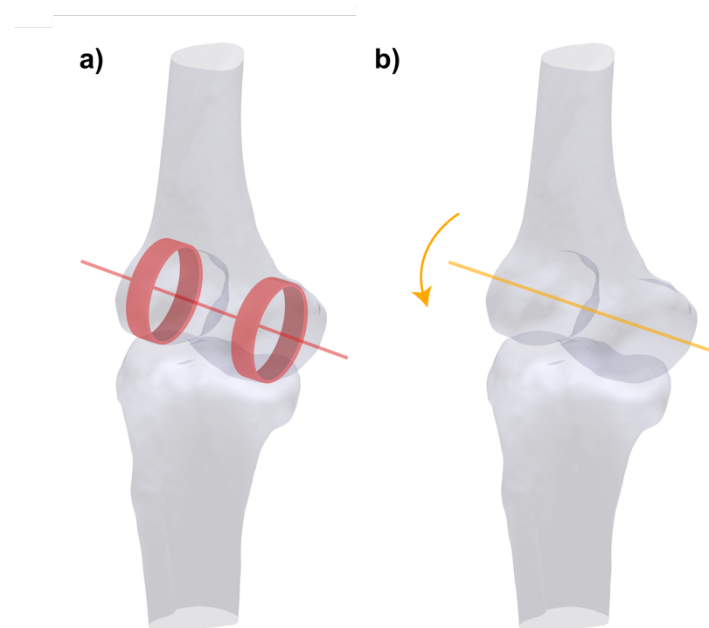
Figure 4. Graphic representation of a) a cylinder axis, and b) a functional flexion axis. Reproduced and adapted with permission from [53].

Previous work has been published suggesting that joint axes approaches based on bone geometry and the position of anatomical landmarks can be used virtually interchangeably with functional-based approaches [54, 55]. It is reasonable to expect however, that for several subjects, the presence of even minor differences between their actual femoral bone geometries and the idealised cylinder model leveraged by a cylinder-based approach will lead to differences between an axis identified functionally *versus* one identified geometrically. The inherent assumption in a considerable portion of the early literature has been that these differences are likely so small that their effect on kinematic signals could be considered mostly negligible [54, 55]. Nevertheless, given the complex nature of rotational data and the tendency of any associated errors to propagate from one plane of motion into the others [56, 57] we decided to perform a basic sensitivity analysis to gain a better understanding of the impact that minor differences between e.g. a cylinder axis and a functional flexion axis could have on the shape of the corresponding kinematic signals.

We began by considering an example set of kinematic signals (Figure 5, in black) over a level walking cycle based on a fluoroscopically defined femoral reference frame. We then simulated a known misalignment between that fluoroscopically defined femoral reference frame and an analogous inertially defined femoral reference frame of $\theta°$ around the femoral anteroposterior (AP) axis, where $\theta \in \{ i \in \mathbb{Z} \mid -5 \leq i \leq 5\}$. The resulting kinematic signals varied in shape and magnitude within a window of $\pm 5°$, especially in ab/adduction (Figure 5a, in blue). We then went on to consider analogous misalignments around the AP axis of the tibial reference frame (Figure 5b, in orange), the proximodistal (PD) axis of the femoral reference frame (Figure 5c, in blue), the PD axis of the tibial reference frame (Figure 5d, in orange), and even combined misalignments around the AP *and* PD axes for first the femoral (Figure 5e, in blue) and then the tibial (Figure 5f, in orange) reference frames. Finally, we illustrated an example of the possible combined effects of misalignments around the AP *and* PD axes of *both* the femoral and tibial reference frames (Figure 6, in grey). In all cases, the underlying relative motion between the joint segments was always kept exactly the same; only artificial differences to static frame alignment were introduced. The results of these analyses clearly demonstrate the non-negligible effects that even minor differences in frame alignment can produce on kinematic signals. Importantly, the impact of these differences on the associated kinematic signals can consist of not just simple offsets to the curves (e.g. Figure 5b, 5d), but also of notable changes in signal shape, potentially transforming a local minimum into a local maximum (e.g. Figure 5c, 5e) or *vice versa*. Furthermore, the combination of misalignments around multiple axes, even if individually small in magnitude ($\leq 5°$), can lead to uncertainty windows as large as 20° (Figure 6), a sizeable degree of error considering the relatively small ranges of motion often observed for ab/adduction and int/external rotation during gait activities. (Note: The sensitivity analysis presented here aimed to assess the effect of finding slightly different flexion/extension axes using the cylinder axis vs. functional flexion axis methods. Errors of misalignment around only the mediolateral axis were therefore excluded here, as a rotation around this axis would not change its direction and would only happen if the cylinder and functional flexion axes were in fact perfectly coincident.)
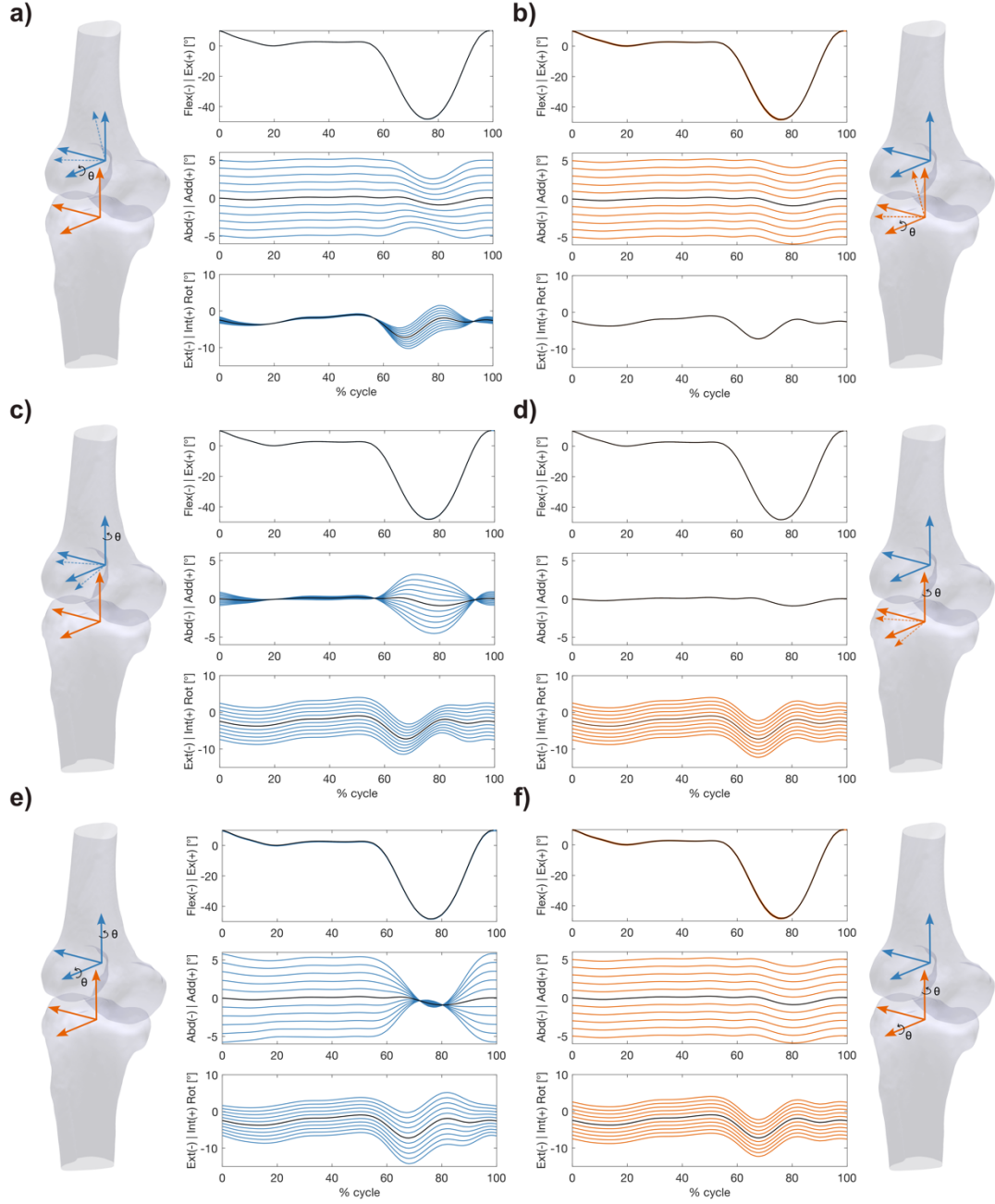
Figure 5. Illustration of the effect of $\theta°$ of frame misalignment around the a) femoral AP axis, b) tibial AP axis, c) femoral PD axis, and d) tibial PD axis, as well as a combination of $\theta°$ of frame misalignment around both the a) femoral AP and PD and b) tibial AP and PD axes. Reference set of tibiofemoral kinematic signals over a sample level walking cycle are illustrated in black; kinematic signals associated with a misaligned femoral frame are blue, and signals associated with a misaligned tibial frame are orange. Graphical representations of the local reference frames within the joint segments are also shown in blue and orange for the femur and tibia, respectively. The kinematic signals resulting from the misaligned frames are depicted for all integer values of θ from -5 to 5.
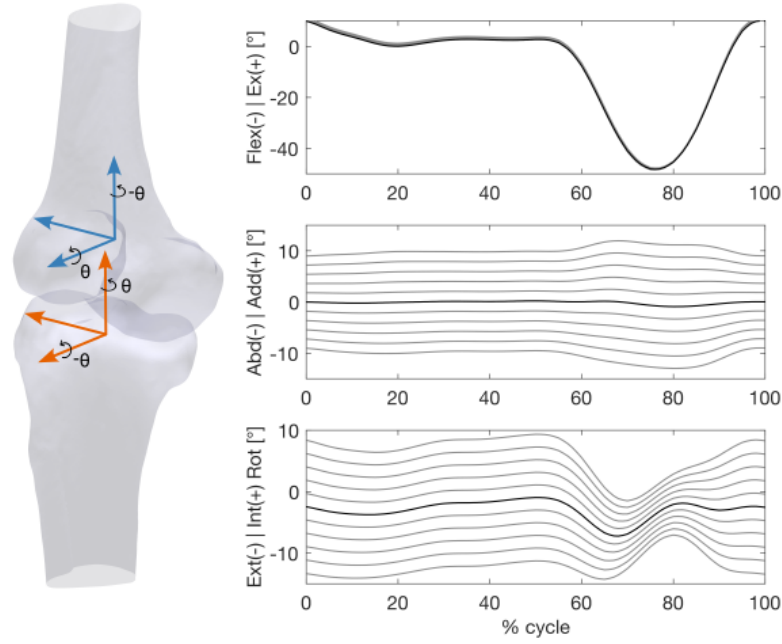
Figure 6. Illustration of the effect of $\theta°$ of frame misalignment around the femoral AP axis and tibial PD axis, in addition to $-\theta°$ around both the femoral PD and tibial AP axes. Reference set of tibiofemoral kinematic signals over a sample level walking cycle are illustrated in black; kinematic signals associated with misaligned frames are shown in grey. Local reference frames within the joint segments are shown in blue and orange for the femur and tibia, respectively. The kinematic signals resulting from the misaligned frames are depicted for all integer values of θ from -5 to 5.

Notably, our sensitivity analysis confirmed that the presence of even minor misalignments between a cylinder-based axis and a functional flexion axis could certainly lead to errors with the characteristics and magnitudes observed between the simulator- and the IMU-based kinematic signals (Figure 2) in Journal Publication I. Evidently, our results were susceptible to a fourth, previously overlooked layer of error, namely, the *cross-talk layer*. The term cross-talk refers to the mechanism by which even small differences in the direction of the joint's primary rotation axis can lead to the artificial amplification of rotations occurring around the other two secondary axes (Figure S1 in [46]). It becomes therefore critical to first compensate for possible differences in the alignment of the local segment frames of each of our two datasets. Only once these differences have been corrected for, can we properly gauge the level of error characterising the sensor fusion algorithm layer. This then motivated a study that was subsequently published in *Nature Scientific Reports* (5-year Impact Factor of 4.3 as of 2023), presented here as Journal Publication II: *A frame orientation optimisation method for consistent interpretation of kinematic signals*.

Considering the lack of consensus surrounding joint axis definitions, it became unclear whether a cylinder-based axis would be considered "more accurate" than a functionally defined flexion axis, or *vice versa*. Without delving too deep into a longer philosophical discussion that would fall outside the scope of this dissertation, at least from a mathematical and engineering perspective, neither axis is more correct than the other, they are simply *different*. The same could be said of axes derived using other approaches, such as the clinical and surgical transepicondylar axis methods [54, 58]. The idealised model of a perfect hinge joint with clear anatomical landmarks marking the direction of the vector representing the joint's axis of rotation is helpful, but realistically flawed. Even excluding measurement

errors, we can reasonably expect to see differences between the joint axes that result from different methods because the underlying axis that each method seeks is based on different information and assumptions, and is therefore, at the most basic level, *inherently different.*

The availability of different approaches to define joint axes and thereby establish local reference frames to represent the moving segments of a joint, paired with a lack of awareness that signals obtained using different axis approaches are not directly comparable, presents a clear problem in the field of biomechanics in general. An inability to compare kinematic signals between studies due to a lack of consensus regarding which axis method to use, as well as differences in the type of information made available by different motion capture modalities (making it impossible to enforce the widespread use of a single joint axis approach, even if one were to be unanimously chosen), make it incredibly challenging to reach a common understanding of tibiofemoral joint motion patterns. There is a pressing need for a more robust and reproducible representation of kinematics, one which is not dependent on the chosen joint axis approach. In Journal Publication II, we therefore present a frame orientation optimisation method (FOOM), a computational approach we developed that visibly demonstrates the potential to address this critical gap in biomechanics research. Moreover, after successful implementation of the FOOM approach on the simulator and IMU-based kinematic signals, our findings clearly established that our IMU-based mobile gait analysis system is certainly accurate enough to capture patients' knee rotational kinematics, at least in the absence of STA. Naturally, further work is required to additionally tackle the accurate estimation of tibiofemoral translations, as well as characterise (and potentially improve) our algorithm's resilience to errors introduced by STA. These investigations have already begun and are being continually explored in collaboration with partner institutions (FAU Erlangen and Medizinische Hochshule Hannover).

5. Revisiting Phenotypes

In light of the new insights obtained from the previously described sensitivity analyses, as well as the results obtained within Journal Publication II, it became necessary to assess the extent to which the cross-talk layer of error could practically affect the identification of functional phenotypes. To perform this assessment, we selected two peer-reviewed articles that fulfilled the following criteria:

(1) have been published within the last five years,
(2) have no authors in common,
(3) report the existence of clinically relevant functional phenotypes, which have been identified by applying data clustering techniques to the *in vivo* kinematic signals of a large (>50) patient cohort,
(4) and report the kinematic signals of each of the identified phenotypes with sufficient detail for these to be digitised for further analysis.

The first study that was selected claimed to have successfully identified three "meaningful phenotypes" based on the application of a clustering model on the 3D kinematic curves of 150 healthy knees during treadmill walking (Figure 7, left) [59]. Each kinematic phenotype was determined by averaging the kinematic curves of all subjects assigned to a given cluster by the clustering algorithm. The study claimed to have thus identified three meaningfully different patterns of knee motion characterising asymptomatic gait. After digitisation of the kinematic signals of the three phenotypes from high-resolution copies of the published figures using an online tool (v4.6; WebPlotDigitizer, Pacifica, California, USA), our FOOM approach was applied to the kinematic signals of Phenotype 2 and Phenotype 3 to optimise the orientations of the associated local femoral and tibial reference frames towards the orientations of the frames used in Phenotype 1. This optimisation effectively re-orientated the underlying

local reference frames towards a common target orientation (dictated in this case by Phenotype 1), after which each phenotype's kinematic signals were recalculated according to these optimised reference frames. As previously mentioned, and described in Journal Publication II, only after possible differences in reference frame orientations have been corrected in this way (thus properly accounting for the cross-talk layer of error) can one reliably conclude that the differences observed between kinematic signals represent real differences in the underlying joint movement patterns of the different groups. After implementation of the described FOOM approach to the data presented by the previous study, the kinematic signals of the original three phenotypes could be observed to reach a much higher level of agreement than before (Figure 7, right). In fact, while minor differences could be detected between the three groups, especially for Phenotype 2, the average kinematic curves essentially overlapped over the entire gait cycle after simply adjusting the orientation of the local segment frames by a maximum of 12.7° around a given axis, with most adjustments falling below 7° (Table 1).
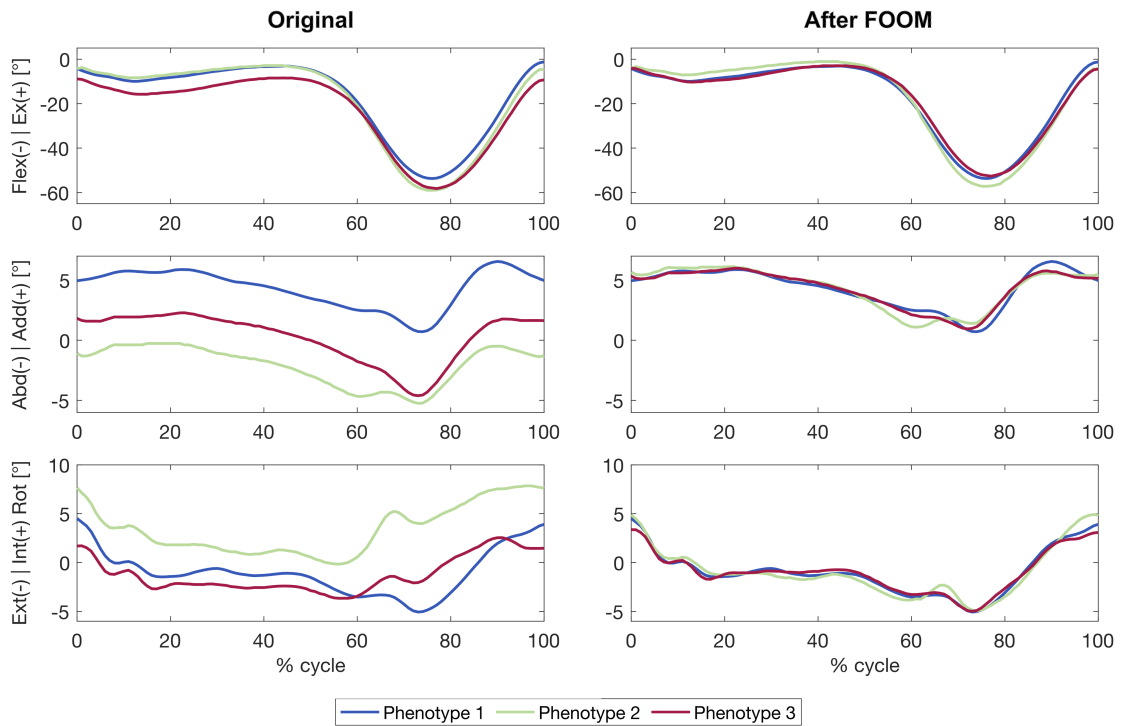
Figure 7. Knee joint angles over one complete exemplary gait cycle (expressed as a percentage) for each of the three phenotypes identified in [59], shown as reported in the original publication (left), as well as after re-orientating the underlying local segment frames by implementing FOOM (right).

Table 1. Corrective rotations in degrees applied to local femoral and tibial reference frames of Phenotypes 2 and 3 by optimisation towards Phenotype 1 with FOOM.

		Phenotype 2	Phenotype 3
Femoral	X	2.0	-7.6
	Y	-6.2	-6.0
	Z	3.5	0.3
Tibial	X	4.4	-2.5
	Y	-12.7	-9.6
	Z	6.1	-1.7

The second study that was selected for further analysis focused on the clustering of patients with knee osteoarthritis, stating to have identified four patient subgroups (referred to here as "phenotypes") (Figure 8, left). The differences between phenotypes were initially considered to be statistically significant and even "clinically relevant", especially when compared against a healthy control group [20]. Implementation of the FOOM approach (in this case, optimising towards Phenotype 4, or G4 in the original publication) however, once again led to visibly better agreement of the kinematic signals of the four phenotypes (Figure 8, right). Here, local reference frames were re-orientated by a maximum of 12.5° around one of the frame axes, with most of the remaining frame orientation changes consisting once more of 7° or less (Table 2).
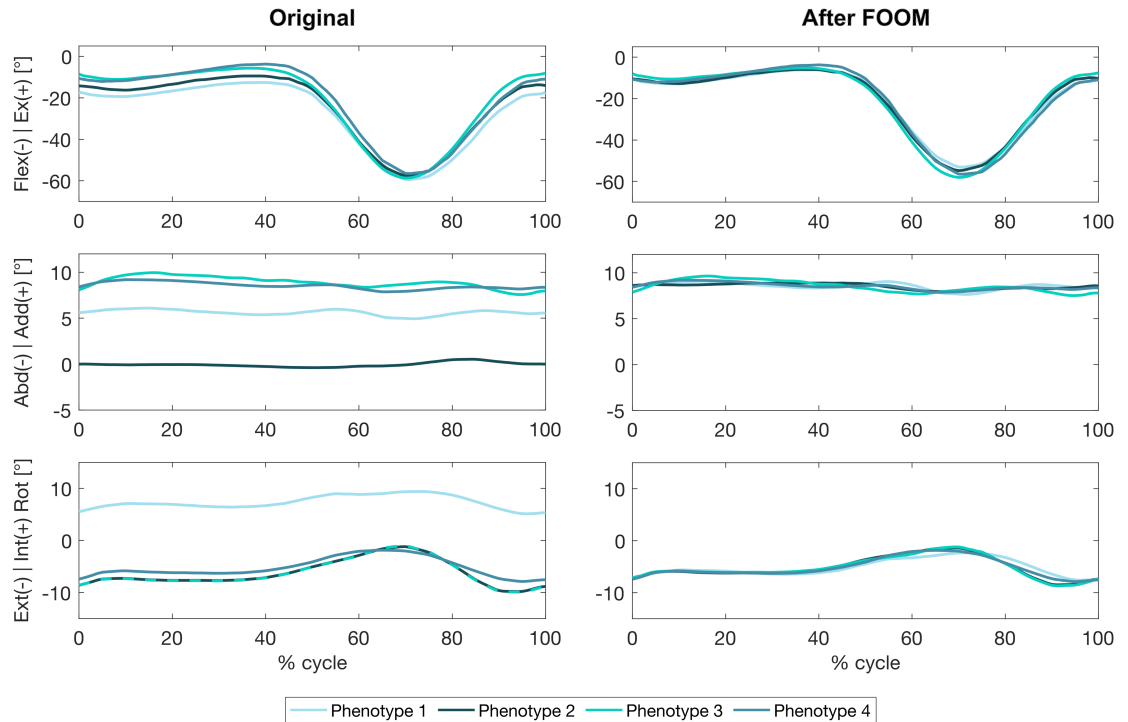
Figure 8. Knee joint angles over one complete exemplary gait cycle (expressed as a percentage) for each of the four phenotypes identified in [20], shown as reported in the original publication (left), as well as after re-orientating the underlying local segment frames by implementing FOOM (right). Note: in bottom left plot, Phenotypes 2 and 3 are overlapping and shown as dashed (rather than solid) lines so that both signals are visible.

Table 2. Corrective rotations in degrees applied to local femoral and tibial reference frames of Phenotypes 1, 2 and 3 by optimisation towards Phenotype 4 with FOOM.

		Phenotype 1	Phenotype 2	Phenotype 3
Femoral	X	-2.9	9.8	-7.0
	Y	1.5	-1.6	-1.9
	Z	-0.2	3.4	0.6
Tibial	X	3.7	5.9	-6.5
	Y	-1.1	-9.3	-0.8
	Z	12.5	-11.4	-0.2

The practical implications of our findings from using FOOM to analyse these two sample studies are important. By adjusting the orientation of local segment frames, differences in the kinematic signals between reported phenotypes previously considered to be "meaningful" or "clinically relevant", were virtually eliminated. This inevitably bears the question: Were the measured differences between the kinematic curves of the different groups so-called "real" differences in the underlying joint motion? Or were they merely the result of, e.g., measurement error in defining joint axes? The first phenotyping study used an optical marker-based system to capture subject kinematics. Even though the system additionally incorporated a rigid knee brace for marker attachment in an attempt to reduce errors associated with STA, previous research has demonstrated that the magnitude of errors affecting kinematic estimates based on stereophotogrammetry can reasonably exceed 10° for the knee and ankle joints [57]. Accordingly, the differences in reference frame orientations enforced by FOOM in this first analysis had magnitudes that could plausibly be explained by measurement error.

The second study considered, however, used biplanar radiographic imaging to ensure better accuracy and precision than traditional marker-based systems [20]. Under ideal testing conditions, validation of the system found errors on bone pose estimation to be below 0.5° [60]. Nevertheless, dynamic validation tests only involved cadaveric specimens performing a simulated squat at an angular speed of 12°/s, a much slower rate than what would be observed *in vivo* at a normal walking speed. At the reported walking speed of 0.83 m/s, angular velocities would have easily exceeded 250°/s [61]. The used imaging frequency of 15Hz was therefore never validated for these higher angular velocities, and accuracy would likely suffer as a result. Similarly, the negative effect of limb overlay (i.e. when the contralateral leg crosses over the target leg, thereby obfuscating the image) was not empirically assessed. The combination of factors such as image resolution, contrast, overlapping contours and equipment setup are known to influence the precision of radiostereometric analysis [62], and could therefore plausibly lead to error values larger than initially presumed. Furthermore, even assuming the image registration process was accurate, the automated algorithm used to define local anatomical coordinate systems was known to be affected by variability. In 10 normal knees, the algorithm varied by about 2.5° around each axis for the femur, and about 2° for the tibia. Moreover, larger differences in morphology between subjects were hypothesised to negatively impact the algorithm's repeatability. In the context of an *in vivo* study with 66 OA patients at different stages of disease progression, higher variability in joint morphology between subjects is certainly reasonable, and so would, by extension, be larger uncertainties. The possibility that measurement error and morphological variability could arguably explain the changes to

frame orientations that were applied during the implementation of FOOM on this second study thus once again brings into question the extent to which the reported phenotypes can be definitively considered to exhibit distinct joint movement patterns.

Our findings stemming from the application of FOOM on the two cited phenotyping studies were by no means conclusive evidence that those phenotypes were invalid or clinically meaningless. What our analysis did achieve, however, was portray why the evidence these studies presented to corroborate the existence of three healthy (or four OA) patient subgroups with allegedly different underlying movement patterns of the tibiofemoral joint should be interpreted with caution. Our exploration clearly demonstrates that frame misalignments well below 13° could in fact artificially lead to very similar differences than the ones observed between the reported phenotypes. More importantly, this analysis serves to highlight that even if the reported differences between the identified subgroups were not the result of measurement error, they were likely not differences between dynamic movement patterns, but rather between *the alignments of each subject's skeletal anatomy*. In this manner, the presence of systematic differences in segment frame orientation between phenotypes could itself be a clinically meaningful observation that should be further explored. Either way, there is a clear need for additional efforts to reliably identify more robust patient phenotypes – phenotypes which even after the application of methods like FOOM to correct frame alignment inconsistencies, still clearly exhibit visibly different joint motion.

6. The REference FRame Alignment MEthod: REFRAME

The identification of robust, reproducible and reliable functional phenotypes requires a re-examination of previously collected data, by additionally post-processing results to exclude possible differences caused by frame alignment inconsistencies. Importantly, the FOOM approach presented thus far targeted only frame orientations, even though kinematic data often comprises both joint rotations and translations. Much like differences in frame orientations can lead to considerable errors in the calculation of joint rotations, differences in the positions of reference frame origins can lead to errors in joint translations. Consequently, the FOOM approach was additionally extended by complementary techniques to analogously optimise coordinate system origins based on translational kinematic signals, resulting in the conception of the REference FRame Alignment MEthod (REFRAME). This flexible, more comprehensive framework was then validated using *in vivo* moving fluoroscopy data of a healthy knee joint during five stair descent cycles.

A full description of REFRAME and the results of validation testing for the first sample subject were drafted into Journal Publication III: *A reproducible representation of healthy tibiofemoral kinematics during stair descent using REFRAME – Part I: REFRAME foundations and validation,* which was published in *Nature Scientific Reports* (5-year Impact Factor of 4.3 as of 2023). In that study, prior to the implementation of REFRAME, for each single motion trial, the use of different axis approaches to define three femoral reference frame variations resulted in clear discrepancies between the kinematic signals associated with each of those reference frames (Figure 9). These differences were present *even though the physical movement of the joint segments* (and the underlying set of raw datapoints) *was known to be one and the same*. It therefore became evident that in the absence of REFRAME, we can no longer operate under the misleading assumption that the presence of differences between sets of kinematic signals inherently implies that there are differences in the underlying movement patterns. Importantly,

however, the convergence of the local reference frames and between the kinematic signals *after* RE-FRAME implementation (Figure 10) provided solid evidence of our method's potential to ensure a consistent and reproducible evaluation of joint motion.
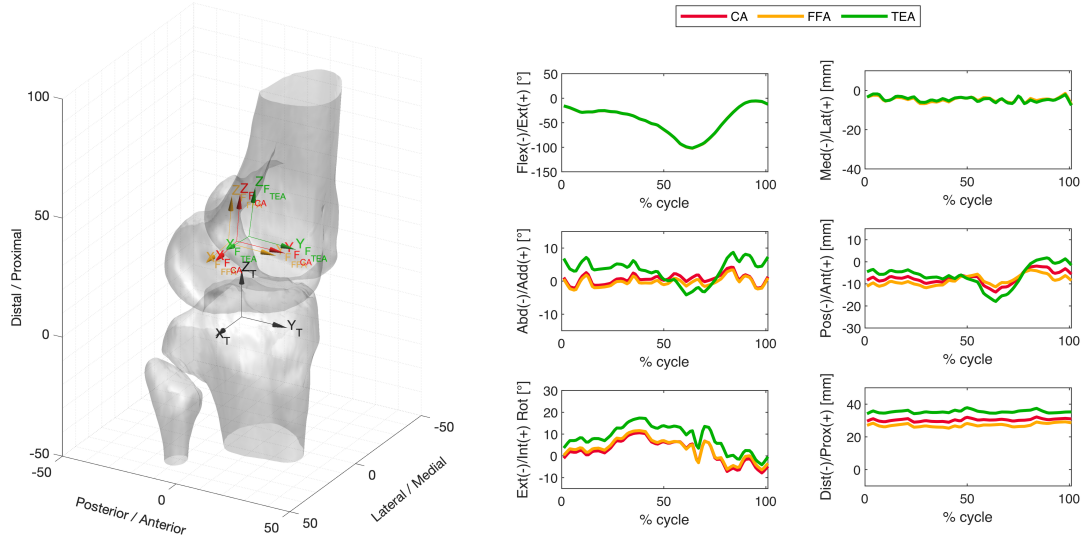
Figure 9. Local segment reference frames (left) and raw kinematic signals (right) for a healthy tibiofemoral joint during a stair descent cycle. Three variations of the kinematic signals were calculated based on three femoral reference frame variations resulting from three distinct joint axis approaches (CA: Cylinder Axis, FFA: Functional Flexion Axis, and TEA: TransEpicondylar Axis).
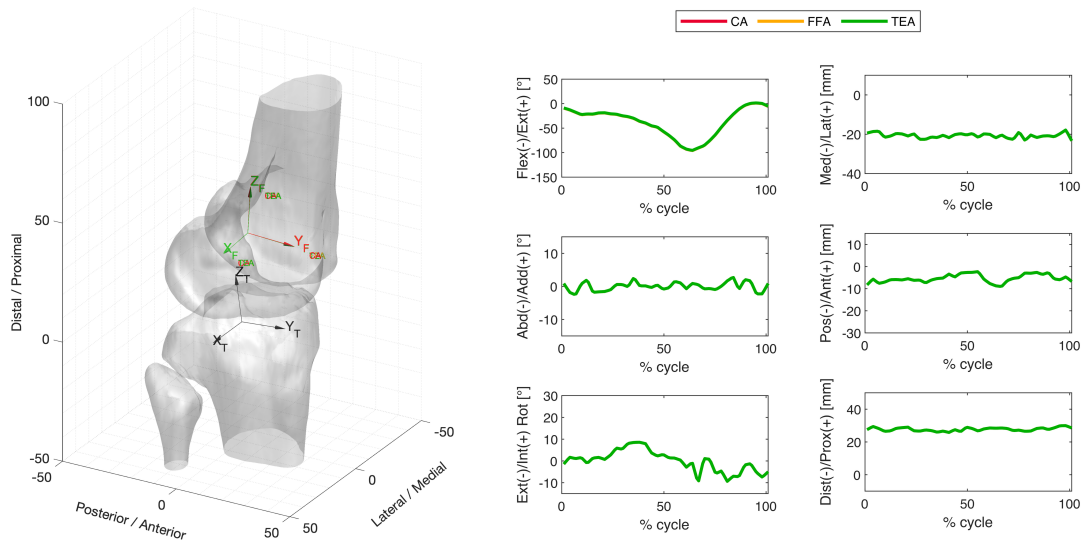
Figure 10. Local segment reference frames (left) and kinematic signals (right) for a healthy tibiofemoral joint during a stair descent cycle, after REFRAME implementation. Three variations of the kinematic signals were calculated based on three femoral reference frame variations resulting from three distinct joint axis approaches (CA: Cylinder Axis, FFA: Functional Flexion Axis, and TEA: TransEpicondylar Axis). REFRAME implementation visibly leads to convergence of the femoral reference frames, as well as of the kinematic signals in all six degrees-of-freedom. (Note: signals from all three axis approaches coincide after REFRAME, so TEA overlaps CA and FFA).

16

While Journal Publication III described the mathematical formulation of the REFRAME framework in detail and presented five stair descent trials of a single subject as preliminary validation and proof-of-concept, a second associated manuscript (Journal Publication VI) was subsequently drafted. Journal Publication IV: *A reproducible representation of healthy tibiofemoral kinematics during stair descent using REFRAME – Part II: Exploring optimisation criteria and inter-subject differences*, which was likewise published in *Nature Scientific Reports* (5-year Impact Factor of 4.3 as of 2023), further validated the method in nine additional subjects (five trials each) and considered the effects of two RE-FRAME implementations on inter-subject differences, while making a first attempt at clinical interpretation of the motion patterns.

In light of the results obtained during first-stage analytical validation of our IMU system prototype and the development of FOOM and REFRAME, additional steps to further test the previously described sensor fusion algorithm in increasingly more complex and/or realistic scenarios were planned and executed. These investigations resulted in the additional publication of two other manuscripts, Journal Publications V and VI. Journal Publication V: *Validation of inertial-measurement-unit-based* ex vivo *knee kinematics during a loaded squat before and after reference-frame-orientation optimisation*, which was also published in the journal *Sensors* (5-year Impact Factor of 3.7 as of 2023), tested the chosen sensor fusion algorithm against an optical system in a more challenging setting than previously described; by considering single iterations of a loaded squat cycle, simulated in each of seven cadaveric specimens on a force-controlled knee rig. In Journal Publication VI: *Comparison of IMU-based knee kinematics with and without harness fixation against an optical marker-based system*, which was published in the journal *Bioengineering* (2023 Journal Impact Factor of 3.8), on the other hand, the STA layer was finally introduced, and 40 asymptomatic knees were tested *in vivo* against an optical marker-based system that leveraged a strategically placed rigid brace (to which the reflective markers were attached). Both studies implemented the REFRAME approach in post-processing, further demonstrating the importance of considering local reference frame definitions when assessing the agreement of kinematic signals.

The collective insights generated while composing the above manuscripts eventually led us to re-evaluate our earlier perception of kinematic signals as a representation of joint motion. This conceptual shift in our understanding is most easily portrayed through what we ultimately labelled *The Book Analogy*, illustrated graphically and described in detail in Appendix A. The analogy essentially proposes that the kinematics of a joint throughout a given motion trial can be thought of as being contained within a book, where a single set of kinematic signals (e.g. the set of six green time series signals in Figure 10) is merely one page of that book, i.e. one possible representation of that joint motion. The set of kinematic signals resulting from representing that same joint motion using local reference frames that are orientated (and positioned) slightly differently would be another page within that book. The entire book could then be thought of as containing all the different possible representations of the same underlying joint motion, with each page corresponding to a different orientation (and position) of the local frames. The implementation of REFRAME essentially aims to enforce consistency in the orientations and positions of the local frames used across the kinematic datasets being compared, which in terms of our book analogy, can be thought of as making sure that *all the books we are comparing are turned to the same page*. The presence of differences between kinematic signals after REFRAME can therefore lead to much more robust conclusions; Since any observed differences can no longer be the result of frame alignment inconsistencies, we can now more confidently infer that they likely reveal actual fundamental differences in joint motion. The implications of REFRAME are thus by no means limited to the identification of functional gait phenotypes or the validation of IMU-based gait analysis. Having access to a method that facilitates a repeatable and robust representation of joint kinematics is extremely

valuable to the biomechanics field in general. Consequently, in order to allow external researchers to independently optimise their kinematic signals and achieve a reproducible representation of joint kinematics across trials, subjects and even institutions, regardless of the joint axis approach used for segment frame definition, REFRAME was developed into an openly available computer application and released online at https://bbraun.info/reframe and https://movement.ethz.ch/data-repository/reframe.html. Accompanied by a detailed user guide (reproduced here in Appendix B) this executable tool is readily available for download and enables users to adapt the implementation of REFRAME to address their specific research needs. REFRAME has in fact already attracted the attention of other research institutions, with which we have since begun collaborative efforts to re-evaluate the comparison of e.g. kinematic signals based on different marker sets, or even marker-less vs. marker-based systems. Moreover, a 2.5-hour hands-on workshop on the theory and application of REFRAME was one of the six pre-courses offered at the 29th Congress of the European Society of Biomechanics (held in Edinburgh in July 2024) and was attended by an audience of both students and professors, with over 35 participants.

7.   Summary & Outlook

This doctoral dissertation was an exploratory investigation meant to establish the necessary foundation required to take on a larger interdisciplinary project. The overarching goal of that project is two-fold: 1) to develop and commercialise a mobile gait analysis system to measure the tibiofemoral kinematics of OA patients in a clinical setting, and 2) to use the kinematic data collected by that system to support the development and validation of a treatment framework that allows physicians to better tailor TKA to individual patient needs, by leveraging the identification of clinically relevant functional phenotypes.

Towards the first objective, this dissertation achieved the identification and first-hand implementation of a sensor fusion algorithm to successfully estimate rotational knee kinematics during a series of gait activities using only two IMU sensors. The total estimated cost of the resulting prototype system was 200 EUR. This system was analytically validated on real kinematic data (previously collected *in vivo* with moving videofluoroscopy) by exploiting a 6 DOFs joint simulator setup (Journal Publication I). Additional testing of the system was also carried out under more challenging conditions in cadaveric specimens each performing a loaded squat cycle (Journal Publication V), as well as *in vivo* under the influence of STA against a commercially available optical motion capture system (Journal Publication VI). Next steps in the development of this mobile gait analysis system will involve further product development and commercialisation. In parallel, the technical feasibility of estimating tibiofemoral translations or an alternative metric for joint stability are now being explored.

Towards the second objective of the project (i.e. the identification of functional gait phenotypes), this dissertation identified a fundamental challenge associated with the comparison of kinematic signals in general: Even minor (e.g. < 5°) differences in reference frame orientation (and/or position) could easily lead to considerably changes in the visible characteristics of kinematic signals (Journal Publication II). The problem was deemed to be relevant not only in the context of the mobile gait analysis system's validation, but additionally within the scope of robust functional phenotype identification. The limited ability to make reliable conclusions from kinematic signal sets where the orientations and/or positions of the underlying local segment frames have not been optimised for consistency represents an important restriction to the clinical relevance of kinematic comparisons. Within the context of this dissertation, this problem was not only identified but also systematically addressed through the development and validation of REFRAME, a reference frame alignment method that is now an openly

accessible solution that can notably facilitate the consistent representation of joint movement patterns, by correcting for differences in reference frame orientations and positions to produce a set of reproducible and repeatable kinematic signals (Journal Publications III and IV). REFRAME thereby represents a valuable step forward in our ability to detect fundamental differences between joint movement patterns.

The valuable advances achieved as part of this dissertation have widespread implications, not only within the scope of the encompassing project but for biomechanics research in general. First of all, the high sensitivity that kinematic signals demonstrated to even minor inconsistencies in reference frame orientation and position strongly indicate that alternative routes to functional phenotyping may prove to be valuable down the line. This is especially relevant considering that only by identifying *robust* phenotypes in our patient population will we really be able to design a treatment framework that will successfully improve patient satisfaction rates. As a result, we strongly recommend that future work explores using REFRAME to develop a patient classification approach that focuses on the extraction of relevant features that characterise joint function, rather than strictly fixating on having to analyse the shape and magnitude of the time series kinematic curves themselves. Second, the deeper implications of REFRAME should also be considered more generally. For example, previous studies evaluating the presence of significant kinematic differences between distinct subject populations may need to be revisited using REFRAME, to conclusively establish whether any detected differences could be plausibly explained by frame alignment inconsistencies rather than different joint motion. Similarly, the clinical meaning and interpretability of kinematic signals both before and after REFRAME optimisation should urgently be studied in more depth. The question of how much value can be attributed to the shape of kinematic signals in objectively representing joint motion, especially in light of how sensitive their visible characteristics are to the measurement process itself, is one that should be critically considered moving forward. To conclude, this doctoral dissertation represents valuable steps forward, not only towards our vision of developing a mobile gait analysis system, and leveraging functional gait phenotyping to improve TKA outcomes, but also towards our fundamental ability to compare kinematic signals and joint movement patterns in musculoskeletal biomechanics in general.

References

1.	Insall, J., Ranawat, C.S., Scott, W.N., and Walker, P., *Total Condylar Knee Replacement: Preliminary Report.* Clinical Orthopaedics and Related Research, 1976(120).
2.	Gkiatas, I. and Sculco, P., *The History of Total Knee Arthroplasty*. 2022. p. 3-14.
3.	Marques, E.M.R., Dennis, J., Beswick, A.D., Higgins, J., Thom, H., Welton, N., Burston, A., Hunt, L., Whitehouse, M.R., and Blom, A.W., *Choice between implants in knee replacement: protocol for a Bayesian network meta-analysis, analysis of joint registries and economic decision model to determine the effectiveness and cost-effectiveness of knee implants for NHS patients—The KNee Implant Prostheses Study (KNIPS).* BMJ Open, 2021. **11**(1): p. e040205.
4.	Rivière, C., Iranpour, F., Auvinet, E., Howell, S., Vendittoli, P.A., Cobb, J., and Parratte, S., *Alignment options for total knee arthroplasty: A systematic review.* Orthopaedics & Traumatology: Surgery & Research, 2017. **103**(7): p. 1047-1056.
5.	Overgaard, A., Lidgren, L., Sundberg, M., Robertsson, O., and W-Dahl, A., *Patient-reported 1-year outcome not affected by body mass index in 3,327 total knee arthroplasty patients.* Acta Orthopaedica, 2019. **90**(4): p. 360-365.
6.	Bryan, S., Goldsmith, L.J., Davis, J.C., Hejazi, S., Macdonald, V., Mcallister, P., Randall, E., Suryaprakash, N., Wu, A.D., and Sawatzky, R., *Revisiting patient satisfaction following total*

knee arthroplasty: a longitudinal observational study. BMC Musculoskeletal Disorders, 2018. **19**(1): p. 423.

7. Choi, Y.J. and Ra, H.J., *Patient Satisfaction after Total Knee Arthroplasty.* Knee Surgery & Related Research, 2016. **28**(1): p. 1-15.

8. Ornetti, P., Maillefert, J.-F., Laroche, D., Morisset, C., Dougados, M., and Gossec, L., *Gait analysis as a quantifiable outcome measure in hip or knee osteoarthritis: A systematic review.* Joint Bone Spine, 2010. **77**(5): p. 421-425.

9. Angerame, M.R., Holst, D.C., Jennings, J.M., Komistek, R.D., and Dennis, D.A., *Total Knee Arthroplasty Kinematics.* The Journal of Arthroplasty, 2019. **34**(10): p. 2502-2510.

10. Blakeney, W.G. and Vendittoli, P.-A., *The future of TKA*, in *Personalized hip and knee joint replacement*. 2020. p. 169-174.

11. Delport, H.P., Vander Sloten, J., and Bellemans, J., *New possible pathways in improving outcome and patient satisfaction after TKA.* Acta Orthopaedica Belgica, 2013. **79**(3): p. 250-254.

12. Delport, H., Labey, L., De Corte, R., Innocenti, B., Vander Sloten, J., and Bellemans, J., *Collateral ligament strains during knee joint laxity evaluation before and after TKA.* Clinical Biomechanics, 2013. **28**(7): p. 777-782.

13. Lim, D., Kwak, D.-S., Kim, M., Kim, S., Cho, H.-J., Choi, J.H., and Koh, I.J., *Kinematically aligned total knee arthroplasty restores more native medial collateral ligament strain than mechanically aligned total knee arthroplasty.* Knee Surgery, Sports Traumatology, Arthroscopy, 2022: p. 1-9.

14. Koh, I.J., Lin, C.C., Patel, N.A., Chalmers, C.E., Maniglio, M., Han, S.B., Mcgarry, M.H., and Lee, T.Q., *Kinematically aligned total knee arthroplasty reproduces more native rollback and laxity than mechanically aligned total knee arthroplasty: A matched pair cadaveric study.* Orthopaedics & Traumatology: Surgery & Research, 2019. **105**(4): p. 605-611.

15. Sappey-Marinier, E., Tibesku, C., Selmi, T.a.S., and Bonnin, M., *Custom Total Knee Arthroplasty*, in *Personalized hip and knee joint replacement*, C. Rivière and P.A. Vendittoli, Editors. 2020. p. 255-264.

16. Buschner, P., Toskas, I., Huth, J., and Beckmann, J., *Improved Knee Function with Customized vs. Off-the-Shelf TKA Implants-Results of a Single-Surgeon, Single-Center, Single-Blinded Study.* Journal of Personalized Medicine, 2023. **13**(8).

17. Herndon, C.L., Frederick, J.S., Farah, O.K., Santos, W., Shah, R.P., and Cooper, H.J., *Customized Individually-Made and Conventional Total Knee Implants are associated with Similar Improvements in Patient-Reported Outcomes.* Journal of Orthopaedic Experience & Innovation, 2022. **3**(2).

18. Beit Ner, E., Dosani, S., Biant, L.C., and Tawy, G.F., *Custom Implants in TKA Provide No Substantial Benefit in Terms of Outcome Scores, Reoperation Risk, or Mean Alignment: A Systematic Review.* Clinical Orthopaedics and Related Research, 2021. **479**(6): p. 1237-1249.

19. Castañeda, S., Roman-Blas, J.A., Largo, R., and Herrero-Beaumont, G., *Osteoarthritis: a progressive disease with changing phenotypes.* Rheumatology, 2013. **53**(1): p. 1-3.

20. Petersen, E.T., Rytter, S., Koppens, D., Dalsgaard, J., Hansen, T.B., Larsen, N.E., Andersen, M.S., and Stilling, M., *Patients with knee osteoarthritis can be divided into subgroups based on tibiofemoral joint kinematics of gait – an exploratory and dynamic radiostereometric study.* Osteoarthritis and Cartilage, 2022. **30**(2): p. 249-259.

21. Wren, T.a.L., Gorton, G.E., Õunpuu, S., and Tucker, C.A., *Efficacy of clinical gait analysis: A systematic review.* Gait & Posture, 2011. **34**(2): p. 149-153.

22. Hecht, G.G., Van Rysselberghe, N.L., Young, J.L., and Gardner, M.J., *Gait Analysis in Orthopaedic Surgery: History, Limitations, and Future Directions.* Journal of the American Academy of Orthopaedic Surgeons, 2022. **30**(21): p. e1366-e1373.

23. Favre, J. and Jolles, B.M., *Gait analysis of patients with knee osteoarthritis highlights a pathological mechanical pathway and provides a basis for therapeutic interventions.* EFORT Open Reviews, 2016. **1**(10): p. 368-374.

24. Delgado-García, G., Vanrenterghem, J., Ruiz-Malagón, E.J., Molina-García, P., Courel-Ibáñez, J., and Soto-Hermoso, V.M., *IMU gyroscopes are a valid alternative to 3D optical motion capture system for angular kinematics analysis in tennis.* Proceedings of the Institution of Mechanical Engineers, Part P: Journal of Sports Engineering and Technology, 2021. **235**(1): p. 3-12.

25. Müller, B., Ilg, W., Giese, M.A., and Ludolph, N., *Validation of enhanced kinect sensor based motion capturing for gait assessment.* PLOS One, 2017. **12**(4): p. e0175813.

26. Albert, J.A., Owolabi, V., Gebel, A., Brahms, C.M., Granacher, U., and Arnrich, B., *Evaluation of the Pose Tracking Performance of the Azure Kinect and Kinect v2 for Gait Analysis in Comparison with a Gold Standard: A Pilot Study.* Sensors, 2020. **20**(18): p. 5104.

27. Vilas-Boas, M.D.C., Choupina, H.M.P., Rocha, A.P., Fernandes, J.M., and Cunha, J.P.S., *Full-body motion assessment: Concurrent validation of two body tracking depth sensors versus a gold standard system during gait.* Journal of Biomechanics, 2019. **87**: p. 189-196.

28. Chen, S., Lach, J., Lo, B., and Yang, G.Z., *Toward Pervasive Gait Analysis With Wearable Sensors: A Systematic Review.* IEEE Journal of Biomedical and Health Informatics, 2016. **20**(6): p. 1521-1537.

29. Simon, S.R., *Quantification of human motion: gait analysis—benefits and limitations to its application to clinical problems.* Journal of Biomechanics, 2004. **37**(12): p. 1869-1880.

30. Kour, N., Gupta, S., and Arora, S., *A Survey of Knee Osteoarthritis Assessment Based on Gait.* Archives of Computational Methods in Engineering, 2021. **28**(2): p. 345-385.

31. Klöpfer-Krämer, I., Brand, A., Wackerle, H., Müßig, J., Kröger, I., and Augat, P., *Gait analysis – Available platforms for outcome assessment.* Injury, 2020. **51**: p. S90-S96.

32. Slade, P., Habib, A., Hicks, J.L., and Delp, S.L., *An Open-Source and Wearable System for Measuring 3D Human Motion in Real-Time.* IEEE Transactions on Biomedical Engineering, 2022. **69**(2): p. 678-688.

33. Jenkins, G.J., Hakim, C.H., Yang, N.N., Yao, G., and Duan, D., *Automatic characterization of stride parameters in canines with a single wearable inertial sensor.* PLOS One, 2018. **13**(6): p. e0198893.

34. Weygers, I., Kok, M., Konings, M., Hallez, H., De Vroey, H., and Claeys, K., *Inertial Sensor-Based Lower Limb Joint Kinematics: A Methodological Systematic Review.* Sensors, 2020. **20**(3).

35. Seel, T., Schauer, T., and Raisch, J. *Joint axis and position estimation from inertial measurement data by exploiting kinematic constraints.* in *2012 IEEE International Conference on Control Applications.* 2012. IEEE.

36. Seel, T., Raisch, J., and Schauer, T., *IMU-based joint angle measurement for gait analysis.* Sensors, 2014. **14**(4): p. 6891-6909.

37. Versteyhe, M., De Vroey, H., Debrouwere, F., Hallez, H., and Claeys, K., *A Novel Method to Estimate the Full Knee Joint Kinematics Using Low Cost IMU Sensors for Easy to Implement Low Cost Diagnostics.* Sensors, 2020. **20**(6).

38. List, R., Postolka, B., Schütz, P., Hitz, M., Schwilch, P., Gerber, H., Ferguson, S.J., and Taylor, W.R., *A moving fluoroscope to capture tibiofemoral kinematics during complete cycles*

of free level and downhill walking as well as stair descent. PLOS One, 2017. **12**(10): p. e0185952.

39. Postolka, B., Taylor, W.R., List, R., Fucentese, S.F., Koch, P.P., and Schütz, P., *ISB clinical biomechanics award winner 2021: Tibio-femoral kinematics of natural versus replaced knees - A comparison using dynamic videofluoroscopy.* Clinical Biomechanics, 2022. **96**: p. 105667.

40. Nagano, Y., Naito, K., Saho, Y., Torii, S., Ogata, T., Nakazawa, K., Akai, M., and Fukubayashi, T., *Association between in vivo knee kinematics during gait and the severity of knee osteoarthritis.* The Knee, 2012. **19**(5): p. 628-632.

41. Rees, J.L., Beard, D.J., Price, A.J., Gill, H.S., Mclardy-Smith, P., Dodd, C.A., and Murray, D.W., *Real in vivo kinematic differences between mobile-bearing and fixed-bearing total knee arthroplasties.* Clinical Orthopaedics and Related Research, 2005(432): p. 204-209.

42. Grood, E.S. and Suntay, W.J., *A joint coordinate system for the clinical description of three-dimensional motions: application to the knee.* Journal of Biomechanical Engineering, 1983. **105**(2): p. 136-144.

43. Sheehan, F.T. and Mitiguy, P., *In regards to the "ISB recommendations for standardization in the reporting of kinematic data".* Journal of Biomechanics, 1999. **32**(10): p. 1135-1136.

44. Macwilliams, B.A. and Davis, R.B., *Addressing some misperceptions of the joint coordinate system.* Journal of Biomechanical Engineering, 2013. **135**(5): p. 54506.

45. Ortigas-Vásquez, A., Taylor, W.R., Postolka, B., Schütz, P., Maas, A., Woiczinski, M., Grupp, T.M., and Sauer, A., *A Reproducible and Robust Representation of Tibiofemoral Kinematics of the Healthy Knee Joint during Stair Descent using REFRAME – Part I: REFRAME Foundations and Validation.* 2024: Preprint on Research Square.

46. Ortigas-Vásquez, A., Taylor, W.R., Maas, A., Woiczinski, M., Grupp, T.M., and Sauer, A., *A frame orientation optimisation method for consistent interpretation of kinematic signals.* Scientific Reports, 2023. **13**(1): p. 9632.

47. Kurosawa, H., Walker, P.S., Abe, S., Garg, A., and Hunter, T., *Geometry and motion of the knee for implant and orthotic design.* Journal of Biomechanics, 1985. **18**(7): p. 487-499.

48. Asano, T., Akagi, M., Tanaka, K., Tamura, J., and Nakamura, T., *In vivo three-dimensional knee kinematics using a biplanar image-matching technique.* Clinical Orthopaedics and Related Research, 2001(388): p. 157-166.

49. Eckhoff, D.G., Dwyer, T.F., Bach, J.M., Spitzer, V.M., and Reinig, K.D., *Three-dimensional morphology of the distal part of the femur viewed in virtual reality.* Journal of Bone and Joint Surgery, 2001. **83-A Suppl 2**(Pt 1): p. 43-50.

50. Ehrig, R.M., Taylor, W.R., Duda, G.N., and Heller, M.O., *A survey of formal methods for determining functional joint axes.* Journal of Biomechanics, 2007. **40**(10): p. 2150-2157.

51. Hosseini Nasab, S.H., Smith, C.R., Postolka, B., Schütz, P., List, R., and Taylor, W.R., *In Vivo Elongation Patterns of the Collateral Ligaments in Healthy Knees During Functional Activities.* Journal of Bone and Joint Surgery, 2021. **103**(17): p. 1620-1627.

52. Schütz, P., Postolka, B., Gerber, H., Ferguson, S.J., Taylor, W.R., and List, R., *Knee implant kinematics are task-dependent.* Journal of the Royal Society Interface, 2019. **16**(151): p. 20180678.

53. Postolka, B., *Natural Knee Kinematics - The Role of Limb Alignment and Activity on Knee Joint Motion*, in *Department of Health Sciences and Technology*. 2020, ETH Zurich: Zurich.

54. Churchill, D.L., Incavo, S.J., Johnson, C.C., and Beynnon, B.D., *The transepicondylar axis approximates the optimal flexion axis of the knee.* Clinical Orthopaedics and Related Research, 1998(356): p. 111-118.

55. Asano, T., Akagi, M., and Nakamura, T., *The functional flexion-extension axis of the knee corresponds to the surgical epicondylar axis: in vivo analysis using a biplanar image-matching technique.* The Journal of Arthroplasty, 2005. **20**(8): p. 1060-1067.

56. Schache, A.G., Baker, R., and Lamoreux, L.W., *Defining the knee joint flexion-extension axis for purposes of quantitative gait analysis: an evaluation of methods.* Gait & Posture, 2006. **24**(1): p. 100-109.

57. Della Croce, U., Leardini, A., Chiari, L., and Cappozzo, A., *Human movement analysis using stereophotogrammetry. Part 4: assessment of anatomical landmark misplacement and its effects on joint kinematics.* Gait & Posture, 2005. **21**(2): p. 226-237.

58. Berger, R.A., Rubash, H.E., Seel, M.J., Thompson, W.H., and Crossett, L.S., *Determining the rotational alignment of the femoral component in total knee arthroplasty using the epicondylar axis.* Clinical Orthopaedics and Related Research, 1993(286): p. 40-47.

59. Mezghani, N., Soltana, R., Ouakrim, Y., Cagnin, A., Fuentes, A., Hagemeister, N., and Vendittoli, P.-A., *Healthy Knee Kinematic Phenotypes Identification Based on a Clustering Data Analysis.* Applied Sciences, 2021. **11**(24).

60. Christensen, R., Petersen, E.T., Jürgens-Lahnstein, J., Rytter, S., Lindgren, L., De Raedt, S., Brüel, A., and Stilling, M., *Assessment of knee kinematics with dynamic radiostereometry: Validation of an automated model-based method of analysis using bone models.* Journal of Orthopaedic Research, 2021. **39**(3): p. 597-608.

61. Mentiplay, B.F., Banky, M., Clark, R.A., Kahn, M.B., and Williams, G., *Lower limb angular velocity during walking at various speeds.* Gait & Posture, 2018. **65**: p. 190-196.

62. Hansen, L., Raedt, S.D., Jørgensen, P.B., Mygind-Klavsen, B., Kaptein, B., and Stilling, M., *Marker free model-based radiostereometric analysis for evaluation of hip joint kinematics.* Bone & Joint Research, 2018. **7**(6): p. 379-387.

II. Journal Publication I

A framework for analytical validation of inertial-sensor-based knee kinematics using a six-degrees-of-freedom joint simulator

Ortigas-Vásquez, A., Maas, A., List, R., Schütz, P., Taylor, W.R. and Grupp, T.M.

Abstract

The success of kinematic analysis that relies on inertial measurement units (IMUs) heavily depends on the performance of the underlying algorithms. Quantifying the level of uncertainty associated with the models and approximations implemented within these algorithms, without the complication of soft-tissue artefact, is therefore critical. To this end, this study aimed to assess the rotational errors associated with controlled movements. Here, data of six total knee arthroplasty patients from a previously published fluoroscopy study were used to simulate realistic kinematics of daily activities using IMUs mounted to a six-degrees-of-freedom joint simulator. A model-based method involving extended Kalman filtering to derive rotational kinematics from inertial measurements was tested and compared against the ground truth simulator values. The algorithm demonstrated excellent accuracy (root-mean-square error ≤0.9°, maximum absolute error ≤3.2°) in estimating three-dimensional rotational knee kinematics during level walking. Although maximum absolute errors linked to stair descent and sit-to-stand-to-sit rose to 5.2° and 10.8°, respectively, root-mean-square errors peaked at 1.9° and 7.5°. This study hereby describes an accurate framework for evaluating the suitability of the underlying kinematic models and assumptions of an IMU-based motion analysis system, facilitating the future validation of analogous tools.

Keywords: gait analysis; IMU; joint angle; knee kinematics; joint simulator

1. Introduction

Research suggests that up to a fifth of total knee arthroplasty (TKA) patients are dissatisfied with their joint functionality post-surgery [1-5]. Experts have previously attributed this deficit to the ubiquitous use of standardised treatment protocols across patients, regardless of their specific kinematic characteristics [6]. It has been suggested that the inclusion of gait analysis could improve clinical decision-making and treatment outcomes [7]. Current state-of-the-art technology includes both marker-based and markerless optical motion capture systems, as well as static and moving fluoroscopic systems [8, 9]. While fluoroscopy offers the considerable advantage of not being affected by soft-tissue artefact, such systems are associated with substantial processing time requirements, infrastructure, expense and complexity, hence limiting their widespread adoption in clinical settings.

The need for cheaper and more mobile gait analysis solutions has recently been addressed with systems based on wearable sensors, such as inertial measurement units (IMUs). A key hurdle of relying on surface-mounted IMUs to derive joint kinematics is accurately estimating the orientation of the underlying bone segments. This task is made especially challenging by the need to estimate kinematic parameters from linear acceleration and angular velocity data instead of direct three-dimensional positions (as is the case with optical motion capture). Vitali and Perkins [10] recently identified four different categories of methods that tackle this challenge. One of these, the group of so-called "model-based" methods, was highlighted as offering obvious advantages, but requiring more thorough validation before widespread adoption is warranted. Unlike "assumed alignment" methods, model-based methods do not rely on a technician's ability to visually align the IMU axes with those of limb segments, nor do they expect subjects to properly execute calibration movements, such as "functional alignment" methods do.

An example of a model-based method to estimate the orientation of underlying bone segments has been laid out by Seel et al. [11, 12]. Their particular implementation of this method, as later refined by Versteyhe et al. [13], stands out by offering four notable advantages:

(1) While numerous IMU-based approaches measuring knee kinematics successfully estimate flexion/extension angles, accurate quantification of ab/adduction and int/external rotation motions are reportedly more challenging. By exploiting a Kalman smoother that leverages two simple mechanical models of the knee joint, this method provides accurate estimates for joint angles in all three anatomical planes.
(2) While the user is offered certain guidelines for correct sensor placement, these are minimally restrictive and easy to follow.
(3) The approach does not require a separate extensive calibration procedure; there are no additional movements that the patient must perform prior to gait assessment.
(4) By avoiding the use of magnetometer data, susceptibility to ferromagnetic disturbances is prevented.

Despite demonstrating promising accuracy in characterising rotational knee kinematics during level walking [13], widespread adoption of the technology in clinical settings remains limited. This is, in part, rooted in the broad spectrum of complex parameter interactions when using IMU-based tools, as well as the associated algorithms that are available. Further variables include sensor placement, pre-processing of raw sensor data, and drift compensation methods [14], to name but a few.

In addition to algorithmic differences, even among systems focused exclusively on capturing rotational knee kinematics, it remains extremely difficult to assess an approach's accuracy, confounded by contrasting sources of ground truth data. As a result, reaching an objective verdict on how different IMU-based systems perform and which system design is most appropriate can be challenging. Indeed, a systematic review conducted by Pacher et al. [15] reached an analogous conclusion.

1.1. Analytical Validation of Inertial-Based Rotational Knee Kinematics

With the goal of establishing a common foundation for evaluating digital tools that support clinical decision-making, including IMU-based kinematic assessment, the Digital Medicine Society has recently presented the V3 framework [16]. The project lays out standard guidelines divided into three steps: verification, analytical validation and clinical validation. Analytical validation, in particular, focuses on assessing the performance of an algorithm in deriving a physiological metric from sample-level sensor data. The importance of analytically validating IMU-based kinematic assessment tools is therefore clear. Algorithms that derive rotational knee kinematics from inertial data without additional input or extensive calibration generally require the use of models and assumptions. These approximations are needed to compensate for the lack of position data in a global frame, but rarely perfectly reflect reality. Characterising the magnitude of this error can be crucial to guiding product development.

Validation of IMU-based systems directly on human subjects using retroreflective markers and optical motion capture systems [17, 18] is difficult due to soft-tissue artefact, whereby the skin on which the sensor is placed moves relative to the underlying bones [19, 20]. With known difficulties associated with assessing the magnitude of soft-tissue artefact alone, it is clear that isolating how much uncertainty is due to the algorithm's models and assumptions, as opposed to soft-tissue artefact itself, is extremely challenging.

Comprehensive analytical validation of an IMU-based system that estimates knee kinematics should therefore occur at two different levels (Figure 1). The first level involves appraising the degree of uncertainty associated with the models, assumptions and approximations that are implemented within the chosen algorithm. In order to isolate this level of error and quantify it experimentally, we require an approach that does not add other considerable sources of error (such as soft-tissue artefact). Current options include the use of manually operated mechanical rigs [21] and industrial robot arms [13, 22]. These methods are subject to limitations, such as dissimilar embodiments, susceptibility to easily overlooked errors in kinematic mapping, and difficulties in recreating physiological movements. Thorough testing against references that are able to generate realistic knee motion without soft-tissue artefact are therefore clearly required before system performance can be assessed in real-life scenarios. This investigation consequently aimed to develop and test a protocol for a first-level analytical validation of IMU-based knee rotational kinematics using real joint kinematics reconstructed in a simulator.
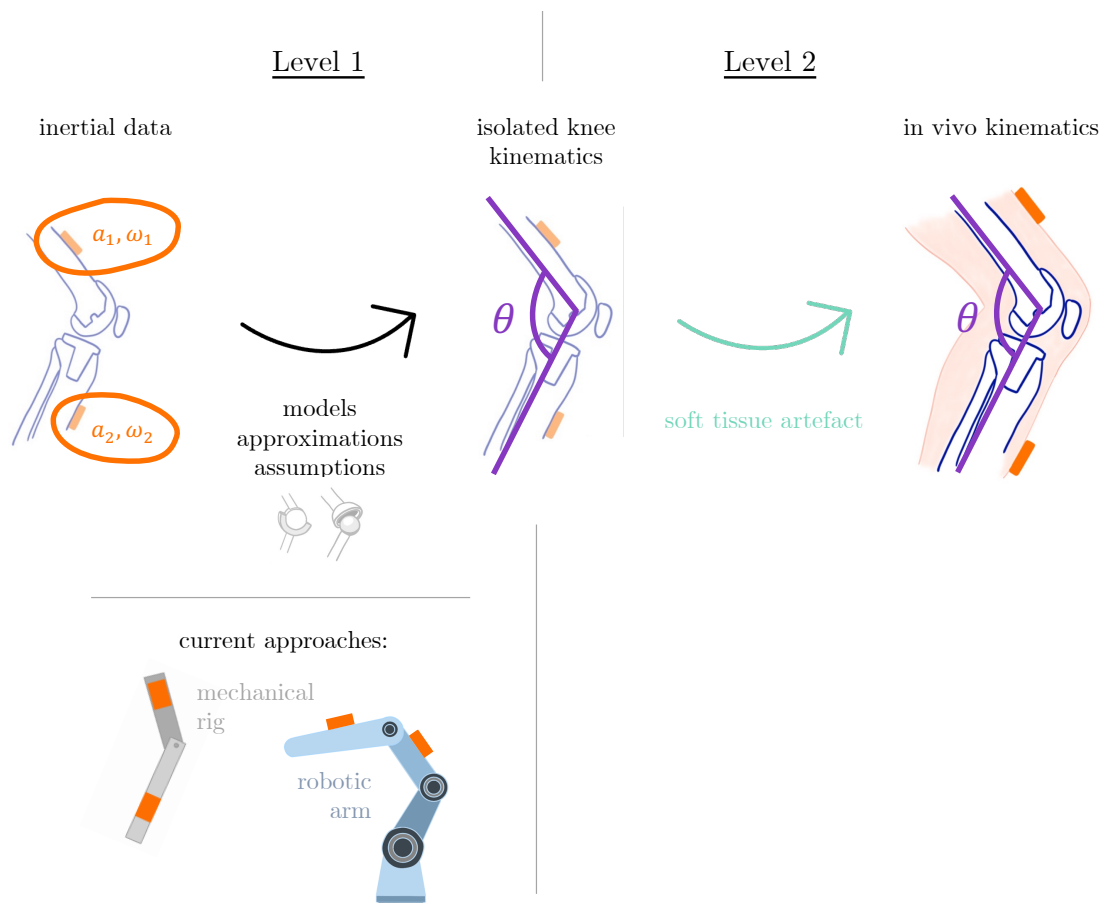
Figure 1. An[...]ial-based tool for kinematic assessment should occur at different levels (e.g., with and without the possibility of soft-tissue artefact) to allow characterisation of different sources of error.

2. Materials and Methods

To investigate the accuracy of IMU-based systems to estimate flexion/extension, ab/adduction, and int/external tibial rotations, we established a simulator setup that was able to recreate tibiofemoral kinematics throughout in vivo measured functional activities of daily living. To achieve this, we applied the open-source kinematic data collected experimentally by Schütz et al. in 2019 [23]. In their study, a moving fluoroscope was employed to capture the tibiofemoral implant kinematics of six total knee arthroplasty (TKA) patients (average age of 72.8 ± 8.5 years; BMI 24.3 ± 2.2 kg/m^2), each with a unilateral PFC Sigma cruciate retaining fixed-bearing prosthesis (Depuy Synthes, Warsaw, IN, USA), during level walking, stair descent, and sit-to-stand-to-sit. At the time of assessment, all subjects showed good functional outcome (Knee Injury and Osteoarthritis Outcome Score 91.2 ± 5.7, no/very low pain) and were measured in the gait lab at least 1 year post-operatively (4.2 ± 3.5 years). This subject-specific data was used as input to guide the kinematics of two independent arms of the joint simulator (described below). Output measurements of the physical rotations actually performed by the simulator then served as ground truth data in order to investigate the accuracy of IMU-based angle derivation.

2.1. Joint Simulator

A six-degrees-of-freedom hydraulically actuated joint simulator (VIVO, AMTI, Watertown, MA), often used for wear testing applications, was selected for use in this study (manufacturer-reported position resolution: <0.1mm, rotation: <0.1°). Displacement mode and the Grood and Suntay joint coordinate system [24] were used to recreate tibial and femoral kinematics of the robotic segments without the influence of the soft-tissue artefact.

To set the reference pose, the upper segment was positioned to correspond with a flexion/extension gimbal arm parallel to the base plate (Figure 2), and ab/adduction actuators at the centre of travel. Meanwhile, the lower segment was centred along both the anteroposterior (AP; Cartesian Y-axis) and mediolateral (Cartesian X-axis) axes, as well as about the int/external rotation actuator axis. Finally, axial translation was set to correspond with an offset of 0 mm from the default (factory-defined) Z position. These axes corresponded to the original subject data captured in the gait laboratory [23]. This specific configuration was set to correspond to the Grood and Suntay translation (0, 0, 0) and angular coordinates (0, 0, 0).

Iterative learning control was enabled on the AP, flexion/extension and int/external rotation axes (gain fractions of 0.5, 0.2 and 0.5, respectively) to ensure that the simulator kinematic pathway accurately replicated the subject joint kinematics. This iterative learning control feature monitors the tracking error, which refers to the difference between the actuator's commands and the actual execution. A compensation signal to minimise this error is generated and applied to the following cycle iteration. Here, the goal was for the compensation signal to rapidly reach equilibrium while avoiding dynamic instability, hence allowing accurate kinematic data to be replicated in the simulator. It was found that by the 50th cycle, all input and output simulator signals had converged (tracking error < 1.0°) and become stable. As a result, cycles of each activity were simulated until the kinematic values for the 50th and 51st iterations could be acquired.
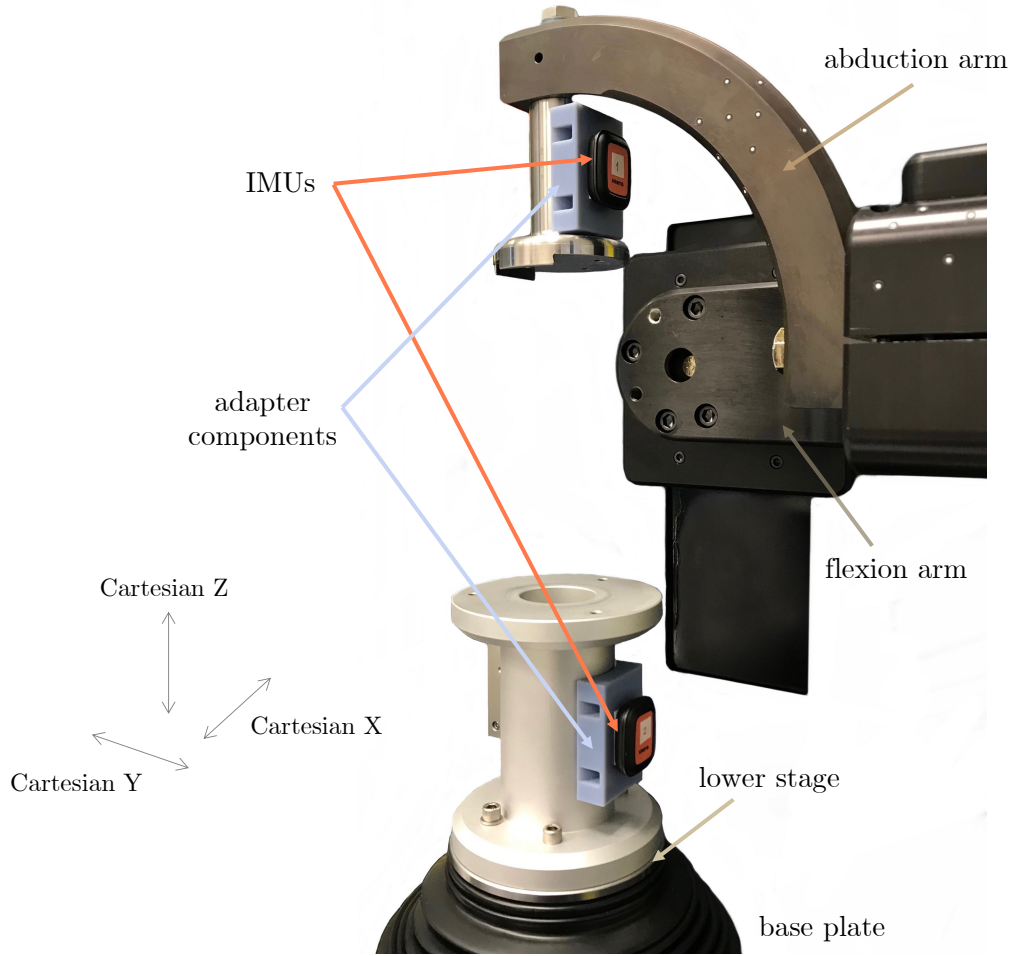
Figure 2. Two inertial sensors were attached to the joint simulator (shown here in reference pose) using mounting adhesive tape: one was attached to the condylar adapter component (top), and the other to the tibial adapter component (bottom). Custom rapid prototype adapters (in blue) were developed to ensure both sensors could be easily adhered onto a flat surface.

Subject-specific kinematic data were made compatible with the simulator coordinate system by expressing rotations of the tibia relative to the femur, as per Grood and Suntay [24]. Standing up and sitting down motions were combined into a single movement by concatenating the respective average signals of each subject in order to ensure a cyclical signal such that the simulator could execute the motion smoothly over multiple iterations. For certain trials in which the subject did not return to their original posture, the kinematic data was smoothed (using De Boor's approach [25] to fit a cubic smoothing spline with a smooth factor of at least 0.5) to remove any jumps in the signal. Here, smoothing was deemed necessary when the simulator failed to complete haptic mapping (an automated process run as part of the iterative learning control feature [26]). Once the necessary smoothing had been applied, kinematic data corresponding to the subject rotations and anteroposterior translations (mean movement pattern of all activity trials) were input (totalling three activities for each of the six subjects). Imported as text files, data were transferred onto the simulator's host PC using a USB flash drive. Here, AP translation and int/external rotation were applied to the tibia, while flexion/extension and ab/adduction were applied to the femur. One cycle iteration was performed per second and sampled at 100 Hz.

2.2. Inertial Motion Sensors

Two Xsens DOT IMUs (Movella, Enschede, Netherlands) were mounted on the simulator using adhesive strips: one on the upper (representing the femoral segment), and one on the lower (representing the tibial segment) adapter (Figure 2). After time synchronisation of the sensors (Xsens DOT software, v2021.0), linear acceleration and angular velocity data were collected at 60 Hz [27, 28] while the simulator performed the kinematic cycles. Data recording was stopped a few seconds after the simulation in order to capture a stationary reference pose.

2.3. IMU-Based Knee Kinematics Estimation

A wide spectrum of algorithms to estimate kinematics based on inertial measurements exist [10, 14]. Upon review, the algorithm implemented by Versteyhe et al. [13] was selected since this computational method relies exclusively on gyroscope and accelerometer measurements. Correction of drift is achieved using an extended Kalman filter and smoother framework (also referred to as a Rauch-Tung-Striebel smoother [29]) in which orientation is parametrised as unit quaternions. In general, the proposed set up requires one IMU sensor to be attached to each of the two limb segments (i.e., thigh, shank). The algorithm relies on a rigid body model that approximates the knee as first a hinge and then a spheroidal joint, such that most rotations occur around one main (flexion/extension) axis, while the algorithm still accounts for small rotations in the other planes. Certain kinematic constraints, [11-13], are implemented in a first stage to optimise estimates of a joint axis and joint centre of rotation. These approximations are fed into the filter as additional input parameters. Using a pseudo-observation approach [30], a series of output constraints [30] is implemented to update model estimates.

The original scripts implemented by Versteyhe et al. [13] and Kresie [21] are openly available as MATLAB m-files (The Mathworks Inc., Natick, USA). Custom MATLAB scripts (vR2021b) based on these works were developed, as well as additional scripts for pre- and post-processing of the data. A fourth order Butterworth filter was applied to the raw inertial signals, with a cut-off frequency of 7 Hz. An offset correction script corrected all timepoints to the reference pose orientation. The resulting waveforms were then normalised to 101 points and plotted as a percentage of one gait cycle.

To temporally synchronise the IMU and simulator data, signal alignment parameters (i.e., the time delay between two input signals) based on the flexion/extension waveforms were estimated using the built-in *alignsignals* function and subsequently used to align all three kinematic curves in time.

2.4. Data Analysis

Knee joint angles were estimated in the sagittal, frontal and transverse planes, corresponding to flexion/extension, ab/adduction and int/external tibial rotation, respectively. Rotational kinematics were plotted and the root-mean-square error (RMSE) between the sensor-estimated kinematics and the simulator-generated ground truth data was assessed over one representative (51st) activity cycle. In addition to RMSE, the maximum absolute error over the assessed representative activity cycle was also computed to more comprehensively judge the magnitude of errors that could potentially occur at a given time point. Finally, Bland-Altman plots [31] were created to establish the agreement (means and differences) between the IMU- and simulator-based kinematics.

3. Results

The collected kinematic data showed the highest levels of accuracy were associated with flexion/extension angles during level walking (Table 1, for subject-specific values see Table A1), with an RMSE below 1.0° for all three rotations (Figure 3). The largest errors in ab/adduction occurred between 60% and 90% of the gait cycle for level walking, and between 40% and 80% for stair descent (Figure 4). In the case of sit-to-stand-to-sit, the highest ab/adduction uncertainties occurred at the beginning and end of the activity cycle, when joint flexion was highest (Figure 5). No clear patterns were recognisable for int/external rotation errors. In general, the flexion/extension rotations were subject to the smallest errors. The largest RMSEs for all three rotations occurred for sit-to-stand-to-sit, with values of 0.9°, 3.1° and 4.8° in the sagittal, frontal and transverse planes, respectively.
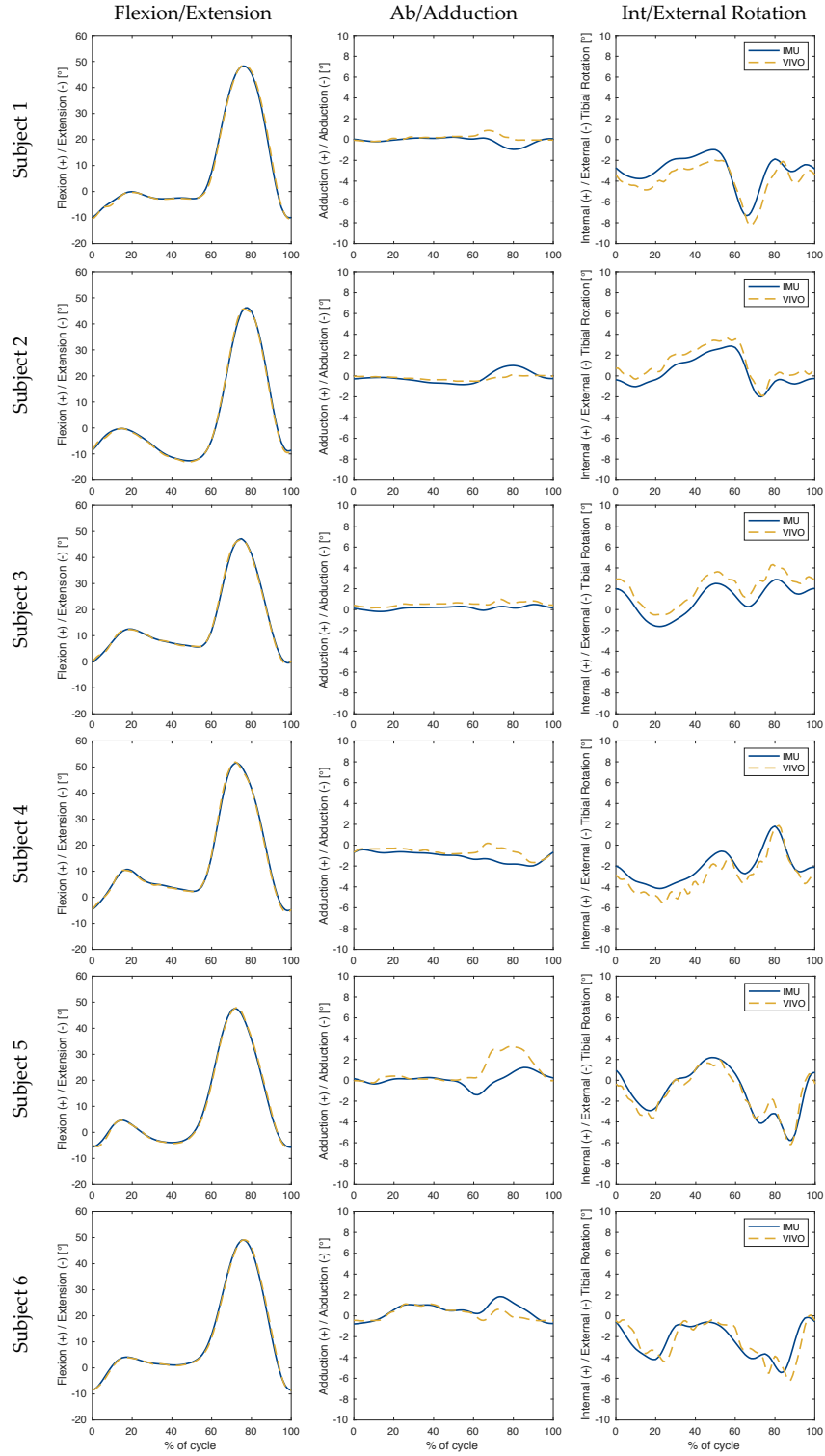
Figure 3. Level Walking: Knee joint angles were plotted over the progression (expressed as a percentage) of one complete gait cycle. The solid blue line illustrates the angles estimated using inertial data. The dashed gold line illustrates the ground truth angles performed by the joint simulator. Each row represents one subject, while each column presents rotations in a different plane relative to the femoral coordinate system.
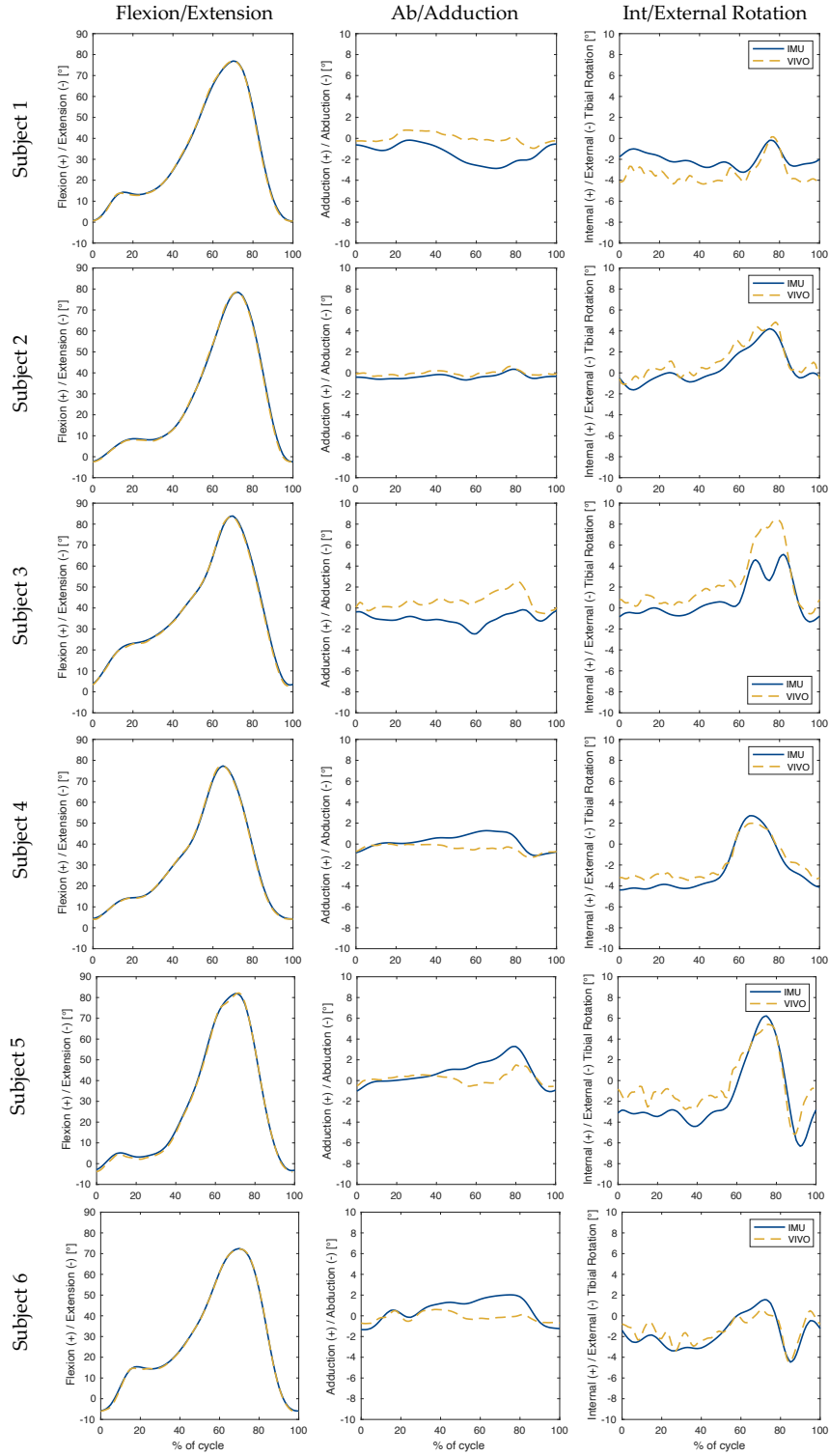
Figure 4. Stair Descent: Knee joint angles were plotted over the progression (expressed as a percentage) of one complete gait cycle. The solid blue line illustrates the angles estimated using inertial data. The dashed gold line illustrates the ground truth angles performed by the joint simulator. Each row represents one subject, while each column presents rotations in a different plane relative to the femoral coordinate system.
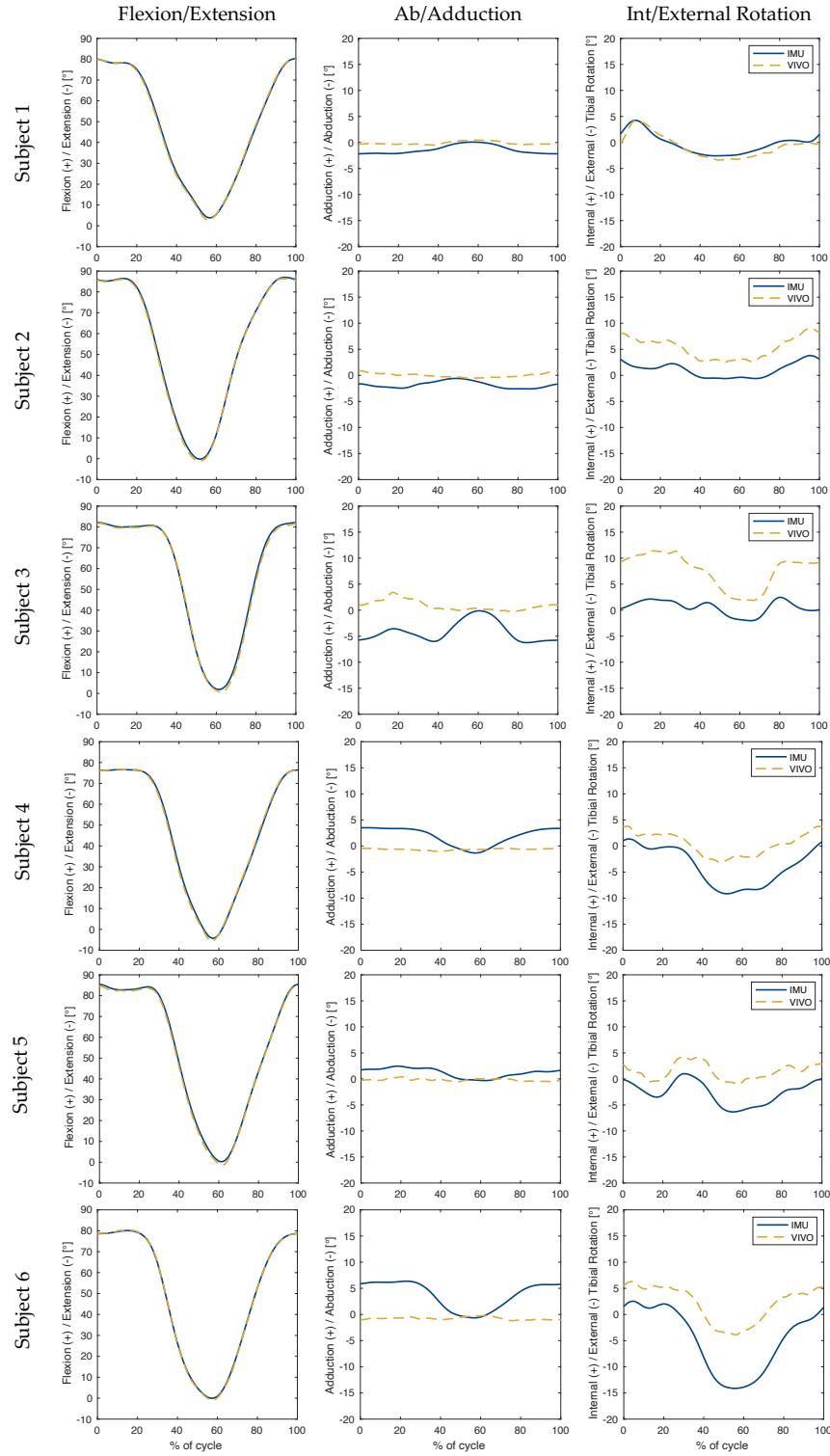
Figure 5. Sit-to-Stand-to-Sit Sequence: Knee joint angles were plotted over the progression (expressed as a percentage) of one complete gait cycle. The solid blue line illustrates the angles estimated using inertial data. The dashed gold line illustrates the ground truth angles performed by the joint simulator. Each row represents one subject, while each column presents rotations in a different plane relative to the femoral coordinate system.

Table 1. Root-mean-square error (in degrees) between sensor-estimated kinematics and simulator-generated ground truth data was calculated over one cycle of every activity, for each of the six subjects. Results are summarised by expressing mean RMSE, ±1 standard deviation, over all subjects, for each of the three planes of rotation.

|	Flexion/Extension	Ab/Adduction	Int/External Rotation
Level Walking	0.7 ± 0.1	0.6 ± 0.3	0.9 ± 0.2
Stair Descent	0.7 ± 0.2	1.2 ± 0.5	1.3 ± 0.5
Sit-to-Stand-to-Sit	0.9 ± 0.3	3.1 ± 1.9	4.8 ± 2.5

Maximum absolute errors for all subjects in the sagittal plane ranged between 1.0° and 2.7° (Table 2, for subject-specific values see Table A2). In the frontal plane, they fell between 0.4° and 7.0°, while errors in the transverse plane ranged from 1.2° to 10.8°. Peak errors for a given plane and activity ranged from 1.6° (sagittal plane in stair descent) to 10.8° (transverse plane in sit-to-stand-to-sit).

Table 2. Maximum absolute errors (in degrees) between sensor-estimated kinematics and simulator-generated ground truth data over all subjects, for every activity type, and each of the three planes of rotation.

	Flexion/Extension	Ab/Adduction	Int/External Rotation
Level Walking	2.3	3.2	2.6
Stair Descent	1.6	3.0	5.2
Sit-to-Stand-to-Sit	2.7	7.0	10.8

Bland-Altman plots revealed that high levels of agreement existed between the IMU and simulator kinematics (Figure A1, Figure A2 and Figure A3). On average, the two approaches differed by 0.5° and presented a mean two-tailed 95% confidence interval of ±2.8°, including results which did not fulfil the assumption of normality (based on a Lilliefors test [32] at 5% significance level). When such cases were excluded, an average difference of 0.2° and a mean confidence interval of ±1.3° was observed.

4. Discussion

Validation of IMU algorithms for estimating joint kinematics is critical before sensor systems can be robustly implemented in clinical settings. In this study, we propose and test a framework for validating sensor technology using a joint simulator to assess the accuracy of IMU-derived joint angles. The simulator was driven using subject-specific data to recreate real kinematic profiles, unaffected by soft-tissue artefact. Operation of the robotic simulator using Grood and Suntay, instead of Cartesian, coordinate systems, has specifically allowed simplification of the data harmonisation process and interpretation of the resulting kinematic curves. The simulator approach presented here can therefore act as a reference standard with which to generate realistic kinematics and assess the accuracy of different sensor systems and algorithms to capture real-world movement patterns.

Demonstration of this framework was achieved using a computational approach previously presented by Seel et al. [11, 12] and later enhanced by Versteyhe et al. [13]. Our results reveal that this algorithm exhibited high average accuracy (RMSE ≤0.9°, maximum absolute errors ≤3.2°) for all three rotations during level walking. This was in line with previous studies [13] in which IMUs were strapped to two segments of a robotic arm, where the segments represented the femur and tibia. In their study, the femur remained fixed in space, while the tibia was programmed to move. They reported quaternion values of the tibial segment in a global reference frame in a comparison against the robotic arm data. Our framework has been able to build on these preliminary findings by implementing a joint simulator setup in which both femoral and tibial segment analogues rotated (and even translated along one axis). This setup has therefore enabled us to compare the joint angle estimates obtained by calculating the relative pose between limb segments, in a scenario in which both segments rotated relative to a global reference frame. Furthermore, our framework allows the complete three-dimensional reconstruction of measured subject-specific knee joint kinematics. By applying the method of Versteyhe et al. to activities other than level walking, it has been possible to assess the accuracy of IMU analysis during a range of functional activities of daily living.

Based on RMSEs, the IMU-based joint angle estimates were most accurate during level walking. Results during stair descent were slightly inferior, followed by sit-to-stand-to-sit. Similar trends were observed in maximum error values, where level walking was once again subject to the smallest peak errors, while maximum absolute errors during sit-to-stand-to-sit increased to over twice those of other activities. This trend may be a reflection of the algorithm's underlying assumptions, which are based around applications comprising straight line walking. Here, the joint flexion angles involved in stair descent deviate only slightly from level walking, where both activities exhibit stance and swing phases, with motion advancing in a straight line by alternating movements of the lower limbs. Sit-to-stand-to-sit, on the other hand, lacks a swing phase and does not involve progressive displacement of the lower limbs relative to the ground. This activity is therefore associated with the greatest deviations from the modelling assumptions, hence providing a plausible explanation for the highest measured errors (Figure 3, Figure 4 and Figure 5).

It is clear that out-of-sagittal-plane rotations were subject to the largest errors across all activities. Moreover, visual inspection of the simulator versus IMU kinematics (especially the first two columns of Figure 3, Figure 4 and Figure 5), suggest a correlation between the magnitude of flexion angles and errors in ab/adduction. This association is indicative of cross-talk, which describes how differences in knee mediolateral axis alignment can lead to an artificial increase in the amplitude of ab/adduction angles [33], and additionally propagate to affect int/external rotation angles. Subsequent work should therefore involve a more in-depth assessment of the accuracy of the orientation of the joint

(flexion/extension) axis identified by the inertial data, as compared to that defined by the simulator. Furthermore, a more detailed analysis of the nature of the apparent relationship between flexion magnitude and out-of-sagittal-plane rotation errors should be performed. Any such investigation should specifically take into account the problematic lack of consensus surrounding joint segment frame definition.

A review by McGinley et al. [34] concluded that errors in excess of 5° should be avoided in gait analysis to prevent incorrectly guiding clinical decision-making. The advantage of approaching analytical validation of IMU-based gait analysis systems in the framework presented here is that we can conclusively establish whether the underlying technology and computational model for joint angle estimation is able to attain results with mean RMSEs that fall within this 5° window. However, in vivo applications will undoubtedly be additionally affected by soft-tissue artefact, which is likely to compound the model's uncertainty to exceed this 5° threshold (especially for out-of-sagittal plane rotations in activities such as sit-to-stand-to-sit). Quantification of the errors associated with soft-tissue artefact is beyond the scope of this investigation, but has been addressed by other works [20, 35, 36]. Minimisation of these uncertainties is known to be challenging and affected by a number of variables, including activity type, movement speed, and subject anatomical characteristics [37]. Nevertheless, the clear advantage offered by the proposed IMU solution is the insensitivity of the approach to sensor placement, which can be leveraged to minimise the effects of soft-tissue artefact [38]. As a result, having established the accuracy of the underlying biomechanical model and its associated assumptions, subsequent work can specifically address soft-tissue artefact and explore promising methods for tackling it.

Although intermittently disrupted by large peak errors (Table 2), the assessed algorithm for IMU-based joint estimation (mainly selected for use in this study due to its flexibility in sensor placement) demonstrated good average accuracy over the assessed activities. Nonetheless, RMSEs of up to 7.5° for individual subjects suggest that the algorithm still requires further enhancement to ameliorate the errors affecting out-of-sagittal plane rotations during activities besides level walking (e.g., by modelling additional constraints imposed by the ankle joint during sit-to-stand-to-sit). Moreover, from a clinical perspective, errors of 7.5° could also critically lead to a different interpretation of joint functionality, particularly if this addresses ab/adduction or int/external rotation. As a result, there is a critical requirement to further develop approaches to mitigate cross-talk in kinematic datasets. Other methods that have attempted to quantify human joint kinematics using IMU technology have utilised different filter implementations [39, 40], sensor fusion methods [12, 40] and biomechanical models [14] to address drift and attain accurate movement patterns. While the algorithm implemented here is only one of many different approaches to joint angle estimation based on inertial data, the presented framework allows for a standard assessment and comparison of similar solutions.

While the use of a six-degrees-of-freedom joint simulator offered advantages over alternative validation techniques, it was not impervious to limitations. Notably, in a clinical context, both joint segments would be free to move in all degrees of freedom. In the simulator used in our framework, however, all translations, as well as rotations around the longitudinal axis, were performed by the bottom segment, while the remaining two rotations were executed by manipulating the upper femoral segment. These complex kinematic interactions pose a challenge to the algorithm when estimating the motions of the simulator, as only one of the sensors measures active rotational information that is valuable for assessing the model. In a clinical context, the availability of inertial data from both sensors can be fused to produce more accurate joint angle estimates, hence improving system performance rather than hindering it. An additional challenge arose from the boundaries of the simulator's physical range of motion. For our particular set up and reference pose combination, maximum flexion was capped at 85.0°.

During our study, Subject 5 reached 89.4° of flexion during sit-to-stand-to-sit, hence requiring kinematic data to be cropped. However, in general, our framework has demonstrated suitability for recreating real-word kinematic data as a setup for testing IMU algorithm accuracy.

The algorithm for IMU-based joint angle estimation employed in this study relied on Rauch-Tung-Striebel smoothing, an extension of Kalman filtering approaches. Here, filter parameters were defined based on sensor manufacturer specifications and manually tuned by visually inspecting the innovation term for zero mean and no correlation between parameters. In order for the technology to be feasibly scalable, parameter tuning should be performed systematically, repeatably and reliably. As a result, it is crucial that any system that uses a Kalman-type-filter, clearly and transparently reports an associated reproducible method for parameter tuning. This seems by no means to be the norm in the relevant literature published thus far, and is an aspect future investigations are encouraged to address more clearly.

In conclusion, quantifying the inherent error of a given algorithm that estimates joint kinematics from inertial data is a pivotal step in establishing an accurate, yet affordable, and mobile solution to knee kinematic assessment. By quantifying accuracy prior to the introduction of soft-tissue artefact, valuable insights into sources of error can be gained, enabling researchers to better compare the performance of different IMU-based solutions, particularly in light of the challenge posed by cross-talk. The framework presented in this study thus offers a straightforward approach to test inertial-sensor-based systems, and to determine the suitability of the underlying biomechanical models and the limitations of their assumptions. Successful development and adoption of such a system would have widespread clinical implications: By enabling gait analysis to become a regular part of the TKA treatment and rehabilitation workflow, it could help healthcare experts gain insights into the biomechanical mechanisms contributing to patient (dis)satisfaction.

Author Contributions

Funding

Data Availability Statement

Datasets used for this study are included in Schütz et al. (2019) [23].

Acknowledgements

Conflicts of Interest

References

1. Robertsson, O., Dunbar, M., Pehrsson, T., Knutson, K., and Lidgren, L., *Patient satisfaction after knee arthroplasty: a report on 27,372 knees operated on between 1981 and 1995 in Sweden.* Acta Orthopaedica Scandinavica, 2000. **71**(3): p. 262-267.
2. Baker, P.N., Van Der Meulen, J.H., Lewsey, J., and Gregg, P.J., *The role of pain and function in determining patient satisfaction after total knee replacement. Data from the National Joint Registry for England and Wales.* Journal of Bone and Joint Surgery, 2007. **89**(7): p. 893-900.
3. Bourne, R.B., Chesworth, B.M., Davis, A.M., Mahomed, N.N., and Charron, K.D., *Patient satisfaction after total knee arthroplasty: who is satisfied and who is not?* Clinical Orthopaedics and Related Research, 2010. **468**(1): p. 57-63.
4. Schulze, A. and Scharf, H., *Zufriedenheit nach Knietotalendoprothesenimplantation.* Der Orthopäde, 2013. **42**(10).
5. Noble, P.C., Conditt, M.A., Cook, K.F., and Mathis, K.B., *The John Insall Award: Patient expectations affect satisfaction with total knee arthroplasty.* Clinical Orthopaedics and Related Research, 2006. **452**: p. 35-43.
6. Hirschmann, M.T. and Behrend, H., *Functional knee phenotypes: a call for a more personalised and individualised approach to total knee arthroplasty?* 2018. **26**: p. 2873-2874.
7. Favre, J. and Jolles, B.M., *Gait analysis of patients with knee osteoarthritis highlights a pathological mechanical pathway and provides a basis for therapeutic interventions.* EFORT Open Reviews, 2016. **1**(10): p. 368-374.
8. List, R., Postolka, B., Schütz, P., Hitz, M., Schwilch, P., Gerber, H., Ferguson, S.J., and Taylor, W.R., *A moving fluoroscope to capture tibiofemoral kinematics during complete cycles of free level and downhill walking as well as stair descent.* PLOS One, 2017. **12**(10): p. e0185952.
9. Guan, S., Gray, H.A., Keynejad, F., and Pandy, M.G., *Mobile Biplane X-Ray Imaging System for Measuring 3D Dynamic Joint Motion During Overground Gait.* IEEE Trans Med Imaging, 2016. **35**(1): p. 326-336.
10. Vitali, R.V. and Perkins, N.C., *Determining anatomical frames via inertial motion capture: A survey of methods.* Journal of Biomechanics, 2020. **106**: p. 109832.
11. Seel, T., Schauer, T., and Raisch, J. *Joint axis and position estimation from inertial measurement data by exploiting kinematic constraints.* in *2012 IEEE International Conference on Control Applications.* 2012. IEEE.
12. Seel, T., Raisch, J., and Schauer, T., *IMU-based joint angle measurement for gait analysis.* Sensors, 2014. **14**(4): p. 6891-6909.

13.   Versteyhe, M., De Vroey, H., Debrouwere, F., Hallez, H., and Claeys, K., *A Novel Method to Estimate the Full Knee Joint Kinematics Using Low Cost IMU Sensors for Easy to Implement Low Cost Diagnostics.* Sensors, 2020. **20**(6).

14.   Weygers, I., Kok, M., Konings, M., Hallez, H., De Vroey, H., and Claeys, K., *Inertial Sensor-Based Lower Limb Joint Kinematics: A Methodological Systematic Review.* Sensors, 2020. **20**(3).

15.   Pacher, L., Chatellier, C., Vauzelle, R., and Fradet, L., *Sensor-to-segment calibration methodologies for lower-body kinematic analysis with inertial sensors: A systematic review.* Sensors, 2020. **20**(11): p. 3322.

16.   Goldsack, J.C., Coravos, A., Bakker, J.P., Bent, B., Dowling, A.V., Fitzer-Attas, C., Godfrey, A., Godino, J.G., Gujar, N., and Izmailova, E., *Verification, analytical validation, and clinical validation (V3): the foundation of determining fit-for-purpose for Biometric Monitoring Technologies (BioMeTs).* npj Digital Medicine, 2020. **3**(1): p. 55.

17.   Takeda, R., Tadano, S., Natorigawa, A., Todoh, M., and Yoshinari, S., *Gait posture estimation using wearable acceleration and gyro sensors.* Journal of Biomechanics, 2009. **42**(15): p. 2486-2494.

18.   Robert-Lachaine, X., Parent, G., Fuentes, A., Hagemeister, N., and Aissaoui, R., *Inertial motion capture validation of 3D knee kinematics at various gait speed on the treadmill with a double-pose calibration.* Gait & Posture, 2020. **77**: p. 132-137.

19.   Mcgrath, T. and Stirling, L., *Body-worn IMU-based human hip and knee kinematics estimation during treadmill walking.* Sensors, 2022. **22**(7): p. 2544.

20.   Taylor, W.R., Ehrig, R.M., Duda, G.N., Schell, H., Seebeck, P., and Heller, M.O., *On the influence of soft tissue coverage in the determination of bone kinematics using skin markers.* Journal of Orthopaedic Research, 2005. **23**(4): p. 726-734.

21.   Kresie, S.W.-J., *Development and Evaluation of an IMU-Based Wearable Device for ACL Injury Research.* 2021, University of California, Davis.

22.   Chiang, C.-Y., Chen, K.-H., Liu, K.-C., Hsu, S.J.-P., and Chan, C.-T., *Data collection and analysis using wearable sensors for monitoring knee range of motion after total knee arthroplasty.* Sensors, 2017. **17**(2): p. 418.

23.   Schütz, P., Postolka, B., Gerber, H., Ferguson, S.J., Taylor, W.R., and List, R., *Knee implant kinematics are task-dependent.* Journal of the Royal Society Interface, 2019. **16**(151): p. 20180678.

24.   Grood, E.S. and Suntay, W.J., *A joint coordinate system for the clinical description of three-dimensional motions: application to the knee.* Journal of Biomechanical Engineering, 1983. **105**(2): p. 136-144.

25.   De Boor, C., *A practical guide to splines.* Vol. 27. 1978: springer-verlag New York.

26.   Advanced Mechanical Technology Inc., *VIVO Control Technical Reference, Version 1.0.0.* 2015, AMTI: Watertown, MA, USA.

27.   Zhou, L., Fischer, E., Tunca, C., Brahms, C.M., Ersoy, C., Granacher, U., and Arnrich, B., *How we found our IMU: Guidelines to IMU selection and a comparison of seven IMUs for pervasive healthcare applications.* Sensors, 2020. **20**(15): p. 4090.

28.   Stergiou, N., *Biomechanics and gait analysis.* 2020, Academic Press: London: UK.

29.   Rauch, H.E., Tung, F., and Striebel, C.T., *Maximum likelihood estimates of linear dynamic systems.* AIAA journal, 1965. **3**(8): p. 1445-1450.

30.   Doran, H.E., *Constraining Kalman filter and smoothing estimates to satisfy time-varying restrictions.* The Review of Economics and Statistics, 1992: p. 568-572.

31.   Bland, J.M. and Altman, D., *Statistical methods for assessing agreement between two methods of clinical measurement.* The Lancet, 1986. **327**(8476): p. 307-310.

32.   Lilliefors, H.W., *On the Kolmogorov-Smirnov test for normality with mean and variance unknown.* Journal of the American statistical Association, 1967. **62**(318): p. 399-402.

33.   Naaim, A., Bonnefoy-Mazure, A., Armand, S., and Dumas, R., *Correcting lower limb segment axis misalignment in gait analysis: A simple geometrical method.* Gait & Posture, 2019. **72**: p. 34-39.

34.   Mcginley, J.L., Baker, R., Wolfe, R., and Morris, M.E., *The reliability of three-dimensional kinematic gait measurements: A systematic review.* Gait & Posture, 2009. **29**(3): p. 360-369.

35.   Akbarshahi, M., Schache, A.G., Fernandez, J.W., Baker, R., Banks, S., and Pandy, M.G., *Non-invasive assessment of soft-tissue artifact and its effect on knee joint kinematics during functional activity.* Journal of Biomechanics, 2010. **43**(7): p. 1292-1301.

36.   Ancillao, A., Aertbeliën, E., and De Schutter, J., *Effect of the soft tissue artifact on marker measurements and on the calculation of the helical axis of the knee during a gait cycle: A study on the CAMS-Knee data set.* Human Movement Science, 2021. **80**: p. 102866.

37.   Peters, A., Galna, B., Sangeux, M., Morris, M., and Baker, R., *Quantification of soft tissue artifact in lower limb human motion analysis: a systematic review.* Gait & Posture, 2010. **31**(1): p. 1-8.

38.   Kratzenstein, S., Kornaropoulos, E.I., Ehrig, R.M., Heller, M.O., Pöpplau, B.M., and Taylor, W.R., *Effective marker placement for functional identification of the centre of rotation at the hip.* Gait & Posture, 2012. **36**(3): p. 482-486.

39.   Al Borno, M., O'day, J., Ibarra, V., Dunne, J., Seth, A., Habib, A., Ong, C., Hicks, J., Uhlrich, S., and Delp, S., *OpenSense: An open-source toolbox for inertial-measurement-unit-based measurement of lower extremity kinematics over long durations.* Journal of NeuroEngineering and Rehabilitation, 2022. **19**(1): p. 1-11.

40.   Weygers, I., Kok, M., De Vroey, H., Verbeerst, T., Versteyhe, M., Hallez, H., and Claeys, K., *Drift-free inertial sensor-based joint kinematics for long-term arbitrary movements.* IEEE Sensors Journal, 2020. **20**(14): p. 7969-7979.

5. Supplementary Material

Table A1. Root-mean-square error (in degrees) between sensor-estimated kinematics and simulator-generated ground truth data, throughout a representative activity cycle. Results are shown for all six subjects, for every activity type, in each of the three rotation planes. (F/E = flexion/extension; A/A = adduction/abduction; I/E = internal/external tibial rotation).

	Level Walking			Stair Descent			Sit-to-Stand-to-Sit		
	F/E	A/A	I/E	F/E	A/A	I/E	F/E	A/A	I/E
Subject 1	0.9	0.5	1.0	0.7	1.6	1.5	0.8	1.4	0.8
Subject 2	0.7	0.4	0.8	0.7	0.3	0.8	0.9	2.0	4.3
Subject 3	0.5	0.4	1.1	0.8	1.9	1.9	1.2	5.5	7.5
Subject 4	0.7	0.7	1.0	0.6	0.9	0.8	1.0	3.0	4.6
Subject 5	0.7	1.3	0.7	0.9	1.2	1.8	1.0	1.4	4.2
Subject 6	0.7	0.6	1.0	0.4	1.2	0.8	0.4	5.2	7.5

Table A2. Maximum absolute error (in degrees) between sensor-estimated kinematics and simulator-generated ground truth data over the same previously analysed cycle. Results are shown for all six subjects, for every activity type, in each of the three rotation planes. (F/E = flexion/extension; A/A = adduction/abduction; I/E = internal/external tibial rotation).

	Level Walking			Stair Descent			Sit-to-Stand-to-Sit		
	F/E	A/A	I/E	F/E	A/A	I/E	F/E	A/A	I/E
Subject 1	2.3	1.1	2.1	1.6	2.7	2.6	1.5	1.9	1.8
Subject 2	1.4	1.0	1.2	1.6	0.4	1.4	1.8	2.7	5.5
Subject 3	1.4	0.7	1.7	1.6	3.0	5.2	2.7	7.0	9.9
Subject 4	1.8	1.5	1.9	1.2	1.7	1.2	2.2	4.0	7.0
Subject 5	1.4	3.2	1.5	1.6	2.5	3.8	1.9	2.3	5.9
Subject 6	1.9	1.4	2.6	1.3	2.1	1.6	1.0	7.0	10.8
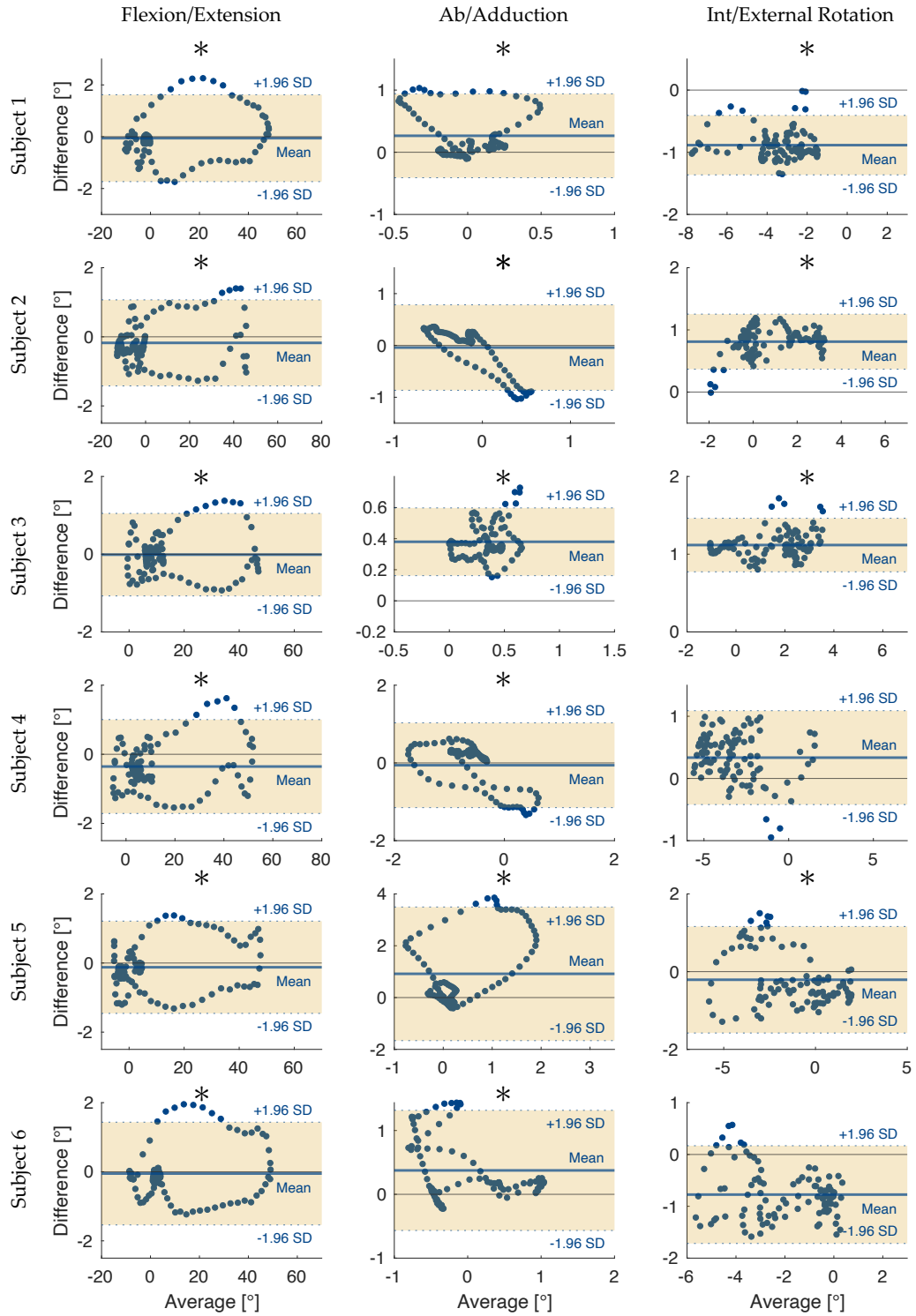
Figure A1. Bland-Altman plots for level walking. Differences between simulator- and IMU-based estimates were plotted against the average of the two measures. Shaded areas denote two-tailed 95% confidence intervals while dotted blue lines represent limits of agreement and solid blue lines show the mean difference. Each row corresponds to a different subject; each column to a different plane of rotation. Inclusion of an asterisk indicates the assumption of normality was not fulfilled.
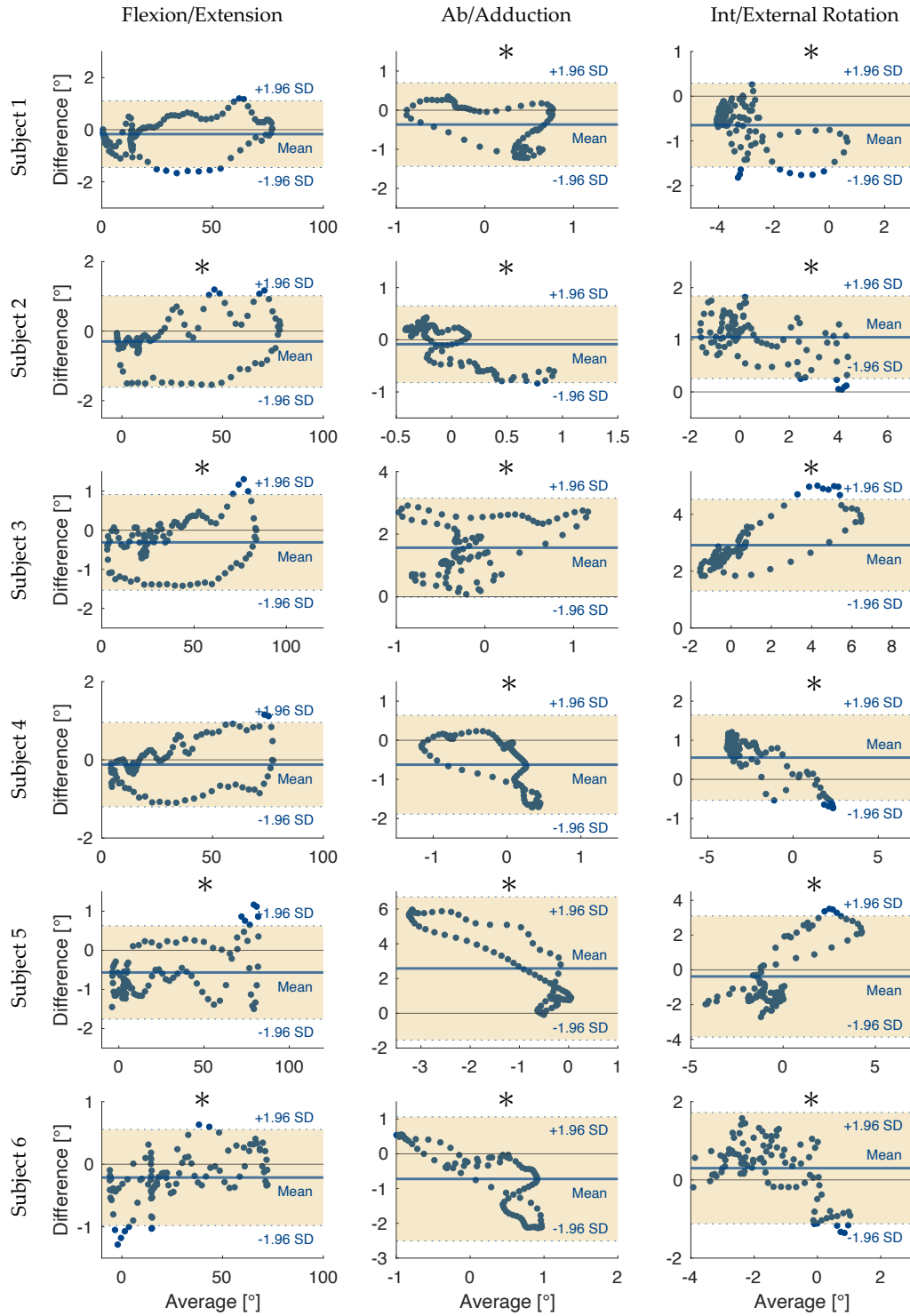
Figure A2. Bland-Altman plots for stair descent. Differences between simulator- and IMU-based estimates were plotted against the average of the two measures. Shaded areas denote two-tailed 95% confidence intervals while dotted blue lines represent limits of agreement and solid blue lines show the mean difference. Each row corresponds to a different subject; each column to a different plane of rotation. Inclusion of an asterisk indicates the assumption of normality was not fulfilled.
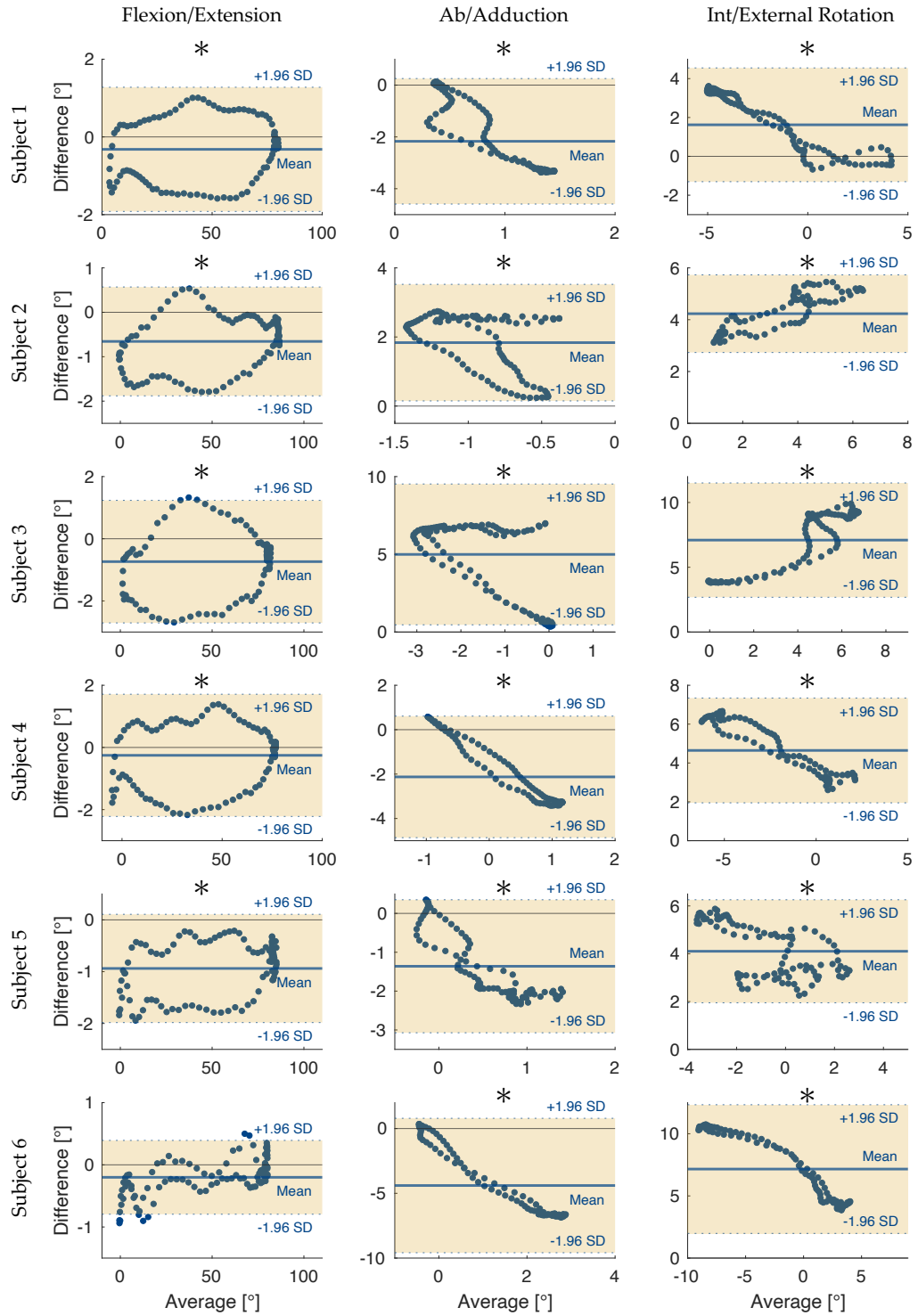
Figure A3. Bland-Altman plots for sit-to-stand-to-sit. Differences between simulator- and IMU-based estimates were plotted against the average of the two measures. Shaded areas denote two-tailed 95% confidence intervals while dotted blue lines represent limits of agreement and solid blue lines show the mean difference. Each row corresponds to a different subject; each column to a different plane of rotation. Inclusion of an asterisk indicates the assumption of normality was not fulfilled.

III. Journal Publication II

A frame orientation optimisation method for consistent interpretation of kinematic signals

Ortigas-Vásquez, A., Taylor, W.R., Maas, A., Woiczinski, M., Grupp, T.M. and Sauer A.

Abstract

In clinical movement biomechanics, kinematic data are often depicted as waveforms (i.e. signals), characterising the motion of articulating joints. Clinically meaningful interpretations of the underlying joint kinematics, however, require an objective understanding of whether two different kinematic signals actually represent two different underlying physical movement patterns of the joint or not. Previously, the accuracy of IMU-based knee joint angles was assessed using a six-degrees-of-freedom joint simulator guided by fluoroscopy-based signals. Despite implementation of sensor-to-segment corrections, observed errors were clearly indicative of cross-talk, and thus inconsistent reference frame orientations. Here, we address these limitations by exploring how minimisation of dedicated cost functions can harmonise differences in frame orientations, ultimately facilitating consistent interpretation of articulating joint kinematic signals.

In this study, we present and investigate a frame orientation optimisation method (FOOM) that aligns reference frames and corrects for cross-talk errors, hence yielding a consistent interpretation of the underlying movement patterns. By executing optimised rotational sequences, thus producing angular corrections around each axis, we enable a reproducible frame definition and hence an approach for reliable comparison of kinematic data. Using this approach, root-mean-square errors between the previously collected (1) IMU-based data using functional joint axes, and (2) simulated fluoroscopy-based data relying on geometrical axes were almost entirely eliminated from an initial range of 0.7°–5.1° to a mere 0.1°–0.8°. Our results confirm that different local segment frames can yield different kinematic patterns, despite following the same rotation convention, and that appropriate alignment of reference frame orientation can successfully enable consistent kinematic interpretation.

Keywords: kinematics; cross-talk; optimisation; knee joint; gait analysis; joint coordinate system; local reference frame; IMU

1. Introduction

The development of an affordable and mobile alternative to current state-of-the-art gait analysis systems (such as marker-based or markerless optical motion capture, and static or moving videofluoroscopy [1, 2]) could allow experts to better incorporate objective assessment of patient function into daily clinical practice. Most notably, the accurate estimation of rotational knee kinematics from inertial measurement units (IMUs) has received considerable attention in recent years [3]. Assessing these technologies to establish which approaches are able to provide a correct interpretation of the underlying kinematics requires their accuracy to be evaluated.

In clinical movement biomechanics, kinematics can be plotted to characterise joint motion over time. Two (or more) of these signals are then often compared to determine whether significant differences in kinematic patterns are associated with, for example, different pathologies [4, 5], disease stages [6, 7], treatment strategies [8, 9], or measurement systems [10-12] . In previous work, inertial-based knee kinematic estimates were compared against ground truth data generated by a calibrated joint simulator, using an analytical approach that allowed flexibility in the orientation of the sensor placement on the joint segments [13]. By assuming that the simulator output represented a true and correct measurement of the joint kinematics, the accuracy of the IMU estimates was quantified by calculating the root-mean-square error (RMSE) and maximum absolute error. This comparison relied on the fundamental assumption that the kinematics originating from each source (IMU-based system and robotic joint simulator) could be directly compared and would ideally be identical, therefore producing a consistent interpretation of the underlying movement patterns. This previous work demonstrated that accuracies (RMSEs) in the ranges of 0.4°-1.2°, 0.3°-5.5° and 0.7°-7.5° for angles in the sagittal, frontal, and transverse planes respectively, could be achieved using a model-based method to derive rotational knee kinematics from IMU data [13]. However, given that the testing scenario did not include deviations due to soft tissue movement, the observed level of errors was thought to be insufficient to reliably support clinical decision-making. Since the underlying segment kinematics were fundamentally the same, it is entirely plausible that the observed errors result from differences in the reference frames. Although this concept is well appreciated in the field of movement science, the practical implementation of consistent reference frames, especially when using IMU technology, has remained almost impossible.

When presenting any set of kinematic data, the associated coordinate frames of the individual joint segments *must* be clearly defined. In general, each body segment is assigned a three-dimensional (3D) Cartesian coordinate system. For rotational kinematics, this coordinate frame definition should, at a minimum, describe how the exact orientation of each of the three axes is determined. In cases where translational data is also included, each segment's coordinate frame should be complemented by an explanation of how the location of the frame's origin is established. Critical problems arise when these core requirements fail to be met. This failure commonly stems from a lack of consensus in the understanding and interpretation of approaches [14]. The popular Grood and Suntay Joint Coordinate System (JCS) was initially presented as non-orthogonal and sequence independent [15]. In practice, use of the JCS to describe e.g. knee kinematics is equivalent to individually assigning the femur and tibia a right-handed 3D Cartesian frame, and calculating a Cardan sequence describing the orientation of the distal (tibial) frame relative to the proximal (femoral) frame. This transformation follows an intrinsic sequence of rotations analogous to what would be clinically construed as: 1) flexion/extension, 2) adduction/abduction, and 3) internal/external rotation. In fact, the mathematical proof substantiating this interpretation has been previously reported, demonstrating the JCS to be both sequence dependent and orthogonal [16, 17]. These controversies have contributed to confusion surrounding the

definition of joint reference frames. Statements such as "kinematics were calculated according to Grood and Suntay" have unfortunately become commonplace, but insufficient if not accompanied by unambiguous details. A multitude of variations in the definition of tibiofemoral frames alone can be observed in the literature, even among those explicitly citing Grood and Suntay [14, 18].

Movement scientists attempt to standardise measurements of motion by using reliable anatomical or functional landmarks. However, different approaches used to analyse consistent kinematics have shown to result in considerably different interpretations of the joint motion [14, 19]. In fact, the authors of this work strongly suggest that cross-talk between the different analysis approaches produces the large errors observed, and are therefore the underlying source of the very different interpretations. Cross-talk itself is a phenomenon whereby the alignment of the local segment coordinate system allows the rotation around one axis to be mixed-up with rotations around the others (see Supplementary Figure S1 for an illustration of this effect). As a result, the measured rotations around each axis heavily depend upon the orientation of the chosen coordinate systems and to date assessment of motion patterns remains insufficiently reliable to support clinical decision-making.

To mitigate this problem, previous studies have explored methods of post-processing kinematic data to eliminate cross-talk. Woltring considered reducing cross-talk by transforming local segment frames so that ab/adduction or both ab/adduction and int/external rotation were zeroed at maximum flexion [20]. From a clinical perspective, however, the inherent assumption that there must be no ab/adduction and/or int/external rotation at maximum knee flexion of a gait cycle is questionable. Baker and co-workers, on the other hand, minimised ab/adduction variance, under the assumption that medio-lateral stability could be approximated as a hinge [21], and therefore any variation in marker-based ab/adduction measurements was a likely result of thigh marker misplacement [22]. Rivest addressed cross-talk by transforming local segment frames to minimise the quadratic variation of ab/adduction and int/external rotation, but only applied the transformations in a weighted manner to minimise between-subject variability [23]. Cross-talk reduction thus depended on the assessed subject population, and post hoc inclusion of any additional participants would require complete recalculation of all subjects' kinematics. Furthermore, for a given subject's trial, the analysis could lead to different kinematic values, simply by being processed as part of different cohorts.

More recently, Baudet and co-workers proposed a cross-talk correction method based on principal component analysis, whereby variables were linearly transformed to eliminate correlations and minimise ab/adduction variance [24]. The authors concluded that the "correction method eliminated the presence of knee joint angle cross-talk, as proved by mean r^2 values close to 0 for the left and right side after correction", where r was the correlation coefficient between flexion/extension and ab/adduction. While r can be used as a descriptive measure of the *linear* association between two variables [25], sensitivity analyses have shown that the relationship between flexion/extension and cross-talk artefact out of the sagittal plane is not linear (Supplementary Figure S1) [26]. By extension, the assumption that cross-talk is equivalent to the linear relationship between flexion/extension and ab/adduction (rather than ab/adduction *error*) is an inherently misleading oversimplification. Furthermore, even if this linearity approximation were justified by limiting analyses to a confined range of knee flexion (i.e. where the relationship could be considered to be linear), r^2 has repeatedly been criticised for being misinterpreted and confused with R^2 (the coefficient of determination) [27, 28]. While numerically equivalent to r^2 under specific conditions, the idea that an R^2 value close to zero indicates that two variables are not related is incorrect. Reducing r^2 (or R^2) between flexion/extension and ab/adduction to zero is therefore not the same as eliminating cross-talk. Moreover, Baudet and co-workers also justified the minimisation of ab/adduction variance by suggesting that previous cadaveric studies had managed to

measure the knee's physiological range of motion (ROM), and this range was small in ab/adduction [29]. This argument ignored the fact that, of all three reported rotations, ab/adduction was likely affected by the largest errors. Importantly, these ab/adduction measurements must have been associated with a set of local segment frames that were themselves susceptible to cross-talk, making it impossible to assume they unequivocally represent the joint's true physiological ROMs.

A new perspective on knee kinematics is therefore critically necessary; one that recognises that any muculoskeletal kinematic measurement is the result of a series of *choices* designed to help us empirically characterise the highly complex 3D and time-dependent motion of an articulating joint. The fact that some of these choices may be more intuitive than others does not imply they are inherently *correct* or *incorrect*. Without the ability to reference values of some known true physiological joint motion, the following question arises: Given sets of kinematic data, can a consistent interpretation of the underlying movement patterns be achieved, independent of the analysis approach used? Answering this question is of critical importance in order to allow a standardised understanding of whether joint movement patterns are fundamentally similar or different, and therefore reliably support clinical decision-making. In this study, we directly address this challenging question by considering a Frame Orientation Optimisation Method (FOOM) that aligns reference frame orientations and corrects for cross-talk errors between kinematic signals derived using two different analysis approaches, with the goal to produce a consistent interpretation of the underlying articulating joint movement patterns.

2. Methods

In this study, we present and investigate a Frame Orientation Optimisation Method that ensures consistent reference frame orientations and corrects for cross-talk errors in kinematic datasets. By executing rotational sequences to minimise cross-talk error between segment frames, we target a reproducible frame definition and hence document an approach for reliable interpretation of articulating joint movement patterns.

Our underlying hypothesis was that if discrepancies between kinematic datasets and the ground truth signals result from differences in frame alignment, then a set of frame rotations should exist, which, if applied to the segment frames, would compensate for misalignment and eliminate cross-talk errors. Such a method could ideally be applied independently to any given kinematic dataset, without requiring access to a full ground truth signal, and thereby provide a reliable and reproducible interpretation of the kinematic patterns for comparison across studies.

In order to describe the mathematical formulation, we initially provide the underlying notation:

Let rotation matrix $\mathbf{R}_B^A$ denote the orientation of frame A relative to frame B. $\mathbf{R}_B^A$ can be expressed in terms of *Tait-Bryan angles* as

$$\mathbf{R}_B^A = \mathbf{R}(\hat{\mathbf{x}}, \alpha) \times \mathbf{R}(\hat{\mathbf{y}}, \beta) \times \mathbf{R}(\hat{\mathbf{z}}, \gamma), \tag{1}$$

for an intrinsic XYZ sequence of rotation, where $\mathbf{R}(\hat{\mathbf{v}}, \theta)$ indicates a positive rotation of θ around an axis in the direction of $\hat{\mathbf{v}}$. Let us define, for convenience, $\mathbf{r}_B^A$ as the corresponding 3×1 column vector, where the vector elements (in order from top to bottom) indicate e.g. knee joint flexion/extension, ab/adduction, and tibial int/external rotation,

$$\mathbf{r}_B^A(t) = \begin{bmatrix} (\mathbf{r}_B^A)_1 \\ (\mathbf{r}_B^A)_2 \\ (\mathbf{r}_B^A)_3 \end{bmatrix} = \begin{bmatrix} \alpha \\ \beta \\ \gamma \end{bmatrix}, \tag{2}$$

at timestep t.

Let us now consider a set of "raw" rotational knee kinematics, established based on measured data, expressed in matrix representation, where $\mathbf{R}_{femur_{raw}}^{tibia_{raw}}$ denotes the orientation of the tibial segment frame, $tibia_{raw}$, relative to the femoral segment frame, $femur_{raw}$, and varies with time (Figure 1a).

a
$femur_{raw}$

$\mathbf{R}_{femur_{raw}}^{tibia_{raw}}$

$tibia_{raw}$

relative orientation
of raw frames

b
$femur_{ideal}$

$\mathbf{R}_{femur_{ideal}}^{tibia_{ideal}}$

$tibia_{ideal}$

relative orientation of ideal
cross-talk-free frames
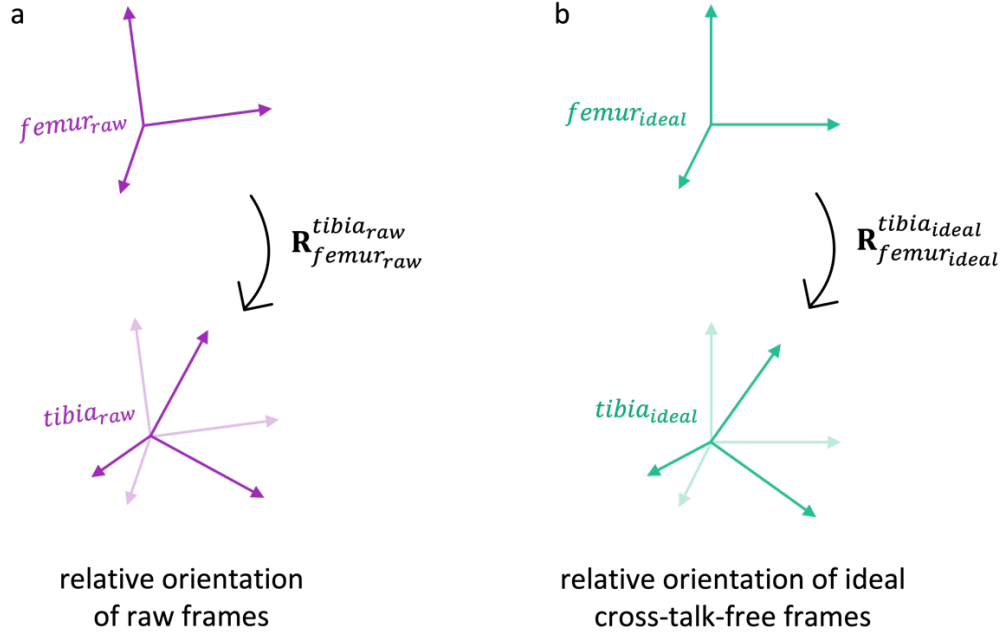
Figure 1. Schematic of local segment frames relative to one another: (a) Measured kinematics are given by rotation matrix $\boldsymbol{R}_{femur_{raw}}^{tibia_{raw}}$, denoting the orientation of the raw tibial segment frame relative to the raw femoral segment frame. (b) A set of ideal kinematics would be given by rotation matrix $\boldsymbol{R}_{femur_{ideal}}^{tibia_{ideal}}$, denoting the orientation of an ideal cross-talk-free tibial segment frame relative to an ideal cross-talk-free femoral frame.

The vector $\mathbf{r}_{femur_{raw}}^{tibia_{raw}}$ highly depends on both the order of the rotation sequence and the exact orientation of the individual femoral and tibial frames. Orientation of these frames is determined by the specific choice of approach used for coordinate system definition; be it landmark-based, functional, or a combination of the two. Any difference in frame orientation, even a very minor one, is known to lead to differences in kinematic patterns, even if the physical relative movement between the underlying joint segments is fundamentally the same [14]. This is especially problematic because for a given set of collected data, any and all estimated segment coordinate systems will be subject to some level of uncertainty or error.

Consider an "ideal", cross-talk-free kinematic signal, $\boldsymbol{R}_{femur_{ideal}}^{tibia_{ideal}}$, resulting from the relative orientation of two frames, $femur_{ideal}$ and $tibia_{ideal}$ (Figure 1b). At any given instant in time, it cannot be assumed that the raw frames are perfectly aligned with the orientation of these hypothetical ideal cross-talk-free frames (Supplementary Figure S2). The difference in orientation between the raw and ideal frame of a given segment is constant over time, since both frames are defined as fixed relative to the (assumed to be) rigid bodies they represent. For measurements affected by soft-tissue artefact, an approach such as the Optical Common Shape Technique based on Procrustes approaches as described in [30] would be required in order to ensure a rigid marker (or sensor) configuration. With sufficient knowledge of the raw frames' and ideal frames' respective orientations, it would then be possible to re-align the raw frames to match the ideal frames, hence allowing a set of "modified" or reorientated femoral and tibial frames, $femur_{mod}$ and $tibia_{mod}$ to be obtained (Figure 2). Let $\mathbf{R}_{femur_{raw}}^{femur_{mod}}$ and $\mathbf{R}_{tibia_{raw}}^{tibia_{mod}}$ denote the orientation of the modified frames relative to the orientation of the raw segment

frames. The relative orientation of these modified frames would yield kinematics given by rotation matrix $\mathbf{R}^{tibia_{mod}}_{femur_{mod}}$, where these modified kinematics are related to the raw kinematics by

$$\mathbf{R}^{tibia_{mod}}_{femur_{mod}} = (\mathbf{R}^{femur_{mod}}_{femur_{raw}})^{-1} * \mathbf{R}^{tibia_{raw}}_{femur_{raw}} * \mathbf{R}^{tibia_{mod}}_{tibia_{raw}} \quad . \tag{3}$$
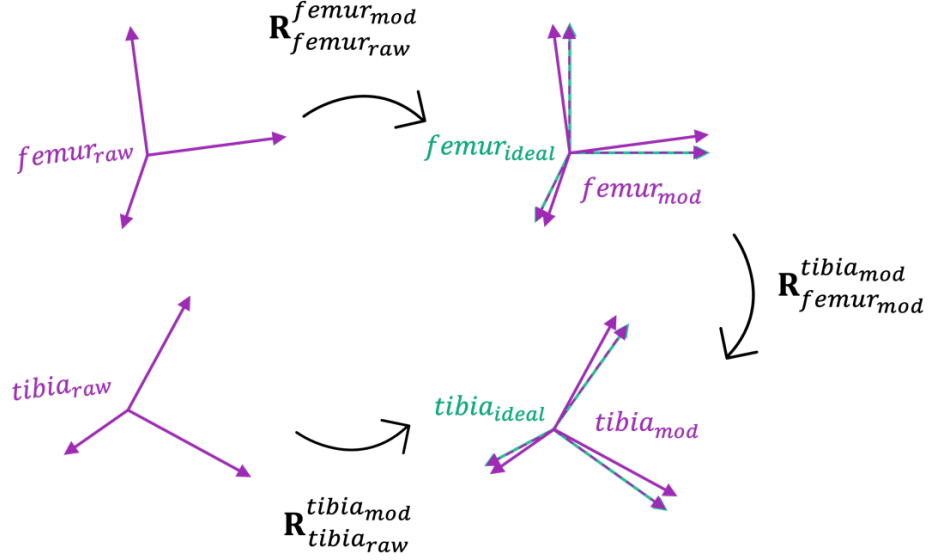
Figure 2. Schematic of raw (solid purple), ideal (solid green) and modified (dashed purple) local segment frames relative to one another, where modified frames are the raw frames after realignment to approximate the orientation of the ideal frames. $\boldsymbol{R}^{femur_{mod}}_{femur_{raw}}$ and $\boldsymbol{R}^{tibia_{mod}}_{tibia_{raw}}$ denote the orientation of the modified frames relative to the orientation of the raw segment frames, and $\boldsymbol{R}^{tibia_{mod}}_{femur_{mod}}$ denotes the orientation of the modified tibia frame relative to the modified femoral frame.

Assuming the orientation of these ideal segment frames relative to the underlying segments are unknown, but the resulting relative rotations between the two segment frames, $\mathbf{R}^{tibia_{ideal}}_{femur_{ideal}}$ (or $\mathbf{r}^{tibia_{ideal}}_{femur_{ideal}}$), *are* known, then mathematical optimisation approaches could be used to solve for the values of $\mathbf{R}^{femur_{mod}}_{femur_{raw}}$ and $\mathbf{R}^{tibia_{mod}}_{tibia_{raw}}$ that minimise the differences between the modified, $\mathbf{r}^{tibia_{mod}}_{femur_{mod}}$, and the ideal, $\mathbf{r}^{tibia_{ideal}}_{femur_{ideal}}$, kinematics.

In most practical cases, knowledge of the numerical value of the hypothetical cross-talk-free ideal kinematics is admittedly not realistic. Although an undisputed definition of optimal segment frame orientations does not exist, partly due to a lack of consensus, but also due to differences in data capture approaches (including the consideration of soft-tissue artefact etc.), there is a common agreement that cross-talk artificially amplifies out-of-sagittal plane rotations (Supplementary Figure S1). If absolutely no cross-talk were present, then pure joint flexion would not produce any artefact kinematic signal around the other axes. In a kinematic measurement, consisting of one dominant (e.g. flexion/extension) axis and two non-dominant (e.g. ab/adduction and int/external rotation) axes, the minimisation of rotations around the two non-dominant axes would inherently maximise rotation around the dominant axis, and therefore would not allow artefact rotations into the non-dominant axes. As a result, the remaining rotations in the non-dominant axes would not be distorted by cross-talk artefact. To achieve

this, finding a frame alignment that is affected by as little cross-talk as possible can be enabled by determining the values of $\mathbf{R}_{femur_{raw}}^{femur_{mod}}$ and $\mathbf{R}_{tibia_{raw}}^{tibia_{mod}}$ that minimise $(\mathbf{r}_{femur_{mod}}^{tibia_{mod}})_2$ and $(\mathbf{r}_{femur_{mod}}^{tibia_{mod}})_3$. While there are clearly various different cost functions that can be applied to minimise these values (each associated with different kinematic targets), for this demonstration of the approach, we have chosen to minimise root-mean-square (RMS). This choice implies that higher deviations from zero are weighted more heavily than if using the sum or average of the absolute values.

By re-aligning the segment frames to minimise the components of the 3D rotation that occur in the transverse and frontal planes, the magnitude of the rotation component in the third (sagittal) plane is thus effectively maximised. We therefore ensure that flexion predominates and that cross-talk is minimised. Furthermore, the need for a second associated kinematic dataset to act as the assumed ideal ground truth is eliminated. In practice, such a minimisation would be applied over the entire activity cycle. As such, it is not possible to entirely mitigate cross-talk errors for every instant of time. However, the overall output will indeed produce a consistent and reliable set of data, and hence allow comparison across trials, subjects, and studies.

2.1. Application

As a first step towards approach verification, results of a previous investigation were used to explore the potential relationships between the magnitude of errors in different planes [13, 31]. In a previous study, *in vivo* kinematics for six subjects over five valid cycles of three activities of daily living (level walking, stair descent, and sit-stand-sit) were derived from moving videofluoroscopy, using a cylindrical axis approach (i.e. based on the fitting of a cylindrical shape to each femoral condyle) to define the primary joint axis [31]. Mean kinematic signals for each subject were then replicated in a six-degrees-of-freedom robotic joint simulator (VIVO, AMTI, Watertown, MA) and measured using IMUs [13]. The ground truth data was then compared against IMU-based estimates obtained using an algorithm that leveraged the combined use of simple biomechanical models and Kalman smoothing [32] to estimate functional axes and the associated knee joint angles from linear acceleration and angular velocity measurements. Although the simulator segment kinematics were consistent and unaffected by soft-tissue artefact, maximum absolute errors between the two kinematic datasets of up to 10.8° were observed. Larger errors in the transverse plane rotations seemingly coincided with higher flexion angles; a trend indicative of cross-talk between coordinate system axes (Supplementary Figure S1).

In a preliminary frame orientation analysis, we first tested the assumption that the observed errors originated from cross-talk by applying mathematical optimisation (in this case, using a Levenberg-Marquardt algorithm [33]) to solve for $\mathbf{R}_{femur_{raw}}^{femur_{mod}}$ and $\mathbf{R}_{tibia_{raw}}^{tibia_{mod}}$ to minimise the RMSE between $\mathbf{r}_{femur_{mod}}^{tibia_{mod}}$ and $\mathbf{r}_{femur_{ideal}}^{tibia_{ideal}}$, (i.e. minimise $\sum_{i=1}^{3}\sqrt{\frac{1}{T}\sum_{t=0}^{T}\left(\left(\mathbf{r}_{femur_{ideal}}^{tibia_{ideal}}(t)\right)_i - \left(\mathbf{r}_{femur_{mod}}^{tibia_{mod}}(t)\right)_i\right)^2}$) under the assumption that IMU-based estimates represented the raw data, and simulator ground truth represented the ideal data. Here, we used a specific implementation of FOOM to rotate the IMU-based reference frames to minimise differences between the IMU and simulator kinematic signals (i.e. FOOM$_{IMU \to Sim}$). By rotating the local femoral and tibial frames associated with the IMU data by $\mathbf{R}_{femur_{IMU}}^{femur_{mod}}$ and $\mathbf{R}_{tibia_{IMU}}^{tibia_{mod}}$, respectively, to align with the ground truth segment frames, a set of modified local frames was established and the resultant relative rotations were calculated. A comparison between the IMU kinematics resulting from these newly aligned frames and the simulator ground truth kinematics was then performed to establish how much of the reported errors were associated with cross-talk.

After this preliminary analysis established the level of cross-talk, the presented stand-alone implementation of FOOM to reorientate the segment reference frames was tested by comparing the IMU and simulator kinematic curves, which were derived from identical motion patterns but with different underlying reference frames. Here, each kinematic dataset was independently optimised by minimising the RMS of ab/adduction and int/external rotation (here, we minimised $\sum_{i=2}^{3} \sqrt{\frac{1}{T} \sum_{t=0}^{T} \left(\mathbf{r}_{femur_{mod}}^{tibia_{mod}}(t) \right)_i^2}$); In contrast to FOOM$_{\text{IMU}\to\text{Sim}}$ in the preliminary analysis (which technically also involves optimising frame orientations to meet certain criteria), this latter broader implementation of FOOM individually considers both the simulator- and IMU-based kinematics as "raw" values in turn, acting as a self-contained approach that does not rely on information encompassed within a second dataset to achieve frame orientation optimisation.

Custom scripts to implement the described optimisations were developed in MATLAB (vR2021b; The Mathworks Inc., Natick, Massachusetts, USA). RMSEs were calculated for both the preliminary analysis (FOOM$_{\text{IMU}\to\text{Sim}}$) and the stand-alone implementation of FOOM. Paired t-tests were then conducted to compare RMSEs before and after frame reorientation, with and without a Bonferroni correction to account for multiple comparisons [34] (assuming two independent comparisons were performed: 1 – No Optimisation vs. FOOM$_{\text{IMU}\to\text{Sim}}$, and 2 – No Optimisation vs. FOOM).

2.2. Ethics declarations

This study used publicly accessible data and therefore did not directly involve humans. Collection of the original fluoroscopy data that was replicated here occurred within the scope of a separate cited study, which states that all subjects "provided written, informed consent to participate in this study, which was approved by the local ethics committee (EK 2011-N-6)" [31].

3. Results

3.1. Preliminary analyses

There were visible differences between the raw IMU-based and raw simulator kinematic patterns, despite identical underlying motion. The preliminary analyses ($FOOM_{IMU \rightarrow Sim}$) that aligned the IMU-based local segment frames to that of the simulator resulted in a clear convergence of the kinematic signals in all three planes, throughout the entire activity cycles and for all subjects – for brevity, only images for level walking are shown (Figure 3), but figures for stair descent and sit-to-stand-to-sit can be viewed in the Supplementary Material (Figures S3-S4), along with the corrective rotations applied to the femoral and tibial frames as part of these analyses (Tables S1-S2). Importantly, these improvements were associated with a considerable reduction in average RMSEs across all three activities for ab/adduction (from 0.7°-3.2° to 0.1°-0.5°) and for int/external rotation (from 0.8°-5.1° to 0.3°-0.6°) (Tables 1-2).
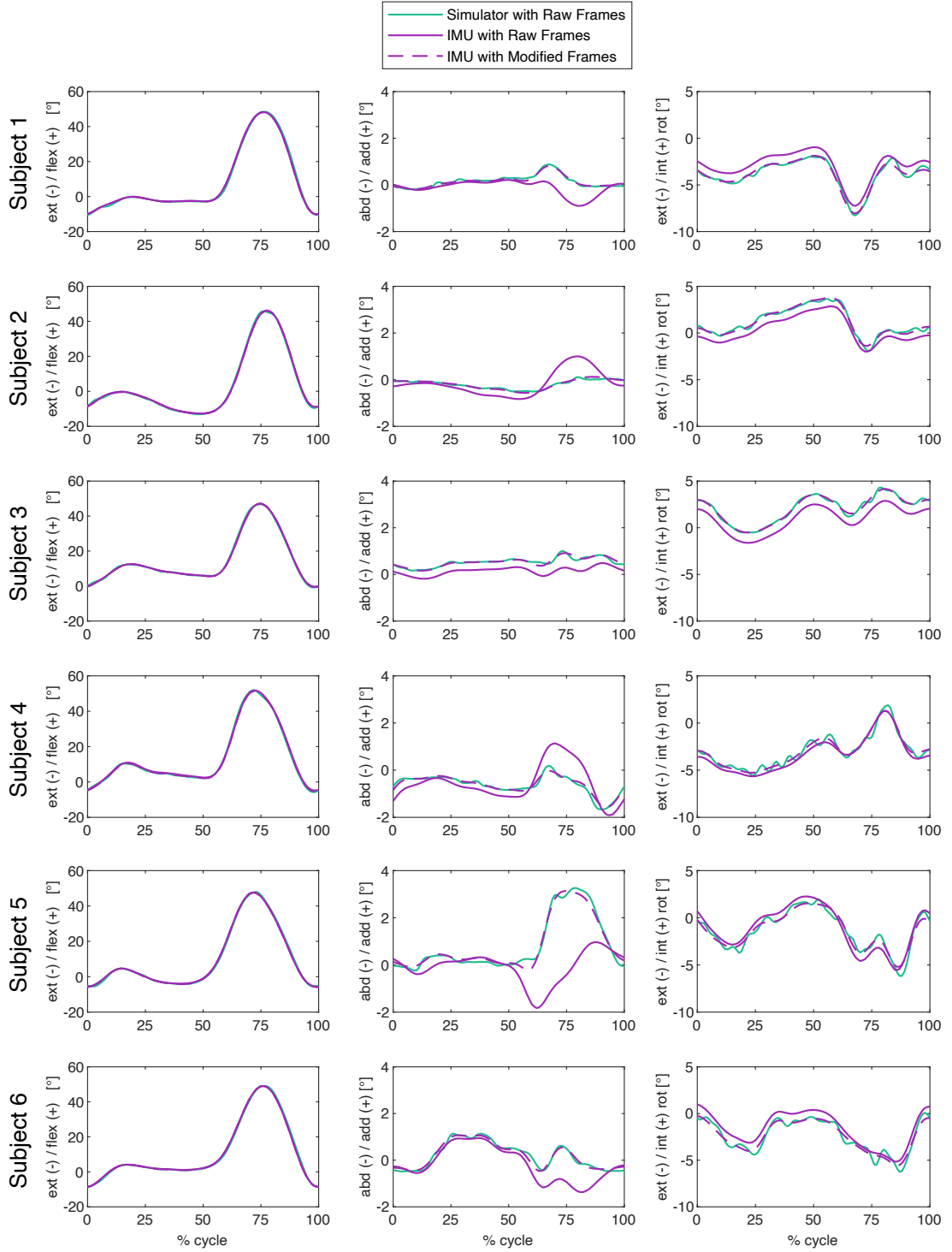
Figure 3. Level walking with raw frames: Knee joint angles are shown over one complete exemplary gait cycle (expressed as a percentage) for each subject. The solid green lines illustrate the simulator kinematics, while the solid purple lines illustrate the IMU-based kinematics. The dashed purple lines show these IMU-based signals after rotation of the IMU- to the simulator reference frames ($FOOM_{IMU \to Sim}$), demonstrating convergence of the signals and a different interpretation of the movement patterns once aligned.

Table 1. RMSE ± standard deviation (in degrees) between the raw IMU-based kinematics and the raw simulator kinematics.

Not Optimised	Flexion/Extension	Ab/Adduction	Int/Ext Rotation
Level Walking	0.7 ± 0.1	0.7 ± 0.5	0.8 ± 0.2
Stair Descent	0.7 ± 0.1	1.4 ± 1.1	1.4 ± 0.9
Sit-to-Stand-to-Sit	0.9 ± 0.3	3.2 ± 1.7	5.1 ± 2.1

Table 2. RMSE ± standard deviation (in degrees) between the IMU-based kinematics with rotated segment frames and the raw simulator kinematics (i.e. $FOOM_{IMU \rightarrow Sim}$).

Preliminary Analyses	Flexion/Extension	Ab/Adduction	Int/Ext Rotation
Level Walking	0.7 ± 0.1	0.1 ± 0.0	0.3 ± 0.1
Stair Descent	0.6 ± 0.1	0.3 ± 0.2	0.4 ± 0.2
Sit-to-Stand-to-Sit	0.8 ± 0.2	0.5 ± 0.2	0.6 ± 0.2

3.2. Frame Orientation Optimisation Method

After independent frame orientation optimisation of each raw dataset using the described FOOM, average RMSEs across all activities decreased to 0.1°-0.5° for ab/adduction and 0.3°-0.6° for int/external rotation (Figure 4, Table 3). Figures for stair descent and sit-to-stand-to-sit can be viewed in the Supplementary Material (Figures S5-S6), along with the corrective rotations applied to the femoral and tibial frames for all three activities (Tables S3-S6).
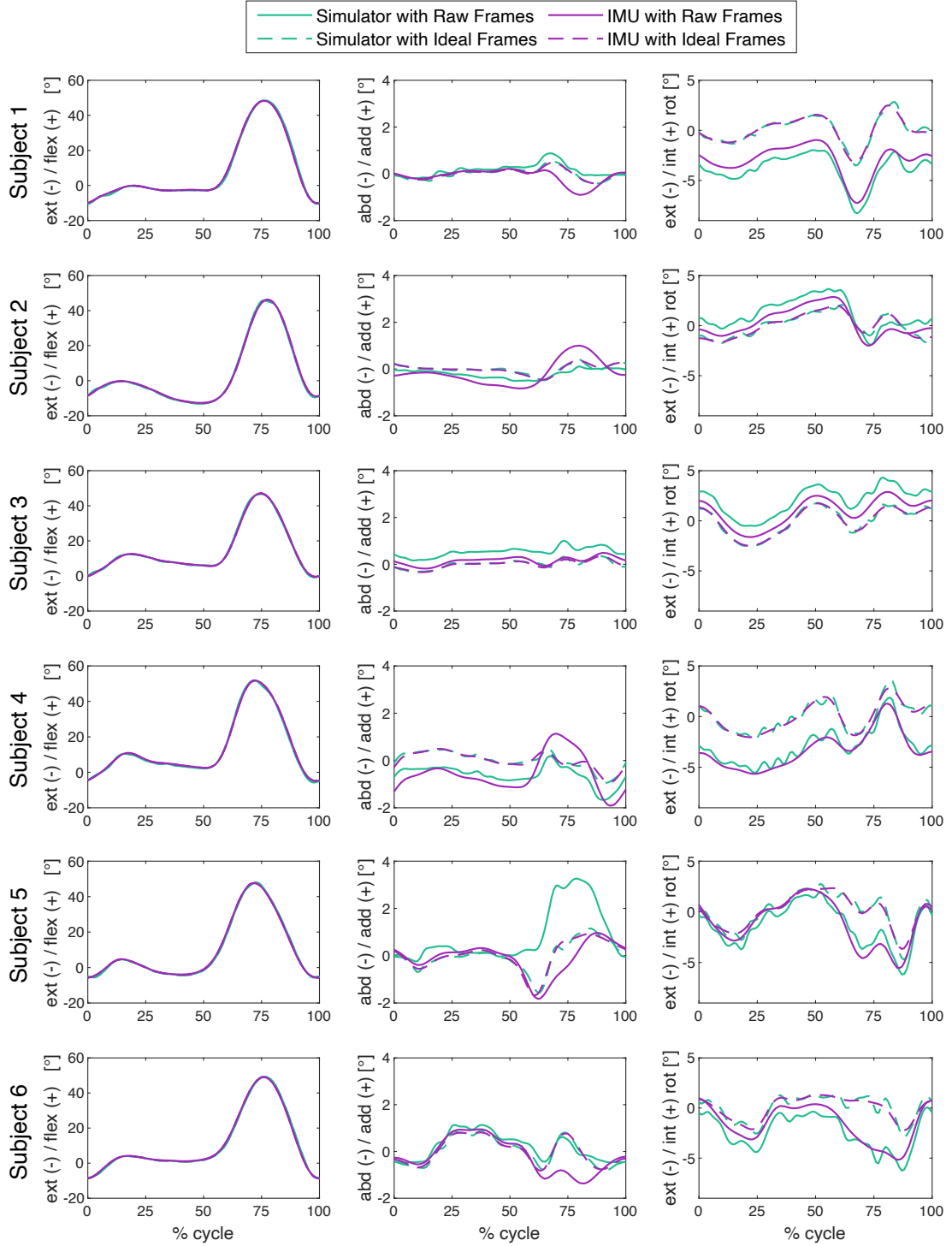
Figure 4. Level walking with ideal frames: Knee joint angles are shown over one complete exemplary gait cycle (expressed as a percentage) for each subject. The solid green lines illustrate the raw simulator kinematics, while the solid purple lines illustrate the raw IMU-based kinematics. The dashed purple lines show these IMU-based kinematics after frame orientation optimisation, while the dashed green lines show the simulator kinematics after optimisation, demonstrating convergence of the two sets of signals and a different interpretation of the movement patterns once aligned. Note that the converged signals differ from both original datasets but become consistent with one another.

Table 3. RMSE ± standard deviation (in degrees) after application of FOOM to both the IMU- and simulator datasets.

Frame Orientation Optimisation Method	Flexion/Extension	Ab/Adduction	Int/Ext Rotation
Level Walking	0.7 ± 0.1	0.1 ± 0.0	0.3 ± 0.1
Stair Descent	0.7 ± 0.2	0.3 ± 0.2	0.4 ± 0.2
Sit-to-Stand-to-Sit	1.0 ± 0.2	0.5 ± 0.2	0.6 ± 0.2

3.3. Statistical analyses

For the most part, neither the $FOOM_{IMU \rightarrow Sim}$ implementation in the preliminary analysis nor the stand-alone implementation of FOOM led to statistically significant changes in flexion/extension RMSE compared to the raw data (with the exception of $FOOM_{IMU \rightarrow Sim}$ analysis of stair descent, when Bonferroni correction was excluded; Figure 5a). On the other hand, paired t-tests showed ab/adduction RMSEs to be significantly improved after frame optimisation for all activities (except stair descent if we perform a Bonferroni correction; Figure 5b). Average RMSEs for ab/adduction decreased from a range of 0.7°-3.2° to 0.1°-0.5° after $FOOM_{IMU \rightarrow Sim}$ analysis, and to 0.1°-0.5° after full frame orientation optimisation (stand-alone FOOM). Similar outcomes were observed for int/external rotation RMSEs, which were significantly reduced for all activities (once again except stair descent if a Bonferroni correction is considered), from an average range of 0.8°-5.1° to 0.3°-0.6° (Figure 5c).
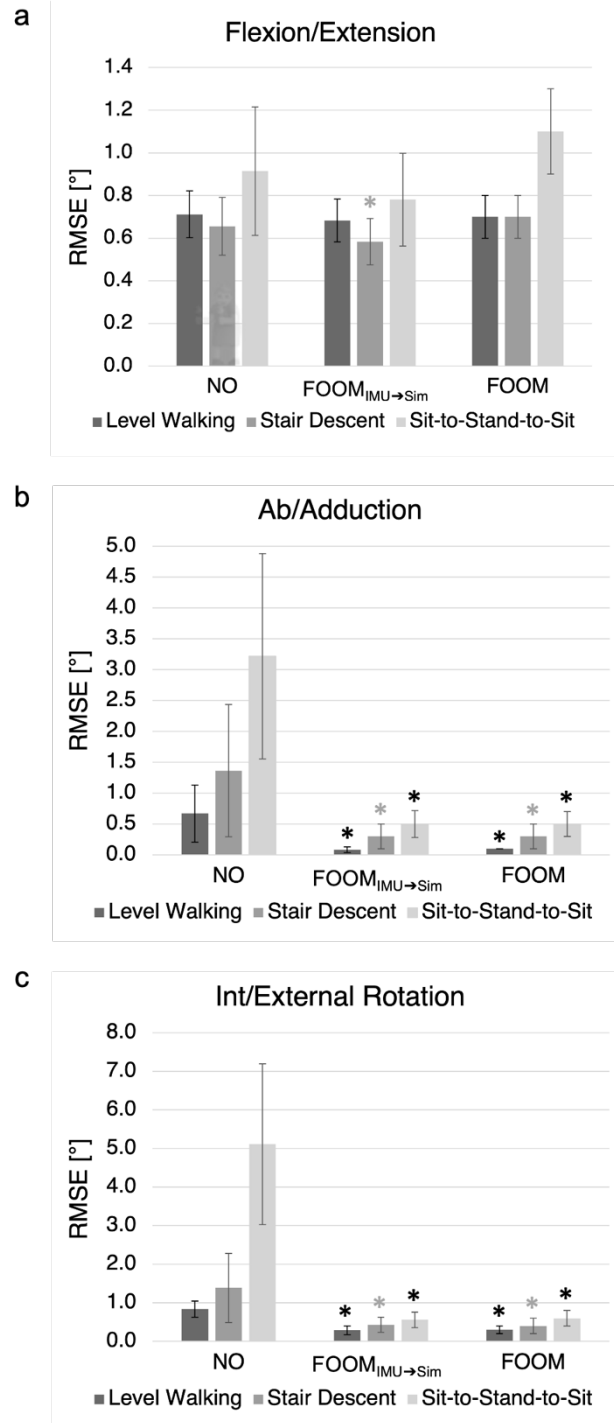
Figure 5. Root-mean-square error (RMSE) comparison: Average root-mean-square errors ± 1 standard deviation, before optimisation (NO – Not Optimised), after initial cross-talk analysis (FOOM$_{\text{IMU}\rightarrow\text{Sim}}$), and frame orientation optimisation based on minimisation of ab/adduction and int/external rotation RMSE (FOOM), for all three activities: (a) flexion/extension, (b) ab/adduction, and (c) int/external rotation. Statistically significant differences based on a paired t-test with significance considered at 0.05 are indicated by an asterisk, where black asterisks indicate statistically significant differences after Bonferroni correction.

4. Discussion

In human movement science, the interpretation of joint motion around each axis is known to strongly depend upon the orientation of the chosen local coordinate frames. Due to variability in measurement and analysis approaches between institutions, the assessment of motion patterns remains insufficiently reliable to support clinical decision-making. In this study, we present the Frame Orientation Optimisation Method that has clearly demonstrated efficacy in unifying frame orientation to mitigate cross-talk in kinematic datasets, thereby providing a repeatable and standardised output, regardless of the analysis approach used. Application of FOOM to measured joint kinematics could therefore provide an approach for universal comparison of movement data.

In our study, we have been able to successfully realise the convergence of kinematic datasets to a reproducible signal using datasets from a previous study [13]. Here, the observed errors between IMU-based estimates and ground truth kinematics from a robotic joint simulator were thought to be indicative of cross-talk – a hypothesis that could be verified by solving for a set of compensatory 3D rotation parameters. The results of applying corrective rotations as part of a preliminary analysis (using FOOM$_{IMU \rightarrow Sim}$) clearly demonstrated that the differences could be almost entirely removed for all tested datasets (Figure 3, Tables 1-2), hence providing strong evidence that almost all of the original errors did indeed stem from differences in frame orientation.

In *in vivo* settings, a set of ground truth values is almost never available, and movement scientists have therefore attempted to standardise clinical motion data in order to allow suitable comparison across studies [15, 19, 35-37]. In order to address this challenge, a fundamental assumption of our FOOM approach was that an ideal orientation exists for each of the segment frames. Consequently, instead of assuming that the ideal segment frames are prescribed by either ground truth data or the measured local segments' anatomical or functional data (like other cross-talk reduction approaches [22, 24]), our premise is that an alternative set of frames exists that is able to minimise cross-talk between axes. In our study, we demonstrated this postulation by minimising the RMS of ab/adduction and int/external rotation. Since it cannot be assumed that the simulator segment frames were defined to comply with the same criteria, an analogous transformation was applied to the simulator-based data (Figure 4). These optimisations resulted in a third converged kinematic signal that could be consistently achieved from different kinematic datasets for the given motion patterns. It is important to note that implementation of the chosen criteria does *not* assume that ideal natural joint motion should consist of pure flexion/extension, nor that the resulting modified signal should approximate to a constant 0°; neither does it imply that the optimisation will actually produce that result. This application of FOOM should, however, maximise flexion/extension and therefore minimise the level of cross-talk artefact between axes.

Although the FOOM approach may redefine the motion planes, the method possesses the considerable advantage of being entirely self-contained; optimisation of a kinematic dataset based on segment frame alignment can be achieved without relying on information contained within a second dataset. While other approaches, such as the determination of functional joint axes [38], also target the optimal orientation of the primary axis of rotation, our approach possesses the benefit of complete 3D frame re-orientation to minimise cross-talk around all axes. Naturally, different criteria might be better suited to optimise the alignment of segment frames during activities where flexion/extension does not clearly dominate, e.g. for a sidestep or crossover cutting manoeuvre. In such cases, out-of-sagittal plane

rotations may themselves be of primary interest, and so minimisation of ab/adduction may not be appropriate.

Acknowledging that any optimisation-based method to standardise the representation of kinematic signals requires some flexibility, and offering this freedom to the user is a key difference between FOOM and methods such as those presented by Woltring [20] or Rivest [23]. Accordingly, whether the implementation of a post-processing method like FOOM in fact leads to a *better* or *more accurate* set of kinematic data remains open for discussion. While finding consensus on the ideal definition of tibiofemoral kinematics is beyond the scope of this study, coordinate system definitions and alignment methods rely on one key assumption: that an optimal (ideal) alignment of the joint segment frames exists. However, *how* this alignment is defined and how it is best approximated based on the available data is ultimately a matter of *choice,* and further investigation towards standardising these choices is clearly required. While a certain choice of frame definition may be more (or less) suitable for answering a particular research question, the respective resultant kinematics cannot be considered to be more (or less) *accurate*, but rather simply a different (and hopefully more repeatable) representation of the same movement.

Here, the FOOM approach redefined the motion planes using rotational sequences, requiring only small angular corrections. In its current formulation, the algorithm could nevertheless find that larger rotations are needed to optimise the objective criteria for a different kinematic dataset. Rotating raw frames by larger angles to reach the desired modified frames does not hinder the underlying goal of determining whether differences in kinematic signals are caused by differences in frame orientation, rather than actual differences in the underlying movement patterns. If, however, the absolute values of the kinematic signals are believed to be clinically relevant, it is possible to ensure only small deviations from reference signals by modifying the underlying objective function to include a term that penalises deviations from one (or more) of the raw signals themselves. For example, it is possible to additionally minimise the difference between raw and ideal flexion values, or by constraining the magnitude of frame rotations permitted for optimisation.

For both the IMU-based data and the simulator values, kinematic calculations followed the globally recognised joint rotation convention of Grood and Suntay; a 3D Cartesian coordinate frame was attached to the femur and tibia, respectively, and angles were calculated as an intrinsic extension-adduction-internal rotation Cardan sequence of the tibia relative to the femur [15-17]. However, the simulator kinematic signals originally stemmed from values derived using a fluoroscopic dataset, where a cylindrical axis approach was used to define the femoral reference frame [31]. The IMU-based signals were derived with no direct information of the bone geometry, and therefore defined segment frames using a functional approach instead [13, 32]. The converged signals of the optimised IMU and optimised simulator kinematics (Figure 4) and the substantial reduction of ab/adduction and int/external rotation RMSEs after frame orientation optimisation (Figure 5) indicate excellent agreement between these two datasets. This observed reduction in RMSEs after frame re-orientation suggests that the two dataset segment frames were not initially consistent with one another and were susceptible to cross-talk artefact, despite the fact they both represented the same underlying motion and followed the same Grood and Suntay rotation convention. It is therefore clear that comparable rotational kinematics require two key components: not only 1) a common joint rotation convention, but importantly also 2) common axis orientations in the local reference frames of the proximal and distal segments. While the former requirement is easily addressed within e.g. the Grood and Suntay convention, the latter is considerably more complicated and often completely ignored. As mentioned, the definition of axis orientations is generally approached geometrically based on the identification of anatomical landmarks, or

functionally based on dynamic joint motion. However, although relationships between geometry and functional movement undoubtedly exist [39], they are neither straightforward nor generalisable. The FOOM approach bypasses the need to relate differently defined axes of rotation by directly producing consistent and reliable kinematic signals.

In conclusion, our study has demonstrated that consideration of the exact orientation of reference frames, beyond basic conventional guidelines, is vital when drawing inferences regarding the (dis)agreement of two (or more) kinematic curves. Moreover, the optimisation of reference frames towards minimisation of cross-talk now allows a clear perspective for reliable comparison of kinematic data collected using different techniques and in different settings. As such, the presented approach provides new options for comparing e.g. IMU data, where the challenge of sensor-to-segment calibration has so far made valid comparisons difficult. Further investigation should clearly attempt to better understand what correct kinematics and optimally aligned joint frames entail, as well as further study methods of cross-talk quantification and their associated clinical applications [40] and implications. Moreover, while the current examination was limited to rotational kinematics, a more comprehensive approach including translational kinematics should also be considered. By consistently standardising local segment frame alignment, such a collectively relevant approach will enable the valid comparison of kinematic data across trials, subjects, and studies.

Author contributions

Data availability

The datasets generated and analysed during the current study are available from the corresponding author on reasonable request.

Acknowledgements

Competing interests

A.O.V., A.M., T.G. and A.S. are employees of B. Braun Aesculap AG, Tuttlingen, Germany. W.T. has received compensation as a member of a scientific advisory board of the company. M.W. leads the applied biomechanics research group at the Musculoskeletal University Center Munich (MUM), which has received research funding from Aesculap AG in the past.

References

1. Guan, S., Gray, H.A., Keynejad, F., and Pandy, M.G., *Mobile Biplane X-Ray Imaging System for Measuring 3D Dynamic Joint Motion During Overground Gait.* IEEE Trans Med Imaging, 2016. **35**(1): p. 326-336.

2. List, R., Postolka, B., Schütz, P., Hitz, M., Schwilch, P., Gerber, H., Ferguson, S.J., and Taylor, W.R., *A moving fluoroscope to capture tibiofemoral kinematics during complete cycles of free level and downhill walking as well as stair descent.* PLOS One, 2017. **12**(10): p. e0185952.

3. Weygers, I., Kok, M., Konings, M., Hallez, H., De Vroey, H., and Claeys, K., *Inertial Sensor-Based Lower Limb Joint Kinematics: A Methodological Systematic Review.* Sensors, 2020. **20**(3).

4. Postolka, B., Taylor, W.R., List, R., Fucentese, S.F., Koch, P.P., and Schütz, P., *ISB clinical biomechanics award winner 2021: Tibio-femoral kinematics of natural versus replaced knees - A comparison using dynamic videofluoroscopy.* Clinical Biomechanics, 2022. **96**: p. 105667.

5. Gibbs, C.M., Hughes, J.D., Popchak, A.J., Chiba, D., Lesniak, B.P., Anderst, W.J., and Musahl, V., *Anterior cruciate ligament reconstruction with lateral extraarticular tenodesis better restores native knee kinematics in combined ACL and meniscal injury.* Knee Surgery, Sports Traumatology, Arthroscopy, 2022. **30**(1): p. 131-138.

6. Nagano, Y., Naito, K., Saho, Y., Torii, S., Ogata, T., Nakazawa, K., Akai, M., and Fukubayashi, T., *Association between in vivo knee kinematics during gait and the severity of knee osteoarthritis.* The Knee, 2012. **19**(5): p. 628-632.

7. Favre, J., Erhart-Hledik, J.C., and Andriacchi, T.P., *Age-related differences in sagittal-plane knee function at heel-strike of walking are increased in osteoarthritic patients.* Osteoarthritis and Cartilage, 2014. **22**(3): p. 464-471.

8. Rees, J.L., Beard, D.J., Price, A.J., Gill, H.S., Mclardy-Smith, P., Dodd, C.A., and Murray, D.W., *Real in vivo kinematic differences between mobile-bearing and fixed-bearing total knee arthroplasties.* Clinical Orthopaedics and Related Research, 2005(432): p. 204-209.

9. Murakami, K., Hamai, S., Okazaki, K., Wang, Y., Ikebe, S., Higaki, H., Shimoto, T., Mizu-Uchi, H., Akasaki, Y., and Nakashima, Y., *In vivo kinematics of gait in posterior-stabilized and bicruciate-stabilized total knee arthroplasties using image-matching techniques.* International Orthopaedics, 2018. **42**(11): p. 2573-2581.

10. Petraglia, F., Scarcella, L., Pedrazzi, G., Brancato, L., Puers, R., and Costantino, C., *Inertial sensors versus standard systems in gait analysis: a systematic review and meta-analysis.* European Journal of Physical and Rehabilitation Medicine, 2019. **55**(2): p. 265-280.

11. D'isidoro, F., Brockmann, C., and Ferguson, S.J., *Effects of the soft tissue artefact on the hip joint kinematics during unrestricted activities of daily living.* Journal of Biomechanics, 2020. **104**: p. 109717.

12. Schmitz, A., Ye, M., Boggess, G., Shapiro, R., Yang, R., and Noehren, B., *The measurement of in vivo joint angles during a squat using a single camera markerless motion capture system as compared to a marker based system.* Gait & Posture, 2015. **41**(2): p. 694-698.

13. Ortigas-Vásquez, A., Maas, A., List, R., Schütz, P., Taylor, W.R., and Grupp, T.M., *A Framework for Analytical Validation of Inertial-Sensor-Based Knee Kinematics Using a Six-Degrees-of-Freedom Joint Simulator.* Sensors, 2022. **23**(1).

14. Postolka, B., Taylor, W.R., Datwyler, K., Heller, M.O., List, R., and Schütz, P., *Interpretation of natural tibio-femoral kinematics critically depends upon the kinematic analysis approach: A survey and comparison of methodologies.* Journal of Biomechanics, 2022. **144**: p. 111306.

15.   Grood, E.S. and Suntay, W.J., *A joint coordinate system for the clinical description of three-dimensional motions: application to the knee.* Journal of Biomechanical Engineering, 1983. **105**(2): p. 136-144.

16.   Sheehan, F.T. and Mitiguy, P., *In regards to the "ISB recommendations for standardization in the reporting of kinematic data".* Journal of Biomechanics, 1999. **32**(10): p. 1135-1136.

17.   Macwilliams, B.A. and Davis, R.B., *Addressing some misperceptions of the joint coordinate system.* Journal of Biomechanical Engineering, 2013. **135**(5): p. 54506.

18.   Hull, M.L., *Coordinate system requirements to determine motions of the tibiofemoral joint free from kinematic crosstalk errors.* Journal of Biomechanics, 2020. **109**: p. 109928.

19.   Sauer, A., Kebbach, M., Maas, A., Mihalko, W.M., and Grupp, T.M., *The Influence of Mathematical Definitions on Patellar Kinematics Representations.* Materials, 2021. **14**(24).

20.   Woltring, H.J., *3-D attitude representation of human joints: a standardization proposal.* Journal of Biomechanics, 1994. **27**(12): p. 1399-1414.

21.   Chao, E.Y., Laughman, R.K., Schneider, E., and Stauffer, R.N., *Normative data of knee joint motion and ground reaction forces in adult level walking.* Journal of Biomechanics, 1983. **16**(3): p. 219-233.

22.   Baker, R., Finney, L., and Orr, J., *A new approach to determine the hip rotation profile from clinical gait analysis data.* Human Movement Science, 1999. **18**(5): p. 655-667.

23.   Rivest, L.P., *A correction for axis misalignment in the joint angle curves representing knee movement in gait analysis.* Journal of Biomechanics, 2005. **38**(8): p. 1604-1611.

24.   Baudet, A., Morisset, C., D'athis, P., Maillefert, J.F., Casillas, J.M., Ornetti, P., and Laroche, D., *Cross-talk correction method for knee kinematics in gait analysis using principal component analysis (PCA): a new proposal.* PLOS One, 2014. **9**(7): p. e102098.

25.   Kutner, M.H., *Applied linear statistical models.* 5th ed. The McGraw-Hill/Irwin series operations and decision sciences. 2005, New York: McGraw-Hill/Irwin. xxviii, 1396.

26.   Kadaba, M.P., Ramakrishnan, H.K., and Wootten, M.E., *Measurement of lower extremity kinematics during level walking.* Journal of Orthopaedic Research, 1990. **8**(3): p. 383-392.

27.   Ijomah and Azubuike, M. *On the Misconception of R2 for (r)2 in a Regression Model.* 2019.

28.   Kvalseth, T.O., *Cautionary Note about R2.* The American Statistician, 1985. **39**(4): p. 279-285.

29.   Blankevoort, L., Huiskes, R., and De Lange, A., *The envelope of passive knee joint motion.* Journal of Biomechanics, 1988. **21**(9): p. 705-720.

30.   Taylor, W.R., Ehrig, R.M., Duda, G.N., Schell, H., Seebeck, P., and Heller, M.O., *On the influence of soft tissue coverage in the determination of bone kinematics using skin markers.* Journal of Orthopaedic Research, 2005. **23**(4): p. 726-734.

31.   Schütz, P., Postolka, B., Gerber, H., Ferguson, S.J., Taylor, W.R., and List, R., *Knee implant kinematics are task-dependent.* Journal of the Royal Society Interface, 2019. **16**(151): p. 20180678.

32.   Versteyhe, M., De Vroey, H., Debrouwere, F., Hallez, H., and Claeys, K., *A Novel Method to Estimate the Full Knee Joint Kinematics Using Low Cost IMU Sensors for Easy to Implement Low Cost Diagnostics.* Sensors, 2020. **20**(6).

33.   Moré, J.J. *The Levenberg-Marquardt algorithm: Implementation and theory.* 1977.

34.   Bonferroni, C.E., *Teoria statistica delle classi e calcolo delle probabilità.* 1936: Seeber.

35.   Taylor, W.R., Kornaropoulos, E.I., Duda, G.N., Kratzenstein, S., Ehrig, R.M., Arampatzis, A., and Heller, M.O., *Repeatability and reproducibility of OSSCA, a functional approach for assessing the kinematics of the lower limb.* Gait & Posture, 2010. **32**(2): p. 231-236.

36.   Davis, R.B., Õunpuu, S., Tyburski, D., and Gage, J.R., *A gait analysis data collection and reduction technique.* Human Movement Science, 1991. **10**(5): p. 575-587.

37. Charlton, I.W., Tate, P., Smyth, P., and Roren, L., *Repeatability of an optimised lower body model.* Gait & Posture, 2004. **20**(2): p. 213-221.

38. Ehrig, R.M., Taylor, W.R., Duda, G.N., and Heller, M.O., *A survey of formal methods for determining functional joint axes.* Journal of Biomechanics, 2007. **40**(10): p. 2150-2157.

39. Martelli, S., Sancisi, N., Conconi, M., Pandy, M.G., Kersh, M.E., Parenti-Castelli, V., and Reynolds, K.J., *The relationship between tibiofemoral geometry and musculoskeletal function during normal activity.* Gait & Posture, 2020. **80**: p. 374-382.

40. Boeth, H., Duda, G.N., Heller, M.O., Ehrig, R.M., Doyscher, R., Jung, T., Moewis, P., Scheffler, S., and Taylor, W.R., *Anterior cruciate ligament-deficient patients with passive knee joint laxity have a decreased range of anterior-posterior motion during active movements.* The American Journal of Sports Medicine, 2013. **41**(5): p. 1051-1057.

5. Supplementary Material
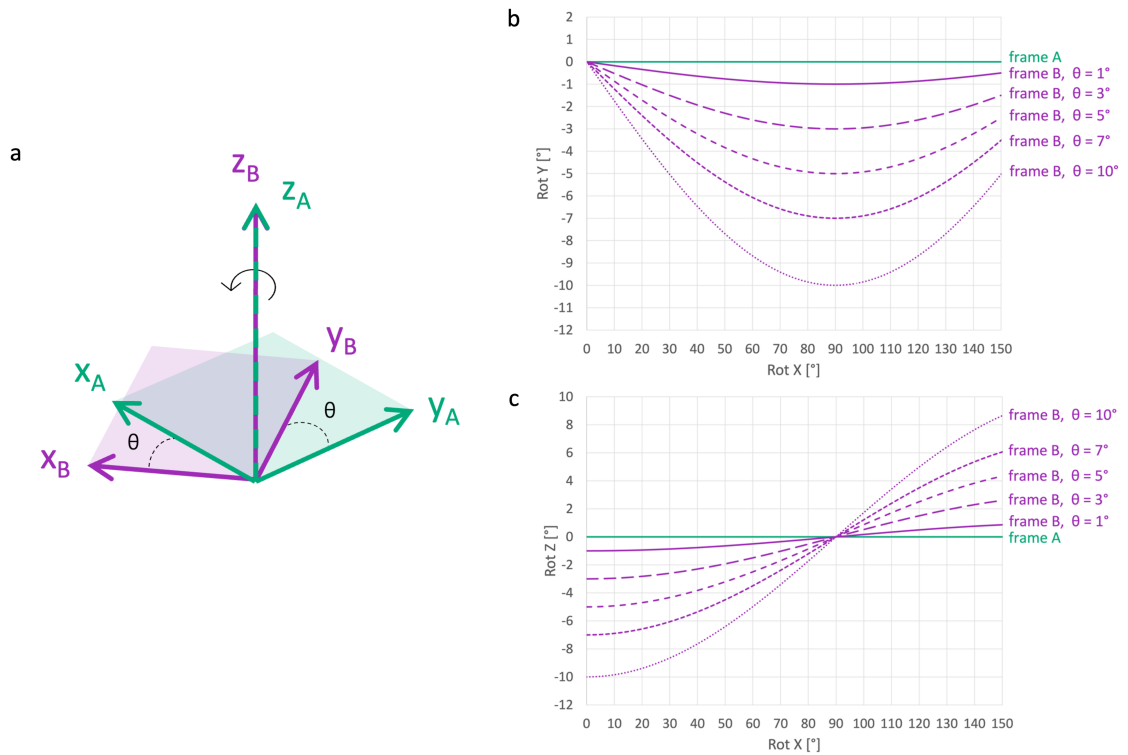
Figure S1. Frame A (green) and Frame B (purple) are misaligned by a rotation of θ around the z-axis (a). A pure rotation around Frame A's x-axis is not perceived by Frame B as a pure rotation around its x-axis, but rather as rotations around its y-axis (b) and z-axis (c) as well.
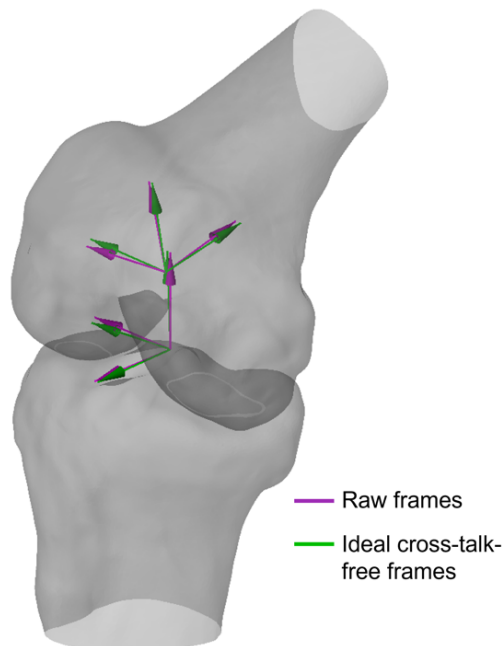
Figure S2. Raw segment frames (purple) may not be perfectly aligned with the orientation of ideal cross-talk-free frames (green).
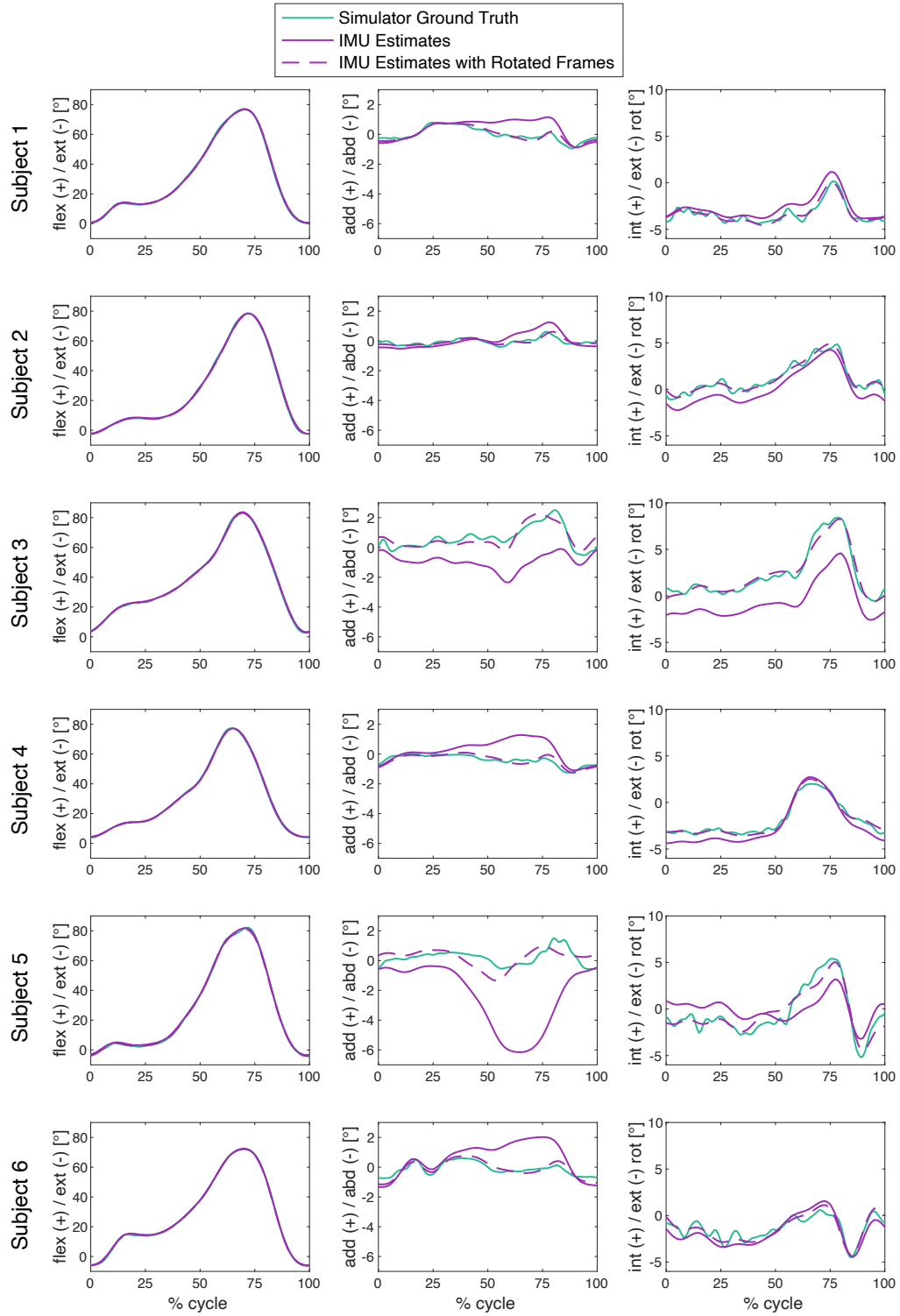
Figure S3. Stair Descent (Preliminary Analyses): Knee joint angles are shown over one complete exemplary gait cycle (expressed as a percentage) for each subject. The solid green lines illustrate the simulator kinematics, while the solid purple lines illustrate the IMU-based kinematics. The dashed purple lines show these IMU-based signals after rotation of the IMU- to the simulator reference frames, demonstrating convergence of the signals and a different interpretation of the movement patterns once aligned.
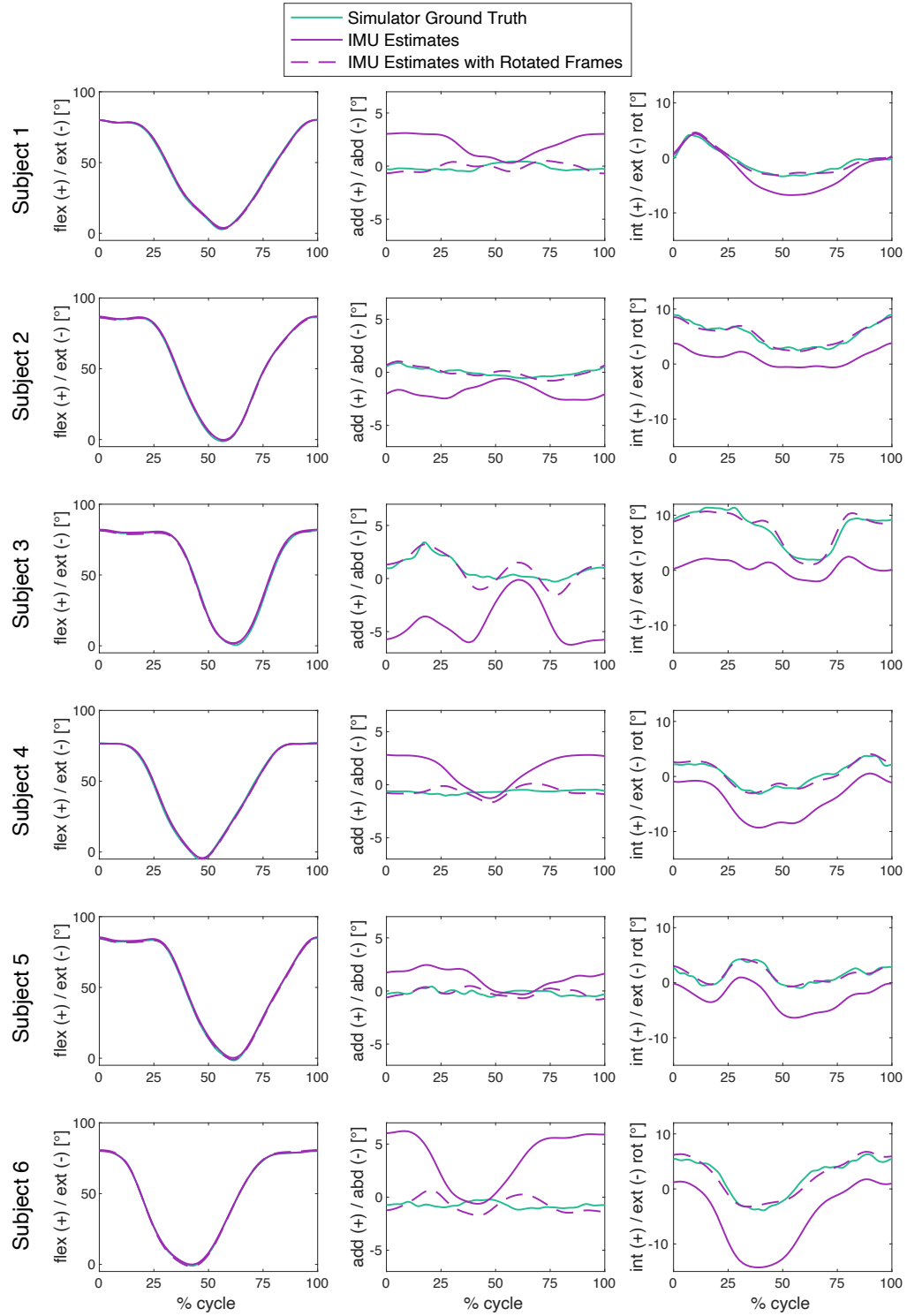
Figure S4. Sit-to-Stand-to-Sit (Preliminary Analyses): Knee joint angles are shown over one complete exemplary gait cycle (expressed as a percentage) for each subject. The solid green lines illustrate the simulator kinematics, while the solid purple lines illustrate the IMU-based kinematics. The dashed purple lines show these IMU-based signals after rotation of the IMU- to the simulator reference frames, demonstrating convergence of the signals and a different interpretation of the movement patterns once aligned.

Table S1. Corrective rotations in degrees applied on **femur** frame in preliminary analysis.

	Level Walking			Stair Descent			Sit-to-Stand-to-Sit		
	F/E	A/A	I/E	F/E	A/A	I/E	F/E	A/A	I/E
Subject 1	0.1	-0.6	1.9	0.0	1.3	-0.3	0.4	4.7	-4.0
Subject 2	0.0	0.6	-1.9	0.3	0.8	-1.6	0.2	-2.7	-2.8
Subject 3	0.0	-0.8	-0.8	0.1	-3.3	-1.5	-0.4	-7.7	-2.6
Subject 4	0.2	1.0	-2.0	0.1	2.0	-1.8	0.3	4.1	-7.2
Subject 5	0.5	-3.5	3.9	0.2	-6.1	3.3	0.9	2.8	-5.6
Subject 6	0.2	-1.5	2.1	0.1	2.1	-2.0	1.6	7.9	-11.8

Table S2. Corrective rotations in degrees applied on **tibia** frame in preliminary analysis.

	Level Walking			Stair Descent			Sit-to-Stand-to-Sit		
	F/E	A/A	I/E	F/E	A/A	I/E	F/E	A/A	I/E
Subject 1	0.0	-0.5	1.0	-0.1	1.5	-0.4	0.0	3.9	0.3
Subject 2	-0.2	0.7	-1.2	-0.1	1.0	-0.3	-0.3	-2.0	0.1
Subject 3	0.0	-0.5	0.2	-0.2	-2.4	0.1	-0.5	-6.1	0.2
Subject 4	0.0	1.3	-1.4	0.1	1.9	-0.4	-0.1	3.7	-0.3
Subject 5	0.3	-3.3	3.3	-0.6	-5.1	1.2	-0.2	2.4	0.3
Subject 6	0.1	-1.5	1.1	-0.1	2.2	-0.9	0.7	6.7	-0.3

IV. Journal Publication III

A reproducible representation of healthy tibiofemoral kinematics during stair descent using REFRAME – Part I: REFRAME foundations and validation

Ortigas-Vásquez, A., Taylor, W.R., Postolka, B., Schütz, P., Maas, A., Woiczinski, M., Grupp, T.M. and Sauer, A.

Abstract

In clinical movement biomechanics, kinematic measurements are collected to characterise the motion of articulating joints and investigate how different factors influence movement patterns. Representative time-series signals are calculated to encapsulate (complex and multidimensional) kinematic datasets succinctly. Exacerbated by numerous difficulties to consistently define joint coordinate frames, the influence of local frame orientation and position on the characteristics of the resultant kinematic signals has been previously proven to be a major limitation. Consequently, for consistent interpretation of joint motion (especially direct comparison) to be possible, differences in local frame position and orientation *must* first be addressed. Here, building on previous work that introduced a frame orientation optimisation method and demonstrated its potential to induce convergence towards a consistent kinematic signal, we present the REference FRame Alignment MEthod (REFRAME) that addresses both rotational and translational kinematics, is validated here for a healthy tibiofemoral joint, and allows flexible selection of optimisation criteria to fittingly address specific research questions. While not claiming to improve the *accuracy* of joint kinematics or reference frame axes, REFRAME does enable a representation of knee kinematic signals that accounts for differences in local frames (regardless of how these differences were introduced, e.g. anatomical heterogeneity, use of different data capture modalities or joint axis approaches, intra- and inter-rater reliability, etc.), as evidenced by peak root-mean-square errors of 0.24° ± 0.17° and 0.03 mm ± 0.01 mm after its implementation. By using a self-contained optimisation approach to systematically re-align the position and orientation of reference frames, REFRAME allows researchers to better assess whether two kinematic signals represent fundamentally similar or different underlying knee motion. The openly available implementation of REFRAME could therefore allow the consistent interpretation and comparison of knee kinematic signals across trials, subjects, examiners, or even research institutes.

Keywords: kinematics; coordinate system; reference frame; joint axis; joint angles; knee motion; movement analysis

1. Introduction

Clinical movement analysis seeks to improve our understanding of human joint motion to better guide treatment development and improve clinical decision-making. To achieve this, reliable analyses require objective quantification of joint movement patterns, i.e. *joint kinematics*. While raw movement data (e.g. marker coordinates in a three-dimensional (3D) global laboratory reference frame) are *measured*, a kinematic signal must be *calculated* from the captured data points to allow a clinical interpretation of the underlying movement patterns of the articulating segments. Importantly, assessment of kinematic signals should inherently lead to a consistent interpretation of joint movement, regardless of the numerical approach used to derive them. Unfortunately, the complexity of fully characterising the motion of a biological joint using classic mechanical engineering principles is challenged by the requirement to present the 3D motion patterns of multiple segments at multiple timepoints in a simple two-dimensional illustration – such that the outcome is mathematically accurate, yet intuitive to clinical practitioners. This complexity has led to the lack of consensus around the calculation of kinematic signals, hence resulting in inconsistency in the interpretation of the underlying movement patterns [1-4].

In 1995, the International Society of Biomechanics (ISB) released an official set of recommendations towards standardising the reporting of joint kinematics [5]. Their guidelines on detailing relative orientations recommended the definition of a rotation convention for each individual joint, citing the work of Grood and Suntay [6] as a suitable example for the knee. Although these guidelines explicitly noted that both the orientations of the local proximal and distal reference frames, as well as the positions of their respective origins, need to be not only clearly specified but also consistent across trials, subjects and/or studies, emphasis was placed on the importance of detailing a common rotation convention. Following the ISB's publication, Grood and Suntay's approach and variations thereof have gained popularity and been widely adopted by the biomechanics community. Importantly, this approach has been repeatedly proven to be mathematically analogous to an extension-adduction-internal rotation Cardan sequence of the distal relative to the proximal segment (excluding Grood and Suntay's modification of positive and negative signs – see Supplementary Figure S1) [7, 8]. Nevertheless, as ISB guidelines suggested and more recent studies have demonstrated [1, 9], a common choice for local segment frame orientation and origin definition is fundamental to the standardised reporting of joint kinematics, but is extremely difficult to achieve in practice. Critically, however, even small inconsistencies from practical application result in a malalignment of the primary joint axis relative to the true instantaneous axis of rotation, which is known to result in artefact translations and therefore differing interpretations of joint movement [1].

Existing literature on the knee joint alone presents abundant approaches seeking to provide consistent interpretations of joint motion by focusing on the exact method used to define the primary (flexion/extension) axis, whereby the secondary axes stem from this definition. On one hand, anatomical-based approaches, such as the transepicondylar axis [10, 11] and the cylinder axis [12-14], leverage the relative location of skeletal landmarks to define joint axes. However, identification of anatomical landmarks is known to be subject to considerable observer variance [15], and previous analyses have demonstrated that even minor differences in landmark location can result in noticeably divergent kinematic signals [16]. On the other hand, functional axes such as the symmetrical axis of rotation (SARA) [17], the least squares estimate method [18, 19] and the mean helical axis [20], are defined based on the relative movement between the joint segments. In fact, some have recommended functional axes over other approaches because of their practical representation of the average instantaneous axis of rotation [1], especially in settings where medical imaging is not available (which is often the case). However, as

described by Postolka et al. [1], knee motion can be composed of a combination of rolling, slipping, and/or gliding between segments. Therefore, functional approaches that rely on approximations of only rolling with slipping (and therefore approximate to a simple – albeit optimised – hinge joint), or those finding the exact instantaneous axis of rotation at each timestep (without a fixed relationship to the bone anatomy), while advantageous, are still inherently limited. Moreover, previous studies have suggested that the reliability of functional methods often suffers due to their sensitivity to functional calibration trial performance [21].

In addition to practical approaches seeking to improve the initial definition of a primary joint axis, post-processing methods looking to realign local segment frames and thus achieve so-called "cross-talk reduction" have also been introduced (where cross-talk refers to the presence of artefact rotations around secondary axes due to a misalignment in primary axis orientation) [22]. A brief summary of relevant examples was provided in one of our recent publications [9], making explicit reference to the work of Woltring [23], Baker et al. [24], Rivest [25], and Baudet et al. [26]. While these methods of post-processing all aim to mitigate the presence of cross-talk in kinematic datasets, they focus predominantly on frame orientation. Even the recent Frame Orientation Optimisation Method (FOOM) accounts exclusively for differences in the orientation of local body axes, offering only consistent *rotational* kinematic signals [9]. The interpretation of *translational* movement patterns, however, is critically dependent not only on the orientation of the reference frames, but even more so on their locations in space [1].

Even studies that specifically use the ISB official guidelines for standardising kinematics, including the Grood and Suntay convention, are not able to produce consistent (i.e. repeatable) local segment frame orientation and location. This is largely due to the overwhelming variety of approaches available to quantify joint kinematics, with differences emerging not only in the choice of joint axis definition (as discussed here), but also in the choice of anatomical model [27-29], data capture modality (e.g. inertial vs. optical), marker set (in the case of marker-based optical motion capture) [30, 31], and computational method (e.g. direct vs. inverse kinematics) [27]. These challenges are further exacerbated by variability across studies related to different e.g. anatomical landmark locations (for example, due to different bone morphologies) [16, 29], examiners [15], equipment and instrumentation (including software) [32, 33], and magnitudes of soft-tissue artefact [34, 35].

Within the context of joint axis definitions, although in some cases the choice of approach to define a primary axis is largely based on study protocol, it can also be driven by the type of measurements available. For example, given the lack of exact data regarding the 3D positions of bony landmarks provided by inertial measurement units (IMUs), calculation of kinematic signals from an IMU-only system is likely to leverage functional axes [36]. Ultimately, the lack of agreement on a universally applicable definition of local segment frames results in a collection of kinematic signals that cannot be directly compared against one another. Importantly, to date, axes derived from functional joint kinematics usually not only require exceeding a range of motion threshold for proper calibration, but also tend to optimise joint motion exclusively around one axis. Even the SARA approach [17], which symmetrically identifies the primary joint axis based on relative motion, is generally limited by placing the origin of the coordinate system along the approximated functional axis, usually at a distance bisecting the medial and lateral condylar landmarks. As a result, any of the approaches currently available will inevitably also lead to inconsistent interpretations of what should be an unambiguous quantification of joint motion [1].

To eventually achieve consistency in clinical interpretation, the biomechanics community critically needs an approach that results in a unique and unambiguous solution before kinematic datasets can be compared across studies in a reliable manner. This can only be accomplished using methods that provide unique solutions in all six degrees of freedom (DOFs). Therefore, towards the vision of standardising kinematic signals for their consistent representation within and across studies, the so-called REference FRame Alignment MEthod (REFRAME) seeks to offer both unified and unambiguous frame orientations and origin locations. Here, we aim to 1) present a general mathematical formulation of REFRAME, 2) perform a preliminary validation for the knee in one subject (see Part II for further validation), and 3) discuss optimisation criteria options.

2. Methods

In this study, we present the REFRAME approach that further develops a previously presented optimisation method for the standardisation of frame orientations [9] to now provide a more generalised formulation that additionally addresses coordinate system origin positions. The combined framework therefore offers a comprehensive approach for standardising kinematic datasets. Finally, the practical implications of establishing frame alignment optimisation criteria based on different combinations of statistical parameters are then investigated by systematically assessing REFRAME's efficacy for producing converging kinematic signals for the same underlying movement pattern. Here, using an illustrative dataset of six DOFs *in vivo* tibiofemoral kinematics that exhibit seemingly different kinematic signals, even though they originate from a single set of kinematic data, we demonstrate the ability of REFRAME to produce converged kinematic signals.

Normally, axes of rotation [17] would be used to describe the movement patterns of segments relative to one another, but the interpretation of the joint kinematics is known to vary greatly according to the analysis approach used [1]. The REFRAME approach is based on the fundamental assumption that kinematics can only be reliably compared if the segment reference frames are completely consistent. Here, we propose a framework to obtain consistent reference frame definitions based on the characteristics of the associated six DOFs kinematic signal and therefore allow reliable comparison of datasets. The approach builds on FOOM [9], which allows orientation alignment of the coordinate systems, to also provide an approach for the reliable determination of joint translations. In the preceding FOOM study, we demonstrated REFRAME's ability to target differences in reference frame orientations when comparing kinematic signals collected using two different data capture modalities (IMUs vs. fluoroscopy/robotic simulator). Not only do we now consider the tibiofemoral kinematics of healthy patients (vs. with total knee replacement in FOOM study), but we also additionally show that even a single set of raw data from a common source (i.e. fluoroscopy) can lead to notably different kinematic signals when processed using distinct axis approaches. Moreover, given all kinematic signal sets compared in this study stem from the same raw measurements (and are therefore all affected by noise equally), we are able to target quasi-perfect convergence of signals after REFRAME in our validation of this method. To mitigate the effects of cross-talk, the REFRAME approach reorientates and translates the segment reference frames in order to optimise rotations and translations of the joint. While we appreciate there is a philosophical argument to be had regarding which parameters should be maximised or minimised, in general, we assume that flexion/extension is dominant throughout gait activities, and therefore provide a proof-of-concept based on this foundation for the healthy knee joint.

2.1. REFRAME: General optimisation method

Kinematics describe the relative pose of two joint segments, where the term *pose* encompasses *position* (translational kinematics) and *orientation* (rotational kinematics). In order to calculate kinematic signals, a reference frame fixed to each (assumed to be rigid) joint segment is defined. Rotational kinematics will depend exclusively on the orientation of the axes of each segment frame, while translational kinematics will depend on each frame's orientation, as well as the exact position of their respective origins. As a result, REFRAME's approach to optimise the pose of segment reference frames is divided into two stages. In stage I, optimal axis orientation is found by minimising criteria of rotational parameters exclusively. Building on the optimal orientations determined in the first stage, stage II then determines the optimal position for each frame's origin by minimising criteria of joint translations. In the

following section, vectorial and multidimensional variables and functions are represented by characters in **bold**, to distinguish these from scalar parameters.

Consider an initial kinematic measurement stemming from an arbitrary set of two segment frames. Let us express this raw measurement using the matrix $\mathbf{K}^0$ of size $M \times N$, where the matrix rows (in order from top to bottom) indicate extension, adduction, internal rotation (of the distal segment), lateral translation, anterior translation, and proximal translation, such that $M = 6$ and N is the total number of timesteps. To allow for column-wise operations, we let n represent the current timestep and borrow $(:, n)$ from programming notation, such that $\mathbf{K}^0_{:,n}$ represents the entire n-th column of matrix $\mathbf{K}^0$. Therefore, $\mathbf{K}^0_{:,n}$ is a 6×1 column vector providing all three raw rotational kinematic values and all three raw translational kinematic values between the joint segments at timestep n.

Similar to the derivation of FOOM [9], we refer to the captured data as "raw", while the REFRAME approach aims to obtain a "modified" or "optimised" set of local segment reference frames, for which the resultant joint kinematics fulfil certain optimisation criteria. (Note: While the term *raw* is usually used to refer to unprocessed primary data from the data capture source, e.g. 3D marker coordinates, in this context we use the term *raw* to differentiate reference frames and/or kinematic signals that have not yet undergone optimisation with REFRAME from those that have.) The relative rotations between the raw and modified frames are given by a 6×1 column vector $\mathbf{r}$ (3 rotations for each of the 2 segment frames = 6 elements). Similarly, the relative translations between the raw and modified frames are given by a 6×1 column vector $\mathbf{t}$. In the optimisation process, $\mathbf{r}$ then $\mathbf{t}$ act as *decision variables* for optimisation stages I then II, respectively.

Let the modified kinematic data $\mathbf{K}$ be given by

$$\mathbf{K} = \boldsymbol{\kappa}(\mathbf{K}^0, \mathbf{r}, \mathbf{t}) \ . \tag{1}$$

Note that function $\boldsymbol{\kappa}$ will depend on the specific joint and associated segment frame conventions chosen. Analogous to $\mathbf{K}^0_{:,n}$, the joint kinematic values resulting from the modified segment frames for a specific timestep, n, will be given by the 6×1 column vector $\mathbf{K}_{:,n}$.

2.1.1. Stage I – Relative Orientations

First, the optimal relative rotations of the reference frames can be found by minimising the objective function c_r, by varying decision variable $\mathbf{r}$ (i.e. by varying the relative orientations between raw and modified segment frames). Given that rotational kinematics are unaffected by the exact position of each frame's origin, decision variable $\mathbf{t}$ can be set to equal a 6×1 zero vector $\mathbf{0}$ during this stage. The optimisation problem at this point can therefore be expressed as

$$\min c_r\big(\mathbf{K}(\mathbf{K}^o, \mathbf{r}, \mathbf{0})\big) \ . \tag{2}$$

An example for such a criterion for the knee joint could be the sum of the root-mean-square (RMS) of adduction and internal rotation,

$$e.g. \quad \min\left(c_r = \sqrt{\frac{1}{N}\sum_{n=0}^{N} \mathbf{K_{2,n}}(\mathbf{K}_{:,n}^0, \mathbf{r}, \mathbf{0})^2} + \sqrt{\frac{1}{N}\sum_{n=0}^{N} \mathbf{K_{3,n}}(\mathbf{K}_{:,n}^0, \mathbf{r}, \mathbf{0})^2}\right). \qquad (3)$$

The relative rotation angles between raw and modified segment frames that minimise c_r are referred to as $\mathbf{r}^*$, and are fixed as a constant model parameter during stage II.

2.1.2. Stage II – Relative Positions

During this second optimisation step, the objective function c_t will be minimised by varying the value of $\mathbf{t}$, given the previously determined rotations, $\mathbf{r}^*$,

$$\min c_t\big(\mathbf{K}(\mathbf{K}^o, \mathbf{r}^*, \mathbf{t})\big). \qquad (4)$$

An example for this criterion applied to the knee joint could be the sum of the RMS of the three translations,

$$e.g. \quad \min\left(c_t = \sqrt{\frac{1}{N}\sum_{n=0}^{N}\big(\mathbf{K_{4,n}}\big)^2} + \sqrt{\frac{1}{N}\sum_{n=0}^{N}\big(\mathbf{K_{5,n}}\big)^2} + \sqrt{\frac{1}{N}\sum_{n=0}^{N}\big(\mathbf{K_{6,n}}\big)^2}\right). \qquad (5)$$

After this second stage, optimal relative frame translations, $\mathbf{t}^*$, are also known and the segment kinematics can thus be represented in the REFRAME reference frames,

$$\mathbf{K}^* = \boldsymbol{\kappa}(\mathbf{K}^0, \mathbf{r}^*, \mathbf{t}^*), \qquad (6)$$

where $\mathbf{K}^*$ represents the updated ("REFRAMEd") kinematic signals.

2.2. Application

In order to validate the ability of REFRAME to achieve convergent kinematic signals in all six DOFs, *in vivo* knee kinematic data from a previous study were utilised. Here, five gait cycles of stair descent were collected using moving videofluoroscopy [37, 38]. In their study, Postolka et al. [1] presented multiple different approaches to define flexion/extension axes and describe the motion of the joint, including the cylindrical axis (CA) [12-14], the functional flexion axis (FFA) based on the symmetrical axis of rotation approach (SARA) [17], and the transepicondylar axis (TEA) [10, 11]. Stair descent was selected for REFRAME validation because it follows the familiar pattern of level walking, while including deeper flexion angles and thus better highlighting cross-talk effects. Importantly, this original study revealed clear differences in the interpretation of the joint movement patterns in the anteroposterior direction according to the analysis approach used (emphasising the need for methods such as RE-FRAME).

In our study (Part I), data from one (female; 22 years old; BMI of 19.3 kg/m²) of these originally evaluated subjects [1] was used as a proof-of-concept for the REFRAME approach. Similar to that previous study, axes for ab/adduction and int/external rotation, as well as a femoral coordinate system origin, were defined based on each of the three primary axis (CA, FFA, TEA) variations, while a single coordinate system was defined for the tibial segment (Figure 1). A temporary shaft axis was first defined by fitting a cylinder to the proximal femoral shaft. The femur anteroposterior axis was then orthogonal to this shaft axis and the primary axis. The femur longitudinal axis was defined orthogonal to the

anteroposterior and primary axes. The tibial longitudinal axis direction was defined based on the orientation of the tibial shaft. Directions for the anteroposterior and mediolateral tibial axes were defined by leveraging two circles fitted to the tibial cortex. The details of this approach have been previously described [38]. For each of the three femoral axis variations, kinematic signals were calculated for all six DOFs. Flexion/extension (around the X-axis), ab/adduction (around the Y-axis) and int/external rotation (around the Z-axis) were derived as rotations of the tibial relative to the femoral segment frame as an XYZ intrinsic rotation sequence (which, again, is numerically equivalent to a Grood and Suntay based approach, but where extension, adduction and internal tibial rotation are positive for a right knee; see Supplementary Figure S1). On the other hand, anteroposterior (AP), mediolateral (ML) and proximodistal (PD) translations were obtained by calculating the position of the femoral origin relative to the tibial origin, along the tibial segment frame axes. Data for the entire ten subject cohort, as well as a hands-on exploration of the effects of different optimisation criteria and of inter-subject differences after REFRAME can be found in an associated study (Part II) and have been excluded here for brevity and clarity.

The REFRAME approach was then applied to each of these three different sets of axis kinematic signals. As previously described, any full implementation of REFRAME to consistently optimise different sets of joint rotations and translations requires a specific selection of optimisation criteria. In the context of healthy knees, for joint rotations, we chose to optimise frame orientation by minimising root-mean-square (RMS) ab/adduction and int/external rotation. Here, this minimisation process inherently ensures that the large flexion/extension rotations are excluded from the ab/adduction and int/external rotations, hence producing frame orientations with minimal cross-talk effects. Joint translations were then optimised by minimising the variances of all three translational kinematic signals (AP, ML and PD), in line with an expected ideal signal with minimal amplitude, where the femoral and tibial origins are not necessarily coincident during a neutral reference pose. All optimisation criteria were weighted equally. The resultant frame transformations were then applied to the raw femoral and tibial frames respectively, to obtain a new set of modified local segment frames. A corresponding set of modified (hereinafter also referred to as "REFRAMEd") kinematic signals was calculated based on the relative orientation and position of these modified frames, and then plotted over the progression of one activity cycle. Finally, root-mean-square error (RMSE) values were calculated between all possible pairwise comparisons of the three sets of kinematic signals, both before (i.e. for raw signals) and after (i.e. for modified signals) REFRAME implementation.

2.3. Statistical Analysis

The goal of statistical analysis was to compare the mean outcomes of applying two different data processing methods (without REFRAME vs. with REFRAME) to multiple trials of the same subject. Given as each gait cycle was processed individually, the (probabilistic) event of REFRAME significantly affecting the RMSEs of any one trial would not change the likelihood that the same or a different effect would be observed for any other trial. Consequently, trials in this context can in fact be considered independent. Shapiro-Wilk tests [39] with a significance level of 5% were used to verify that the assumption of a normal distribution could not be excluded. Paired t-tests [40] were then used to evaluate whether differences were statistically significant at a 5% significance level. To account for the fact that three comparisons were performed (1 – CA vs. FFA, 2 – CA vs. TEA, 3 – FFA vs. TEA), significance levels were Bonferroni corrected with n = 3 to 1.67%. In cases where Shapiro-Wilk tests led to rejection of the normality assumption, the non-parametric alternative to paired t-testing was additionally performed, i.e. Wilcoxon Signed Rank testing [41] (left-tailed, 5% significance level). Processing of

kinematic data was performed using custom MATLAB scripts (vR2022a; The Mathworks Inc., Natick, Massachusetts, USA). Statistical analyses were run using GraphPad Prism 9 (v9.5.1; GraphPad Software Inc.; San Diego, CA, USA).
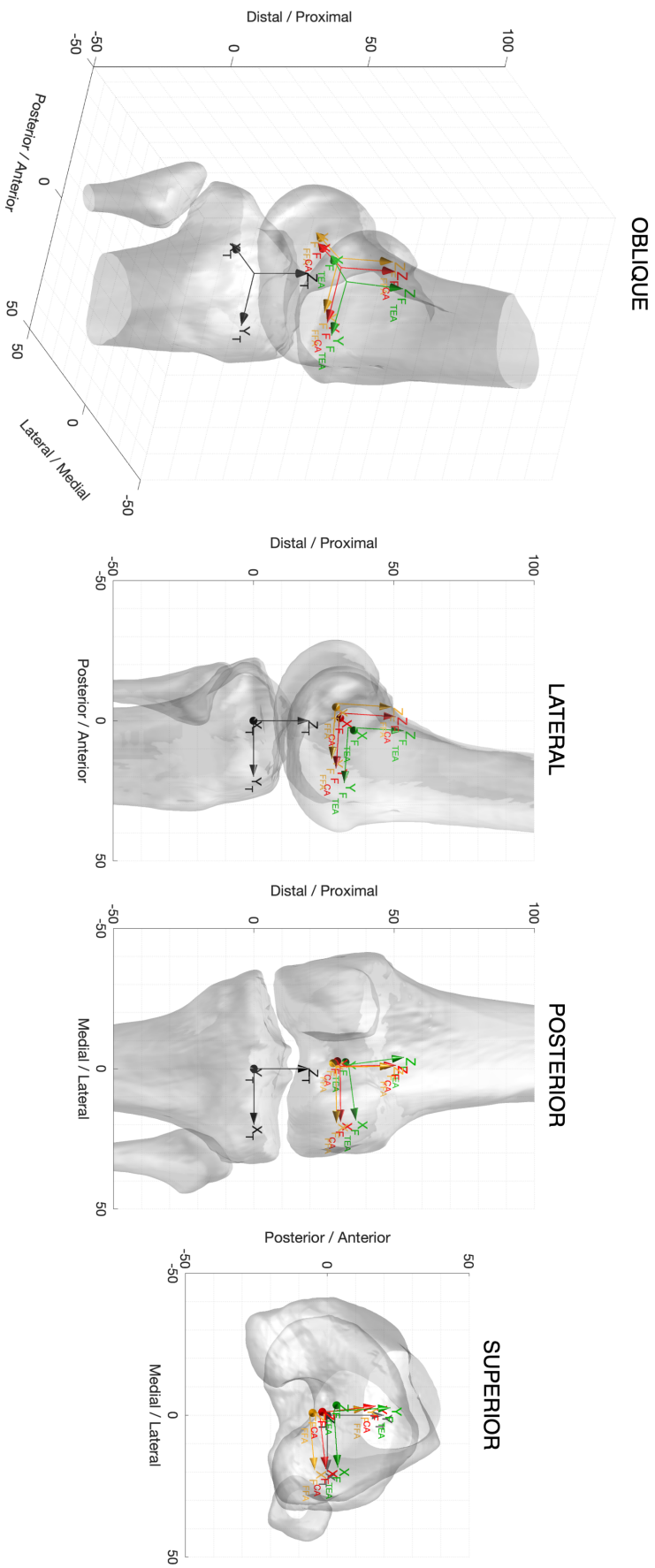
Figure 1. Raw local segment reference frames: Three different femoral reference frames (in red, yellow and green) were defined based on each of three analysis approaches (CA: cylindrical axis; FFA: functional flexion axis; TEA: transepicondylar axis). A single common raw reference frame was defined for the tibia (in black). All coordinate systems and bone segments are shown here relative to the raw tibial coordinate system (i.e. the raw tibia origin is at 0,0,0).

83

3. Results

Differences could be observed between the three raw sets of kinematic signals for the five trials of stair descent according to the analysis approach used (CA, FFA, TEA). For rotations, the largest differences were observed primarily in the frontal and transverse planes (Figure 2); for translations, primarily in the sagittal plane (Figure 3).

Application of the REFRAME approach to the raw kinematic signals originating from the same underlying movement then led to local frame reorientation and translation of 4.47° (around the corresponding screw axis; for XYZ intrinsic Cardan angle sequence see Table 1 and Supplementary Table S1) and 14.1 mm (net absolute displacement; for individual displacement along each axis see Table 1 and Supplementary Table S1) on average for the femoral frame, and 9.99° and 0 mm on average for the tibial frame (Figure 4), resulting in convergence of the modified kinematic signals for all three rotations throughout the entire activity cycle (Figure 2) – for brevity, only trial 1 is shown, but trials 2-5 are presented in the Supplementary Material (Figures S2, S4, S6 and S8). Visible improvements in signal convergence were substantiated by maximum differences between curves (quantified by peak mean RMSEs) of 0.24° ± 0.17° after REFRAME optimisation (Table 2).

Similarly, after application of REFRAME to the reference frame translations, almost no obvious differences were discernible between the optimised translational kinematic signals (Figure 3) – trial 1 shown; trials 2-5 are given in the Supplementary Material (Figures S3, S5, S7 and S9). Peak mean RMSEs for ML (from 0.54 mm ± 0.09 mm to 0.03 mm ± 0.01 mm), AP (from 4.91 mm ± 0.10 mm to 0.02 mm ± 0.01 mm) and PD (from 8.32 mm ± 0.05 mm to 0.02 mm ± 0.00 mm) translations decreased across all trials (Table 2).

In the pairwise comparison between axis approaches, decreases in the RMSEs of out-of-sagittal plane rotations as a result of REFRAME implementation were deemed statistically significant (Figure 5). (Differences in int/external rotation between CA vs. FFA did not pass the Shapiro-Wilk test for normality, so a left-tailed Wilcoxon Signed Rank test was performed in addition to the default paired t-test. The decrease was still found to be statistically significant with a p-value of 0.03125. Notably, however, for a sample size of 5 pairs with a non-zero difference, the minimum p-value that can be obtained with a Wilcoxon Signed Rank test in the extreme case where all values in one group are greater than the other is in fact 0.03125 [42].) Similarly, statistically significant decreases were observed in the RMSEs of joint translations, especially for the anteroposterior and mediolateral directions (Figure 6). The statistically significant effects identified here (except for CA vs. FFA int/external rotation) would withstand even more conservative implementations of the Bonferroni correction, e.g. if the number of comparisons were to be considered 18 (6 degrees of freedom x 3 axis comparisons) instead of 3.
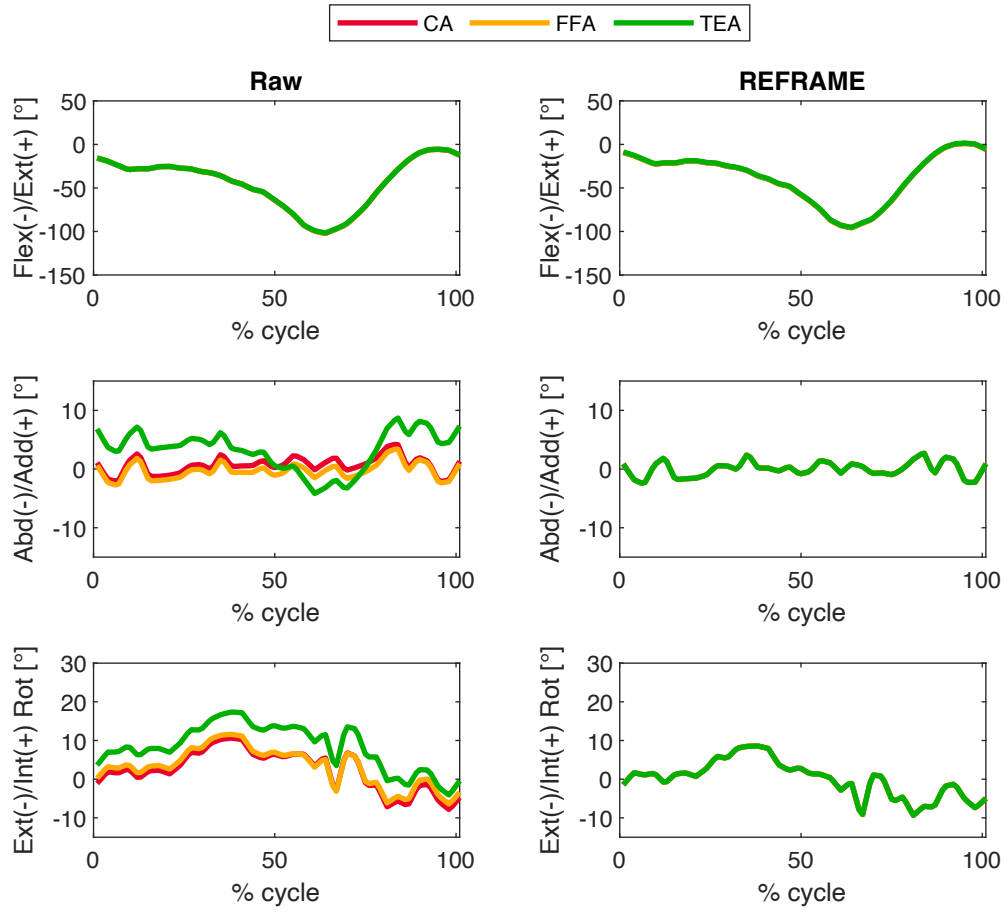
Figure 2. Rotational kinematics: Joint rotations (in degrees) of the tibial relative to the femoral segment frame for one sample cycle of stair descent (trial 1), before (Raw) and after REFRAME optimisation, for all three axis approaches (CA: cylindrical axis; FFA: functional flexion axis; TEA: transepicondylar axis). Curves overlap in right-hand side plots; CA and FFA are almost fully covered by TEA.
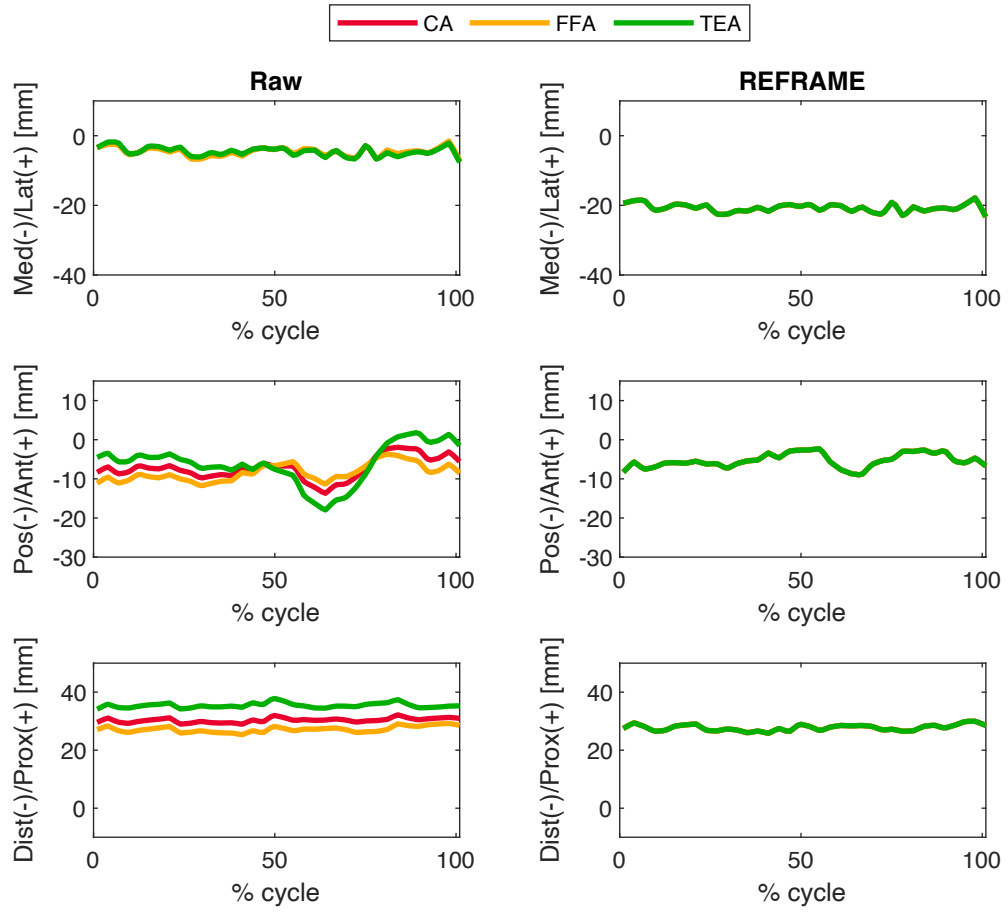
Figure 3. Translational kinematics: Joint translations (in mm) of the femoral relative to the tibial origin for one sample cycle of stair descent (trial 1), before (Raw) and after application of the REFRAME optimisation, for all three axis approaches (CA: cylindrical axis; FFA: functional flexion axis; TEA: transepicondylar axis). Curves overlap in right-hand side plots; CA and FFA are almost fully covered by TEA.

Table 1. Average (of absolute values) rotations (in degrees) and translations (in mm) applied to raw local reference frames to transform them into the REFRAMEd reference frames; Rotations are expressed as an XYZ intrinsic Cardan angle sequence.

		CA	FFA	TEA
Femur				
Rot [°]	X	0.02 ± 0.03	0.02 ± 0.01	0.20 ± 0.18
	Y	1.52 ± 1.00	1.42 ± 1.00	8.29 ± 1.00
	Z	2.36 ± 1.71	1.47 ± 1.16	1.53 ± 0.69
Trans [mm]	X	12.92 ± 3.30	12.86 ± 3.30	13.17 ± 3.22
	Y	2.66 ± 0.60	0.52 ± 0.39	8.21 ± 0.50
	Z	1.95 ± 0.53	0.50 ± 0.22	3.77 ± 0.86
Tibia				
Rot [°]	X	9.39 ± 6.43	9.40 ± 6.42	9.34 ± 6.43
	Y	1.41 ± 1.33	1.41 ± 1.33	1.41 ± 1.33
	Z	2.26 ± 1.17	2.26 ± 1.17	2.26 ± 1.17
Trans [mm]	X	0.00 ± 0.00	0.00 ± 0.00	0.00 ± 0.00
	Y	0.00 ± 0.00	0.00 ± 0.00	0.00 ± 0.00
	Z	0.00 ± 0.00	0.00 ± 0.00	0.00 ± 0.00
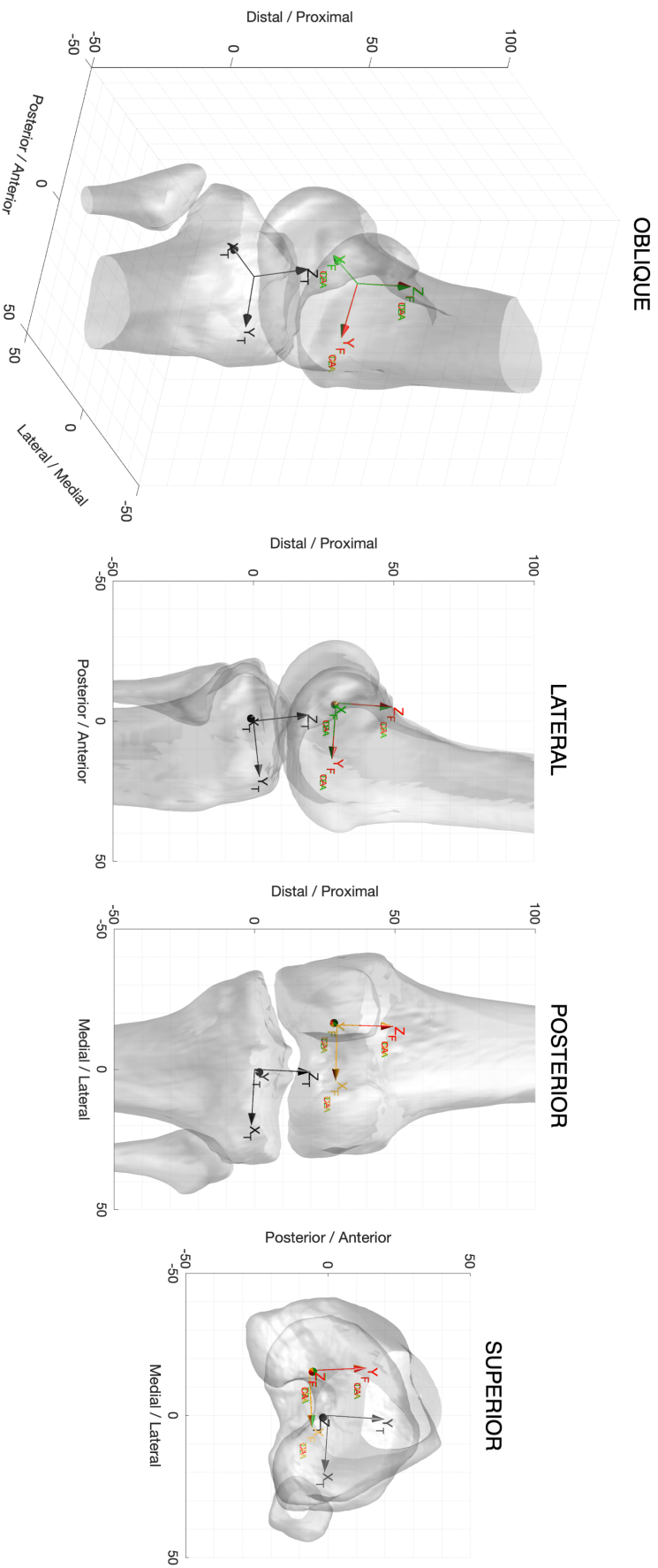
Figure 4. Optimised local segment reference frames after REFRAME: The previously differently oriented and positioned femoral reference frames (CA: cylindrical axis in red; FFA: functional flexion axis in yellow; TEA: transepicondylar axis in green) visibly coincide in 3D space after REFRAME. A single representative optimised tibia reference frame is illustrated here in black (transformations of the tibia frame as result of REFRAME were consistent across all three datasets to 0.1° and 0.00001mm). All coordinate systems and bone segments are shown relative to the raw tibial coordinate system (i.e. the raw tibia origin is at 0,0,0).

88

Table 2. Root-mean-square error (rotations in degrees, translations in mm; ML – mediolateral, AP – anteroposterior, PD – proximodistal) between kinematic signals resulting from different axis approaches ((CA: cylindrical axis; FFA: functional flexion axis; TEA: transepicondylar axis), before ((Raw)) and after REFRAME implementation.

	Trial 1		Trial 2		Trial 3		Trial 4		Trial 5		Mean ± SD	
	Raw	REFRAME	Raw	REFRAME	Raw	REFRAME	Raw	REFRAME	Raw	REFRAME	Raw	REFRAME
CA vs. FFA												
Flex/Ext	0.08	0.06	0.06	0.05	0.08	0.06	0.08	0.09	0.07	0.08	0.07 ± 0.01	0.07 ± 0.02
Ab/Add	0.99	0.00	1.01	0.00	1.01	0.00	1.01	0.00	1.02	0.00	1.01 ± 0.01	0.00 ± 0.00
Int/Ext	1.01	0.00	0.99	0.00	0.99	0.00	0.99	0.00	0.99	0.00	0.99 ± 0.01	0.00 ± 0.00
ML	0.20	0.02	0.23	0.02	0.17	0.03	0.24	0.02	0.27	0.01	0.22 ± 0.04	0.02 ± 0.01
AP	2.06	0.00	2.00	0.00	2.04	0.01	2.03	0.01	1.96	0.00	2.02 ± 0.04	0.00 ± 0.00
PD	3.17	0.01	3.20	0.01	3.18	0.01	3.18	0.01	3.22	0.01	3.19 ± 0.02	0.01 ± 0.00
CA vs. TEA												
Flex/Ext	0.24	0.43	0.24	0.15	0.31	0.08	0.26	0.14	0.27	0.42	0.26 ± 0.03	0.24 ± 0.17
Ab/Add	4.20	0.00	4.09	0.01	4.15	0.01	4.14	0.01	4.03	0.00	4.12 ± 0.07	0.01 ± 0.00
Int/Ext	6.09	0.01	6.17	0.01	6.12	0.01	6.13	0.02	6.22	0.01	6.15 ± 0.05	0.01 ± 0.00
ML	0.28	0.01	0.34	0.01	0.24	0.04	0.33	0.03	0.39	0.02	0.32 ± 0.06	0.02 ± 0.01
AP	2.96	0.01	2.89	0.01	2.96	0.04	2.95	0.02	2.82	0.01	2.92 ± 0.06	0.02 ± 0.01
PD	5.12	0.01	5.15	0.01	5.12	0.01	5.12	0.01	5.19	0.01	5.14 ± 0.03	0.01 ± 0.00
FFA vs. TEA												
Flex/Ext	0.19	0.37	0.22	0.10	0.25	0.01	0.21	0.05	0.23	0.34	0.22 ± 0.02	0.18 ± 0.17
Ab/Add	4.58	0.01	4.45	0.01	4.50	0.01	4.47	0.01	4.42	0.01	4.49 ± 0.06	0.01 ± 0.00
Int/Ext	5.37	0.01	5.47	0.01	5.43	0.01	5.45	0.01	5.50	0.01	5.44 ± 0.05	0.01 ± 0.00
ML	0.48	0.03	0.57	0.02	0.41	0.02	0.57	0.05	0.65	0.03	0.54 ± 0.09	0.03 ± 0.01
AP	5.00	0.01	4.87	0.01	4.98	0.04	4.96	0.02	4.76	0.02	4.91 ± 0.10	0.02 ± 0.01
PD	8.28	0.01	8.35	0.02	8.29	0.02	8.29	0.02	8.41	0.02	8.32 ± 0.05	0.02 ± 0.00
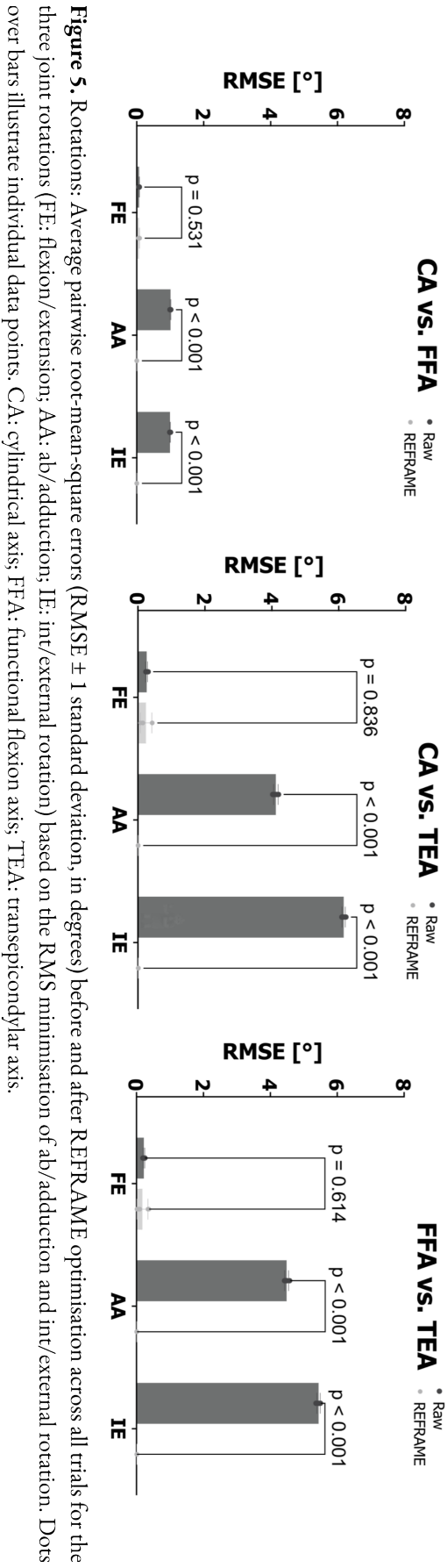
Figure 5. Rotations: Average pairwise root-mean-square errors (RMSE ± 1 standard deviation, in degrees) before and after REFRAME optimisation across all trials for the three joint rotations (FE: flexion/extension; AA: ab/adduction; IE: int/external rotation) based on the RMS minimisation of ab/adduction and int/external rotation. Dots over bars illustrate individual data points. CA: cylindrical axis; FFA: functional flexion axis; TEA: transepicondylar axis.
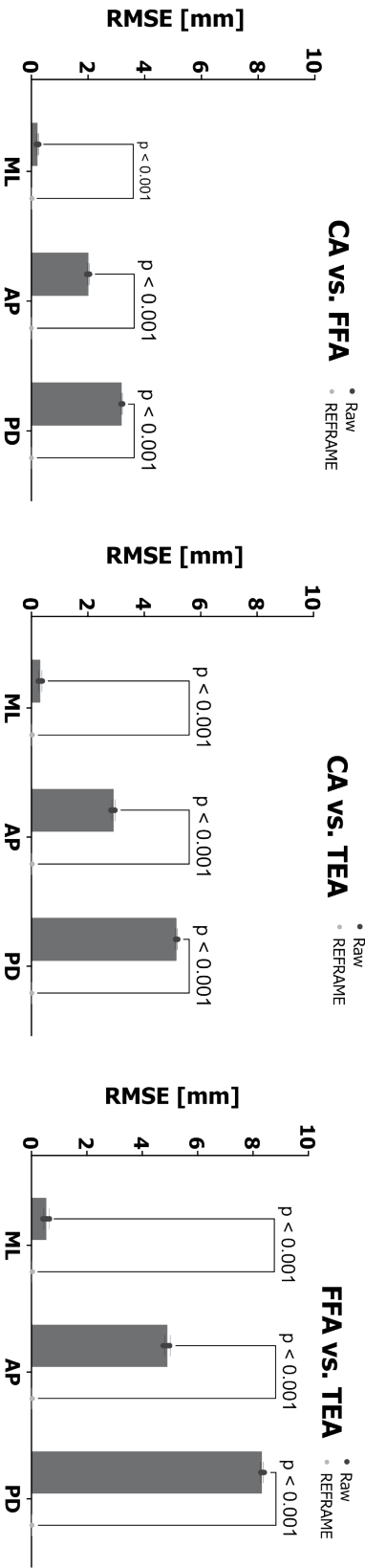
Figure 6. Translations: Average pairwise root-mean-square errors (RMSE ± 1 standard deviation, in mm) before and after REFRAME optimisation across all trials for the three joint translations (ML: mediolateral; AP: anteroposterior; PD: proximodistal) based on the RMS minimisation of ab/adduction and int/external rotation, as well as of AP, ML and PD translations. Dots over bars illustrate individual data points. CA: cylindrical axis; FFA: functional flexion axis; TEA: transepicondylar axis.

90

4. Discussion

In clinical movement biomechanics, analysis of kinematic data is often tackled by focusing on rotations around (or translations along) a single joint axis at a time. For example, a single kinematic curve may depict flexion/extension (i.e. rotations around the mediolateral axis only). Moreover, the origin of each segment coordinate system is often based on anatomical or only limited (e.g. to a calibration trial) functional movement data. Importantly, while this type of analysis demands the definition of segment-fixed axes, previous work has demonstrated that the instantaneous axis or centre of rotation in a joint most likely varies throughout the progression of an activity [1]. Unfortunately, recent work has also shown that even minor differences in the orientation and position of joint segment frames can lead to substantial variation in the characteristics of the resulting kinematic signals [1, 9, 43]. The challenges to provide consistent frame definition and present complex time-dependent 3D kinematic signals in a simplified manner has therefore led to a number of kinematic analysis methods being presented [1, 17]. Use of different analysis approaches has thus resulted in a collection of kinematic signals presented across the literature which, if directly compared without further analysis, easily leads to questionable and/or inconsistent conclusions [1]. In this study, we expand on the previously presented FOOM approach [9] to address these inconsistencies towards mitigating kinematic cross-talk and providing an approach to standardise movement signals of the tibiofemoral joint. Here, to achieve this, we have now considered coordinate system locations (in addition to our previous optimisation of orientations) to provide a general framework, the so-called REFRAME approach, to enable the standardisation of tibiofemoral joint kinematics in all six DOFs. Offered as a set of adaptable MATLAB scripts (vR2022a; The Mathworks Inc., Natick, Massachusetts, USA) upon request, as well as an openly available online tool (accessible through Aesculap AG, https://bbraun.info/reframe, and the ETH Zürich, https://movement.ethz.ch/data-repository/reframe.html), REFRAME allows researchers to independently implement the presented approach and thereby standardise kinematic signals for reproducible representation across trials, subjects, and institutions, regardless of the initial underlying segment frame definitions used.

In this study, we successfully developed the conceptual framework and applied REFRAME to a sample subject's knee kinematic data for five cycles of stair descent. Here, the visible differences in the magnitude and characteristics of the raw kinematic signals obtained from processing the same set of fluoroscopically obtained datapoints with three distinct axis approaches (Figures 2 and 3) corroborate the findings of previous studies [1, 2, 9] and demonstrate the substantial effect that frame pose has on kinematic signals (and thus, by extension, on the clinical understanding of joint motion). Using an implementation of REFRAME that minimises ab/adduction and int/external rotation RMS, and then the variance of all three translations, femoral and tibial segment frames are transformed and become aligned, achieving convergence of the three seemingly distinct raw kinematic signals to a new solution. From over 6° rotation and over 8 mm translation, application of REFRAME has achieved mean RMSEs between approaches of well below 0.5° for rotations and 0.05 mm for translations over five trials. Such results therefore suggest that consistent outcomes and interpretations of kinematic signals can be achieved regardless of the initial analysis method used, but that application of an approach such as REFRAME is required before different kinematic datasets can be compared.

As previously described, the particular combination of optimisation criteria applied in our study is based on the underlying assumption that minimising out-of-sagittal-plane rotations inherently maximises flexion/extension and thus minimises cross-talk [9]. Furthermore, optimisation of joint translations by targeting minimal variances for all three translation signals is consistent with the clinical

expectation that, in the absence of trauma or pathology, any relative displacement between joint segments will be small in magnitude, without requiring that the tibial and femoral origins perfectly coincide at neutral stance. The initial implementation of REFRAME presented in this study is presumed to be suitable for most applications assessing asymptomatic flexion-dominant knee movement patterns, and we therefore tentatively recommend selecting this implementation for gait activities such as level and inclined walking, as well as stair ascent/descent. However, it is important to note that while minimising the RMS of both out-of-sagittal-plane rotations, followed by the variance of all three translations, is a reasonable choice based on expected gait patterns, other less common activities may require a bespoke implementation of REFRAME to ensure that relevant movement characteristics can be discriminated.

Importantly, while REFRAME offers users the flexibility to choose between different objective parameters, the underlying assumptions associated with this choice of optimisation criteria should be critically considered. In the previous example, the optimisation criteria for joint rotations inherently assume that a sinusoidal correlation between flexion/extension and out-of-sagittal-plane rotations is the result of cross-talk and therefore not a "real" movement pattern [9]. Consider a hypothetical subject for whom ab/adduction and int/external rotation values are sinusoidally related to the degree of tibiofemoral flexion/extension; The recommended REFRAME implementation would interpret this relationship as artefact and propose a new set of local frame orientations that suppresses that pattern as far as possible, potentially hiding clinically relevant information. It is therefore crucial that users are aware of such implications before clinically interpreting optimised kinematic signals. In fact, the application of REFRAME based on *any* choice of optimisation criteria will be associated with some underlying assumption(s) about joint behaviour, and local segment frames will, in turn, be modified to fulfil these assumptions as much as possible. As such, implementation of REFRAME for understanding the motion of joints other than the human knee, clearly requires further investigation to provide recommendations of best practice usage. However, for several clinically relevant assessments of the normal knee, REFRAME does now plausibly provide a post-analysis approach for standardising and comparing kinematic signals.

The majority of previously proposed standardisation methods (especially those presented as post-processing cross-talk reduction approaches), have been evaluated on their ability to reduce the correlation between e.g. flexion/extension and ab/adduction [26]. Enforcement of these assumptions is merely a means by which these approaches seek to standardise kinematic signals, but reduced correlations are inherent to the approach and are therefore not an appropriate outcome metric. We therefore suggest that kinematic standardisation methods should be instead evaluated by ensuring 1) that two representations of the same motion can be identified as corresponding to a single underlying movement pattern by simple visual inspection, and 2) that substantial differences between two kinematic signals after they have been properly standardised are a reliable indication that fundamentally different motion profiles are presented. Our results indicate that REFRAME holds the potential to fulfil both of these requirements, therefore making it a strong candidate for kinematic standardisation and repeatable representation of tibiofemoral movement patterns.

## 4.1. Tailoring the optimisation criteria

The optimisation criteria in REFRAME (previously c_r and c_t for rotations and translations, respectively) consist of mathematical functions that characterise the properties of a set of kinematic signals. The choice of optimisation parameter(s) should be methodically suited to address each specific

underlying research question, and is expected to vary for different joints, pathologies, and activities. Aside from the previously introduced RMS, examples of possible functions include e.g. the minimisation of variance, the sum of absolute values, the maximum absolute value, and/or the range of motion over an activity cycle. Whichever criteria are selected, these functions will be used to quantify the extent to which a specific kinematic signal deviates from an assumed or expected behaviour (Table 3). Here, for example, our implementation of REFRAME that minimised the RMS of ab/adduction and int/external rotation inherently orients the reference frames to produce the best possible hinge joint at the knee. Any remaining signal around these secondary axes is then assumed to be the cross-talk-free motion of the knee joint. However, it is entirely reasonable to use different optimisation criteria to best understand other joint movement patterns where flexion/extension is not necessarily the dominant joint rotation (e.g. sidestep cutting or knee rotational laxity tests [44]).

REFRAME optimisation criteria can also be given different weights to specify how their fulfilment should be prioritised within the optimisation process. The use of different functions to define the optimisation criteria clearly has different effects on the characteristics of the resulting kinematic signals (Figure 7). Needless to say, it is possible to combine the use of different functions for different kinematic parameters (e.g. minimise the *RMS* of int/external rotation, but the *variance* of ab/adduction, equally weighted). Furthermore, as previously shown [9], it is also possible to optimise the joint segment frames towards an "ideal" reference kinematic pattern by minimising the RMSE against a reference dataset, e.g. within mechanical or simulator setups. Moreover, customised objective functions can be designed that similarly penalise deviations from such reference signals, or even from one (or more) of the raw signals themselves (e.g. if we assume that certain raw rotation values are sufficiently accurate and should not be considerably affected by REFRAME optimisation). In this sense, REFRAME is highly flexible and can be tuned to address individual needs in many different fields.

Table 3. Examples of possible building blocks for the objective functions.

Parameter	Associated expected behaviour
Sum of absolute values or average of absolute values	Very small (or zero) rotations/translations
RMS or quadratic mean (i.e. RMSE against a constant zero reference signal)	Very small (or zero) rotations/translations; higher deviations have a greater weight
Variance	Any (close to) constant value
Maximum absolute value	Extrema occur at small values of rotation/translation
Range of motion over the activity cycle (i.e. *maximum-minimum*)	Small peak-to-peak amplitude
RMSE against reference data	"Ideal" kinematic curve given by a reference dataset
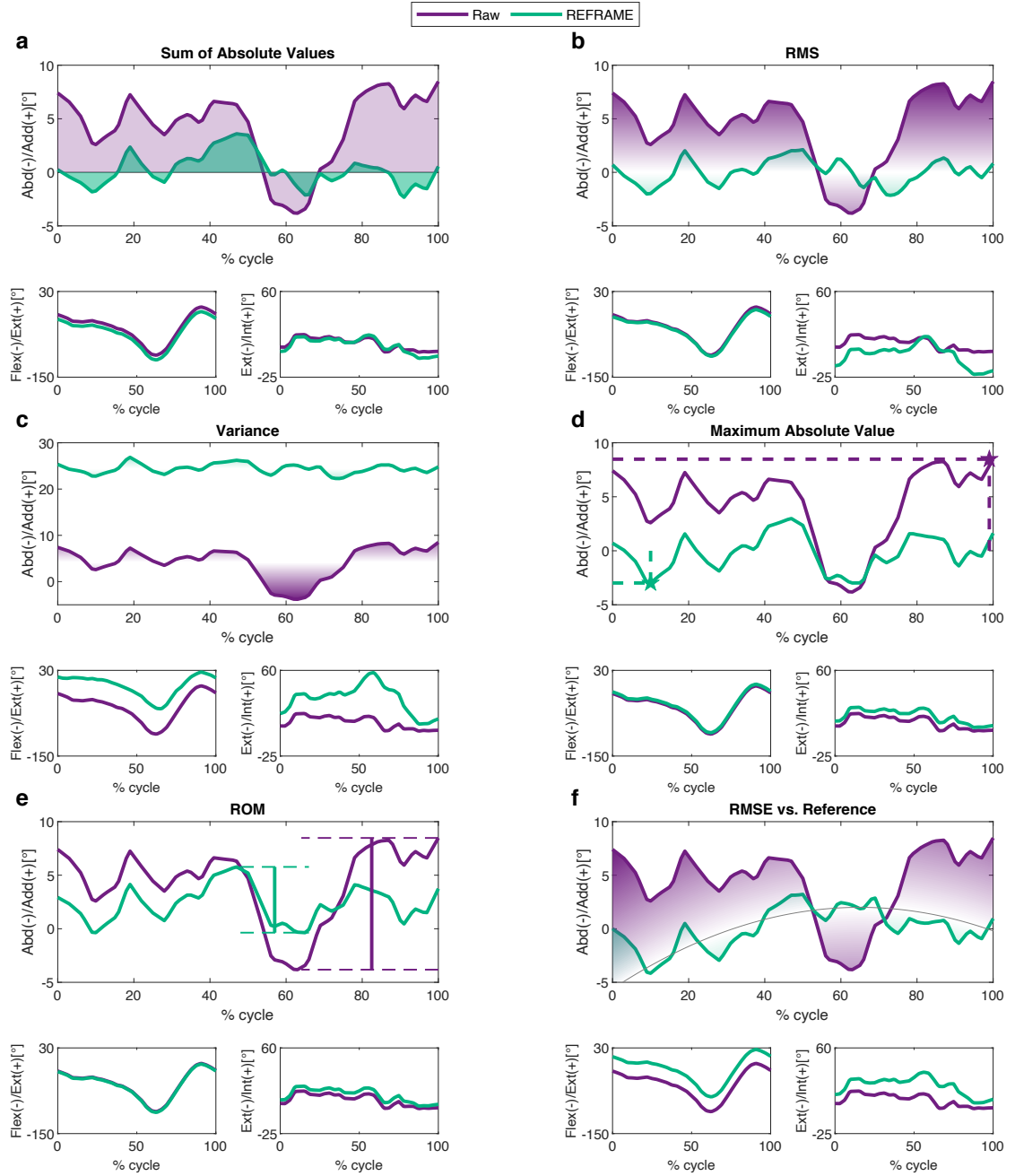
Figure 7. Illustration of the effects of optimising ab/adduction based on different statistical parameters – Joint rotations (in degrees) of the tibial relative to the femoral segment frame during stair descent (trial 2) based on a transepicondylar axis approach. "Raw" signals (green) are processed using six different REFRAME implementations to yield REFRAMEd signals (purple). Each figure panel illustrates minimisation of a different statistical parameter: a) Sum of absolute values – i.e. shaded area (deviation from zero) is minimised; b) Root-mean-square – i.e. shaded area (deviation from zero) is minimised, colour gradient reflects higher weighting of values further from zero; c) Variance – i.e. shaded area (deviation from mean) is minimised, colour gradient reflects higher weighting of larger deviations; d) Maximum absolute value – i.e. peak absolute value (indicated with a star) is minimised; e) Range of motion – i.e. difference between maximum and minimum values (indicated by annotation) is minimised; f) Root-mean-square error vs. an arbitrary sample reference signal $f(t) = -4.5 \left(\frac{t-65}{50} \right)^2 + 2$ – i.e. shaded area is minimised, colour gradient reflects higher weighting of differences with a larger absolute magnitude.

94

Although the use of different parameters potentially influences the characteristics of the RE-FRAMEd signals (Figure 7), five different REFRAME implementations did achieve convergence for all three rotational signals, regardless of the optimisation parameter selected (Figure 8). Similar results were observed for joint translations, demonstrating convergence after REFRAME optimisation (Figure 9). The exclusive use of variance or ROM to guide the optimisation of joint translations is at this time recommended only with great caution, as these two parameters are not thought to guarantee signal convergence. This hypothesis is associated with the fact that while RMS, sum of absolute values, and maximum absolute value all involve a quantification of the signal's absolute *magnitude* (whether on average or at a discrete timepoint), ROM and variance exclusively target the signal's *amplitude.* Our reasoning suggests that multiple (possibly infinite) solutions that minimise ROM or variance may exist, and therefore signal convergence is not guaranteed for joint translations based on these optimisation criteria. In the example presented in this study, by restricting only the level of *variation* in the position of the femoral origin (expressed in the tibial frame), but not its *absolute* value, the optimisation may propose femoral and tibial origins that are either very close to each other, very far from each other, or anything in between, while still achieving the same level of variation in the femoral frame's position. The same effect is not observed when using ROM or variance to optimise joint rotations, presumably due to the order-dependent nature of rotational sequences (although further work is needed to better understand these effects).
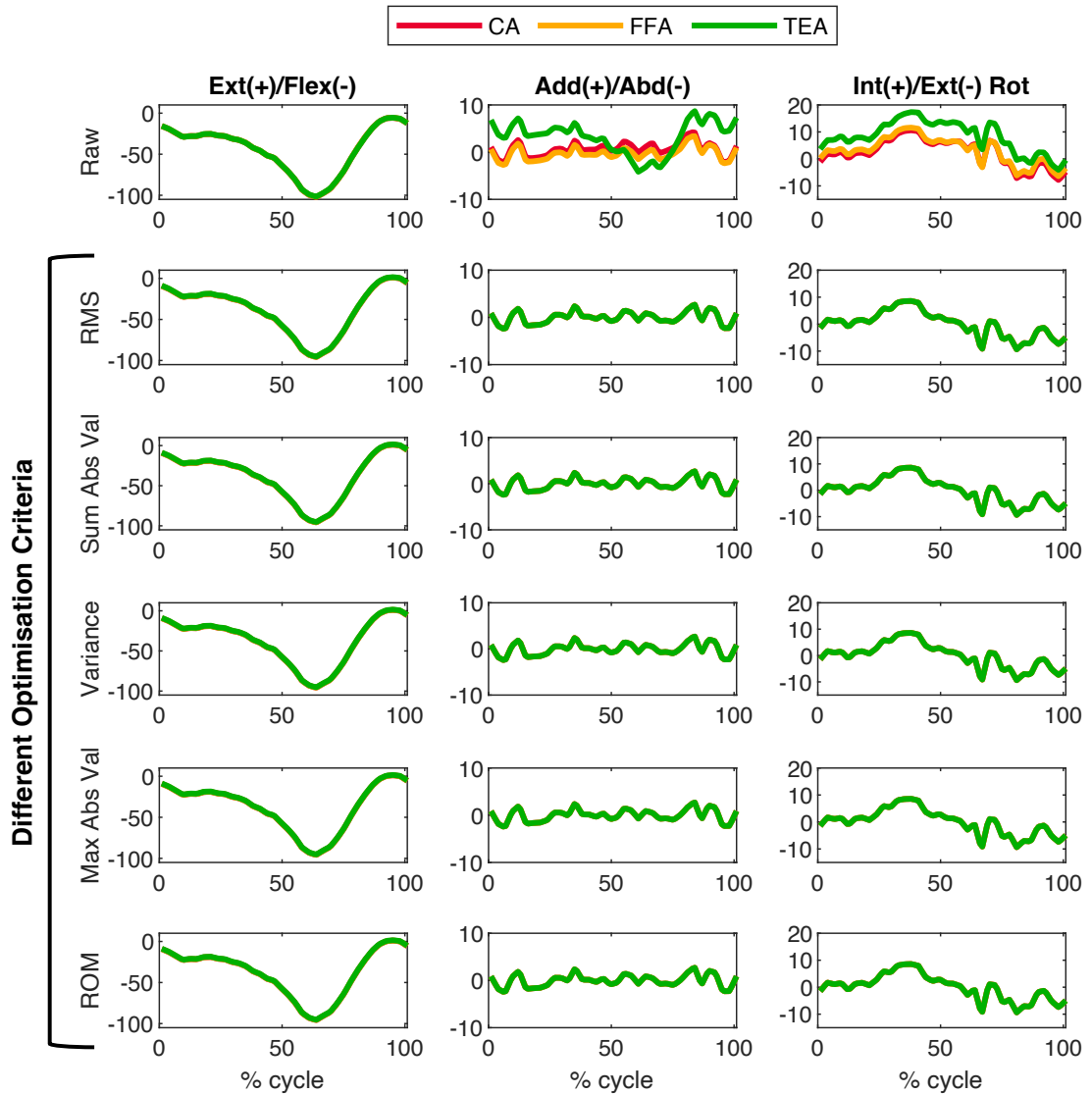
Figure 8. Different parameters as optimisation criteria – Rotational kinematics: Joint rotations (in degrees) of the tibial relative to the femoral segment frame during one cycle of stair descent (trial 1) for all three axis approaches (CA: cylindrical axis; FFA: functional flexion axis; TEA: transepicondylar axis). Kinematic signals are shown before (row 1) and after (rows 2-6) five different REFRAME implementations, where each implementation minimises one of five statistical parameters for ab/adduction and int/external rotation (RMS: Root-mean-square; Sum Abs Val: Sum of absolute values; Variance; Max Abs Val: Maximum absolute value; ROM: Range of motion over single activity cycle). Note: In several plots, CA and FFA are covered by TEA.
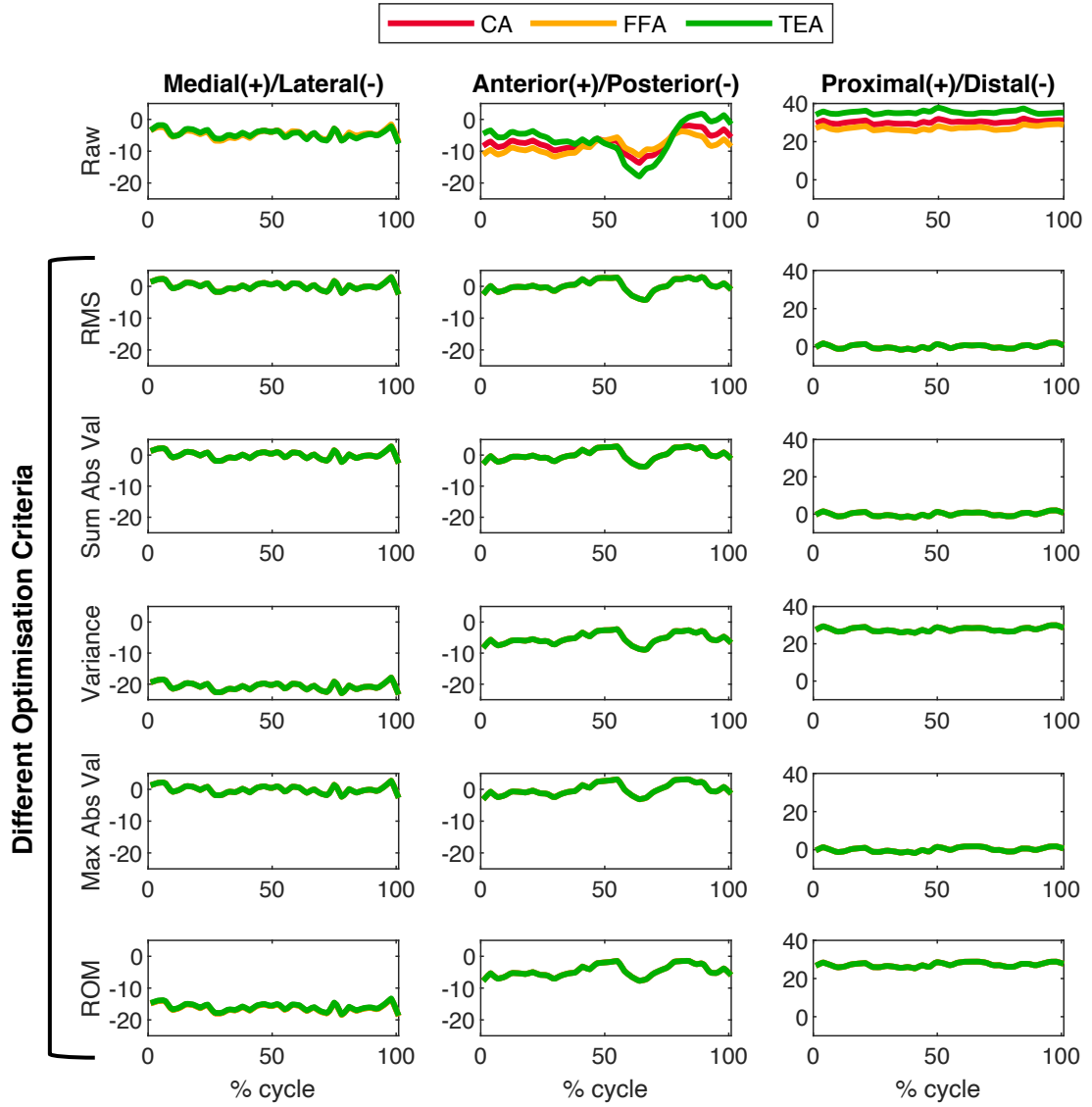
Figure 9. Different parameters as optimisation criteria – Translational kinematics: Joint translations (in mm) of femoral origin relative to tibial origin, along tibial frame axes over one cycle of stair descent (trial 1) for all three flexion/extension axis approaches (CA: cylindrical axis; FFA: functional flexion axis; TEA: transepicondylar axis). Kinematic signals are shown before (row 1) and after (rows 2-6) five different REFRAME implementations, where each implementation minimises RMS of ab/adduction and int/external rotation in stage I, followed by a minimisation of one of five statistical parameters for all three joint translations (RMS: Root-mean-square error; Sum Abs Val: Sum of absolute values; Variance; Max Abs Val: Maximum absolute value; ROM: Range of motion over single activity cycle). Note: In several plots, CA and FFA are partially covered by TEA.

4.2. Clinically interpreting REFRAMEd kinematic signals

We have demonstrated that signal convergence can be achieved using a variety of different statistical parameters to define REFRAME's underlying objective function (Figures 8 and 9). However, results also showed that the magnitudes and characteristics of the optimised kinematic signals are influenced by this choice of statistical parameter (Figure 7). Application of REFRAME therefore leads to a

fundamental far-reaching question: How can we clinically interpret REFRAMEd kinematic signals? While this overarching issue is largely philosophical in nature, reaching a consensus will inevitably require a discussion of its practical implications. Biomechanical engineers need to work closely with clinical practitioners to ultimately agree on a representation of joint kinematics that is not only objectively unambiguous and mathematically coherent, but also intuitive to clinicians and in keeping with their occupational understanding of physiological joint movement. Interestingly, while it is true that applying objective functions that target different statistical parameters of a *single* DOF clearly leads to different optimised signals (Figure 7), application of objective functions that target the same statistical parameter for two or more DOFs led to a rather consistent set of optimised signals (Figures 8 and 9). In fact, in this study, the optimised signals for joint translations are fairly uniform across statistical parameters. Comparison of the rotational and translational results clearly reveals convergence of the rotational signals, but variation in the magnitude of the translational values, even though the patterns are almost identical. Preliminary attempts at interpreting these signals can be achieved through reconciliation with existing knowledge. For example, after REFRAME optimisation, translational kinematics repeatedly converged on an AP signal with a range of about 7 mm for this particular subject. Intuitively, envisioning solely what is usually clinically understood by AP translation between the femur and tibia (i.e. excluding any cross-talk effects entirely) in a healthy subject with intact soft-tissue structures, 7 mm of displacement seems highly plausible, especially considering the proximal tibia has an average AP dimension of about 50 mm [45, 46]). However, notwithstanding the possibility to make further first crude attempts at clinically interpreting REFRAMEd signals, the clinical "accuracy" of the values given by the REFRAMEd kinematic signals is very much open for debate, and additional efforts are certainly needed before any kind of consensus can be reached. Importantly, REFRAME does not aim to improve the clinical accuracy of raw kinematic signals, nor does it claim to find the *true* or *correct* flexion/extension axis, etc., but rather aims to make it easier to determine whether two kinematic signals represent fundamentally similar or different underlying motion.

4.3. Conclusion

This study confirmed that reconciling any possible differences in segment frame pose is essential to allow the consistent interpretation and comparison of articulating joint kinematic signals across studies. Furthermore, while a complete understanding of the clinical significance of optimised kinematic signals will certainly require further investigation *and* discussion, REFRAME demonstrates flexibility and consistency in its ability to optimise local segment frame orientation and position. While this potential was established here for understanding tibiofemoral kinematics, REFRAME is presumed to offer similar possibilities for other articulating joints towards understanding movement patterns and e.g. joint stability/laxity [47], although additional work will be necessary to corroborate these conjectures. Importantly, our results have highlighted that without an approach like REFRAME, we cannot exclude the possibility that differences observed between two (or more) kinematic signals are simply the result of discrepancies in frame alignment. Neither can we, by extension, make reliable conclusions about clinical differences in joint movement patterns without REFRAME (except for in very specific scenarios). Consequently, by holding the potential to enable reliable comparisons of kinematic signals across trials, subjects, examiners, motion capture systems, or even research institutes, REFRAME represents a valuable step forward in improving our collective understanding of articulating joint motion, at least within the context of the tibiofemoral joint.

Author contributions

Data availability

The presented method (REFRAME) can be openly implemented by downloading the standalone application and accompanying user documentation available in https://bbraun.info/reframe and https://movement.ethz.ch/data-repository/reframe.html. Additional MATLAB files to enable advanced custom features are also available under license from the corresponding author upon reasonable request. The original subject data used during the current study to validate the proposed method is part of a larger dataset generated within the scope of a separate, previously published study [1]. For further information regarding the data availability of this referenced kinematic dataset, please refer to the original article available here: https://doi.org/10.1016/j.jbiomech.2022.111306; and/or contact the respective corresponding author of that study.

Acknowledgements

Ethics declarations

This study relied on previously published datasets and therefore did not directly involve humans. Collection of the original fluoroscopy data that was analysed here as part of the method's validation occurred within the scope of a separate cited study, stating that "all subjects provided written, informed consent to participate in this study, which was approved by the local ethics committee (KEK-ZH-Nr. 2016-00410)" [1].

Competing interests

A.O.V., A.M., T.G. and A.S. are employees of B. Braun Aesculap AG, Tuttlingen, Germany. W.T. has received compensation as a member of a scientific advisory board of the company. M.W. leads the applied biomechanics research group at the Musculoskeletal University Center Munich (MUM), which has received research funding from Aesculap AG in the past. A.O.V., A.S., and A.M. are all listed as co-inventors on a pending patent application submitted by Aesculap AG under number DE102022125697A1, which claims a system for standardising axis orientation and position in kinematic data relating to a patient's body joint. A version of the REFRAME code is nevertheless openly available upon request for non-commercial purposes.

References

1.   Postolka, B., Taylor, W.R., Datwyler, K., Heller, M.O., List, R., and Schütz, P., *Interpretation of natural tibio-femoral kinematics critically depends upon the kinematic analysis approach: A survey and comparison of methodologies.* Journal of Biomechanics, 2022. **144**: p. 111306.

2.   Sauer, A., Kebbach, M., Maas, A., Mihalko, W.M., and Grupp, T.M., *The Influence of Mathematical Definitions on Patellar Kinematics Representations.* Materials, 2021. **14**(24).

3.   Lenz, A.L., Strobel, M.A., Anderson, A.M., Fial, A.V., Macwilliams, B.A., Krzak, J.J., and Kruger, K.M., *Assignment of local coordinate systems and methods to calculate tibiotalar and subtalar kinematics: A systematic review.* Journal of Biomechanics, 2021. **120**: p. 110344.

4.   Kolz, C.W., Sulkar, H.J., Aliaj, K., Tashjian, R.Z., Chalmers, P.N., Qiu, Y., Zhang, Y., Foreman, K.B., Anderson, A.E., and Henninger, H.B., *Reliable interpretation of scapular kinematics depends on coordinate system definition.* Gait & Posture, 2020. **81**: p. 183-190.

5.   Wu, G. and Cavanagh, P.R., *ISB recommendations for standardization in the reporting of kinematic data.* Journal of Biomechanics, 1995. **28**(10): p. 1257-1261.

6.   Grood, E.S. and Suntay, W.J., *A joint coordinate system for the clinical description of three-dimensional motions: application to the knee.* Journal of Biomechanical Engineering, 1983. **105**(2): p. 136-144.

7.   Sheehan, F.T. and Mitiguy, P., *In regards to the "ISB recommendations for standardization in the reporting of kinematic data".* Journal of Biomechanics, 1999. **32**(10): p. 1135-1136.

8.   Macwilliams, B.A. and Davis, R.B., *Addressing some misperceptions of the joint coordinate system.* Journal of Biomechanical Engineering, 2013. **135**(5): p. 54506.

9.   Ortigas-Vásquez, A., Taylor, W.R., Maas, A., Woiczinski, M., Grupp, T.M., and Sauer, A., *A frame orientation optimisation method for consistent interpretation of kinematic signals.* Scientific Reports, 2023. **13**(1): p. 9632.

10.   Berger, R.A., Rubash, H.E., Seel, M.J., Thompson, W.H., and Crossett, L.S., *Determining the rotational alignment of the femoral component in total knee arthroplasty using the epicondylar axis.* Clinical Orthopaedics and Related Research, 1993(286): p. 40-47.

11.   Churchill, D.L., Incavo, S.J., Johnson, C.C., and Beynnon, B.D., *The transepicondylar axis approximates the optimal flexion axis of the knee.* Clinical Orthopaedics and Related Research, 1998(356): p. 111-118.

12.   Kurosawa, H., Walker, P.S., Abe, S., Garg, A., and Hunter, T., *Geometry and motion of the knee for implant and orthotic design.* Journal of Biomechanics, 1985. **18**(7): p. 487-499.

13.   Asano, T., Akagi, M., Tanaka, K., Tamura, J., and Nakamura, T., *In vivo three-dimensional knee kinematics using a biplanar image-matching technique.* Clinical Orthopaedics and Related Research, 2001(388): p. 157-166.

14.   Eckhoff, D.G., Dwyer, T.F., Bach, J.M., Spitzer, V.M., and Reinig, K.D., *Three-dimensional morphology of the distal part of the femur viewed in virtual reality.* Journal of Bone and Joint Surgery, 2001. **83-A Suppl 2**(Pt 1): p. 43-50.

15.   Robinson, M., Eckhoff, D.G., Reinig, K.D., Bagur, M.M., and Bach, J.M., *Variability of landmark identification in total knee arthroplasty.* Clinical Orthopaedics and Related Research, 2006. **442**: p. 57-62.

16.   Morton, N.A., Maletsky, L.P., Pal, S., and Laz, P.J., *Effect of variability in anatomical landmark location on knee kinematic description.* Journal of Orthopaedic Research, 2007. **25**(9): p. 1221-1230.

17.   Ehrig, R.M., Taylor, W.R., Duda, G.N., and Heller, M.O., *A survey of formal methods for determining functional joint axes.* Journal of Biomechanics, 2007. **40**(10): p. 2150-2157.

18.   Asano, T., Akagi, M., and Nakamura, T., *The functional flexion-extension axis of the knee corresponds to the surgical epicondylar axis: in vivo analysis using a biplanar image-matching technique.* The Journal of Arthroplasty, 2005. **20**(8): p. 1060-1067.

19.   Gamage, S.S. and Lasenby, J., *New least squares solutions for estimating the average centre of rotation and the axis of rotation.* Journal of Biomechanics, 2002. **35**(1): p. 87-93.

20.   Besier, T.F., Sturnieks, D.L., Alderson, J.A., and Lloyd, D.G., *Repeatability of gait data using a functional hip joint centre and a mean helical knee axis.* Journal of Biomechanics, 2003. **36**(8): p. 1159-1168.

21.   Kainz, H., Hajek, M., Modenese, L., Saxby, D.J., Lloyd, D.G., and Carty, C.P., *Reliability of functional and predictive methods to estimate the hip joint centre in human motion analysis in healthy adults.* Gait & Posture, 2017. **53**: p. 179-184.

22.   Sangeux, M., *Computation of hip rotation kinematics retrospectively using functional knee calibration during gait.* Gait & Posture, 2018. **63**: p. 171-176.

23.   Woltring, H.J., *3-D attitude representation of human joints: a standardization proposal.* Journal of Biomechanics, 1994. **27**(12): p. 1399-1414.

24.   Baker, R., Finney, L., and Orr, J., *A new approach to determine the hip rotation profile from clinical gait analysis data.* Human Movement Science, 1999. **18**(5): p. 655-667.

25.   Rivest, L.P., *A correction for axis misalignment in the joint angle curves representing knee movement in gait analysis.* Journal of Biomechanics, 2005. **38**(8): p. 1604-1611.

26.   Baudet, A., Morisset, C., D'athis, P., Maillefert, J.F., Casillas, J.M., Ornetti, P., and Laroche, D., *Cross-talk correction method for knee kinematics in gait analysis using principal component analysis (PCA): a new proposal.* PLOS One, 2014. **9**(7): p. e102098.

27.   Kainz, H., Modenese, L., Lloyd, D.G., Maine, S., Walsh, H.P.J., and Carty, C.P., *Joint kinematic calculation based on clinical direct kinematic versus inverse kinematic gait models.* Journal of Biomechanics, 2016. **49**(9): p. 1658-1669.

28.   Leardini, A., Belvedere, C., Nardini, F., Sancisi, N., Conconi, M., and Parenti-Castelli, V., *Kinematic models of lower limb joints for musculo-skeletal modelling and optimization in gait analysis.* Journal of Biomechanics, 2017. **62**: p. 77-86.

29.   Brito Da Luz, S., Modenese, L., Sancisi, N., Mills, P.M., Kennedy, B., Beck, B.R., and Lloyd, D.G., *Feasibility of using MRIs to create subject-specific parallel-mechanism joint models.* Journal of Biomechanics, 2017. **53**: p. 45-55.

30.   Kerkhoff, A., Wagner, H., and Peikenkamp, K., *Comparison of six different marker sets to analyze knee kinematics and kinetics during landings.* Current Directions in Biomedical Engineering, 2020. **6**(2).

31.   Ferrari, A., Benedetti, M.G., Pavan, E., Frigo, C., Bettinelli, D., Rabuffetti, M., Crenna, P., and Leardini, A., *Quantitative comparison of five current protocols in gait analysis.* Gait & Posture, 2008. **28**(2): p. 207-216.

32.   Chiari, L., Croce, U.D., Leardini, A., and Cappozzo, A., *Human movement analysis using stereophotogrammetry: Part 2: Instrumental errors.* Gait & Posture, 2005. **21**(2): p. 197-211.

33.   Benedetti, M.G., Merlo, A., and Leardini, A., *Inter-laboratory consistency of gait analysis measurements.* Gait & Posture, 2013. **38**(4): p. 934-939.

34.   Peters, A., Galna, B., Sangeux, M., Morris, M., and Baker, R., *Quantification of soft tissue artifact in lower limb human motion analysis: a systematic review.* Gait & Posture, 2010. **31**(1): p. 1-8.

35.   Leardini, A., Chiari, L., Della Croce, U., and Cappozzo, A., *Human movement analysis using stereophotogrammetry. Part 3. Soft tissue artifact assessment and compensation.* Gait & Posture, 2005. **21**(2): p. 212-225.

36. Seel, T., Schauer, T., and Raisch, J. *Joint axis and position estimation from inertial measurement data by exploiting kinematic constraints*. in *2012 IEEE International Conference on Control Applications*. 2012.

37. List, R., Postolka, B., Schütz, P., Hitz, M., Schwilch, P., Gerber, H., Ferguson, S.J., and Taylor, W.R., *A moving fluoroscope to capture tibiofemoral kinematics during complete cycles of free level and downhill walking as well as stair descent*. PLOS One, 2017. **12**(10): p. e0185952.

38. Postolka, B., Schütz, P., Fucentese, S.F., Freeman, M.a.R., Pinskerova, V., List, R., and Taylor, W.R., *Tibio-femoral kinematics of the healthy knee joint throughout complete cycles of gait activities*. Journal of Biomechanics, 2020. **110**: p. 109915.

39. Shapiro, S.S. and Wilk, M.B., *An analysis of variance test for normality (complete samples)†*. Biometrika, 1965. **52**(3-4): p. 591-611.

40. Ross, A. and Willson, V.L., *Paired samples T-test*, in *Basic and Advanced Statistical Tests*. 2017, Brill. p. 17-19.

41. Wilcoxon, F., *Individual Comparisons by Ranking Methods*. Biometrics Bulletin, 1945. **1**(6): p. 80-83.

42. Wilcoxon, F., Katti, S., and Wilcox, R.A., *Critical values and probability levels for the Wilcoxon rank sum test and the Wilcoxon signed rank test*. Selected Tables in Mathematical Statistics, 1970. **1**: p. 171-259.

43. Ortigas-Vásquez, A., Maas, A., List, R., Schütz, P., Taylor, W.R., and Grupp, T.M., *A Framework for Analytical Validation of Inertial-Sensor-Based Knee Kinematics Using a Six-Degrees-of-Freedom Joint Simulator*. Sensors, 2022. **23**(1).

44. Moewis, P., Duda, G.N., Jung, T., Heller, M.O., Boeth, H., Kaptein, B., and Taylor, W.R., *The Restoration of Passive Rotational Tibio-Femoral Laxity after Anterior Cruciate Ligament Reconstruction*. PLOS One, 2016. **11**(7): p. e0159600.

45. Chaurasia, A., Tyagi, A., Santoshi, J.A., Chaware, P., and Rathinam, B.A., *Morphologic Features of the Distal Femur and Proximal Tibia: A Cross-Sectional Study*. Cureus, 2021. **13**(1): p. e12907.

46. Mukhopadhaya, J., Kashani, A., Kumar, N., and Bhadani, J.S., *Evaluation of Anthropometric Measurements of the Aspect Ratio of Knee in Indian Population and its Correlation with the Sizing of Current Knee Arthroplasty System*. Indian Journal of Orthopaedics, 2023. **57**(1): p. 110-116.

47. Boeth, H., Duda, G.N., Heller, M.O., Ehrig, R.M., Doyscher, R., Jung, T., Moewis, P., Scheffler, S., and Taylor, W.R., *Anterior cruciate ligament-deficient patients with passive knee joint laxity have a decreased range of anterior-posterior motion during active movements*. The American Journal of Sports Medicine, 2013. **41**(5): p. 1051-1057.

5. Supplementary Material
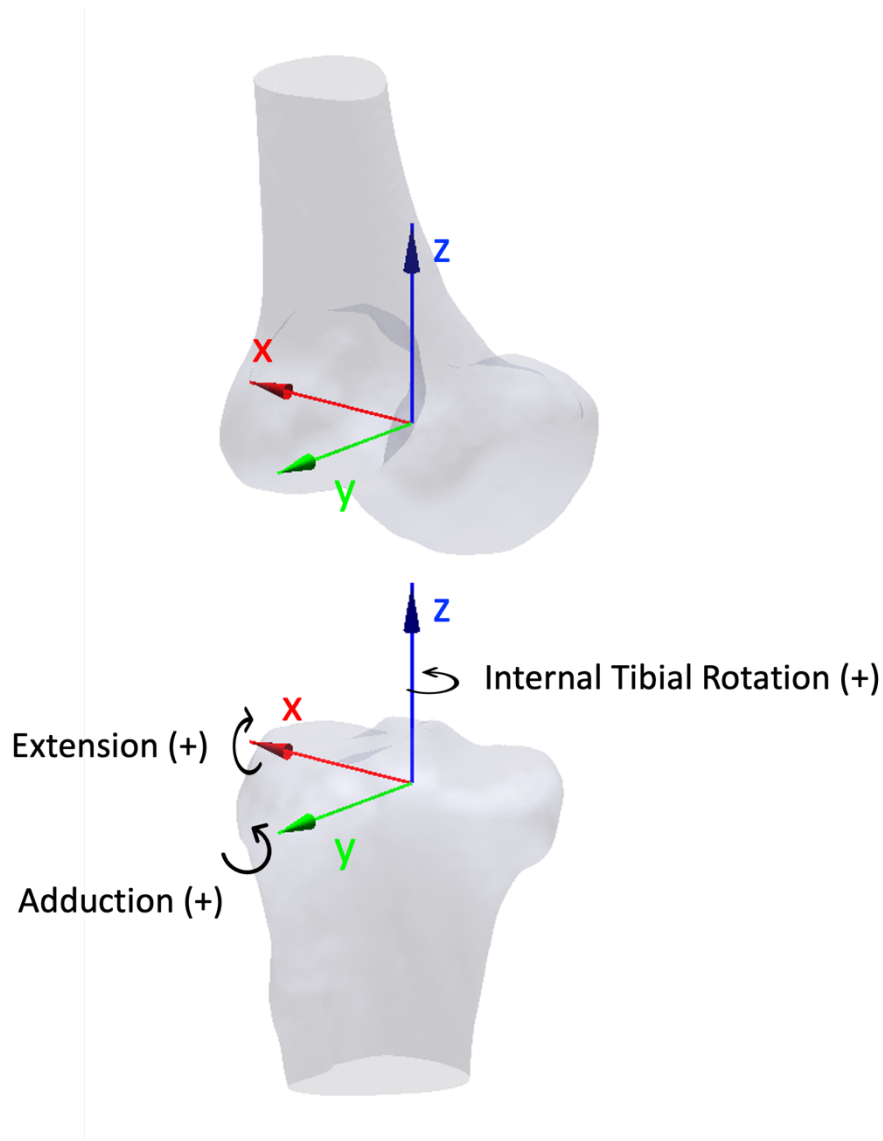
Supplementary Figure S1. Joint angle calculation for a right knee. Tibiofemoral kinematics were calculated as an <u>intrinsic XYZ rotation sequence of the tibial relative to the femoral frame</u> (i.e. as the sequence of rotations needed to transform the femoral frame into the tibial frame). Joint angle signs were determined according to the right-hand rule: Extension represents a positive rotation around the x-axis, adduction represents a positive rotation around the y-axis, and internal tibial rotation represents a positive rotation around the z-axis. The magnitude of joint angles derived this way is numerically equivalent to that obtained using the Grood & Suntay approach [7, 8]. However, it is important to note that Grood & Suntay define flexion, abduction and external tibial rotation as positive for a right knee [6].

Supplementary Table S1. Rotational (in degrees) and translational (in mm) values applied to raw local reference frames to transform them into the REFRAMEd reference frames; Rotations are expressed as an XYZ intrinsic Cardan angle sequence.

		Trial 1			Trial 2			Trial 3			Trial 4			Trial 5		
		CA	FFA	TEA	CA	FFA	TEA	CA	FFA	TEA	CA	FFA	TEA	CA	FFA	TEA
Femur																
Rot [°]	X	0.00	-0.03	-0.43	0.00	0.02	-0.08	-0.02	-0.02	-0.11	0.01	0.01	-0.03	0.08	0.02	-0.37
	Y	2.32	2.23	9.10	0.96	0.87	7.73	1.44	1.34	8.20	0.22	0.12	6.98	2.66	2.57	9.45
	Z	-3.92	-2.51	-0.86	-2.01	-0.60	0.99	-0.92	0.83	2.42	-0.92	0.49	2.07	-4.34	-2.93	-1.28
Trans [mm]	X	-15.20	-15.16	-15.40	-9.32	-9.26	-9.64	-9.30	-9.24	-9.65	-15.59	-15.53	-15.80	-15.18	-15.12	-15.36
	Y	-1.96	1.03	-7.63	-2.78	0.36	-8.14	-3.47	-0.33	-8.83	-2.92	0.07	-8.60	-2.19	0.81	-7.86
	Z	-1.35	0.34	-2.89	-2.36	-0.66	-4.60	-2.48	-0.78	-4.72	-2.13	-0.44	-3.64	-1.44	0.25	-3.00
Tibia																
Rot [°]	X	6.44	6.45	6.41	6.45	6.46	6.41	5.33	5.35	5.24	7.96	7.98	7.92	20.76	20.77	20.72
	Y	2.81	2.81	2.81	-0.34	-0.34	-0.35	0.65	0.65	0.64	-0.34	-0.34	-0.34	2.91	2.91	2.90
	Z	-3.74	-3.74	-3.73	-2.96	-2.96	-2.96	-2.08	-2.08	-2.07	-1.90	-1.90	-1.89	-0.64	-0.64	-0.63
Trans [mm]	X	0.00	0.00	0.00	0.00	0.00	0.00	0.00	0.00	0.00	0.00	0.00	0.00	0.00	0.00	0.00
	Y	0.00	0.00	0.00	0.00	0.00	0.00	0.00	0.00	0.00	0.00	0.00	0.00	0.00	0.00	0.00
	Z	0.00	0.00	0.00	0.00	0.00	0.00	0.00	0.00	0.00	0.00	0.00	0.00	0.00	0.00	0.00

Supplementary Figure S2. Trial 2 – Rotational kinematics: Joint rotations (in degrees) of the tibial relative to the femoral segment frame for one cycle of stair descent, before (Raw) and after REFRAME optimisation, for all three axis approaches (CA: cylindrical axis; FFA: functional flexion axis; TEA: transepicondylar axis). Curves overlap in right-hand side plots; CA and FFA are partially covered by TEA.
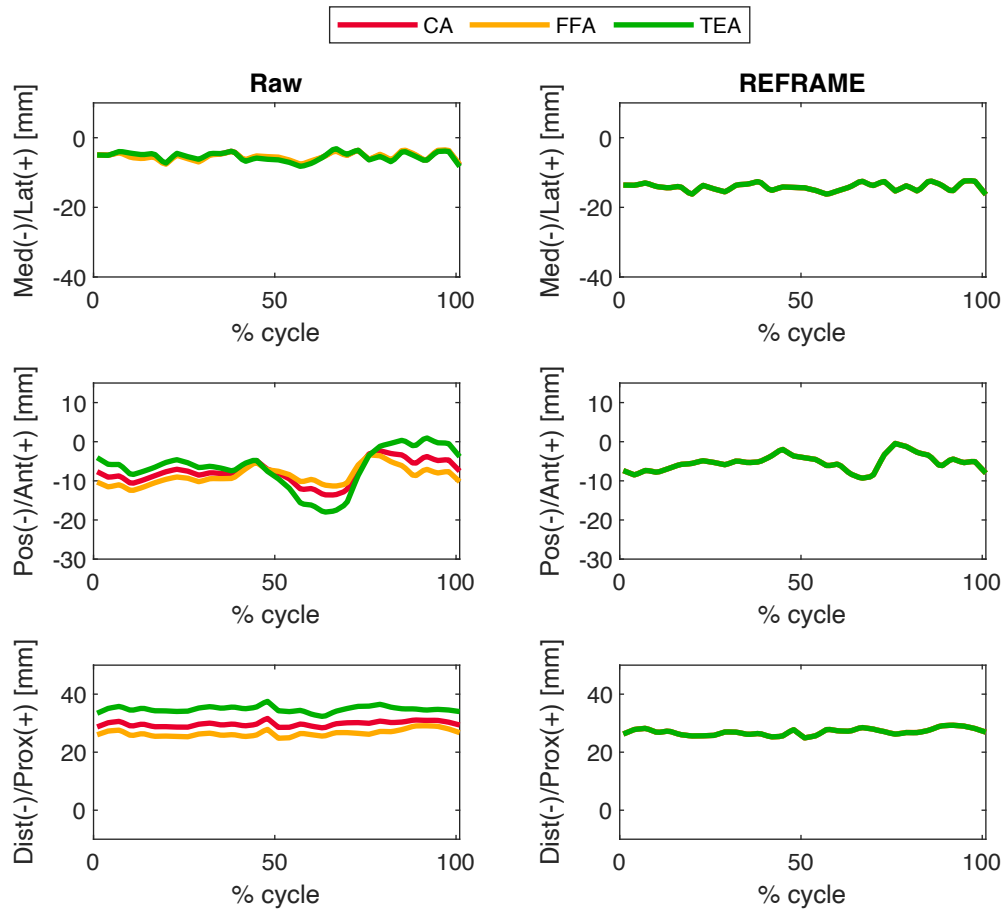
Supplementary Figure S3. Trial 2 – Translational kinematics: Joint translations (in mm) of the femoral relative to the tibial origin for one cycle of stair descent, before (Raw) and after application of the REFRAME optimisation, for all three axis approaches (CA: cylindrical axis; FFA: functional flexion axis; TEA: transepicondylar axis). Curves overlap in right-hand side plots; CA and FFA are partially covered by TEA.

Supplementary Figure S4. Trial 3 – Rotational kinematics: Joint rotations (in degrees) of the tibial relative to the femoral segment frame for one cycle of stair descent, before (Raw) and after REFRAME optimisation, for all three axis approaches (CA: cylindrical axis; FFA: functional flexion axis; TEA: transepicondylar axis). Curves overlap in right-hand side plots; CA and FFA are partially covered by TEA.

Supplementary Figure S5. Trial 3 – Translational kinematics: Joint translations (in mm) of the femoral relative to the tibial origin for one cycle of stair descent, before (Raw) and after application of the REFRAME optimisation, for all three axis approaches (CA: cylindrical axis; FFA: functional flexion axis; TEA: transepicondylar axis). Curves overlap in right-hand side plots; CA and FFA are partially covered by TEA.
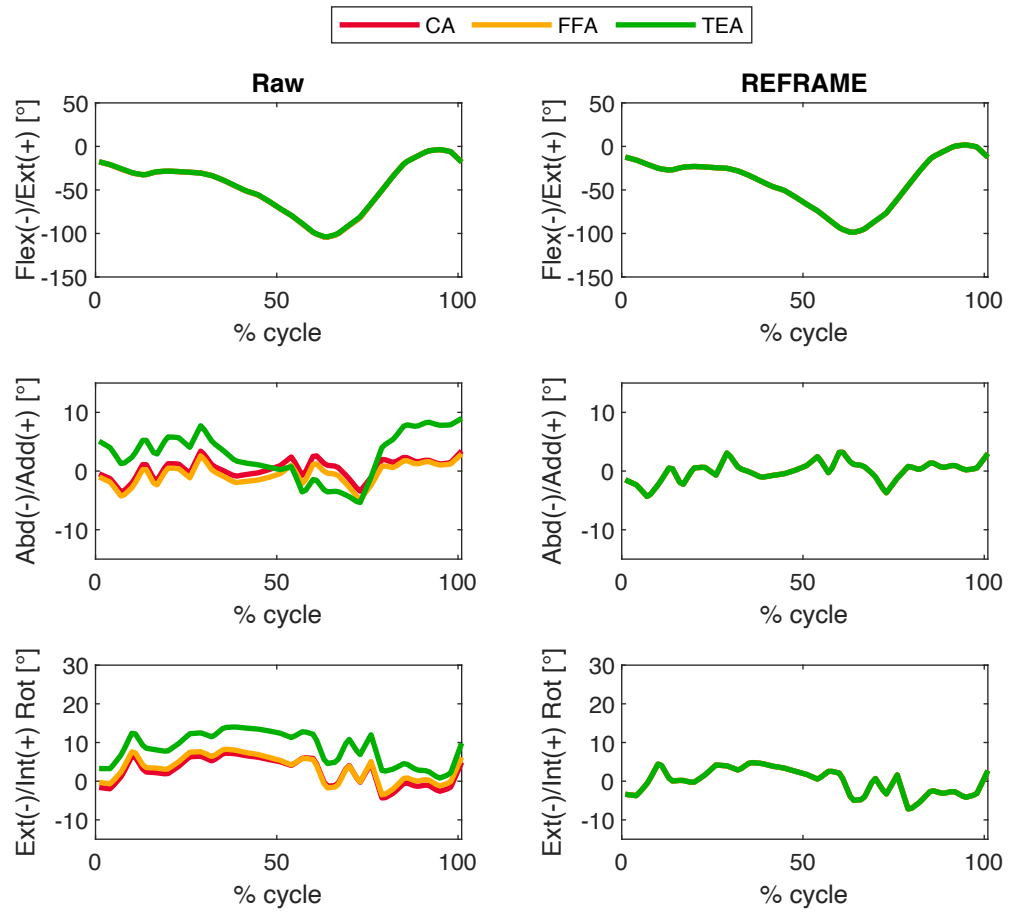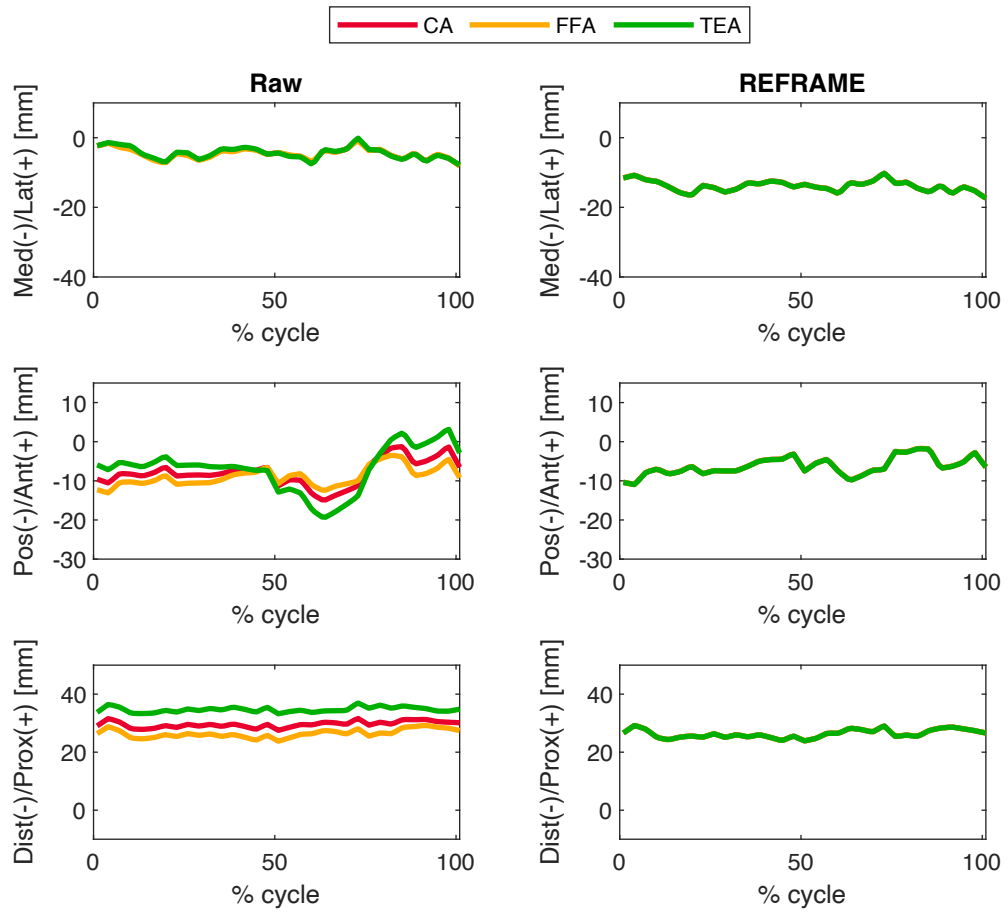
Supplementary Figure S6. Trial 4 – Rotational kinematics: Joint rotations (in degrees) of the tibial relative to the femoral segment frame for one cycle of stair descent, before (Raw) and after REFRAME optimisation, for all three axis approaches (CA: cylindrical axis; FFA: functional flexion axis; TEA: transepicondylar axis). Curves overlap in right-hand side plots; CA and FFA are partially covered by TEA.
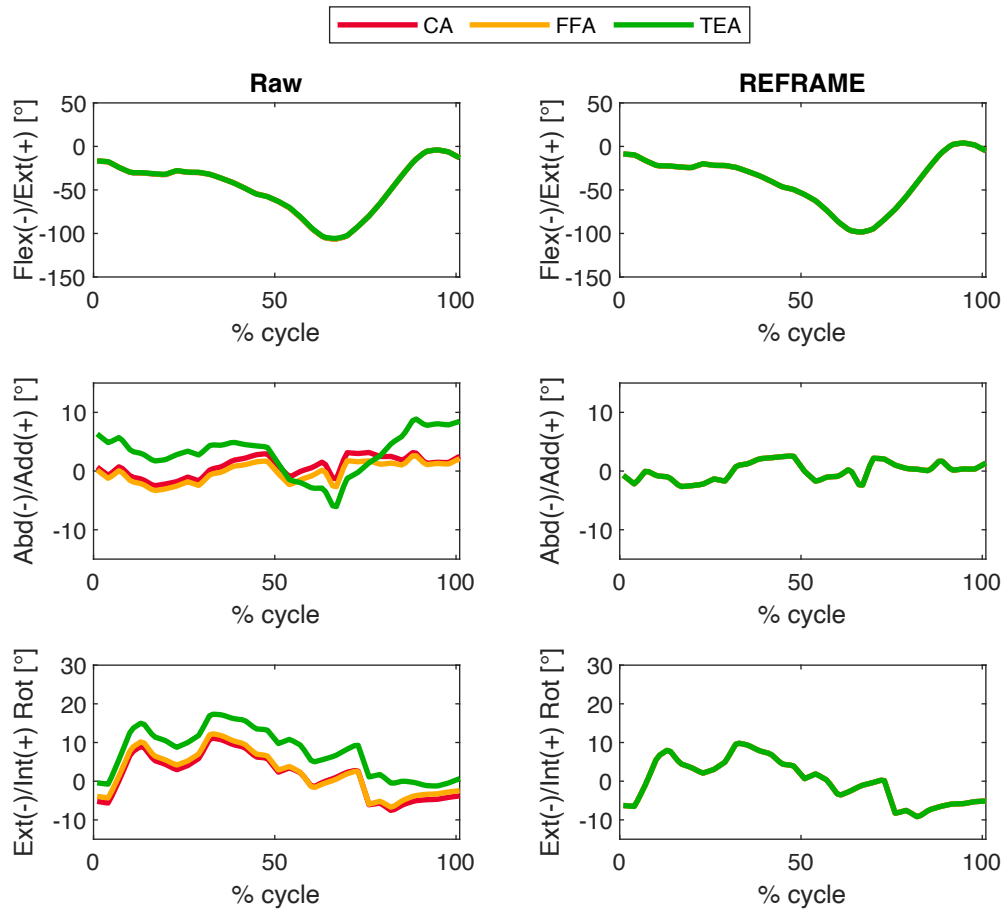
Supplementary Figure S7. Trial 4 – Translational kinematics: Joint translations (in mm) of the femoral relative to the tibial origin for one cycle of stair descent, before (Raw) and after application of the REFRAME optimisation, for all three axis approaches (CA: cylindrical axis; FFA: functional flexion axis; TEA: transepicondylar axis). Curves overlap in right-hand side plots; CA and FFA are partially covered by TEA.
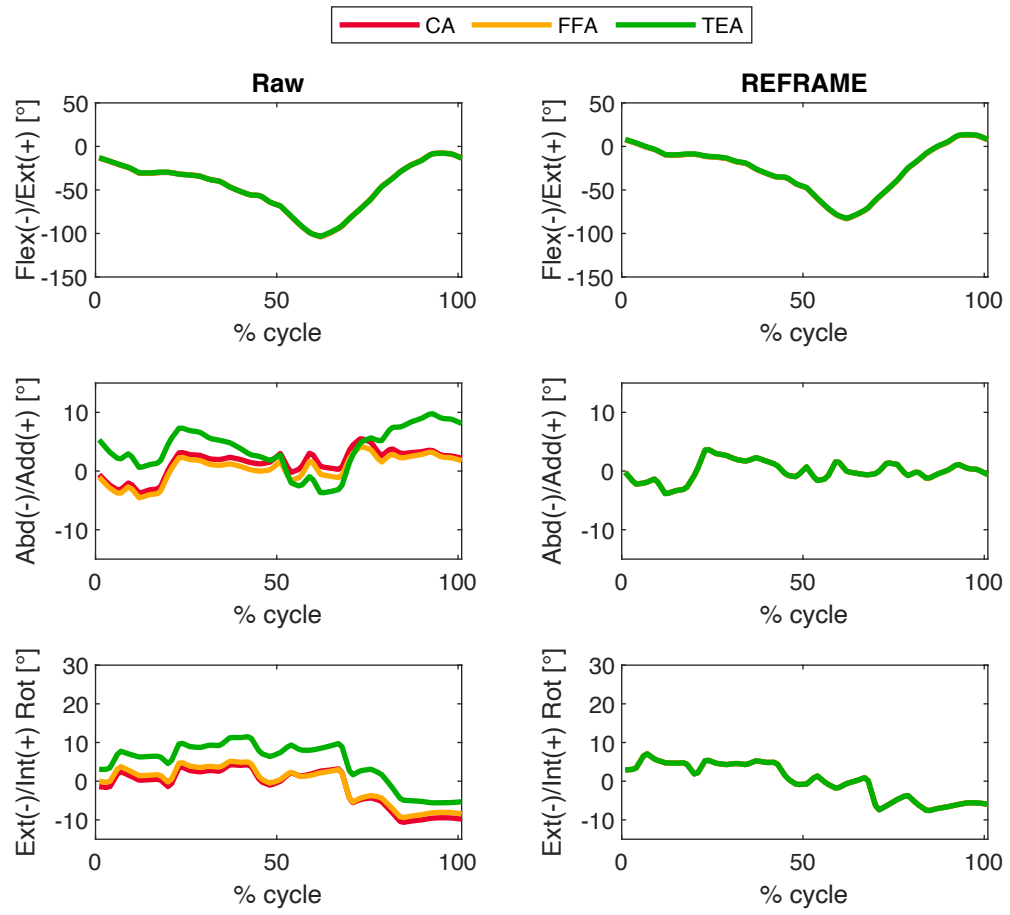
Supplementary Figure S8. Trial 5 – Rotational kinematics: Joint rotations (in degrees) of the tibial relative to the femoral segment frame for one cycle of stair descent, before (Raw) and after REFRAME optimisation, for all three axis approaches (CA: cylindrical axis; FFA: functional flexion axis; TEA: transepicondylar axis). Curves overlap in right-hand side plots; CA and FFA are partially covered by TEA.
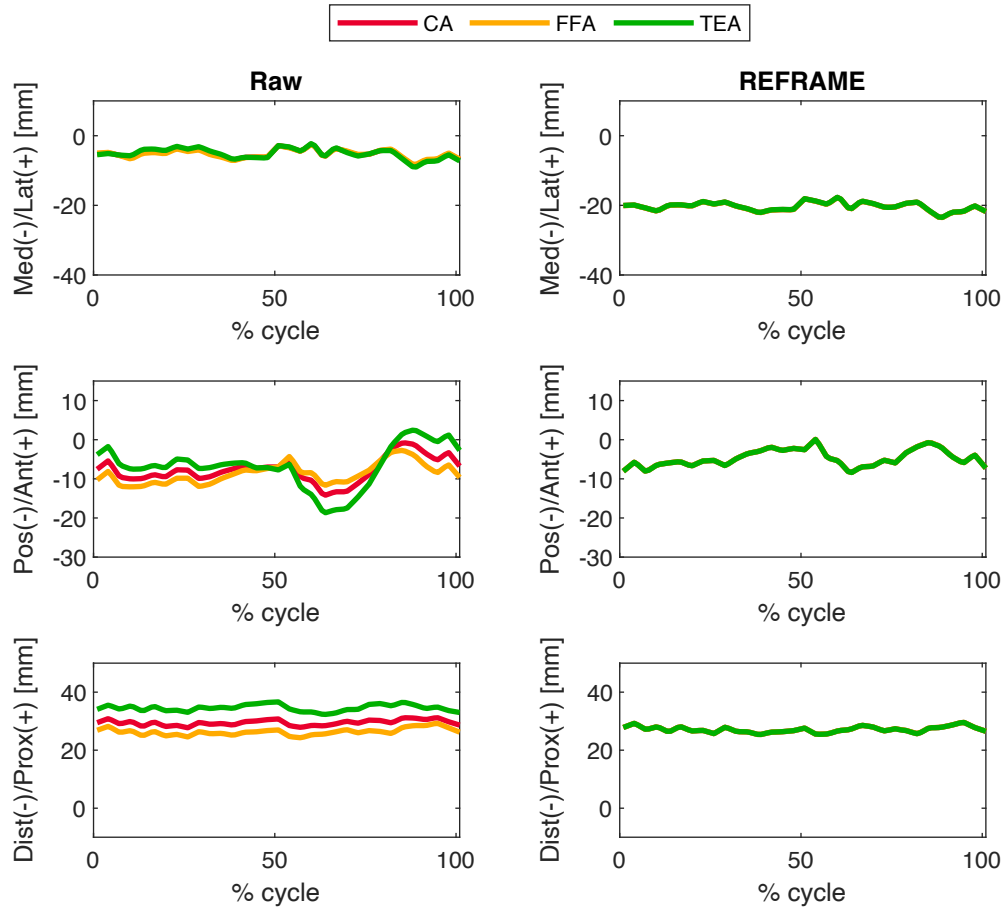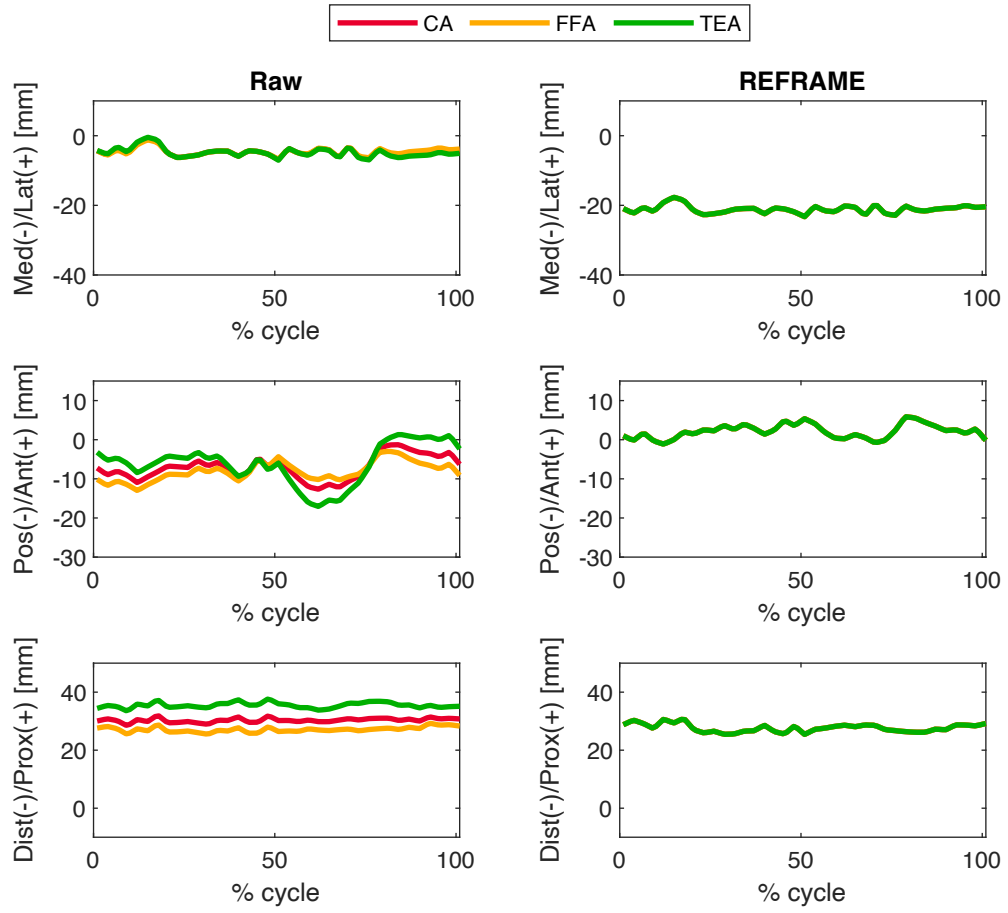
Supplementary Figure S9. Trial 5 – Translational kinematics: Joint translations (in mm) of the femoral relative to the tibial origin for one cycle of stair descent, before (Raw) and after application of the REFRAME optimisation, for all three axis approaches (CA: cylindrical axis; FFA: functional flexion axis; TEA: transepicondylar axis). Curves overlap in right-hand side plots; CA and FFA are partially covered by TEA.

V. Journal Publication IV

A reproducible representation of healthy tibiofemoral kinematics during stair descent using REFRAME – Part II: Exploring optimisation criteria and inter-subject differences

Ortigas-Vásquez, A., Taylor, W.R., Postolka, B., Schütz, P., Maas, A., Grupp, T.M. and Sauer, A.

Abstract

Kinematic analysis is a central component of movement biomechanics, describing the relative motion of joint segments during different activities, in different subject cohorts, and at different timepoints. Establishing whether two sets of kinematic signals represent fundamentally similar or different underlying motion patterns is especially challenging, given 1) the lack of consensus around reference frame and joint axis definition, and 2) the substantial effect that minimal variations in frame position and orientation are known to have on signal magnitude and characteristics. As such, enormous variability in the reporting of tibiofemoral kinematics has resulted in joint movement patterns that remain controversially discussed. Previously, we demonstrated the ability of the REference FRame Alignment MEthod (REFRAME) to reorientate and reposition differently aligned local segment frames to achieve convergence in signals representing the same underlying motion, thereby offering a novel approach to consistently report joint motion.

In this study, for the first time, we apply REFRAME to assess the rotational and translational *in vivo* tibiofemoral motion of ten healthy subjects during stair descent based on kinematic signals collected using a moving videofluoroscope. Kinematics were analysed before and after different REFRAME implementations, revealing generally neutral ab/adduction behaviour, accompanied by varying degrees of a sinusoidal int/external tibial rotation pattern over the activity cycle. Our data demonstrate that different selected implementations of REFRAME are able to highlight different characteristics of the motion patterns: Minimisation of the translational root-mean-square revealed proximodistal translation patterns with overall neutral progression, while anteroposterior translation showed seemingly different levels of correlation with flexion/extension in different subjects. On the other hand, REFRAME minimisation of translational variances exposed differences in the relative mean displacement between the femoral and tibial origins between subjects, highlighting differences in mean centre of rotation positions. This early application of REFRAME for providing an understanding of tibiofemoral kinematics demonstrates the potential of this novel approach to bring clarity to an otherwise complex representation of highly variable time-series signals, while highlighting the philosophical challenges of clinically interpretating kinematic signals in the first place.

Keywords: gait analysis; knee; tibiofemoral; kinematics; joint coordinate system; reference frame; motion capture; stair descent

1. Introduction

In clinical movement biomechanics, motion analysis can be divided into two main components, joint *kinematics* and *kinetics*, where the former investigates the relative *movement* of joint segments. At the most basic level, joint kinematics fundamentally describe the rotational and/or translational displacements of a rigid body relative to another, where both rigid segments are connected by an articulating joint. Characterisation of these displacements can be achieved by defining a coordinate frame fixed to each segment, and tracking the movement of one frame with respect to the other. The position and orientation of each frame relative to the segment it represents can be defined based on e.g. anatomical landmarks [1, 2] or functional calibration movements [3, 4]. The exact *pose* (i.e. orientation and position) of a segment's local coordinate frame will depend on the specific frame definition approach; in other words, for a single joint segment, two different approaches will, in almost all cases, lead to two different reference frames [5]. As a result, the set of joint axes identified using one landmark-based approach will not necessarily match the set of axes identified by a different landmark-based approach, let alone axes identified using a functional method.

In the specific case of the knee joint, early studies inferred that different axes could be used interchangeably. For instance, Churchill and co-workers stated that the transepicondylar axis "closely approximates" the optimal flexion axis, where the latter "can be considered the true flexion axis of the knee" [2]. Such statements have been misinterpreted to mean that the transepicondylar axis and a functional flexion axis could be suitable substitutions for one another, which inherently assumes that minor differences between joint axes lead to proportionally small differences between the kinematic signals stemming from those reference frames. This notion has, in turn, contributed to the false impression that, when comparing two or more sets of kinematic signals, clearly visible differences in their shape and magnitude could immediately be interpreted as evidence of fundamentally different underlying joint motion patterns. Despite the subsequent publication of studies that have explicitly challenged these early simplified models [5-7], as well as official attempts to establish uniformity across studies to allow comparisons between datasets [8], a clear understanding that different kinematic signals do not necessarily imply different underlying joint motion patterns is not ubiquitous among the biomechanics community.

In recent years, our investigations have conclusively shown that even minor (e.g. < 3°) differences in frame orientation can lead to substantial variation in the shape and magnitude of kinematic signals due to cross-talk between reference frames [9, 10]; an effect that is further exacerbated by differences in frame origin position, which can be present even when relying on a single common joint axis approach [11, 12]. As a result, an easily reconcilable representation and understanding of movement patterns remains lacking [5], hence limiting our ability to compare kinematic datasets across studies and between labs, and even hindering a consistent clinical interpretation of joint motion patterns. To address this issue, we previously presented the REference FRame Alignment MEthod (REFRAME) [13], which expands on the Frame Orientation Optimisation Method (FOOM) [9] by enhancing flexibility and incorporating joint translations (see Supplementary Material for details on how FOOM relates to REFRAME), to allow consistent local reference frame alignment even among datasets derived using different joint axis approaches.

Importantly, considerable work has already been undertaken to investigate knee movement patterns during different functional activities [14-17]. Our recent analysis found that healthy knees exhibited a range of motion (ROM) of approximately 13° in int/external tibial rotation and 6° in

ab/adduction during stair descent [14]. Results also indicated that although there was large variation in the degree of int/external tibial rotation present at heel strike, subjects consistently demonstrated a tendency to rotate their tibia internally during the stance phase to reach peak internal rotation shortly before toe-off, ending with an externally rotating tibia in preparation for the next heel strike.

Given that the aforementioned studies were also potentially susceptible to the cross-talk effects described above, it is important to assess whether past work needs to be revisited, and explore whether a revised analysis that incorporates tools such as REFRAME produces a different interpretation of the underlying joint movement patterns. Since REFRAME offers the ability to retrospectively analyse datasets and account for inherent cross-talk artefact, we therefore aimed to understand whether new insights into the interpretation of functional joint kinematics can be gained through application of these techniques. In this study, we thus expand on the aforementioned investigations by including a larger cohort of ten healthy subjects in order to explore how subject differences manifest before and after REFRAME implementation.

2. Methods

One clear requirement prior to comparing kinematic signals before and after REFRAME implementation was to further validate REFRAME's ability to produce convergence in kinematic signals that were derived using different joint axis approaches, yet correspond to a single common underlying movement pattern. Here, we relied on *in vivo* kinematic data previously collected as part of a separate study [14]. In that study, moving videofluoroscopy [18] was used to capture the tibiofemoral kinematics of ten healthy subjects with neutral knee alignments as they performed a minimum of five valid cycles of stair descent. Similar to our previous investigation [5, 13] three different approaches were used to establish a primary flexion axis: a cylindrical axis approach (CA), a functional flexion axis approach (FFA), and a transepicondylar axis approach (TEA) (for further details on axis definitions see [1-3, 5, 19-21]). By designating corresponding ab/adduction and int/external rotation axes, as well as a femoral reference frame origin, three local femoral frames were defined based on the three specified flexion axis variations. Conversely, a single common local reference frame was defined for the tibial segment. Six degrees-of-freedom (DOFs) tibiofemoral kinematics (i.e. joint rotations and translations) were calculated according to each of these three variations of the femoral segment frame. Joint rotations were given by the relative orientations of the tibial relative to the femoral segment frame, following an intrinsic XYZ (extension-adduction-internal tibial rotation for a right knee) rotation sequence as previously described [13, 22]. (Extension, adduction, and tibial internal rotation are positive rotations as per the right-hand rule). Joint translations were dictated by the position of the femoral frame origin relative to the tibial frame origin, in the tibial coordinate system.

After raw CA, FFA and TEA kinematic signals had been derived, reference frame orientations were optimised based on an adaptation of our previously presented FOOM approach [9] (a precursor and specific sub-implementation of the larger REFRAME framework) that we recommended for flexion dominant gait activities. (Note: the term *raw* is used to refer to reference frames and/or kinematic signals that have not yet undergone optimisation with REFRAME.) This configuration of REFRAME consisted of minimising the root-mean-square (RMS) of ab/adduction and int/external rotation, both with a weighting of 1. Transformations of the raw tibial frame consisting of rotations around the mediolateral axis were restricted to zero. Additionally, transformations of the raw femoral frame consisting of rotations around the mediolateral axis were minimally penalised (criteria weighting: 0.0001). This REFRAME configuration prevented considerable changes in the orientations of the local frames' anteroposterior and longitudinal axes in the sagittal plane. The effect of the additional constraints ensured the REFRAMEd kinematics could still be reconciled with our general existing clinical understanding of joint angles (Supplementary Figure S1). Based on the resulting optimally oriented local reference frames, the REFRAMEd rotational tibiofemoral kinematics were calculated for each individual subject and trial.

After optimisation of the coordinate system orientations, two different REFRAME variations were investigated for the optimisation of frame origin positions (i.e. joint translations). The first consisted of a minimisation of the RMS of mediolateral (ML), anteroposterior (AP), and proximodistal (PD) translations, while the second minimised the variance of the same three joint translations. In both cases, all three minimisations were weighted equally with a weighting of 1. Once again, REFRAMEd translational kinematic signals were calculated according to each of the two presented REFRAME implementations. All REFRAME implementations were executed in MATLAB (vR2022a; The Mathworks Inc., Natick, Massachusetts, USA).

For each subject and trial, kinematic signals were plotted to assess differences between axis approaches, as well as whether signal convergence can be achieved for all individual trials through application of REFRAME. Mean intra-subject kinematic signals (and the corresponding standard deviations) were additionally plotted to examine tibiofemoral movement profiles with and without REFRAME. Finally, box plots were made to illustrate the different subject mean ROMs (calculated from each subject's mean curve) in each DOF.

3. Results

Differences between the three raw sets of kinematic signals were strongly apparent according to the joint axis approach used (CA, FFA, TEA). For several subjects, raw CA-based signals visually displayed a higher level of agreement with raw FFA-based signals than with TEA (see e.g. Subject 2, Supplementary Figures S15-24). Furthermore, raw TEA-based signals presented clear indications of being affected by cross-talk artefact, as evidenced by visible amplifications of AP translation signals with flexion angle (see e.g. Subject 1, Supplementary Figures S5-14). Despite the stronger similarity observed between raw CA- and FFA-based signals in most participants and most DOFs, two subjects (3 and 8) displayed high agreement in the raw translation signals derived from CA and TEA approaches (Supplementary Figures S26,28,30,32,34 and S76,78,80,82,84).

Much like in our previous investigation [13], essentially no visible differences were discernible between the three sets of tibiofemoral kinematics after REFRAME implementation in all six DOFs (Supplementary Figures S5-104), consistent with the notion that all three datasets corresponded to a single common underlying motion pattern.

3.1. Joint Rotations – Raw Signals

In the sagittal plane, no notable differences were visible between the three sets of raw flexion/extension signals (Figure 1). Average ROM was consistent across joint axis approaches, falling between 90.7° ± 5.4° and 90.9° ± 5.3° (Figure 2). In the frontal plane, the lowest inter-subject variability was seen in the raw CA-based ab/adduction signals, followed by FFA- and finally TEA-based signals (Figure 3). While average ab/adduction ROMs were 4.3° ± 1.1° and 4.3° ± 1.0° for CA and FFA, respectively, TEA-based signals reached an average ROM of 8.9° ± 2.7° (Figure 4). In the transverse plane, raw CA- and FFA-based int/external rotation signals were generally similar for most subjects, with both signal sets displaying higher inter-subject variation than TEA (Figure 5). On average, TEA-based signals exhibited higher ROM (13.9° ± 3.7°) than CA- (11.1° ± 3.2°) and FFA-based (11.1° ± 3.6°) int/external rotation signals (Figure 6).

3.2. Joint Translations – Raw Signals

Raw ML translation signals were comparable among the three joint axes approaches (Figure 7), as were average raw ROMs along the ML axis (3.5 mm ± 0.9 mm, 3.6 mm ± 1.0 mm, and 3.7 mm ± 1.0 mm for CA-, FFA-, and TEA-based signals, respectively; Figure 8). The average position of the raw femoral frame origin relative to the tibial origin was fairly constant (roughly 7 mm medially) in the ML direction. Among the three sets of raw AP translations, TEA-based signals seemed to be the most affected by cross-talk, as indicated by the visible association between AP translation and flexion/extension; FFA-based signals, on the other hand, appeared to be the least affected (Figure 9). FFA-based translation signals along the AP axis also displayed the lowest levels of inter-subject variability out of the three axis approaches investigated. Mean AP translation ROMs varied between the axis approaches, ranging from 6.7 mm ± 1.6 mm for FFA-based signals, to 11.3 mm ± 4.8 mm for CA-based signals, and 17.5 mm ± 3.3 mm for TEA-based signals (Figure 10). Lastly, of the three PD translation signals, TEA-based signals once more appeared to be the most susceptible to cross-talk artefact (especially Subject 7), while CA- and FFA-based signals displayed similar levels of inter-subject variability (Figure 11). Regarding PD translation signals, before REFRAME implementation, the average PD position of the femoral

frame origin relative to the tibial origin varied little throughout the gait cycle for most subjects. Femoral origins were mostly positioned between approximately 25 and 40 mm proximal to the tibial origin. Average translational ROM along the PD axis was highest for TEA-based signals (5.0 mm ± 2.7 mm), followed by FFA- (2.9 mm ± 0.7 mm) and CA-based signals (2.5 mm ± 1.0 mm) (Figure 12).

3.3. Joint Rotations – After REFRAME

In the sagittal plane, implementation of REFRAME did not lead to distinguishable changes in the flexion/extension signal (Figure 1). Similarly, flexion/extension ROM was not substantially affected by the optimisation of local frame orientations, averaging 90.9° ± 5.4° after REFRAME (Figure 2). For rotations in the frontal plane, implementation of REFRAME led to comparatively less variable ab/adduction signals (Figure 3), and a reduced average ROM of 4.1° ± 0.8° (Figure 4). In the transverse plane, REFRAME also decreased inter-subject variability of int/external tibial rotation signals, resulting in a perceivable sinusoidal pattern over the activity cycle (Figure 5), and a decrease in ROM from peak values as high as 19.8° (Subject 4, FFA) to an average of 10.1° ± 3.0° (Figure 6).

For the femoral reference frame, the differences in orientation between raw and REFRAMEd coordinate systems were virtually negligible around the ML axis. Orientation differences averaged 2.8° ± 2.7° and 2.6° ± 2.5° across all joint axis approaches, subjects, and trials around the AP and PD axes, respectively (Table 1). For the tibial frame, no changes were applied to the local segment frame around the ML axis (in line with our chosen optimisation constraints), while average rotational changes around the AP and PD axes were 2.3° ± 1.5° and 5.2° ± 4.2°, respectively.

3.4. Joint Translations – After REFRAME (Minimising RMS)

REFRAME optimisation based on the minimisation of translation RMSs led to an offset in the ML translation signals, such that the mean ML position of the femoral origin relative to the tibial origin was approximately 0 mm (Figure 7). These effects were in line with our previous investigation of the impact of choosing RMS as the optimisation parameter [13]. Translational ROM along this axis was not substantially affected by the implementation of REFRAME, averaging 3.7 mm ± 1.2 mm (Figure 8), although it did increase for one of the ten subjects, leading to a larger interquartile range. For AP translation, REFRAME implementation visibly reduced inter-subject variability, and similarly to ML, consistently shifted the mean AP values towards 0 mm (Figure 9). After REFRAME, subtle differences in the levels of variation in AP signal magnitude with flexion/extension were discernible among different subjects. AP ROM also noticeably declined, reaching an average of 5.2 mm ± 1.4 mm (Figure 10). In terms of PD translation, REFRAMEd signals exhibited fairly constant behaviour throughout the entire activity cycle, once again settling at approximately 0 mm (Figure 11), as upheld by the minimisation of RMS. After minimisation of translational RMSs through REFRAME, average ROM along the PD axis was 2.4 mm ± 0.5 mm (Figure 12).

This REFRAME implementation resulted in modifications to the femoral origin position of up to 25.9 mm along the ML axis, and 10.9 mm along both the AP and PD raw femoral axes. The tibial origin, on the other hand, was translated a maximum of 33.8 mm along the ML axis, 10.9 mm along the AP axis and 30.9 mm along the PD axis.

3.5. Joint Translations – After REFRAME (Minimising variance)

As previously described, a second REFRAME adaptation was implemented to optimise the position of local reference frame origins based on the minimisation of variance (instead of RMS) for all three translations. After this alternative implementation of REFRAME, the general patterns of all three translational signals were consistent with the results obtained after minimising RMS. This second version of REFRAME led to greater inter-subject variability in mean translation values, especially along the ML and AP axes (Figures 7 and 9). Despite this increased variation, ML translation signals for all subjects became negative, indicating a medially located joint centre of rotation relative to the tibial origin. On the other hand, mean tibiofemoral PD translation values for all subjects fell between 20 and 35 mm for the relative position of the femoral relative to the tibial origin, coherent with a femoral origin that was located proximally to the tibial origin (Figure 11). Average ROMs were comparable to those resulting from REFRAME optimisation based on RMS, averaging 3.7 mm ± 1.2 mm, 5.1 mm ± 1.4 mm, and 2.5 mm ± 0.6 mm for ML, AP and PD translations, respectively (Figures 8, 10, and 12).

The implementation of REFRAME based on translational variance minimisation led to changes in the position of the femoral origin within the bone segment as high as 26.8 mm, 10.8 mm and 10.8 mm around the ML, AP and PD axes, respectively. Changes in the position of the tibial origin as a result of REFRAME implementation were negligible in all directions. In fact, the largest translation applied to the raw tibial origin along any given axis by the optimisation was 3.9×10^{-5} mm, i.e. virtually 0 mm.
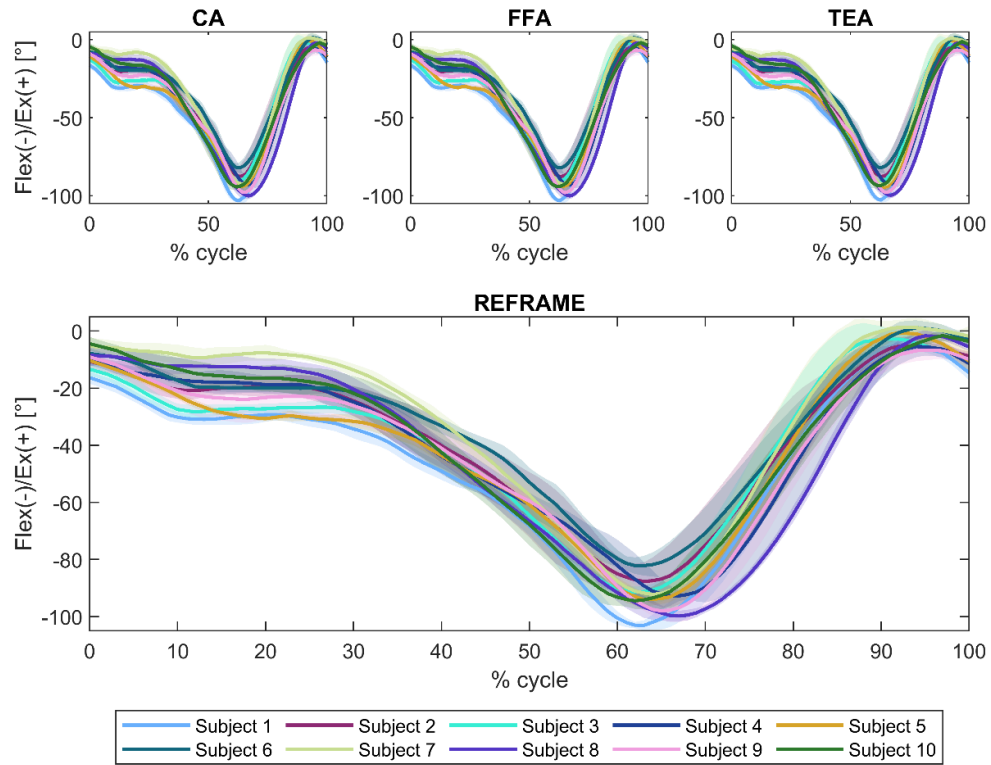
Figure 1. Rotational kinematics: Flexion(flex)/extension(ex) (in degrees) of the tibial relative to the femoral segment frame over a stair descent cycle. Solid lines represent the mean across all trials for each subject, while the corresponding shaded areas depict the associated standard deviations for each individual. Values are illustrated for each of the three joint axis approaches (CA: cylindrical axis; FFA: functional flexion axis; TEA: transepicondylar axis) before REFRAME (top), and after REFRAME (bottom). Note: kinematic patterns for all three axes converge to a single solution upon application of REFRAME, and therefore coincide graphically. Additional note to readers from a clinical background: knee extension is illustrated here as **positive** because following the right-hand rule it corresponds with a positive rotation around the laterally pointing mediolateral axis for a right knee.
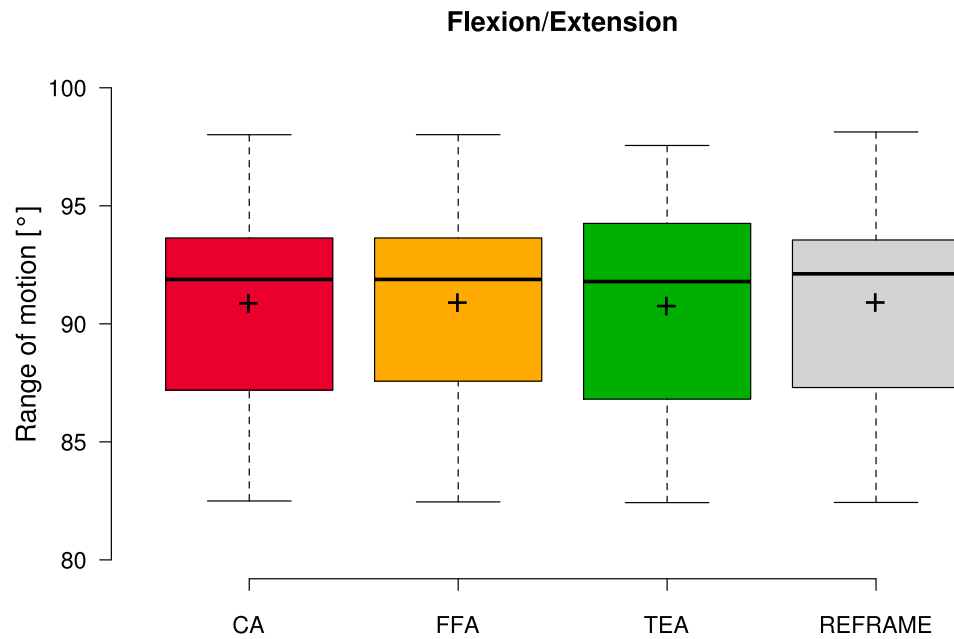
Flexion/Extension

Figure 2. Box plot of flexion/extension range of motion (all subjects and repetitions) according to each of the three different axis approaches (CA: cylindrical axis; FFA: functional flexion axis; TEA: transepicondylar axis), as well as after REFRAME implementation. Centre lines illustrate the medians, while box limits depict the 25th and 75th percentiles. Whiskers extend to data points that are less than 1.5 times the interquartile range away from the 1st and 3rd quartiles. Note: kinematic patterns for all three axes converge to a single solution upon application of REFRAME, and therefore all display the same range of motion values.
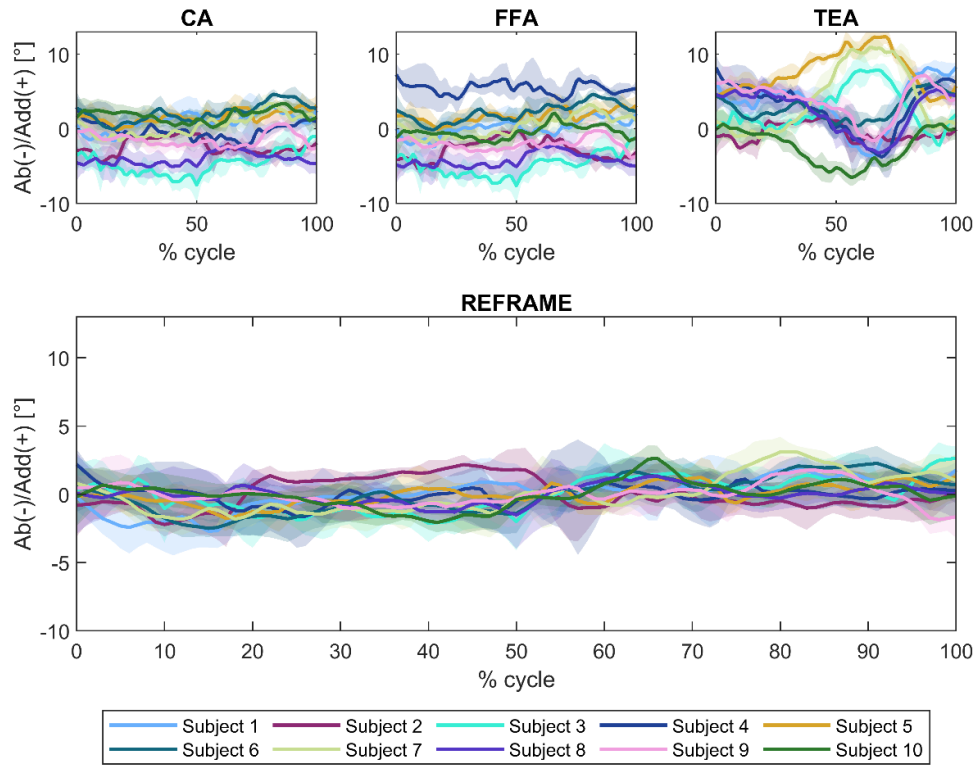
Figure 3. Rotational kinematics: Abduction(ab)/adduction(add) (in degrees) of the tibial relative to the femoral segment frame over a stair descent cycle. Solid lines represent the mean across all trials for each subject, while the corresponding shaded areas depict the associated standard deviations for each individual. Values are illustrated for each of the three joint axis approaches (CA: cylindrical axis; FFA: functional flexion axis; TEA: transepicondylar axis) before REFRAME (top), and after REFRAME (bottom). Note: kinematic patterns for all three axes converge to a single solution upon application of REFRAME, and therefore coincide graphically.
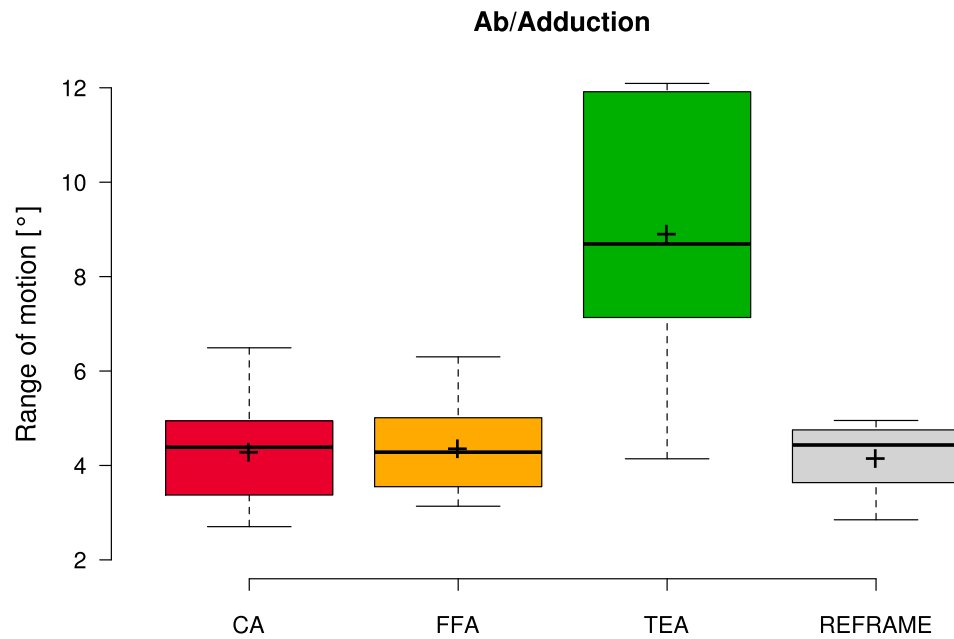
Ab/Adduction

Figure 4. Box plot of ab/adduction range of motion (all subjects and repetitions) according to each of the three different axis approaches (CA: cylindrical axis; FFA: functional flexion axis; TEA: transepicondylar axis), as well as after REFRAME implementation. Centre lines illustrate the medians, while box limits depict the 25th and 75th percentiles. Whiskers extend to data points that are less than 1.5 times the interquartile range away from the 1st and 3rd quartiles. Note: kinematic patterns for all three axes converge to a single solution upon application of REFRAME, and therefore all display the same range of motion values.

Figure 5. Rotational kinematics: External(ext)/internal(int) rotation (in degrees) of the tibial relative to the femoral segment frame over a stair descent cycle. Solid lines represent the mean across all trials for each subject, while the corresponding shaded areas depict the associated standard deviations for each individual. Values are illustrated for each of the three joint axis approaches (CA: cylindrical axis; FFA: functional flexion axis; TEA: transepicondylar axis) before REFRAME (top), and after RE-FRAME (bottom). Note: kinematic patterns for all three axes converge to a single solution upon application of REFRAME, and therefore coincide graphically.
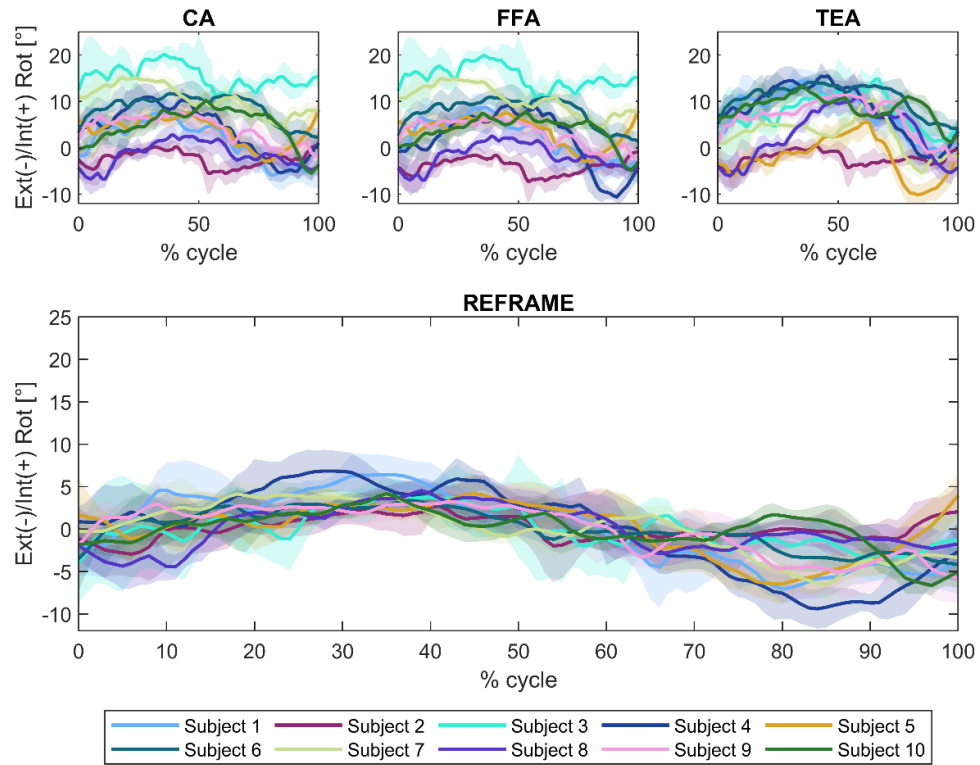
Int/External Rotation
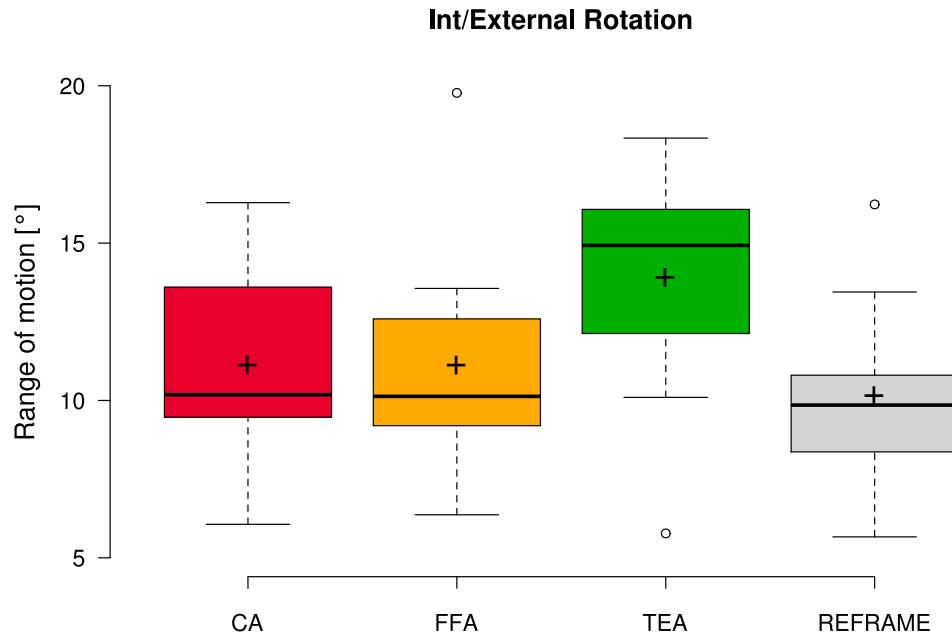
Figure 6. Box plot of int/external rotation range of motion (all subjects and repetitions) according to each of the three different axis approaches (CA: cylindrical axis; FFA: functional flexion axis; TEA: transepicondylar axis), as well as after REFRAME implementation. Centre lines illustrate the medians, while box limits depict the 25th and 75th percentiles. Whiskers extend to data points that are less than 1.5 times the interquartile range away from the 1st and 3rd quartiles. Outliers are indicated by circles. Note: kinematic patterns for all three axes converge to a single solution upon application of RE-FRAME, and therefore all display the same range of motion values.

Figure 7. Translational kinematics: Medio(med)-lateral(lat) translation (in mm) of the femoral relative to the tibial segment frame over a stair descent cycle. Solid lines represent the mean across all trials for each subject, while the corresponding shaded areas depict the associated standard deviations for each individual. Values are illustrated for each of the three joint axis approaches (CA: cylindrical axis; FFA: functional flexion axis; TEA: transepicondylar axis) before REFRAME (top), after minimisation of root-mean-square using REFRAME (middle), and after minimisation of variance using REFRAME (bottom). Note: kinematic patterns for all three axes converge to a single solution upon application of REFRAME, and therefore coincide graphically.
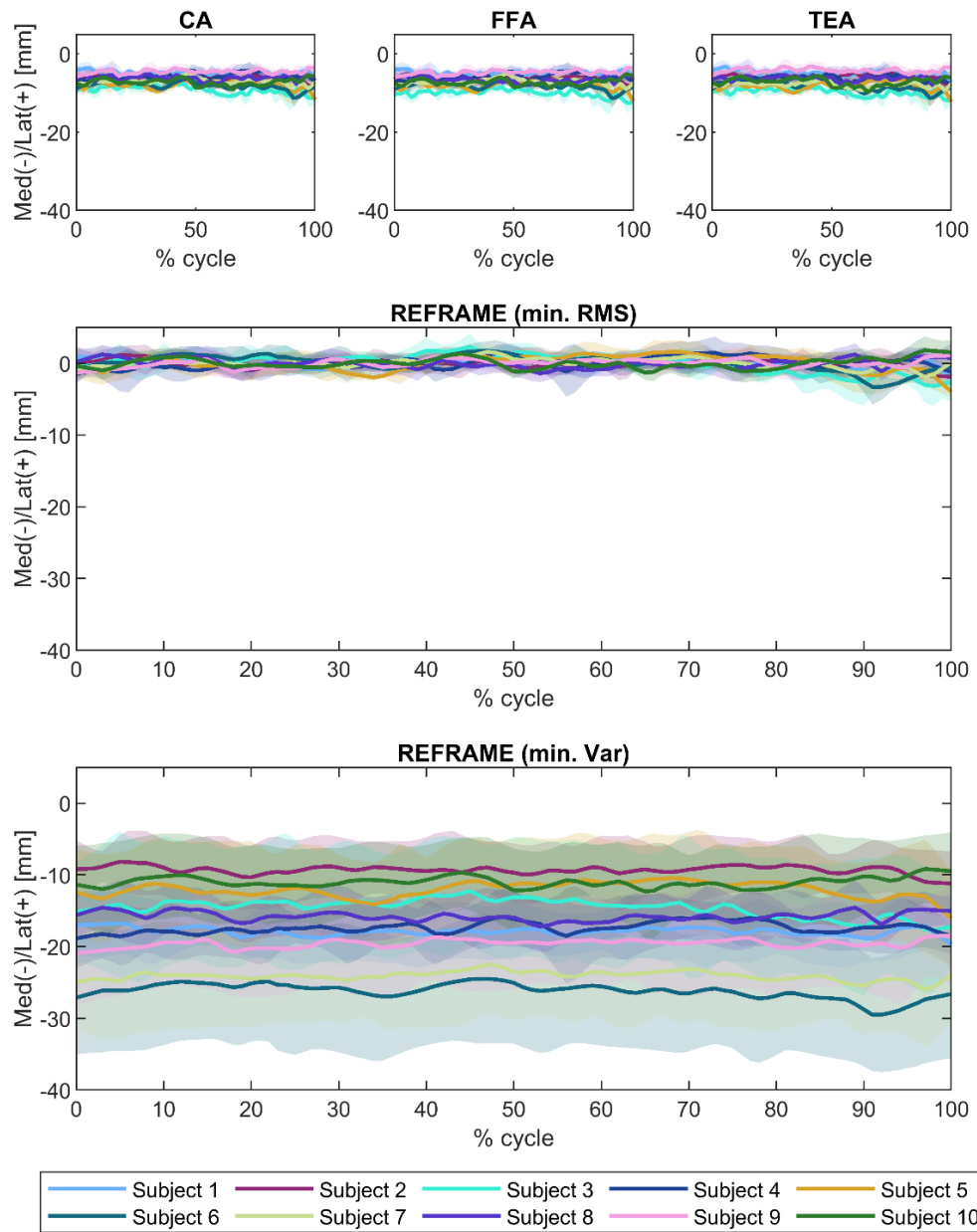
Mediolateral Translation

Figure 8. Box plot of mediolateral translation range of motion (all subjects and repetitions) according to each of the three different axis approaches (CA: cylindrical axis; FFA: functional flexion axis; TEA: transepicondylar axis), as well as after REFRAME implementation. Centre lines illustrate the medians, while box limits depict the 25th and 75th percentiles. Whiskers extend to data points that are less than 1.5 times the interquartile range away from the 1st and 3rd quartiles. Outliers are indicated by circles. Note: kinematic patterns for all three axes converge to a single solution upon application of RE-FRAME, and therefore all display the same range of motion values.

Figure 9. Translational kinematics: Antero(ant)-posterior(pos) translation (in mm) of the femoral relative to the tibial segment frame over a stair descent cycle. Solid lines represent the mean across all trials for each subject, while the corresponding shaded areas depict the associated standard deviations for each individual. Values are illustrated for each of the three joint axis approaches (CA: cylindrical axis; FFA: functional flexion axis; TEA: transepicondylar axis) before REFRAME (top), after minimisation of root-mean-square using REFRAME (middle), and after minimisation of variance using REFRAME (bottom). Note: kinematic patterns for all three axes converge to a single solution upon application of REFRAME, and therefore coincide graphically.
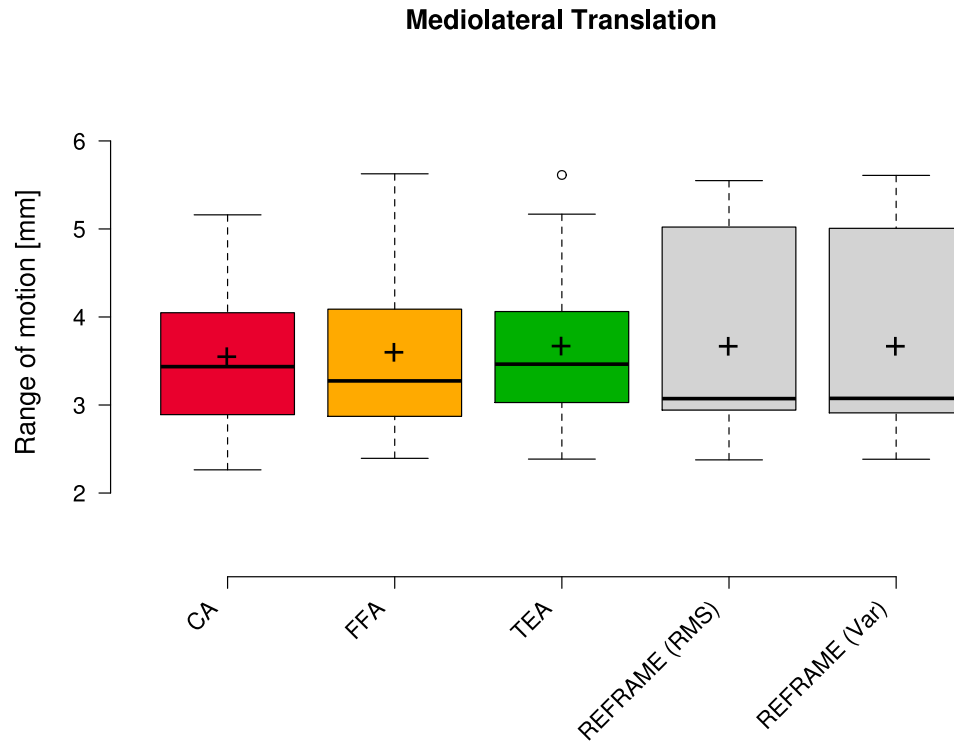
Figure 10. Box plot of anteroposterior range of motion (all subjects and repetitions) according to each of the three different axis approaches (CA: cylindrical axis; FFA: functional flexion axis; TEA: transepicondylar axis), as well as after REFRAME implementation. Centre lines illustrate the medians, while box limits depict the 25th and 75th percentiles. Whiskers extend to data points that are less than 1.5 times the interquartile range away from the 1st and 3rd quartiles. Outliers are indicated by circles. Note: kinematic patterns for all three axes converge to a single solution upon application of REFRAME, and therefore all display the same range of motion values.
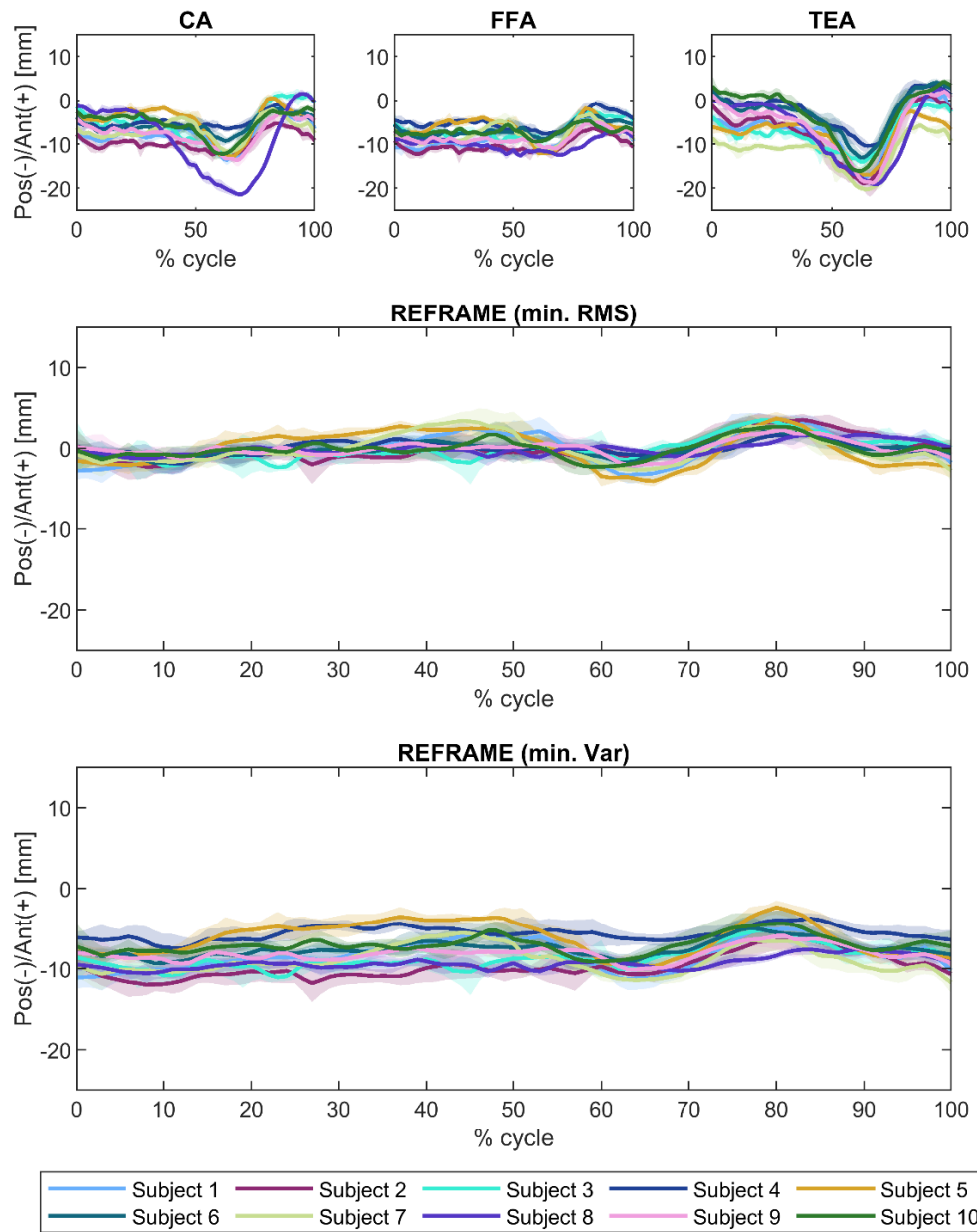
Figure 11. Translational kinematics: Proximo(prox)-distal(dist) translation (in mm) of the femoral relative to the tibial segment frame over a stair descent cycle. Solid lines represent the mean across all trials for each subject, while the corresponding shaded areas depict the associated standard deviations for each individual. Values are illustrated for each of the three joint axis approaches (CA: cylindrical axis; FFA: functional flexion axis; TEA: transepicondylar axis) before REFRAME (top), after minimisation of root-mean-square using REFRAME (middle), and after minimisation of variance using REFRAME (bottom). Note: kinematic patterns for all three axes converge to a single solution upon application of REFRAME, and therefore coincide graphically.
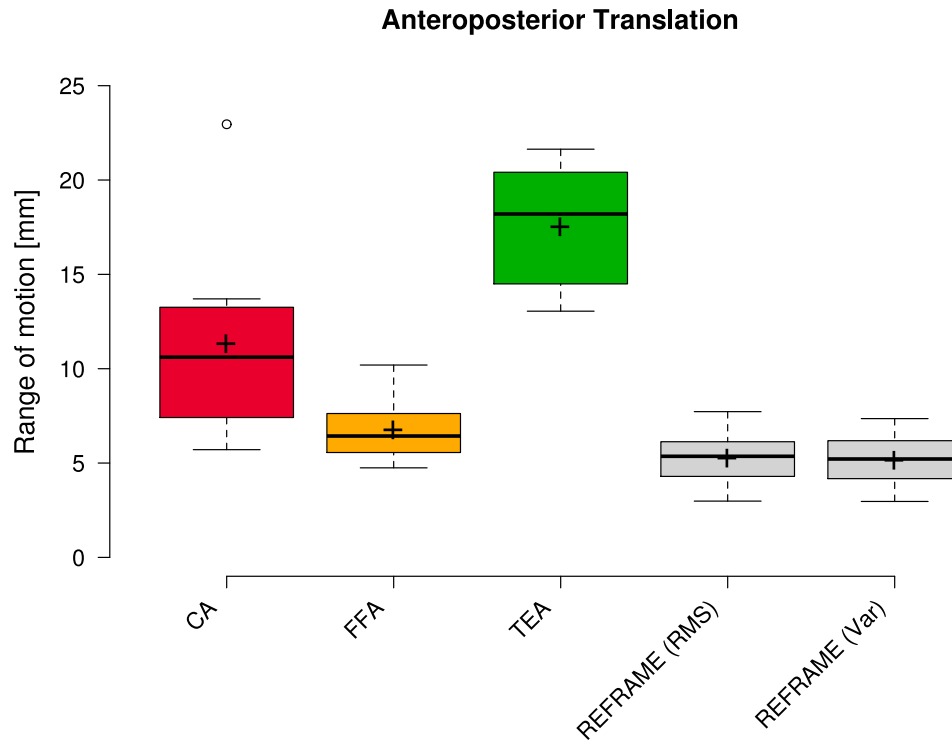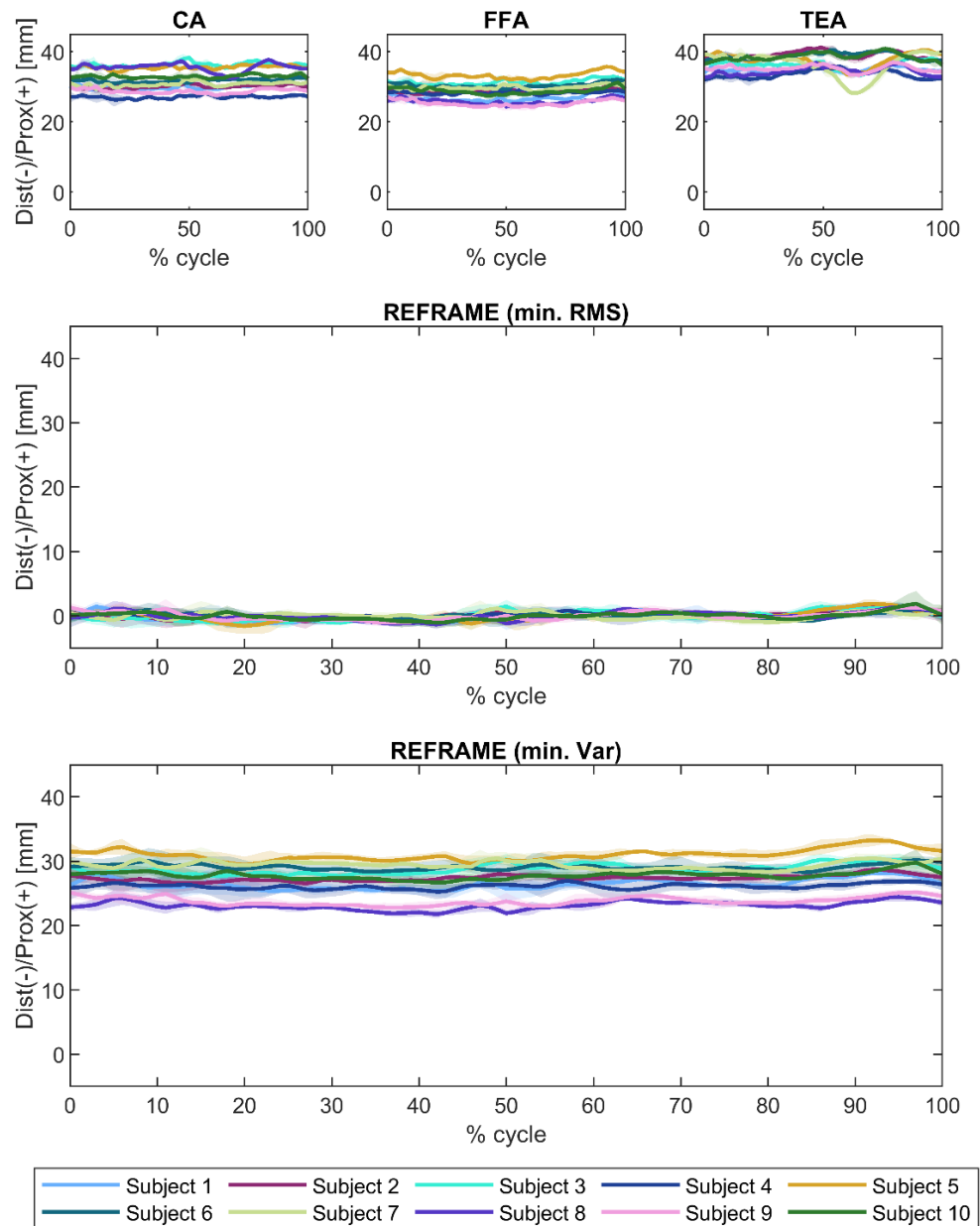
Proximodistal Translation

Figure 12. Box plot of proximodistal range of motion (all subjects and repetitions) according to each of the three different axis approaches (CA: cylindrical axis; FFA: functional flexion axis; TEA: transepicondylar axis), as well as after REFRAME implementation. Centre lines illustrate the medians, while box limits depict the 25th and 75th percentiles. Whiskers extend to data points that are less than 1.5 times the interquartile range away from the 1st and 3rd quartiles. Outliers are indicated by circles. Note: kinematic patterns for all three axes converge to a single solution upon application of REFRAME, and therefore all display the same range of motion values.
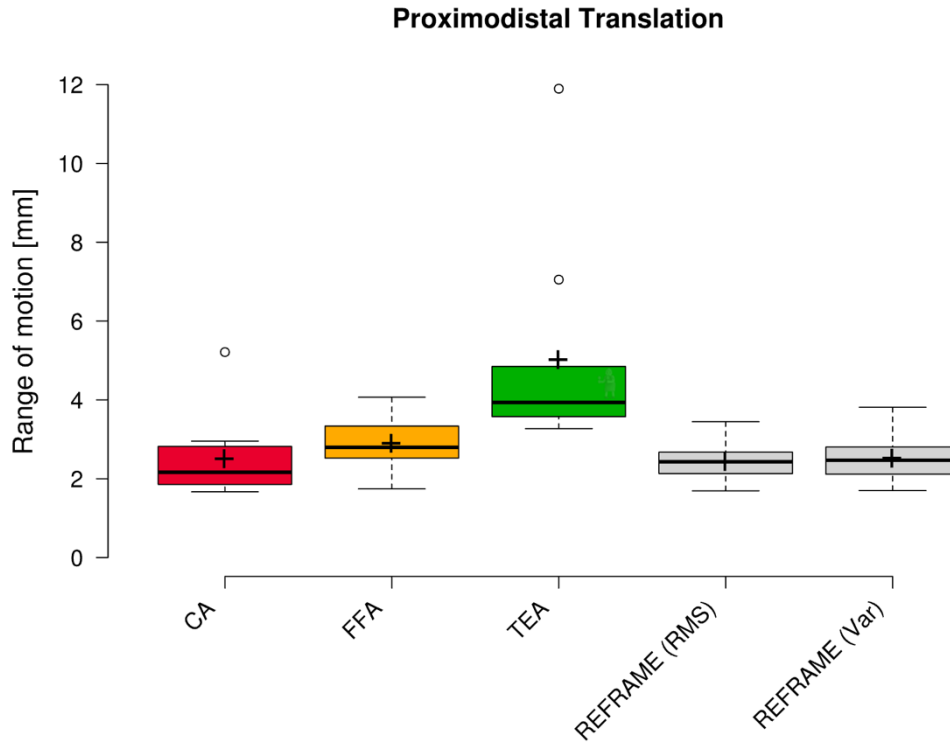
	Absolute Values			
	Maximum	Mean	±	SD
Femur				
Rot [°] X	0.0	0.0	±	0.0
Rot [°] Y	11.6	2.8	±	2.7
Rot [°] Z	10.1	2.6	±	2.5
Trans [mm] (min. RMS) X	25.9	10.2	±	6.6
Trans [mm] (min. RMS) Y	10.9	3.8	±	3.6
Trans [mm] (min. RMS) Z	10.9	3.7	±	2.9
Trans [mm] (min. Var) X	26.8	10.5	±	7.0
Trans [mm] (min. Var) Y	10.8	4.0	±	3.6
Trans [mm] (min. Var) Z	10.8	3.7	±	2.9
Tibia				
Rot [°] X	0.0	0.0	±	0.0
Rot [°] Y	7.2	2.3	±	1.5
Rot [°] Z	15.0	5.2	±	4.2
Trans [mm] (min. RMS) X	33.8	16.7	±	6.9
Trans [mm] (min. RMS) Y	10.9	6.2	±	2.2
Trans [mm] (min. RMS) Z	30.9	27.8	±	2.1
Trans [mm] (min. Var) X	0.0	0.0	±	0.0
Trans [mm] (min. Var) Y	0.0	0.0	±	0.0
Trans [mm] (min. Var) Z	0.0	0.0	±	0.0

Table 1. Maxima and mean values ± standard deviation of absolute values of rotations (in degrees) and translations (in mm) applied to raw local reference frames as part of REFRAME implementation; Rotations are expressed as an XYZ intrinsic Cardan angle sequence; Transformations are expressed in the corresponding raw reference coordinate systems (x-axis = mediolateral; y-axis = anteroposterior; z-axis = proximodistal).

4. Discussion

Despite multiple studies showing that kinematic signals are sensitive to the orientation of the knee flexion axis [5, 23-25], the influence of local 3D reference frame orientation and position is frequently underestimated (or in some cases, haphazardly ignored), especially in investigations involving the comparison and interpretation of kinematic signals. Difficulties in achieving a repeatable and reproducible representation of human joint motion has therefore limited our ability to attain a robust understanding of knee kinematics, even among asymptomatic populations, let alone detect differences in pathological joints. In this study, the fluoroscopy-based tibiofemoral kinematics of ten healthy subjects were analysed before and after the implementation of REFRAME, thereby substantiating results obtained in a previous investigation [13] in nine additional subjects. Moreover, these latest findings served as a starting point for the analysis of inter-subject differences in kinematic signals in which cross-talk artefacts due to frame alignment inconsistencies have been addressed repeatably.

Analysis of the raw kinematic signals obtained from calculating tibiofemoral rotations and translations based on three different joint axis methodologies, strongly indicated that the CA and FFA approaches produced generally closer approximations of each other than the TEA approach. We therefore challenge Churchill and colleagues' early proposal that a TEA based on the palpation of bony landmarks acts as an accurate approximation of the knee joint's functional flexion axis [2]. Instead, in the absence of post-processing methods such as REFRAME, our results partially support the findings of our recent work [5] favouring the use of an FFA or CA approach to avoid the high susceptibility to cross-talk artefact demonstrated by TEA-based kinematics. Under the assumption that joint segments are rigid bodies (for measurements affected by soft-tissue artefact, pre-processing raw data with dedicated algorithms to reduce motion artefact and approximate rigid marker configurations would be required), REFRAME then additionally allows users to optimise frame pose in all six DOFs, rather than performing no frame optimisation (e.g. TEA, CA) or only optimising the orientation of the ML axis (e.g. FFA). Notably, joint axes defined using REFRAME are effectively functional in nature (and as such both subject- and activity-dependent), as they leverage information contained within the kinematic signals to arrive at the optimised reference frames (thus inherently less susceptible to intra- and inter-observer errors). In this study, the availability of fluoroscopic data to assess the pose of local segment frames relative to each subject's bone geometry after REFRAME optimisation could potentially be crucial to explore whether kinematic signals represent similar motion in different subjects (Supplementary Figure S2). It is important to note, however, that the pose of the true instantaneous axis of rotation (i.e. axis with zero translational velocity) is not constant relative to the moving segment's bone geometry. As a result, any anatomically fixed axis will deviate from the instantaneous axis of rotation as soon as complex motion like e.g. rolling without slipping occurs, leading to cross-talk between flexion and translation (Supplementary Figure S3). Consequently, any segment-fixed axis may be able to correctly characterise relative segment motion at particular timepoints (whenever the axis coincides with the instantaneous axis of rotation) but will likely introduce translational cross-talk over the rest of the movement cycle. While an exploration of the philosophical discussion that arises regarding the advantages and pitfalls of anatomically fixed axes versus functional joint axes is beyond the scope of this study, researchers should stay aware of the implications that choosing one type of axes over the other has on the interpretability of their reported results.

Comparison of raw kinematic signals in all six DOFs was followed by optimisation of frame orientations and positions using REFRAME. In line with the previously presented two-stage implementation of REFRAME [13], only frame orientations were optimised in the first stage, followed by the

optimisation of frame origin positions in the second stage. In this study, we chose to minimise ab/adduction and int/external rotation RMS, while restricting changes in the orientation of the tibial local reference frame around the ML (x-) axis, and minimally penalising analogous changes to the femoral reference frame. This REFRAME configuration was selected to minimise cross-talk artefact and maximise rotations in the sagittal plane, which we previously recommended for aligning the axes in clearly flexion-dominant activities [13]. Here, the most notable changes that resulted from REFRAME axis realignment were present in out-of-sagittal-plane rotations. After REFRAME, the resultant ab/adduction patterns over stair descent became both more constant and neutral, while subjects exhibited subtly varying degrees of a sinusoidal pattern in their int/external rotation. These observations are consistent with previous interpretations that suggest knee motion is dominated by rotation in the sagittal and transverse planes [2]. Even though the resulting kinematic signals appear smaller in magnitude, it is important to note here that REFRAME minimisation does not reduce the actual motion that occurs in the joint. Given as the transformations applied to the local segment reference frames are constant over the entire cycle, REFRAME can help illustrate *the same* articulating movement patterns while excluding artefact amplifications linked to cross-talk [13]. Notably, the magnitude of rotations around the AP (y-) and PD (z-) axes performed by REFRAME to reconcile the orientation of local reference frames averaged only $2.8° \pm 2.7°$ and $2.6° \pm 2.5°$, respectively, for the femur. For the tibia, they averaged $2.3° \pm 1.5°$ around the AP axis, and $5.2° \pm 4.2°$ around the PD axis. These magnitudes were well within the range of uncertainty typically associated with joint axis methods [11, 26], especially considering that while *absolute* changes to the tibial frame orientation did exceed 5° around the PD axis, *relative* changes between femur and tibia did not. Researchers are encouraged to review cases where relative changes in frame orientation drastically exceed 5° to evaluate the possible clinical implications of such transformations. Importantly, the standardisation of kinematic signals towards a single repeatable representation (c.f. Subject 8 in Figure 9) brings us closer to achieving a common and consistent interpretation of joint motion patterns between subjects, studies and even laboratories. By excluding any signal differences that could be explained by distinctions in analysis methodology (specifically, by harmonising reference frame orientations and positions), optimised signals offer stronger evidence of potential differences in joint motion.

The first REFRAME configuration we explored for the optimisation of local frame origin locations relied on a minimisation of the RMS of joint translations along all three coordinate frame axes, targeting a zero-mean signal with minimal variation over the activity cycle. While this choice of objective criteria held the potential to highlight inter-subject differences by minimising signal variability, it targeted mean value of 0 mm along all three axes, corresponding with the underlying assumption that the femoral and tibial origins would ideally coincide or be only minimally offset.

A second implementation of REFRAME was also investigated, which minimised translational variance instead of RMS. The minimisation of variance for all three joint translations effectively minimised signal amplitude over the activity cycle (consistent with the notion that changes in joint translation are generally small in magnitude), while allowing for any mean translation value. This philosophy better aligns with a more clinically intuitive model of the knee that does not assume the femoral and tibial origins should be coincident during standing. Instead, this second implementation facilitates a knee model in which the femoral and tibial origins are likely offset by roughly fixed distances of easily 10 mm or more (Supplementary Figure S4).

For joint translations, these two different implementations of REFRAME each appear to highlight different relevant aspects of joint motion during stair descent. The first REFRAME minimisation of translation RMS aimed for coincident origins along all axes, thereby "flattening" the kinematic signals

towards a common mean close to 0. This implementation emphasised differences in the progression of the kinematic signal over the activity cycle, especially in AP translation. While PD translation appears to have been rather constant, ML translation signals showed slightly more local fluctuations around a constant mean. These fluctuations, however, are likely the result of out-of-plane errors in the 2D/3D registration of uniplanar fluoroscopy data. Moreover, for one of the ten subjects, the set of optimal orientations and positions found after REFRAME were associated with an increase in average ML ROM. This effect could be explained by the choice to weigh the minimisation of all parameters equally, such that the subtle increase in ML ROM was offset by the comparably larger decrease in e.g. AP ROM, rendering that solution for the objective function to nevertheless be optimal. Given the limitations of single-plane fluoroscopy, the ML translation results presented in this study should be interpreted with caution, especially considering that the ML registration of images had to be manually adjusted for several trials [14, 27]. Future research leveraging state-of-the-art dual-plane moving fluoroscopy could lead to confirmation of this interpretation, as well as support insights into the advantages provided by other REFRAME implementations. On the other hand, AP translation patterns displayed subtle peaks at approximately 50% and 80% of the gait cycle, with a slight global minimum between 60% and 70%. While this general overall pattern was fairly repeatable across all subjects, signal amplitude varied between subjects, likely a manifestation of variation in the degree to which different individuals' AP translation relates to knee flexion.

The second implementation of REFRAME minimising translation variance effectively "flattened" the curve (similar to RMS) but towards a mean value (not necessarily 0) for each individual. Although differences in pattern progression over the activity cycle are less evident than when minimising RMS, this implementation minimising variance reveals potentially interesting differences in the mean values after optimisation. The translational offset between the femoral and tibial origins axially is consistently between 20 mm and 35 mm over the entire gait cycle which, when combined with the almost negligible ab/adduction ROM, suggests that little (if any) condylar lift-off occurs in healthy knees. This REFRAME interpretation is more compatible with current clinical understanding of joint motion (e.g. that effectively no condylar lift-off takes place in healthy knees during gait) than the far more extreme interpretation of movement patterns suggested by the raw joint axes (e.g. that the joint gap is compressed by over 10 mm in Subject 7, according to TEA, Figure 11).

The location of the REFRAME origins can also provide critical insights into other aspects of joint functionality, especially considering the optimised origin after translation variance minimisation is conceptually comparable to an average pivot point. Taking into account that the initial mediolateral position of the tibial origin was at the midpoint between lateral and medial epicondyles, and that this origin barely moved with REFRAME optimisation, our results suggest a joint centre of rotation that is located medially, in line with Freeman and Pinskerova's proposed general description of knee motion [28, 29]. Here, one valuable aspect of REFRAME is that such functional characteristics of joint motion can be directly extracted without further analysis (although additionally exploring the motion of specific bony landmarks can certainly still be valuable in several cases). Notably, even though the variance-based implementation of REFRAME predictably led to larger differences in the mean relative displacement of femoral and tibial origins, results show that both REFRAME implementations led to almost identical average translational ROM along all three axes. These results exemplify how different REFRAME implementations could emphasise different motion characteristics, highlighting intra- and inter-subject patterns that become noticeable only after REFRAME has successfully excluded signal variations associated with reference frame pose. Nevertheless, the practical implications of different REFRAME formulations are highly nuanced, and further investigations are necessary before a full understanding of the potential of this approach for interpreting joint kinematics can be gained.

In this study, our results clearly demonstrate that the numerical magnitude of kinematic signals can vary greatly depending on the exact orientation and position of joint axes. For example, for a unique physical motion pattern, an AP displacement measurement of -10 mm, could easily become 0 mm or +5 mm after slight local frame reorientation and/or repositioning [9, 13]. As a result, evidence suggests that any attempt to clinically interpret joint kinematics based on the plots of joint angles and/or translations should generally avoid extracting inferences from their *absolute values*. Instead, the focus should be on assessing *relative differences*, either for a single knee joint (e.g. at different instances in time), or between knees (e.g. left knee vs. right knee of the same subject, or different subjects). On the one hand, there may be a potential advantage to switching our focus from the interpretation of kinematic pattern shape and instead concentrating on the extraction of discrete, yet informative, kinematic features (e.g. position of the femoral origin after minimisation of translational variances to examine the centre of rotation in the transverse plane). On the other, however, as long as traditional plots of kinematic time series continue to be used for interpretation, our findings clearly substantiate that the removal of kinematic signal differences caused by inconsistent representations of joint segments is critical to allow the detection of actual differences in joint motion (while showcasing REFRAME's ability to tackle a key component of this challenge). In this manner, this study compellingly illustrates the pivotal role that methods like REFRAME (which can successfully account for differences in frame orientation and position) stand to play in our clinical understanding of joint movement patterns.

Author contributions

Conceptualisation: A.O.V., W.T., B.P., P.S., A.S.; Methodology: A.O.V., A.S.; Software: A.O.V., A.S.; Formal analysis: A.O.V., B.P., P.S., A.S.; Investigation: A.O.V., A.S.; Resources: W.T., B.P., P.S., A.M., T.G.; Data curation: A.O.V., B.P., P.S., A.S.; Writing—original draft: A.O.V., W.T., A.S.; Writing—review and editing: A.O.V., W.T., B.P., P.S., A.M., T.G., A.S.; Supervision: W.T., A.M., T.G., A.S.; Project administration: W.T., T.G., A.S.; Funding acquisition: W.T., A.M., T.G. All authors have read and agreed to the published version of the manuscript.

Data availability

The implemented method (REFRAME) can be openly accessed by downloading the standalone application and accompanying user documentation available in https://bbraun.info/reframe and https://movement.ethz.ch/data-repository/reframe.html. Additional MATLAB files to enable advanced custom features are also available under license from the corresponding author upon reasonable request. The original subject data used during the current study to validate the proposed method is part of a dataset generated within the scope of a separate, previously published study [5]. For further information regarding the data availability of this referenced kinematic dataset, please refer to the original article available here: https://doi.org/10.1016/j.jbiomech.2022.111306; and/or contact the respective corresponding author of that study.

Acknowledgements

Ethics declarations

Collection of the original fluoroscopy data that was analysed here occurred within the scope of a separate cited study, which was performed in accordance with relevant guidelines and states that all subjects "provided written, informed consent to participate in this study, which was approved by the local ethics committee (KEK-ZH-Nr. 2016-00410)" [5].

Competing interests

A.O.V., A.M., T.G. and A.S. are employees of B. Braun Aesculap AG, Tuttlingen, Germany. W.T. has received compensation as a member of a scientific advisory board of the company. A.S., and A.M. are all listed as co-inventors on a pending patent application submitted by Aesculap AG under number DE102022125697A1, which claims a system for standardising axis orientation and position in kinematic data relating to a patient's body joint. A version of the REFRAME code is nevertheless openly available upon request for non-commercial purposes.

References

1.   Berger, R.A., Rubash, H.E., Seel, M.J., Thompson, W.H., and Crossett, L.S., *Determining the rotational alignment of the femoral component in total knee arthroplasty using the epicondylar axis.* Clinical Orthopaedics and Related Research, 1993(286): p. 40-47.

2.   Churchill, D.L., Incavo, S.J., Johnson, C.C., and Beynnon, B.D., *The transepicondylar axis approximates the optimal flexion axis of the knee.* Clinical Orthopaedics and Related Research, 1998(356): p. 111-118.

3.   Ehrig, R.M., Taylor, W.R., Duda, G.N., and Heller, M.O., *A survey of formal methods for determining functional joint axes.* Journal of Biomechanics, 2007. **40**(10): p. 2150-2157.

4.   Ehrig, R.M., Taylor, W.R., Duda, G.N., and Heller, M.O., *A survey of formal methods for determining the centre of rotation of ball joints.* Journal of Biomechanics, 2006. **39**(15): p. 2798-2809.

5.   Postolka, B., Taylor, W.R., Datwyler, K., Heller, M.O., List, R., and Schütz, P., *Interpretation of natural tibio-femoral kinematics critically depends upon the kinematic analysis approach: A survey and comparison of methodologies.* Journal of Biomechanics, 2022. **144**: p. 111306.

6.   Victor, J., *Rotational alignment of the distal femur: A literature review.* Orthopaedics & Traumatology: Surgery & Research, 2009. **95**(5): p. 365-372.

7.   Feng, Y., Tsai, T.Y., Li, J.S., Rubash, H.E., Li, G., and Freiberg, A., *In-vivo analysis of flexion axes of the knee: Femoral condylar motion during dynamic knee flexion.* Clinical Biomechanics, 2016. **32**: p. 102-107.

8.   Wu, G. and Cavanagh, P.R., *ISB recommendations for standardization in the reporting of kinematic data.* Journal of Biomechanics, 1995. **28**(10): p. 1257-1261.

9.   Ortigas-Vásquez, A., Taylor, W.R., Maas, A., Woiczinski, M., Grupp, T.M., and Sauer, A., *A frame orientation optimisation method for consistent interpretation of kinematic signals.* Scientific Reports, 2023. **13**(1): p. 9632.

10.   Ortigas-Vásquez, A., Maas, A., List, R., Schütz, P., Taylor, W.R., and Grupp, T.M., *A Framework for Analytical Validation of Inertial-Sensor-Based Knee Kinematics Using a Six-Degrees-of-Freedom Joint Simulator.* Sensors, 2022. **23**(1).

11. Jenny, J.Y. and Boeri, C., *Low reproducibility of the intra–operative measurement of the transepicondylar axis during total knee replacement.* Acta Orthopaedica Scandinavica, 2004. **75**(1): p. 74-77.

12. Jerosch, J., Peuker, E., Philipps, B., and Filler, T., *Interindividual reproducibility in perioperative rotational alignment of femoral components in knee prosthetic surgery using the transepicondylar axis.* Knee Surgery, Sports Traumatology, Arthroscopy, 2002. **10**(3): p. 194-197.

13. Ortigas-Vásquez, A., Taylor, W.R., Postolka, B., Schütz, P., Maas, A., Woiczinski, M., Grupp, T.M., and Sauer, A., *A Reproducible and Robust Representation of Tibiofemoral Kinematics of the Healthy Knee Joint during Stair Descent using REFRAME – Part I: REFRAME Foundations and Validation.* 2024: Preprint on Research Square.

14. Postolka, B., Schütz, P., Fucentese, S.F., Freeman, M.a.R., Pinskerova, V., List, R., and Taylor, W.R., *Tibio-femoral kinematics of the healthy knee joint throughout complete cycles of gait activities.* Journal of Biomechanics, 2020. **110**: p. 109915.

15. Hamai, S., Moro-Oka, T.A., Dunbar, N.J., Miura, H., Iwamoto, Y., and Banks, S.A., *In vivo healthy knee kinematics during dynamic full flexion.* Biomed Res Int, 2013. **2013**: p. 717546.

16. Hoshino, Y., Wang, J.H., Lorenz, S., Fu, F.H., and Tashman, S., *The effect of distal femur bony morphology on in vivo knee translational and rotational kinematics.* Knee Surgery, Sports Traumatology, Arthroscopy, 2012. **20**(7): p. 1331-1338.

17. Thomeer, L., Guan, S., Gray, H., Schache, A., De Steiger, R., and Pandy, M., *Six-Degree-of-Freedom Tibiofemoral and Patellofemoral Joint Motion During Activities of Daily Living.* Annals of Biomedical Engineering, 2021. **49**(4): p. 1183-1198.

18. List, R., Postolka, B., Schütz, P., Hitz, M., Schwilch, P., Gerber, H., Ferguson, S.J., and Taylor, W.R., *A moving fluoroscope to capture tibiofemoral kinematics during complete cycles of free level and downhill walking as well as stair descent.* PLOS One, 2017. **12**(10): p. e0185952.

19. Kurosawa, H., Walker, P.S., Abe, S., Garg, A., and Hunter, T., *Geometry and motion of the knee for implant and orthotic design.* Journal of Biomechanics, 1985. **18**(7): p. 487-499.

20. Asano, T., Akagi, M., Tanaka, K., Tamura, J., and Nakamura, T., *In vivo three-dimensional knee kinematics using a biplanar image-matching technique.* Clinical Orthopaedics and Related Research, 2001(388): p. 157-166.

21. Eckhoff, D.G., Dwyer, T.F., Bach, J.M., Spitzer, V.M., and Reinig, K.D., *Three-dimensional morphology of the distal part of the femur viewed in virtual reality.* Journal of Bone and Joint Surgery, 2001. **83-A Suppl 2**(Pt 1): p. 43-50.

22. Grood, E.S. and Suntay, W.J., *A joint coordinate system for the clinical description of three-dimensional motions: application to the knee.* Journal of Biomechanical Engineering, 1983. **105**(2): p. 136-144.

23. Most, E., Axe, J., Rubash, H., and Li, G., *Sensitivity of the knee joint kinematics calculation to selection of flexion axes.* Journal of Biomechanics, 2004. **37**(11): p. 1743-1748.

24. Walker, P.S., Heller, Y., Yildirim, G., and Immerman, I., *Reference axes for comparing the motion of knee replacements with the anatomic knee.* The Knee, 2011. **18**(5): p. 312-316.

25. Piazza, S.J. and Cavanagh, P.R., *Measurement of the screw-home motion of the knee is sensitive to errors in axis alignment.* Journal of Biomechanics, 2000. **33**(8): p. 1029-1034.

26. Yin, L., Chen, K., Guo, L., Cheng, L., Wang, F., and Yang, L., *Identifying the Functional Flexion-extension Axis of the Knee: An In-Vivo Kinematics Study.* PLOS One, 2015. **10**(6): p. e0128877.

27.   Postolka, B., List, R., Thelen, B., Schütz, P., Taylor, W.R., and Zheng, G., *Evaluation of an intensity-based algorithm for 2D/3D registration of natural knee videofluoroscopy data.* Medical Engineering & Physics, 2020. **77**: p. 107-113.

28.   Freeman, M.a.R. and Pinskerova, V., *The movement of the normal tibio-femoral joint.* Journal of Biomechanics, 2005. **38**(2): p. 197-208.

29.   Iwaki, H., Pinskerova, V., and Freeman, M.A., *Tibiofemoral movement 1: the shapes and relative movements of the femur and tibia in the unloaded cadaver knee.* Journal of Bone and Joint Surgery, 2000. **82**(8): p. 1189-1195.

5. Supplementary Material

A full copy of the supplementary material for this article is available online and can be downloaded from the following link:

https://static-content.springer.com/esm/art%3A10.1038%2Fs41598-024-76275-3/MediaObjects/41598_2024_76275_MOESM1_ESM.pdf

VI. Journal Publication V

Validation of inertial-measurement-unit-based *ex vivo* knee kinematics during a loaded squat before and after reference-frame-orientation optimisation

Sagasser, S., Sauer, A., Thorwächter, C., Weber, J.G., Maas, A., Woiczinski, M., Grupp, T.M. and **Ortigas-Vásquez, A.**

Abstract

Recently, inertial measurement units have been gaining popularity as a potential alternative to optical motion capture systems in the analysis of joint kinematics. In a previous study, the accuracy of knee joint angles calculated from inertial data and an extended Kalman filter and smoother algorithm was tested using ground truth data originating from a joint simulator guided by fluoroscopy-based signals. Although high levels of accuracy were achieved, the experimental setup leveraged multiple iterations of the same movement pattern and an absence of soft tissue artefacts. Here, the algorithm is tested against an optical marker-based system in a more challenging setting, with single iterations of a loaded squat cycle simulated on seven cadaveric specimens on a force-controlled knee rig. Prior to the optimisation of local coordinate systems using the REference FRame Alignment MEthod (REFRAME) to account for the effect of differences in local reference frame orientation, root-mean-square errors between the kinematic signals of the inertial and optical systems were as high as 3.8° ± 3.5° for flexion/extension, 20.4° ± 10.0° for abduction/adduction and 8.6° ± 5.7° for external/internal rotation. After REFRAME implementation, however, average root-mean-square errors decreased to 0.9° ± 0.4° and to 1.5° ± 0.7° for abduction/adduction and for external/internal rotation, respectively, with a slight increase to 4.2° ± 3.6° for flexion/extension. While these results demonstrate promising potential in the approach's ability to estimate knee joint angles during a single loaded squat cycle, they highlight the limiting effects that a reduced number of iterations and the lack of a reliable consistent reference pose inflicts on the sensor fusion algorithm's performance. They similarly stress the importance of adapting underlying assumptions and correctly tuning filter parameters to ensure satisfactory performance. More importantly, our findings emphasise the notable impact that properly aligning reference-frame orientations before comparing joint kinematics can have on results and the conclusions derived from them.

Keywords: kinematics; optimisation; knee joint; local reference frame; IMU; knee rig

1. Introduction

In the field of orthopaedics, the use of joint kinematic data to objectively quantify patient function and mobility before and after treatment can markedly improve medical outcomes [1-3]. Current gold standard technologies are often considered to be static [4, 5] or dynamic [3, 6, 7] fluoroscopy or in some cases even marker-based optical motion capture systems [8, 9]. Both fluoroscopic and optical systems are unfortunately not only time- and cost-intensive but also require a large laboratory space and the involvement of experienced technicians [9, 10], thereby limiting their use in regular clinical workflows. In recent years, inertial measurement units (IMUs) have been explored as a cheaper and more flexible alternative to the aforementioned gold standards [11]. At the most basic level, IMUs consist of at least (1) a gyroscope that measures angular velocity and (2) an accelerometer that measures linear acceleration. The accuracy and reliability of the kinematic signals estimated from the measured inertial datapoints highly depend on the performance and robustness of the sensor fusion algorithm implemented, as well as the ability to address sources of errors, like drift [9, 12]. Consequently, the thorough validation of said algorithms is a crucial step towards the standard application of IMU-based gait analysis systems in a clinical setting, which could in turn lead to an improvement in orthopaedic patient care and satisfaction.

Previously, a particular implementation [13] of a Rauch–Tung–Striebel smoother was selected for further exploration based on a number of advantages: flexible sensor placement, non-susceptibility to ferromagnetic disturbances, and no need for extensive calibration [14]. A first set of tests to explore the algorithm's accuracy in the absence of soft tissue artefacts was designed, in which real knee motion patterns that had been previously collected in vivo during level walking, stair decent and sit-to-stand using moving videofluoroscopy [15] were used to guide a six degrees of freedom joint simulator. Knee kinematics estimated based on the two IMUs that had been rigidly attached to the simulator demonstrated promising accuracy for level walking, but errors were larger for the other activities, especially the more they differed from a standard gait. Notably, every simulator trial consisted of at least 50 iterations of each activity cycle. On one hand, this number of repetitions was necessary to ensure accurate execution of the motion by the robotic simulator; on the other hand, however, it could have represented an unrealistic advantage for the performance of the sensor fusion algorithm (especially considering the recursive nature of Rauch–Tung–Striebel smoothing, where a forward pass based on an extended Kalman filter is followed by a backward recursion smoother, and accuracy generally improves with additional iterations) [16].

In this study, in order to further evaluate the effectiveness and reliability of a promising IMU-based gait analysis system [13, 14, 17], a prototype was tested in a different, more challenging experimental setup. This served as an intermediate step between the initial tests that relied on the controlled execution of simulated data and future in vivo tests in real-use cases. Originally designed and conducted as part of a separate study, experiments consisted of simulating a single loaded squat in each of seven cadaveric specimens using a force-controlled knee rig. By additionally attaching IMU sensors to that knee rig setup, IMU-based rotational knee kinematics could be estimated and compared against an optical-marker-based reference system. Moreover, the potential effects of inconsistencies between the local reference frames defined by the IMU- vs. optical-based motion capture systems were subsequently assessed by using the REference FRame Alignment MEthod (REFRAME) [17, 18]. Differences in the kinematic signals stemming from each system were then evaluated both before and after the implementation of REFRAME. In this manner, this study represents an additional step in the validation process of a promising IMU-based gait analysis system, bringing us closer to its possible application in clinics.

2. Materials and Methods

2.1. Experimental setup

Data used for this investigation were collected as part of a study that was approved by the ethics committee of the Ludwig Maximilians University Munich (ID 58-16). Data collection and management complied with all the relevant institutional, national, and international guidelines and legislation. Seven cadaveric knees (fresh frozen specimens; 3 female; 2 right; aged 80.4 ± 4.6 years; Table 1) were tested on the Munich knee rig, an established force-controlled device [19-21]. Exclusion criteria included any previous surgical intervention to the specimen's knee or hip, as well as any records of symptoms pointing to a musculoskeletal pathology of the knee. Moreover, legs with a varus/valgus deformity greater than 10° were excluded from the study. Notably, qualitative observations on bone quality and soft tissue conditions were recorded and are available upon specific request. Kinematic profiles were collected strictly to assess agreement between measuring systems and should not necessarily be interpreted as representative of a "healthy" knee joint. Three additional specimens that were originally tested unfortunately had to be excluded from the analyses because of missing datapoints (e.g., due to corrupted or missing raw data files from either the optical or IMU systems). Specimen tests were carried out by five of the listed study authors (see Author Contributions; Investigation), including the laboratory supervisor, the lead knee rig operator, and the developer of the IMU system prototype used. Specimen handling was additionally overseen by an experienced orthopaedic surgeon. All specimen tests took place within a span of four months. Each specimen was tested within 36 h of thawing, as well as within 60 h of having been removed from a freezing temperature.

Table 1. Specimen characteristics

Specimen ID	Age (years)	Sex	Left / Right
1	73	Male	Right
2	88	Male	Right
3	83	Female	Left
4	80	Male	Left
5	78	Female	Left
6	77	Male	Left
7	84	Female	Left
Mean	80.4		
SD	4.6		

 Bone cuts were made 20 cm proximally and 22 cm distally from the epicondylar line, after which the femur and tibia were embedded in metal pots with epoxy resin (RenCast FC 52/53 Isocyanate & FC 53 Polyol, Huntsman Advanced Materials GmbH, The Woodlands, TX, USA). A cortical screw was used to attach the fibula head to the proximal tibia, and a constant muscle force of 20 N was applied throughout the entire load cycle by attaching metallic finger traps (Bühler-Instrumente Medizintechnik GmbH, Tuttlingen, Germany) to the vastus medialis, vastus lateralis, musculus semitendinosus,

and biceps femoris. The mentioned loads were applied in the directions of the respective muscle origins to simulate a physiological line of action (Figure 1; for more information on the direction of forces see Figure 2 in [19]. Further details on this general setup have been described in prior studies [21-23].
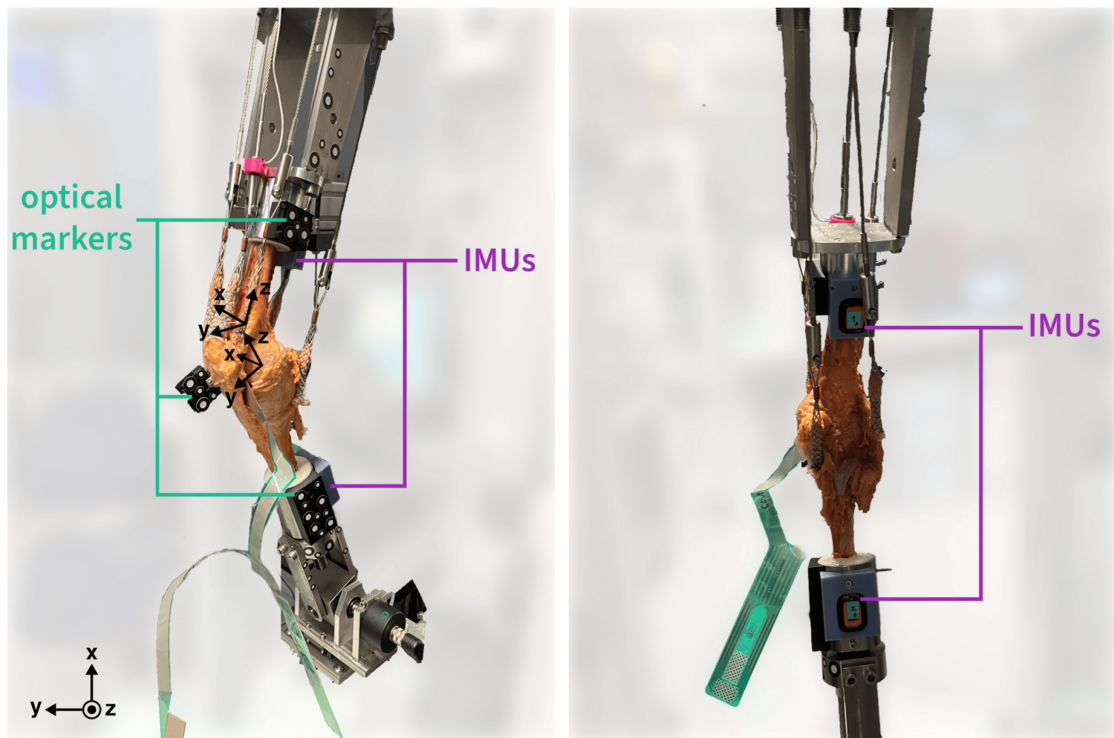
Figure 2. Cadaveric knee on the knee rig, side-view with optical markers (left) and from behind with IMU sensors (right).

A squat from approximately 30° to 130° of the knee flexion (as measured by two angular sensors placed on the hip and ankle joint, respectively; 8820, Burster, Gernsbach, Germany) was performed with a constant angular velocity of 3°/s. In line with previous studies that demonstrated that the shapes of kinematic profiles do not change considerably by increasing ground reaction forces, a controlled muscle force was applied to the rectus femoris to achieve a constant ground reaction force of 50 N. As per Müller et al. [24], further increasing the load would unnecessarily stress both the specimens and equipment but not guarantee better qualitative outcomes. Rotational tibio-femoral kinematics were calculated based on the measurements from two different systems. One system consisted of two IMUs (Xsens Dot, Movella, Enschede, Netherlands), where the sensors were fixed to the metal pots at the ends of the femur and tibia using custom 3D printed parts (Figure 1, right, in blue). Furthermore, the second system comprised a high-resolution 3D camera (Aramis, GOM, Braunschweig, Germany) and 2D optical markers attached to 3D printed parts fixed to the femur, tibia and patella (Figure 1, left, in black).

2.2. Calculation of tibio-femoral kinematics

IMUs were used to sample linear acceleration and angular velocity at 60 Hz. Estimates of tibio-femoral joint angles were obtained from these raw inertial measurements based on a sensor fusion algorithm that leveraged Rauch-Tung-Striebel smoothing (i.e., extended Kalman filtering and smoothing) as per

Versteyhe et al. [12-14, 25]. While an earlier formulation of the algorithm included an offset correction step that relied on the assumption that the subject would start and end the trial at a neutral reference pose with 0° of knee flexion, this operation was adapted to account for a starting flexion angle of approximately 30° by calibrating the flexion value at the first timepoint to match that of the marker-based system.

A high-resolution camera system was used to track the 3D coordinates of selected anatomical landmarks based on rigid clusters of adhesive reflective markers (Figure 1). A right-handed global coordinate system was automatically determined by the camera system software such that the general directions of the x-, y- and z- axes were up, left and towards the camera setup, respectively. Local reference frames were defined for both the femur and tibia segments. The medio-lateral axis of the femoral reference frame was oriented laterally, in the direction of a vector connecting the medial and lateral epicondyles, with the femoral origin located at the midpoint between the two landmarks. The antero-posterior axis of the femur was defined to be positive anteriorly, orthogonal to the medio-lateral axis and a vector connecting the fossa intercondylaris to a point along the longitudinal axis of the femoral shaft, at the centre of the proximal surface of the top metal pot. Lastly, the femoral proximo-distal axis pointed proximally, in a direction orthogonal to the previously defined medio-lateral and antero-posterior axes. For the tibial reference frame, the origin was set at the midpoint between the tubercles of the tibial intercondylar eminence. The tibial medio-lateral axis pointed laterally in the direction of a vector pointing from the medial to the lateral tibial condyle. The tibial antero-posterior axis, on the other hand, pointed anteriorly, orthogonal to the medio-lateral axis and a vector from the centre of the tibial intercondylar eminence to a point along the longitudinal axis of the tibial shaft, at the centre of the distal surface of the bottom metal pot. The proximo-distal axis was then defined as orthogonal to the first two axes, pointing in the proximal direction.

For both IMU and optical systems, joint rotations were expressed as the orientation of the local tibia frame relative to the local reference frame of the femur. Moreover, Cardan angles were calculated based on an intrinsic XYZ rotation sequence from the femoral to the tibial frame, where the x-axis was pointed laterally, the y-axis anteriorly and the z-axis proximally for a right knee (left knees were mirrored into right knees). The knee joint angles in the sagittal, frontal and transversal planes corresponded to extension(+)/flexion(−), adduction(+)/abduction(−) and internal(+)/external(−) rotation, respectively. In this manner, two sets of kinematic signals were derived for each trial: one based on inertial and the other on optical measurements. These kinematic signals were then plotted over the progression of the activity cycle and the root-mean-square errors (RMSEs) between data capture systems were calculated for rotations around each of the three axes. RMSE was chosen as one of the most common metrics used to assess the performance of predictive models [26], like the one leveraged by the IMU-based algorithm, and effectively consists of calculating the square root of the average of the squared differences between observed (here, optical) and predicted (here, IMU) outcomes.

2.3. REFRAME

The primary flexion axis assumed by the optical system was defined based on the position of bony landmarks, as described above. On the other hand, the IMU-based system instead leveraged functional calibration methods (finding a best fit primary axis by first approximating the knee joint as a perfect hinge and then expanding the model to consider a ball-and-socket joint) to define the analogous joint axis. Given that natural knees do not behave as perfect hinges, the anatomical axis assumed by the optical system will inevitably differ to some degree from the functional axis used by the inertial system.

Notably, previous studies have highlighted the importance of accounting for differences in local reference-frame orientations prior to comparing joint movement patterns based on kinematic signals [17]. Consequently, after the two aforementioned sets of rotational kinematics had been calculated (inertial and optical), REFRAME [17, 18] was applied to each of the datasets, to optimise the orientation of the associated local segment reference frames and thus ensure consistency in our comparison of the joint angles.

Two different implementations of the REFRAME approach were explored. The first (REFRAME$_{IMU \rightarrow GOM}$; i.e., "optimising IMU towards GOM") minimised the RMSEs of the IMU-based kinematic signals versus the optical-based estimates. Additionally, frame transformations consisting of rotations around the femoral x-axis during optimisation were restricted to prevent non-physiological frame orientations. Rotations around the different segment frame axes have an intuitive clinical meaning only within certain ranges (e.g., if the femoral longitudinal axis is roughly in the direction of the femoral shaft or the vector connecting the knee joint centre to the hip joint centre). Mathematically, however, it would be possible to, e.g., keep a consistent clinically meaningful flexion angle between femoral and tibial frames (by rotating both frames simultaneously), even while using a set of local frame orientations that no longer holds clinical meaning (e.g., if the longitudinal axes of the femur and tibia local segment reference frames are both at a 45° from the direction of the respective bone shafts). Restricting REFRAME transformations consisting of rotations around the mediolateral axis for one of the two segment frames is therefore a way to avoid this effect. The goal of this implementation was to determine whether, despite any initial apparent differences between the inertial and optical joint kinematic signals (due to differences in local reference-frame orientation), the underlying motion being characterised was in fact the same. Given the described experimental setup, both systems were known to measure the same underlying joint motion and, in the absence of errors, their kinematic signals should therefore coincide after the implementation of REFRAME. This method would inherently transform the orientation of the IMU-based reference frames to match that of the optical based frames, so optimisation of the inertial dataset was not entirely independent as it relied on information contained within the optical dataset.

A second implementation of REFRAME (REFRAME$_{RMS}$) was also explored that independently minimised the root-mean-square (RMS) of abduction/adduction and external/internal rotation signals (both with criteria weighting of 1). Optimisation rotations around the femoral x-axis were once again restricted. Finally, in an effort to maintain clinical interpretability after REFRAME, flexion/extension was anchored to its raw values by minimising the RMSE between raw and optimised signals, with a criterion weighting of 0.1.

After REFRAME analysis, the resulting kinematic signals were once again plotted over the progression of the activity cycle, and the RMSEs between data-capture systems were calculated for rotations around each of the three axes. Paired t-tests at a 5% significance level were executed to compare RMSEs before and after REFRAME$_{IMU \rightarrow GOM}$, as well as before and after REFRAME$_{RMS}$. The sensor fusion algorithm, joint angle estimates, REFRAME implementation, and RMSE calculations were all performed in MATLAB (vR2022b; The Mathworks Inc., Natick, MA, USA). Paired t-tests were performed in GraphPad Prism 10 (v10.1.0; GraphPad Software Inc.; San Diego, CA, USA).

3. Results

An analysis of the IMU- and GOM-based kinematics before REFRAME ("raw") showed agreement only between flexion/extension signals (Figure 2). Clear differences were visible between the two systems for abduction/adduction and external/internal rotation, with RMSEs up to 20.4° ± 10.0° for abduction/adduction and 8.6° ± 5.7° for external/internal rotation (Table 2). Notably, the magnitude of errors affecting abduction/adduction angles was seemingly associated with the joint flexion, possibly indicating the presence of a crosstalk artefact.

Nevertheless, after the first REFRAME implementation, REFRAME$_{IMU \to GOM}$, there was a significant improvement in the agreement between the two datasets for all three movement directions (RMSE of 3.0° ± 2.0° for flexion/extension, 0.9° ± 0.4° for abduction/adduction and 1.4° ± 0.7° for external/internal rotation) (Figure 3, Table 2). REFRAME$_{IMU \to GOM}$ led to transformations of the local femoral reference frame of 0° around the x-axis (restricted by the optimisation formulation), 13.5° ± 13.7° around the y-axis, and 2.0° ± 3.1° around the z-axis, on average (Table 3). On the other hand, the tibia frame was on average transformed by 0.7° ± 4.5° around the x-axis, 19.3° ± 10.8° around the y-axis and 4.4° ± 6.9° around the z-axis. (Although traditional mean and standard deviation values are provided here for context, attempts at interpretation should consider that standard operators act non-commutatively when dealing with transformations.)

A second self-contained implementation of the REFRAME approach, REFRAME$_{RMS}$, whereby the optimisation of a dataset was achieved using only information contained within itself, likewise resulted in visible improvement in the agreement of the inertial and optical kinematic signals for two of the joint angles (RMSE of 0.9° ± 0.4° for abduction/adduction and 1.5° ± 0.7° for external/internal rotation) (Figure 4, Table 2). Only for flexion/extension was there a slight deterioration in the correspondence of the IMU and GOM signals (RMSE of 4.2° ± 3.6°) (Table 2). On average, the changes in frame orientations associated with the IMU signals resulting from the implementation of REFRAME$_{RMS}$ were 15.0° ± 10.1° and 0.6° ± 0.7° around the y- and z- femoral axes, respectively (Table 4). Changes to the orientation of the tibial frame, on the other hand, averaged 2.0° ± 2.1° around x, 13.6° ± 9.2° around y and 6.1° ± 3.7° around z. Analogously, the orientation of the GOM-based femoral reference frame was transformed by 1.4° ± 4.3° around y and −1.4° ± 3.0° around z, on average (Table 5). Finally, the GOM tibial frame was rotated 0.0° ± 0.6° around the x-axis, −5.9° ± 4.3° around the y-axis and 2.0° ± 3.4° around the z-axis.

The results of paired t-tests indicated that the change in RMSE for flexion/extension was not statistically significant for either REFRAME implementation (Figure 5a). However, the decreases in RMSE values for abduction/adduction and external/internal rotation brought about by the REFRAME application were found to be statistically significant for a p-value of 0.05 (Figure 5b, c). In fact, even after Bonferroni correction to account for the double comparison (raw vs. after REFRAME$_{IMU \to OPT}$, and raw vs. after REFRAME$_{RMS}$), the decrease in the RMSEs of out-of-sagittal-plane rotations was still considered statistically significant.
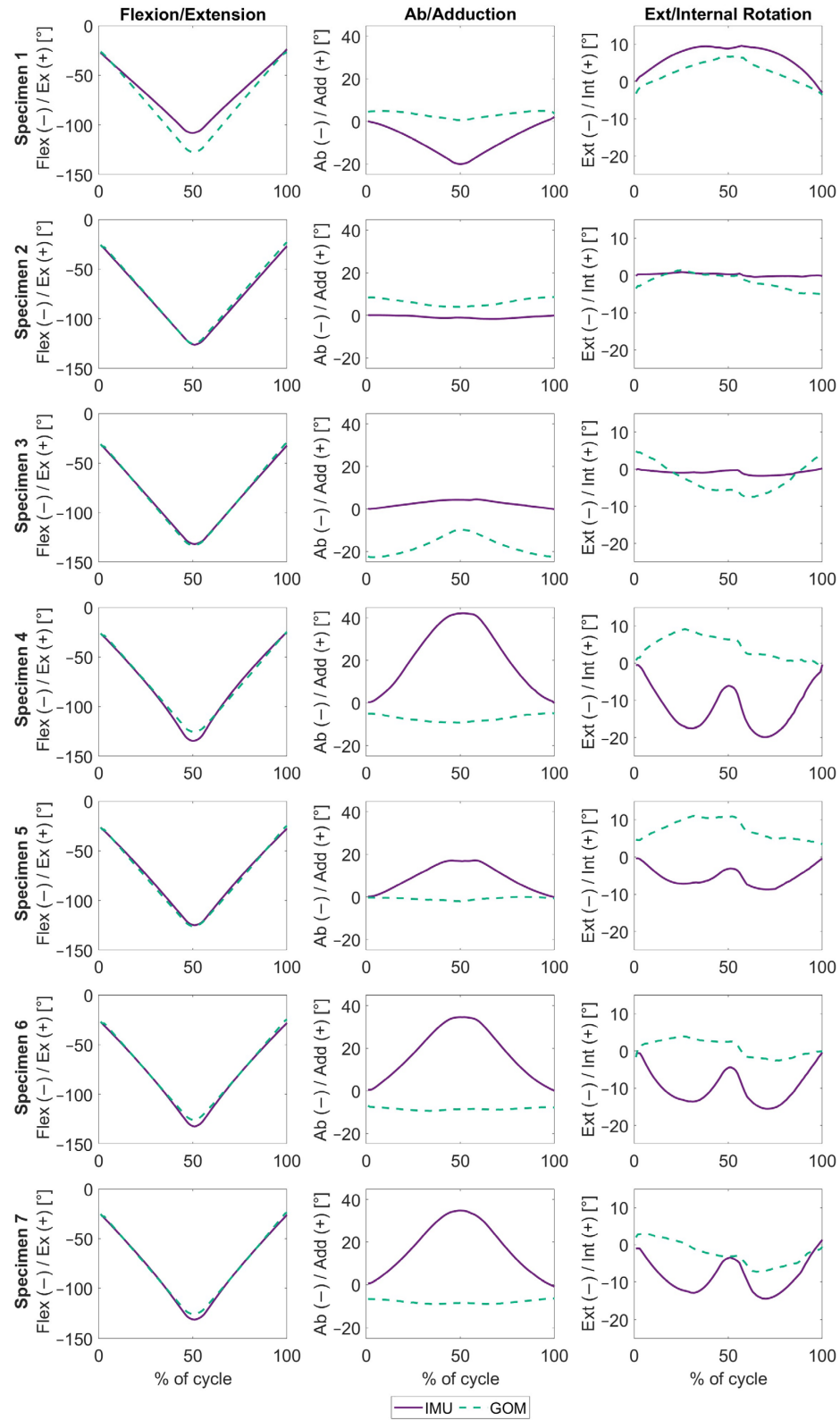
Figure 3. Raw knee joint angles, plotted over the entire squat movement, expressed as a percentage. The solid purple lines represent the angles estimated using inertial data. The dashed green lines represent the angles measured by the optical marker-based system. Each row represents one subject, while the columns represent flexion/extension, ab/adduction and ext/internal rotation (from left to right).

Table 1. Average root-mean-square error (in degrees) for flexion/extension, ab/adduction and ext/internal rotation between IMU-based data and optical marker-based data, before and after REFRAME$_{IMU \rightarrow GOM}$ and REFRAME$_{RMS}$.

	Flexion/Extension	Ab/Adduction	Ex/Internal Rotation
Raw	3.8 ± 3.5	20.4 ± 10.0	8.6 ± 5.7
REFRAME$_{IMU \rightarrow GOM}$	3.0 ± 2.0	0.9 ± 0.4	1.4 ± 0.7
REFRAME$_{RMS}$	4.2 ± 3.6	0.9 ± 0.4	1.5 ± 0.7

Figure 4. REFRAME$_{\text{IMU}\rightarrow\text{GOM}}$ knee joint angles, plotted over the entire squat movement, expressed as a percentage. The solid purple lines represent the angles estimated using inertial data. The dashed green lines represent the angles measured by the optical marker-based system. Each row represents one subject, while the columns represent flexion/extension, ab/adduction and ext/internal rotation (from left to right).

Table 3. Rotational (Rot) transformations (in degrees) of the IMU-based local femoral and tibial reference frames through REFRAME$_{IMU \rightarrow GOM}$ around the x-, y- and z-axis for each specimen.

		Specimen 1	Specimen 2	Specimen 3	Specimen 4	Specimen 5	Specimen 6	Specimen 7
Femur								
	X	0.0	0.0	0.0	0.0	0.0	0.0	0.0
Rot [°]	Y	12.5	-2.7	-6.2	30.1	14.0	23.4	23.2
	Z	5.2	1.3	6.0	-1.1	-2.1	0.6	4.1
Tibia								
	X	-8.6	2.1	0.9	4.4	-0.8	4.0	3.2
Rot [°]	Y	10.9	5.3	14.2	34.5	14.4	29.7	26.1
	Z	9.6	-3.8	-3.2	7.4	-1.1	8.4	13.2

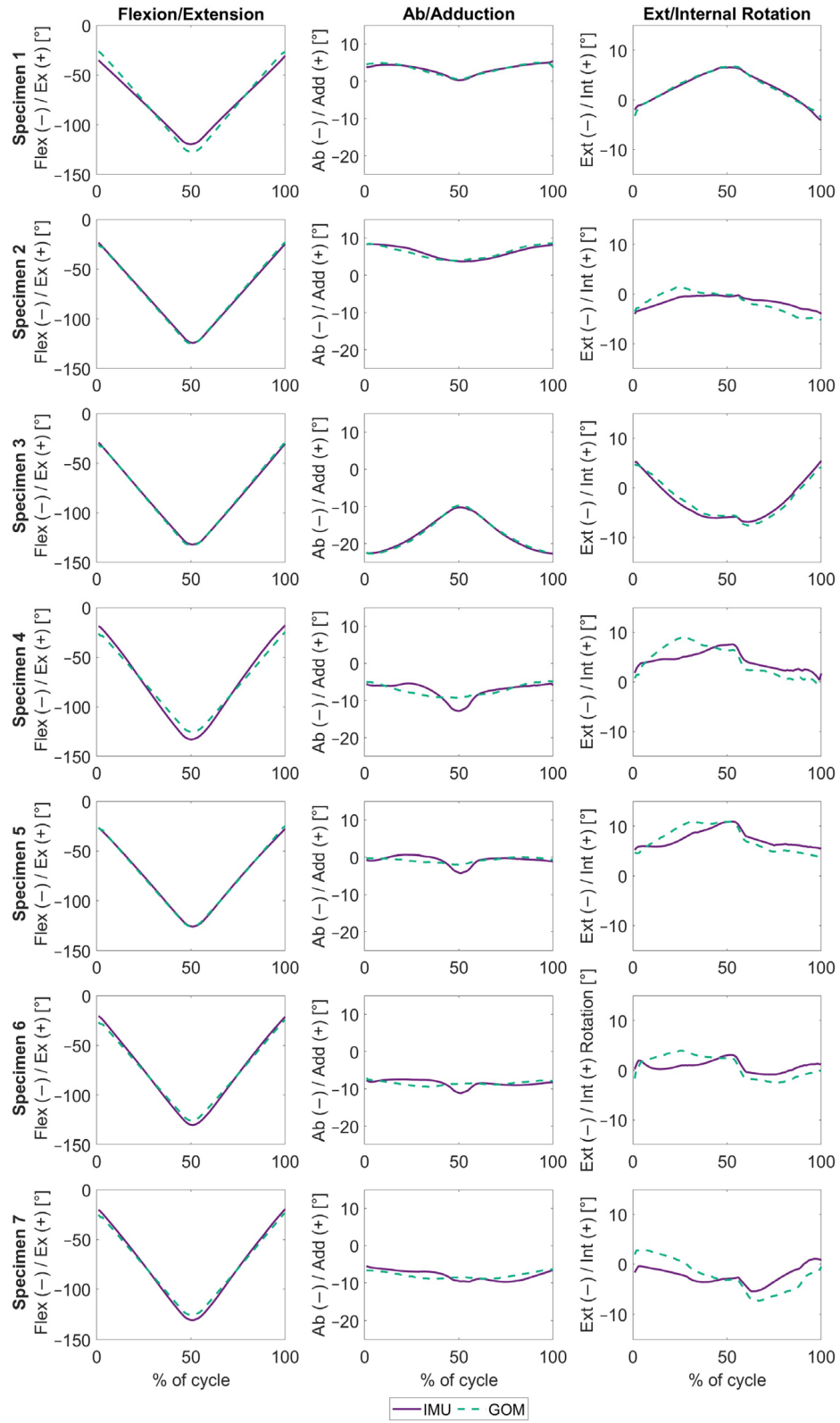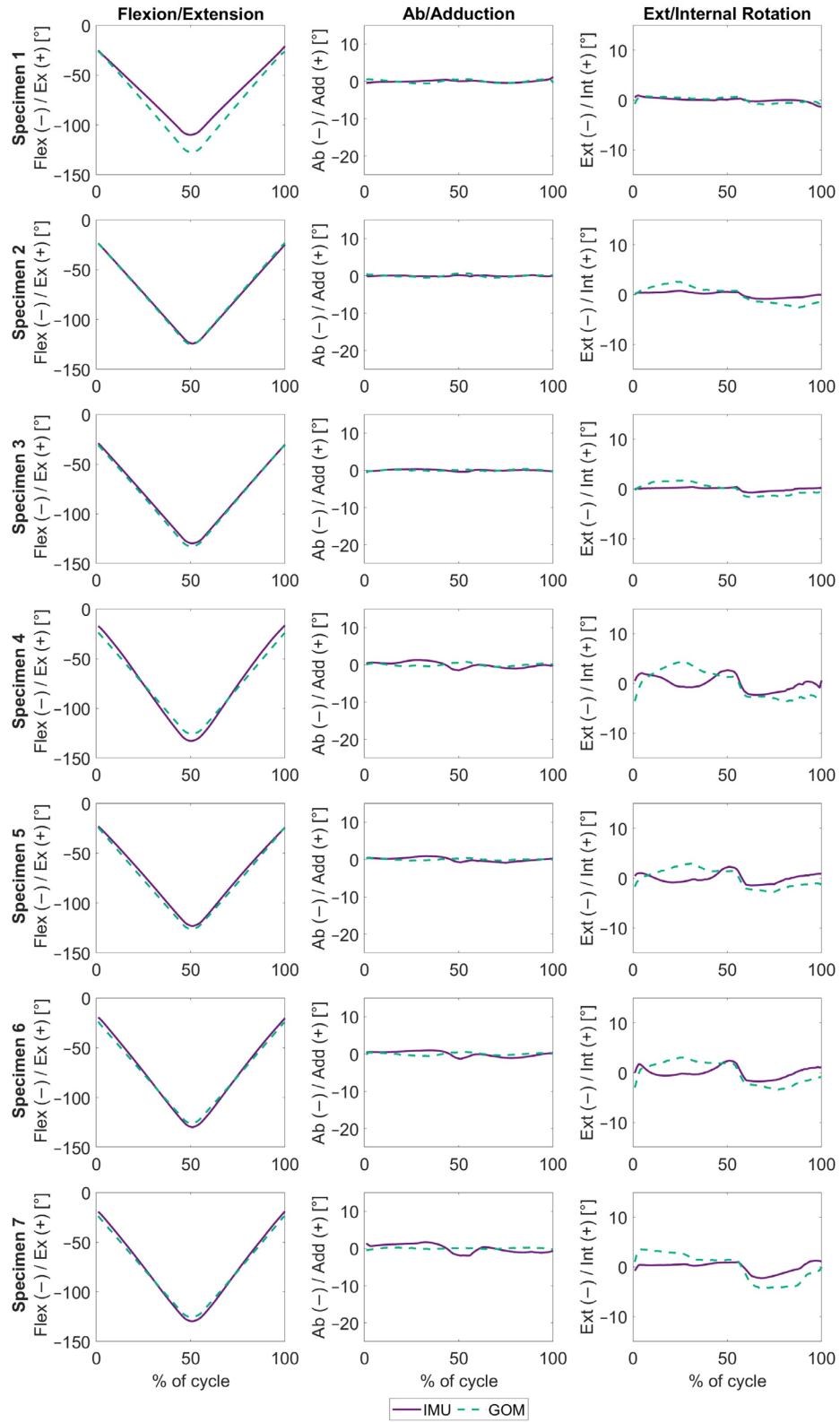**Figure 5.** REFRAME$_{RMS}$ knee joint angles, plotted over the entire squat movement, expressed as a percentage. The solid purple lines represent the angles estimated using inertial data. The dashed green lines represent the angles measured by the optical marker-based system. Each row represents one subject, while the columns represent flexion/extension, ab/adduction and ext/internal rotation (from left to right).

Table 4. Rotational (Rot) transformations (in degrees) of the IMU-based local femoral and tibial reference frames through REFRAME$_{RMS}$ around the x-, y- and z-axis for each specimen.

		Specimen 1	Specimen 2	Specimen 3	Specimen 4	Specimen 5	Specimen 6	Specimen 7
Femur								
	X	0.0	0.0	0.0	0.0	0.0	0.0	0.0
Rot [°]	Y	16.8	0.9	3.0	26.8	12.4	22.7	22.7
	Z	-0.6	0.2	0.1	0.9	1.0	1.1	1.5
Tibia								
	X	1.0	0.0	0.0	5.5	1.0	3.6	3.1
Rot [°]	Y	15.0	0.9	2.7	25.0	10.9	20.4	20.0
	Z	7.4	0.6	1.7	8.9	5.2	8.7	10.0

Table 5. Rotational (Rot) transformations (in degrees) of the GOM-based local femoral and tibial reference frames through REFRAME$_{RMS}$ around the x-, y- and z-axis for each specimen.

		Specimen 1	Specimen 2	Specimen 3	Specimen 4	Specimen 5	Specimen 6	Specimen 7
Femur								
	X	0.0	0.0	0.0	0.0	0.0	0.0	0.0
Rot [°]	Y	3.8	3.6	9.1	-3.2	-1.7	-0.7	-0.8
	Z	-4.8	-0.8	-5.1	1.1	2.9	-0.3	-3.0
Tibia								
	X	-0.2	0.1	-1.1	0.7	0.4	0.2	-0.2
Rot [°]	Y	1.5	-4.7	-11.9	-8.8	-3.5	-8.4	-5.7
	Z	-0.2	4.3	4.4	1.9	6.6	0.2	-3.5
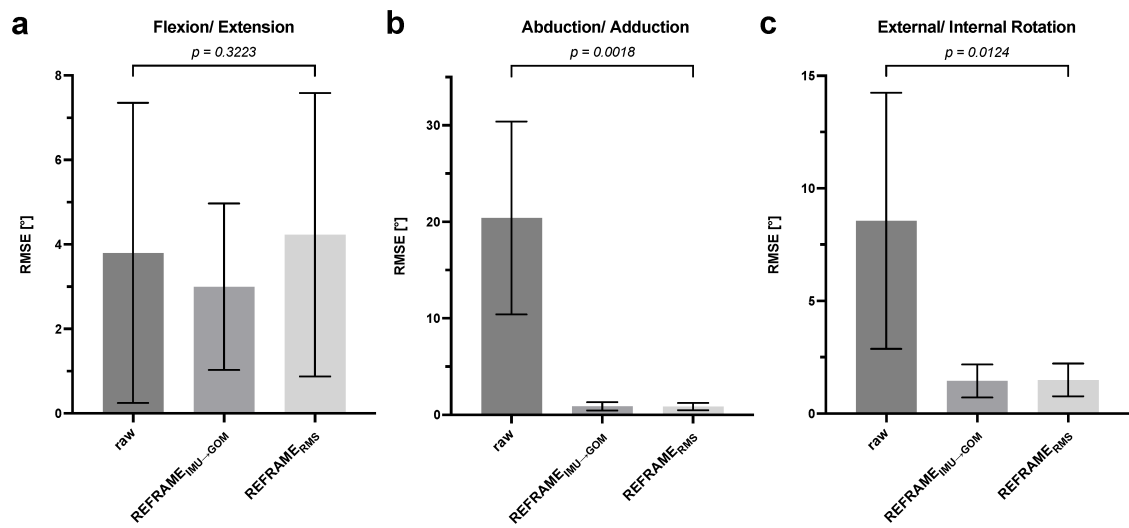
Figure 6. Root-mean-square error (RMSE) comparison: average root-mean-square errors ± standard deviation, before optimisation (raw), after REFRAME$_{IMU \to GOM}$, and REFRAME$_{RMS}$: (a) flexion/extension, (b) abduction/adduction, and (c) external/internal rotation. Statistical significance of differences (*p*-values) based on a paired *t*-test between raw and REFRAME$_{IMU \to GOM}$ and raw and REFRAME$_{RMS}$.

4. Discussion

An IMU-based tool capable of accurately capturing tibio-femoral joint angles during activities of daily living could be extremely valuable in improving patient outcomes in orthopaedic care. In previous work, we adapted and performed first-level validation testing of a prototype system consisting of two IMUs and the implementation of an extended Kalman filter and smoother algorithm [14]. Testing occurred under idealised conditions using a six-degrees of freedom joint simulator and fluoroscopy-based data collected in vivo. Additional work then explored the implementation of a frame orientation optimisation method [17], demonstrating its relevance in ensuring valid conclusions were reached regarding the similarity of and/or difference in joint movement patterns. Importantly, this work determined that even minor inconsistencies in the alignment of joint axes can lead to unreliable kinematic signals. In this study, we therefore tested seven cadaver specimens on a force-controlled knee rig to evaluate the accuracy of the aforementioned IMU-based system in estimating joint kinematics under more challenging conditions than previously tested. This represented a valuable transition from testing on a robotic simulator to testing on real cadaveric specimens, before eventually progressing to the intended in vivo testing conditions. The simulated squat movement was additionally analysed using an optical marker-based system for reference. To ensure reliable comparisons, the kinematic signals stemming from both motion-capture systems were processed using REFRAME, in an effort to align the underlying local coordinate systems of the IMU- and optical-marker-based systems.

Prior to the implementation of REFRAME, our results revealed agreement between the IMU and GOM kinematics for flexion/extension only, showing clear differences for abduction/adduction and external/internal rotation. Moreover, standard deviation values revealed that the implemented IMU algorithm performs differently on different subjects (at least within our limited sample of seven), and these variations seemed to remain even after REFRAME implementation, an effect that was not clearly evident when assessing multiple iterations of repetitive motion patterns, like gait. Importantly, the Rauch-Tung-Striebel smoother assumed by default a reference pose of 0° flexion, 0° adduction and 0° tibial rotation. In the previous study using a six-degrees of freedom joint simulator [14], the assumption of a perfectly neutral reference pose was accurate. In the current study, however, specimens were known to start closer to 30° of flexion, and so the flexion angle at the reference pose assumed by the IMU-based system was appropriately adjusted. Reference abduction/adduction and external/internal rotation values were not analogously adapted, under the assumption that they would be negligible. The resulting discrepancies between the IMU and GOM signals for abduction/adduction and external/internal rotation observed at the beginning of most cycles therefore highlights the importance of having appropriate estimates for all three joint angles in the reference pose to obtain reliable kinematic measurements, especially in the absence of post-processing methods, like REFRAME.

The patterns of errors in abduction/adduction and external/internal rotation seen in the raw kinematic patterns are clearly indicative of cross-talk, which refers to how differences in the alignment of the knee's medio-lateral axis lead to an artificial increase in the amplitude of out-of-sagittal plane rotations (Figure 2). In an idealised representation of cross-talk, with a frame misalignment of a non-zero angle around one of the three frame axes, what should be perceived as pure flexion around a single axis would instead result in artefact non-zero rotations around the remaining two axes (for a visual representation of this effect, please refer to Supplementary Figure S1 of Ortigas-Vásquez et al. [17]). Around one axis, this effect would follow a sine wave pattern, starting at zero with zero flexion, peaking at 90° of flexion and progressively decreasing back to zero by 180° of flexion. This is the case for int/external rotation in Figure 2 (c.f. specimens 4, 6 and 7), as errors peak at approximately 90° of flexion, beyond

which they decrease back down again until peak flexion halfway through the cycle, only for the effect to be mirrored as the knee extends in the second half of the squat. Around the other secondary axis, the artefact would behave like a cosine wave, starting at its peak high (or low) at 0° of flexion, reaching zero at 90° of flexion and continuing on to reach its peak low (or high) at 180° of flexion. This error pattern is clearly reflected for ab/adduction in Figure 2 (c.f. specimens 4, 6 and 7), where the error progressively increases, even past 90° of flexion, and peaks at peak flexion and then decreases back down with extension. Notably, for specimen 3 (Figure 2), the GOM-based kinematic signals for out-of-sagittal-plane rotations were more visibly indicative of crosstalk than the IMU-based signals, highlighting that neither GOM-based nor IMU-based kinematics are necessarily more objectively "accurate" than the other, but rather just graphically different.

The fact that the knee joint does not behave like a proper hinge (which can only rotate about a single fixed axis), but instead displays the complex motion pattern of a six-degrees-of-freedom joint, poses a unique challenge. For activities of daily living (e.g., level walking, stair descent, squat) any true instantaneous axis of rotation will in general not have a constant orientation relative to the bony anatomy, which fundamentally implies that any joint axis identified by palpating bony landmarks on, e.g., the distal femur, will be inherently "flawed" or at least different. This logic suggests that approximating a landmark-based joint axis using only IMU data (and thus functional methods) would be next to impossible. The first REFRAME implementation, REFRAME$_{\text{IMU}\rightarrow\text{GOM}}$, was therefore a necessary step to ascertain whether the differences observed between IMU- and GOM-based signals could potentially be explained by inconsistencies in local reference-frame orientations, rather than reflecting definitive differences in joint motion. After applying REFRAME$_{\text{IMU}\rightarrow\text{GOM}}$, there was a visible improvement in the agreement between the IMU and GOM systems for all three joint angles, suggesting that indeed most of the differences observed between the kinematic signals could be explained by differences in the orientations of the joint axes identified by the two systems. After REFRAME$_{\text{IMU}\rightarrow\text{GOM}}$ had been implemented to ensure a consistent axis orientation, there was considerable improvement in the agreement between IMU- and GOM-based signals for all three rotations, especially abduction/adduction and external/internal rotation (Figure 3). This suggests that REFRAME effectively reduced the impact of crosstalk artefacts, drastically improving the agreement to under 3° of deviation between joint angles around all axes. While certainly sufficient for most applications, given the small range of motion in, e.g., external/internal rotation, errors of 1.4° ± 0.7° (Table 2) may still be critical in some use cases (especially in combination with soft tissue artefacts), suggesting that further work to improve system accuracy could still be beneficial. Importantly, this analysis revealed that, while the IMU system was subject to some measurement error, most of the initially observed differences between IMU and GOM actually stemmed from problems with calibration of the sensor fusion algorithm, rather than IMU sensor inaccuracies.

The transformations applied during REFRAME$_{\text{IMU}\rightarrow\text{GOM}}$ (Table 3) effectively describe the rotations needed to align the IMU-based local femoral and tibial reference frames with those of the GOM system. These transformations can most likely be attributed to two key components. The first is the difference in frame orientations that results from the "incorrect" assumption of 0° abduction and 0° tibial rotation at the first timepoint. For example, according to the GOM system, specimen 3 begins the squat cycle with over 20° of abduction (Figure 2). As a result, reconciliation of the IMU and GOM signals will undeniably demand a change of approximately 20° in the relative orientation of the raw IMU femoral and tibial frames. This is substantiated by the results, as REFRAME$_{\text{IMU}\rightarrow\text{GOM}}$ leads to the transformation of the IMU femoral and tibial frames around the corresponding y-axes by −6.2° and 14.2°, respectively. The second key component contributing to the transformations implemented by REFRAME stems from fundamental differences in the types of joint axes identified by the two systems.

159

While the GOM system defines joint axes based on the 3D coordinates of specific anatomical landmarks, IMU-based kinematics are restricted to purely functional methods. Angular deviations between functional and anatomical axes have been previously estimated to be 1°–5° in the knee joint [27-29]. Consequently, up to 5° (or potentially more considering crosstalk) of the frame transformations by REFRAME$_{IMU \to GOM}$ could easily be attributed to such differences.

The ideal post-processing approach we envision to ensure consistent frame orientations and positions fulfils three key criteria: (1) the resulting signals are clinically interpretable, (2) it should ensure consistent frame orientations and positions regardless of the initial choice of raw frames, and (3) it should be self-contained (i.e., aside from the objective criteria fed by the user, optimisation should rely exclusively on information contained within the set of signals being optimised itself). Although REFRAME$_{IMU \to GOM}$ fulfilled the first two, the third was violated; the implementation relied on the GOM-based signals, optimising the IMU-based signals towards them. Despite this shortcoming, REFRAME$_{IMU \to GOM}$ provided valuable insight into just how much of the differences between the raw IMU and GOM signals could potentially be explained by reference-frame alignment inconsistencies. RMSE values after REFRAME$_{IMU \to GOM}$ thus quantified the magnitude of the measurement error that could not possibly be attributed to frame alignment issues. In contrast, the second REFRAME implementation, REFRAME$_{RMS}$, did fulfil the independence criterion; each dataset was optimised without any input from its counterpart. The minimisation of abduction/adduction and external/internal rotation RMS inherently minimised crosstalk artefacts in both sets of kinematic signals [17], leading to improved agreement between the systems (as evidenced by the reduction in RMSEs of out-of-sagittal-plane rotations compared to raw RMSEs). Notably, the objective criteria for REFRAME$_{RMS}$ only slightly considered (criteria weighting of 0.1) changes to the flexion/extension, thereby resulting in a slight increase in this rotation's RMSE. The fact that RMSEs after REFRAME$_{RMS}$ were marginally larger than after REFRAME$_{IMU \to GOM}$ suggests that although consistency in frame alignment improved after both optimisations, the level of convergence between local reference frames achieved after REFRAME$_{RMS}$ was not quite as precise as with REFRAME$_{IMU \to GOM}$. This helpfully illustrates the challenges associated with trying to fulfil all three key criteria with a single method, which in our experience is extremely difficult (if not impossible). Finally, in terms of the frame transformations applied to the femoral and tibial frames as part of REFRAME$_{RMS}$ optimisation (Table 4 and Table 5), the combined magnitudes of individual rotations strongly support the assumption that almost the same level of convergence was reached as with REFRAME$_{IMU \to GOM}$. For example, REFRAME$_{IMU \to GOM}$ transformations indicated that for specimen 3, frame alignment required a −6.2° rotation around the femoral y-axis. Similarly, REFRAME$_{RMS}$ led to femoral frame transformations of 3.0° around y for the IMU frames and 9.1° for the GOM frames, totalling about −6.1° net relative rotation around y, much like with REFRAME$_{IMU \to GOM}$. Analogous effects were observed in all other subjects.

In conclusion, our study demonstrates the importance of incorporating an approach, such as REFRAME, when evaluating the so-called accuracy (or rather, agreement) between different motion-capture technologies that are known to rely on different methods of joint axis definition. Not only are consistent reference-frame orientations crucial for a robust comparison of kinematic signals, REFRAME analysis has the potential to reveal valuable information about the possible sources of error affecting our measures. Importantly, our work also emphasises the difficulty in developing an ideal post-processing method for reference-frame alignment, especially in light of what are conflicting, sometimes even mutually exclusive, objectives. Finally, we established that although the assessed sensor fusion algorithm does leverage the repetitive nature of gait activities to improve performance, IMU-based joint angles can still achieve promising accuracy for single movement cycles, especially when reliable reference pose values in all three dimensions are available. Nevertheless, the possibility of varying

performance in different subjects for non-repetitive motion patterns should be further investigated. Next steps shall involve in vivo experiments using a larger subject cohort, as well as an evaluation of the effects of soft tissue artefacts.

Author contributions

Funding

Data availability

The raw data supporting the conclusions of this article will be made available by the authors on reasonable request.

Ethics declarations

This study was approved by the ethics committee of the University of Munich, Germany (approval 58–16, 23.02.2016) and carried out in accordance with relevant guidelines and regulations. Informed consent for donation to scientific research had been signed before death by the donors or after death by their relatives.

Competing interests

S.S., A.S., J.G.W., A.M., T.M.G. and A.O.V. are/were employees of B. Braun Aesculap AG, Tuttlingen, Germany. M.W. led the applied biomechanics research group at the Musculoskeletal University Center Munich (MUM), which has received research funding from Aesculap AG in the past.

References

1. Favre, J. and Jolles, B.M., *Gait analysis of patients with knee osteoarthritis highlights a pathological mechanical pathway and provides a basis for therapeutic interventions.* EFORT Open Reviews, 2016. **1**(10): p. 368-374.
2. Feng, J., Wick, J., Bompiani, E., and Aiona, M., *Applications of gait analysis in pediatric orthopaedics.* Current Orthopaedic Practice, 2016. **27**(4): p. 455-464.
3. Postolka, B., Taylor, W.R., List, R., Fucentese, S.F., Koch, P.P., and Schütz, P., *ISB clinical biomechanics award winner 2021: Tibio-femoral kinematics of natural versus replaced knees - A comparison using dynamic videofluoroscopy.* Clinical Biomechanics, 2022. **96**: p. 105667.

4.   Tanifuji, O., Sato, T., Mochizuki, T., Koga, Y., Yamagiwa, H., Endo, N., Kobayashi, K., and Omori, G., *Three-dimensional in vivo motion analysis of normal knees using single-plane fluoroscopy.* Journal of Orthopaedic Science, 2011. **16**(6): p. 710-718.

5.   Cross, J.A., Mchenry, B.D., Molthen, R., Exten, E., Schmidt, T.G., and Harris, G.F., *Biplane fluoroscopy for hindfoot motion analysis during gait: A model-based evaluation.* Medical Engineering & Physics, 2017. **43**: p. 118-123.

6.   List, R., Postolka, B., Schütz, P., Hitz, M., Schwilch, P., Gerber, H., Ferguson, S.J., and Taylor, W.R., *A moving fluoroscope to capture tibiofemoral kinematics during complete cycles of free level and downhill walking as well as stair descent.* PLOS One, 2017. **12**(10): p. e0185952.

7.   Guan, S., Gray, H.A., Keynejad, F., and Pandy, M.G., *Mobile Biplane X-Ray Imaging System for Measuring 3D Dynamic Joint Motion During Overground Gait.* IEEE Trans Med Imaging, 2016. **35**(1): p. 326-336.

8.   Akhtaruzzaman, M., Shafie, A.A., and Khan, M.R., *Gait analysis: systems, technologies, and importance.* Journal of Mechanics in Medicine and Biology, 2016. **16**: p. 1630003.

9.   Klöpfer-Krämer, I., Brand, A., Wackerle, H., Müßig, J., Kröger, I., and Augat, P., *Gait analysis – Available platforms for outcome assessment.* Injury, 2020. **51**: p. S90-S96.

10.   Yunus, M.N.H., Jaafar, M.H., Mohamed, A.S.A., Azraai, N.Z., and Hossain, M.S., *Implementation of Kinetic and Kinematic Variables in Ergonomic Risk Assessment Using Motion Capture Simulation: A Review.* International Journal of Environmental Research and Public Health, 2021. **18**(16).

11.   Weygers, I., Kok, M., Konings, M., Hallez, H., De Vroey, H., and Claeys, K., *Inertial Sensor-Based Lower Limb Joint Kinematics: A Methodological Systematic Review.* Sensors, 2020. **20**(3).

12.   Seel, T., Raisch, J., and Schauer, T., *IMU-based joint angle measurement for gait analysis.* Sensors, 2014. **14**(4): p. 6891-6909.

13.   Versteyhe, M., De Vroey, H., Debrouwere, F., Hallez, H., and Claeys, K., *A Novel Method to Estimate the Full Knee Joint Kinematics Using Low Cost IMU Sensors for Easy to Implement Low Cost Diagnostics.* Sensors, 2020. **20**(6).

14.   Ortigas-Vásquez, A., Maas, A., List, R., Schütz, P., Taylor, W.R., and Grupp, T.M., *A Framework for Analytical Validation of Inertial-Sensor-Based Knee Kinematics Using a Six-Degrees-of-Freedom Joint Simulator.* Sensors, 2022. **23**(1).

15.   Schütz, P., Postolka, B., Gerber, H., Ferguson, S.J., Taylor, W.R., and List, R., *Knee implant kinematics are task-dependent.* Journal of the Royal Society Interface, 2019. **16**(151): p. 20180678.

16.   Rauch, H.E., Tung, F., and Striebel, C.T., *Maximum likelihood estimates of linear dynamic systems.* AIAA journal, 1965. **3**(8): p. 1445-1450.

17.   Ortigas-Vásquez, A., Taylor, W.R., Maas, A., Woiczinski, M., Grupp, T.M., and Sauer, A., *A frame orientation optimisation method for consistent interpretation of kinematic signals.* Scientific Reports, 2023. **13**(1): p. 9632.

18.   Ortigas-Vásquez, A., Taylor, W.R., Postolka, B., Schütz, P., Maas, A., Woiczinski, M., Grupp, T.M., and Sauer, A., *A Reproducible and Robust Representation of Tibiofemoral Kinematics of the Healthy Knee Joint during Stair Descent using REFRAME – Part I: REFRAME Foundations and Validation.* 2024: Preprint on Research Square.

19.   Steinbrück, A., Schröder, C., Woiczinski, M., Fottner, A., Müller, P., and Jansson, V., *Patellofemoral contact patterns before and after total knee arthroplasty: An in vitro measurement.* Biomedical engineering online, 2013. **12**: p. 58.

20. Steinbrück, A., Schröder, C., Woiczinski, M., Fottner, A., Müller, P.E., and Jansson, V., *The effect of trochlea tilting on patellofemoral contact patterns after total knee arthroplasty: an in vitro study.* Archives of Orthopaedic and Trauma Surgery, 2014. **134**(6): p. 867-872.

21. Steinbrück, A., Schröder, C., Woiczinski, M., Fottner, A., Pinskerova, V., Müller, P.E., and Jansson, V., *Femorotibial kinematics and load patterns after total knee arthroplasty: An in vitro comparison of posterior-stabilized versus medial-stabilized design.* Clinical Biomechanics, 2016. **33**: p. 42-48.

22. Steinbrück, A., Schröder, C., Woiczinski, M., Glogaza, A., Müller, P.E., Jansson, V., and Fottner, A., *A lateral retinacular release during total knee arthroplasty changes femorotibial kinematics: an in vitro study.* Archives of Orthopaedic and Trauma Surgery, 2018. **138**(3): p. 401-407.

23. Bauer, L., Woiczinski, M., Thorwächter, C., Melsheimer, O., Weber, P., Grupp, T.M., Jansson, V., and Steinbrück, A., *Secondary Patellar Resurfacing in TKA: A Combined Analysis of Registry Data and Biomechanical Testing.* Journal of Clinical Medicine, 2021. **10**(6).

24. Müller, O., Lo, J., Wünschel, M., Obloh, C., and Wülker, N., *Simulation of force loaded knee movement in a newly developed in vitro knee simulator.* Biomed Tech (Berl), 2009. **54**(3): p. 142-149.

25. Seel, T., Schauer, T., and Raisch, J. *Joint axis and position estimation from inertial measurement data by exploiting kinematic constraints.* in *2012 IEEE International Conference on Control Applications.* 2012. IEEE.

26. Kuhn, M. and Johnson, K., *A Review of the Predictive Modeling Process*, in *Feature Engineering and Selection: A Practical Approach for Predictive Models*, J. Kimmel, Editor. 2019, CRC Press: Boca Raton, FL. p. 36-39.

27. Eckhoff, D.G., Bach, J.M., Spitzer, V.M., Reinig, K.D., Bagur, M.M., Baldini, T.H., and Flannery, N.M., *Three-dimensional mechanics, kinematics, and morphology of the knee viewed in virtual reality.* Journal of Bone and Joint Surgery, 2005. **87 Suppl 2**: p. 71-80.

28. Eckhoff, D., Hogan, C., Dimatteo, L., Robinson, M., and Bach, J., *Difference between the epicondylar and cylindrical axis of the knee.* Clinical Orthopaedics and Related Research, 2007. **461**: p. 238-244.

29. Churchill, D.L., Incavo, S.J., Johnson, C.C., and Beynnon, B.D., *The transepicondylar axis approximates the optimal flexion axis of the knee.* Clinical Orthopaedics and Related Research, 1998(356): p. 111-118.

VII. Journal Publication VI

Comparison of IMU-based knee kinematics with and without harness fixation against an optical marker-based system

Weber, J.G., **Ortigas-Vásquez, A.**, Sauer, A., Dupraz, I., Maas, A. and Grupp, T.M.

Abstract

The use of inertial measurement units (IMUs) as an alternative to optical marker-based systems has the potential to make gait analysis part of the clinical standard of care. Previously, an IMU-based system leveraging Rauch–Tung–Striebel smoothing to estimate knee angles was assessed using a six-degrees-of-freedom joint simulator. In a clinical setting, however, accurately measuring abduction/adduction and external/internal rotation of the knee joint is particularly challenging, especially in the presence of soft tissue artefacts. In this study, the *in vivo* IMU-based joint angles of 40 asymptomatic knees were assessed during level walking, under two distinct sensor placement configurations: (1) IMUs fixed to a rigid harness, and (2) IMUs mounted on the skin using elastic hook-and-loop bands (from here on referred to as "skin-mounted IMUs"). Estimates were compared against values obtained from a harness-mounted optical marker-based system. The comparison of these three sets of kinematic signals (IMUs on harness, IMUs on skin, and optical markers on harness) was performed before and after implementation of a REference FRame Alignment MEthod (REFRAME) to account for the effects of differences in coordinate system orientations. Prior to the implementation of REFRAME, in comparison to optical estimates, skin-mounted IMU-based angles displayed mean root-mean-square errors (RMSEs) up to 6.5°, while mean RMSEs for angles based on harness-mounted IMUs peaked at 5.1°. After RE-FRAME implementation, peak mean RMSEs were reduced to 4.1°, and 1.5°, respectively. The negligible differences between harness-mounted IMUs and the optical system after REFRAME revealed that the IMU-based system was capable of capturing the same underlying motion pattern as the optical reference. In contrast, obvious differences between the skin-mounted IMUs and the optical reference indicated that the use of a harness led to fundamentally different joint motion being measured, even after accounting for reference frame misalignments. Fluctuations in the kinematic signals associated with harness use suggested the rigid device oscillated upon heel strike, likely due to inertial effects from its additional mass. Our study proposes that optical systems can be successfully replaced by more cost-effective IMUs with similar accuracy, but further investigation (especially *in vivo* and upon heel strike) against moving videofluoroscopy is recommended.

Keywords: IMU; gait analysis; knee kinematics; REFRAME; motion capture; movement biomechanics; wearables

1. Introduction

Gait analysis is the systematic study of locomotion of human legs during gait and can be used in both clinical and research settings, such as patient diagnostics and biomechanical studies. One of the dominant state-of-the-art technologies is optical marker-based motion capture (OMC) systems. Kinematic signals are determined computationally based on the tracked positions of reflective markers in three-dimensional space using multiple infrared cameras [1]. Maintaining consistent environmental conditions is important, as factors such as lighting and reflective surfaces can affect the accuracy of dynamic measurements, so setup typically requires an expert and is time-consuming. These characteristics tend to tie OMC systems to laboratory conditions and associate them with high costs [2].

In recent years, the field of gait analysis has witnessed a significant shift towards the development of more mobile solutions with the emergence of wearable technologies such as inertial measurement units (IMUs). These systems offer a promising alternative to traditional optical marker-based approaches for assessing human movement patterns, particularly in the context of measuring rotational knee kinematics [3-6]. IMU-based systems are associated with more affordable prices, are more user-friendly, have smaller dimensions, and are therefore particularly well-suited for capturing motion inside and outside of laboratory settings [6, 7]. Their application usually relies on processing linear acceleration data collected using an accelerometer, and angular velocity data collected using a gyroscope, to then estimate joint kinematics using sensor fusion algorithms. One of the key benefits of IMU-based systems is thus their potential to make gait analysis more accessible and cost-effective, enabling their use outside of laboratory settings, potentially even as part of routine clinical patient pathways.

Prior to clinical application, any gait analysis system should be thoroughly validated [8]. To that end, the accuracy of an IMU-based system to estimate knee joint angles was previously assessed using a six-degrees-of-freedom joint simulator [9]. Guided by fluoroscopy-based signals originally captured *in vivo*, the simulator replicated the tibiofemoral motion of six total knee arthroplasty patients performing daily activities [10], while excluding the possible influence of soft tissue artefact. Raw inertial data collected using a pair of IMUs attached to the simulator were then processed using a Rauch–Tung–Striebel smoother to derive flexion/extension, abduction/adduction, and internal/external tibial rotation based on IMU measurements. To evaluate differences between the simulator and IMU-based signals, the root-mean-square errors (RMSEs) between them were calculated. For level walking, results showed mean RMSEs of 0.7° ± 0.1° for flexion/extension, 0.6° ± 0.3° for abduction/adduction, and 0.9° ± 0.2° for external/internal rotation, indicating promising accuracy. Another study tested the algorithm against an optical marker-based system with single iterations of a loaded squat cycle simulated on seven cadaveric specimens on a force-controlled knee rig and achieved mean RMSE values after aligning the underlying reference frames of 4.2° ± 3.6°, 0.9° ± 0.4°, and 1.5° ± 0.7° for flexion/extension, abduction/adduction, and external/internal rotation, respectively [11]. In a clinical setting, however, motion capture systems consisting of skin-mounted sensors (whether optical or inertial) are usually subject to errors caused by non-rigid movements of the skin (and other soft tissue) relative to the underlying bone. This phenomenon, known as soft tissue artefact (STA), can involve either (a) the collective displacement of a group of markers, or (b) the variation in individual inter-marker distances due to skin elasticity [12, 13].

Consequently, a next step in the analytical validation of the described IMU-based knee kinematics analysis system is therefore to utilise the system *in vivo*, where results may be affected by errors due to STA. In the following study, we present an *in vivo* examination of IMU-based tibiofemoral kinematic estimates, considering two distinct configurations of IMU placement: (1) IMUs attached to a rigid

166

harness (referred to as "IMUs on harness", i.e., with harness fixation), and (2) IMUs mounted "on the skin" using elastic hook-and-loop bands (referred to as "IMUs on skin", i.e., without harness fixation). (Note that "IMUs on skin" were technically not directly adhered onto the skin). Both datasets were then compared against a reference signal calculated from optical markers attached to the rigid harness ("OMC on harness", i.e., the KneeKG system) [14-16] The underlying sensor fusion algorithm used to calculate the IMU-based knee joint angle estimates presented here was based on Ortigas-Vásquez et al.'s adaptation [9] of the approaches previously developed by Seel et al. [3] and Versteyhe et al. [17] IMU-based knee joint angles were estimated using the previously tested adaptation of Rauch–Tung–Striebel smoothing, after which the REference FRame Alignment MEthod (REFRAME) [18, 19] was implemented to account for differences in coordinate system orientations, thus enabling a more rigorous comparison between the three sets of kinematic data (IMUs on harness, IMUs on skin, OMC on harness). Previous studies implementing the REFRAME approach on IMU data tested either on a robotic joint simulator [9] or on cadaveric specimens [11]. This is thus the first study to account for potential differences in local segment reference frame orientations using an optimisation-based approach such as REFRAME within an *in vivo* evaluation of IMU-based tibiofemoral kinematics against optical motion capture.

2. Materials and Methods

2.1. Participants

The study was conducted according to the guidelines of the Declaration of Helsinki, and approved by the Institutional Review Board (or Ethics Committee) of the medical faculty at Ludwig Maximilian University Munich. Thirty volunteers participated in the study after screening for exclusion criteria (Table 1). After exclusion of all incomplete trials due to (a) equipment failure or (b) missing or corrupted data files, a total of 40 individual knees were considered in the final analysis (sex: 20 female, 20 male; side: 20 right, 20 left; mean age: 31.0 ± 9.6 years; mean height: 1.74 ± 0.07 m; mean body mass: 71.9 ± 13.1 kg; mean body mass index (BMI): 23.7 ± 3.4 kg/m^2; mean selected walking speed: 3.9 ± 0.7 km/h).

Table 1. Inclusion and exclusion criteria for participation in the gait analysis study

Inclusion criteria	Exclusion criteria
Employment at Aesculap AG in Tuttlingen	Impairment due to lower extremity, spine or pelvic injury, or neurological disease
Ability to walk independently on a treadmill for at least five minutes at a time	Last surgical procedure less than six months ago
BMI ≤ 40 kg/m^2	Pregnancy

2.2. Reference motion capture system

As a reference system, a non-invasive and marker-based OMC system was used (KneeKG, Emovi Inc., Laval, QC, Canada). The system consisted of an infrared camera (Polaris Spectra camera, Northern Digital Inc., Waterloo, ON, Canada), a personal computer equipped with dedicated software (Knee3D, v5.20.7 and v5.20.8, Emovi Inc., Laval, QC, Canada), and passive markers attached to a rigid harness [20]. The computational method employed to define bone-embedded anatomical frames from marker positions and thus estimate knee joint angles has been previously described in detail by Hagemeister et al. [15]. Briefly, the calibration method used by the optical reference system combined the identification of anatomical landmarks and functional calibration tasks. Specifically, during a static trial, the medial and lateral malleoli, and the medial and lateral epicondyles were identified using a pointer (which was itself equipped with optical markers that could be tracked by the cameras). Additionally, participants were asked to perform functional calibration trials to determine the hip and knee joint centres, as well as their postural alignment during neutral standing. In an attempt to minimise STA, the system's manufacturer trains users to strategically position the provided rigid harness on selected anatomical landmarks [14, 20]. Flexion/extension, abduction/adduction, and external/internal rotation values measured by the system have been previously validated at discrete intervals of knee flexion during a quasi-static weight-bearing squatting activity against radiographic images [16]. To the authors' knowledge, a comprehensive validation of the system during treadmill walking (the system's intended use) against fluoroscopic imaging is not yet available in the literature. Although the extent to which the device minimises STA during level walking has therefore yet to be directly assessed, multiple

studies that utilise the optical reference system as a validated clinical gait analysis system or "silver standard" have been previously published [21-23]. Further studies by, e.g., Lustig et al. [20], Clement et al. [16], and Northon et al. [24], commenting on the validity of the KneeKG system are also available for review. Mean repeatability values have similarly been reported by Hagemeister et al. [15] as ranging between 0.4° and 0.8° for joint rotations, although these values are expected to be highly optimistic and representative of a best-case scenario.

2.3. Study protocol

In addition to total body height and mass, the individual circumferences of each participant's hip, waist, neck, thighs, and shanks were in turn measured and recorded. Prior to the acquisition of kinematic gait data, each participant underwent a familiarisation trial at a self-selected walking speed (0.5 to 6 km/h) in light-coloured socks (as indicated by the optical system's manufacturer). The trial order (right knee assessed first vs. left knee assessed first) was randomised for each participant. The KneeKG marker system ("OMC on harness") was carefully positioned on each participant by a certified technician (as instructed during official training by the manufacturer of the KneeKG). Additionally, two IMU pairs (Xsens DOT, Movella, Enschede, Netherlands) were attached to the same leg, with one pair of sensors ("IMUs on harness") adhered to the optical reference's rigid thigh and shank harness components using double-sided mounting tape, and the other pair ("IMUs on skin") placed facing (approximately) anterior using elastic hook-and-loop straps secured around the thigh and shank circumferences (Figure 1).
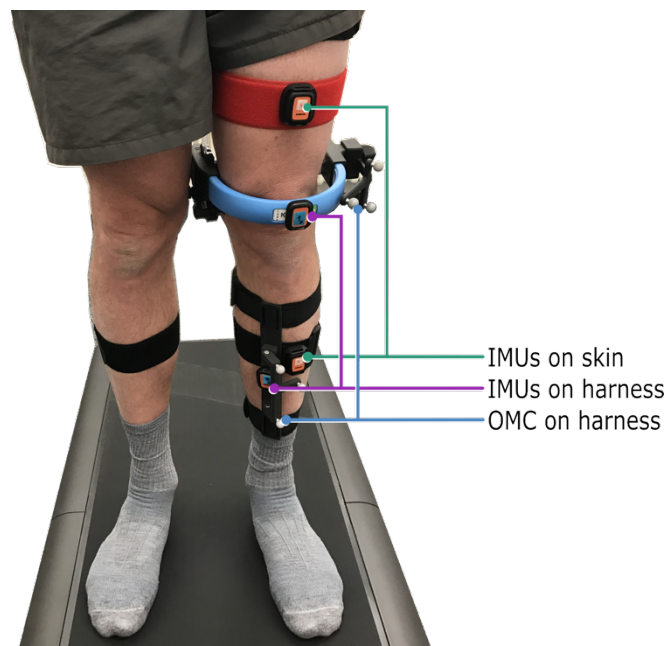
Figure 1. The optical harness-based reference system, as well as two pairs of IMU sensors, were carefully positioned on each participant by a certified technician. One IMU pair was attached to the rigid harness of the reference system ("IMUs on harness"), and a second IMU pair was mounted on elastic hook-and-loop bands ("IMUs on skin"). As per the optical system manufacturer's instructions, participants walked in socks on the treadmill.

All four IMUs were time-synchronised immediately prior to data collection and set to a sampling rate of 60 Hz. Participants were instructed to begin each trial by spending a minimum of three seconds

in a static neutral standing pose, with both knees in full extension and feet facing a direction parallel to the treadmill belt. Participants were instructed to then start the treadmill and set it to increase to the self-selected speed they identified during the preliminary familiarisation trial. A few seconds after the chosen walking speed had been reached, data were collected with the OMC system for 45 s. A second set of OMC data was then collected shortly after the first, for another 45 s. Participants then turned off the treadmill, progressively slowing their pace to reach a full stop, and finally adopted the initial neutral reference pose once more, for a minimum of three seconds. At this point, data collection with the IMUs stopped and the entire procedure was repeated for the contralateral knee.

2.4. Data processing

For each knee, three initial sets of "raw" (non-optimised) kinematic signals were first considered: two sets stemming from the two IMU configurations (IMUs on harness, IMUs on skin), and a third set from the reference system (OMC on harness). The underlying sensor fusion algorithm used for analysis of the IMU data was based on Ortigas-Vásquez et al.'s adaptation [9] of the approaches previously developed by Seel et al. [3] and Versteyhe et al. [17], which leverage Rauch-Tung-Striebel smoothing [25]. This iterative method relied first on a hinge joint model to find an optimal axis of rotation, followed by a ball-and-socket joint model to determine an optimal joint centre. The periods of static neutral standing at the beginning and end of each trial were used during post-processing as a reference pose to calibrate any possible offsets in the kinematic signals. For further details, the reader is referred to [3, 9, 17]. This allowed calculation of knee joint angles from the raw data sampled by each pair of IMUs, using custom Matlab scripts (vR2021b; The Mathworks Inc., Natick, MA, USA). In contrast, the OMC system used built-in software to automatically output joint angle estimates following an approach developed by the manufacturer [15]. Due to the proprietary nature of the software, details regarding, e.g., how the raw marker data were filtered for processing, were not readily available, although previous studies implementing the same harness system have described the use of a zero-lag 2nd-order Butterworth filter with automatically calculated cut-off frequencies [26-28]. Each of the resulting sets of kinematic signals consisted of the three rotational kinematic values of the tibiofemoral joint throughout the gait cycle, i.e., flexion/extension, abduction/adduction, and external/internal tibial rotation. Values corresponded to the intrinsic XYZ Cardan angle sequence that transformed the femoral frame into the tibial frame at each time point, where local axis directions were pointed laterally for a right knee for X, anteriorly for Y, and proximally for Z (the resulting joint angles are comparable to those described by Grood and Suntay [29, 30]).

IMU- and OMC-based signals were time-synchronised relative to each other by estimating the delay between the OMC-based flexion/extension signal with respect to the IMUs on harness flexion/extension signal (using cross-correlation). The estimated delay was then consistently corrected on all three OMC-based joint angles to collectively align them in time with the IMU-based estimates. (The IMUs on skin and IMUs on harness had already been time-synchronised prior to data collection using dedicated software, as described in Section 2.3). Prior to the implementation of a gait detection algorithm for the identification of individual gait cycles, raw angular velocity values in the sagittal plane of the shank IMU were filtered using a fourth-order Butterworth filter with cut-off frequency at 7 Hz. The negative peaks of the filtered signal were then used for heel strike detection and thus identified the start and end of each stride [31]. The period of every individual cycle was calculated, and cycles with a duration below the 5th or above the 95th percentile were excluded from further analyses, leaving at least ten valid gait cycles per knee. Each of these 400 gait cycles (40 knees * 10 cycles) were then time-normalised from 0% to 100%.

In order to ensure consistent orientations of local segment coordinate systems across the three sets of kinematic signals, the REference FRame Alignment MEthod (REFRAME) [19] was applied to the normalised cycles. Two different implementations of REFRAME were explored. The first, RE-FRAME$_{IMU \rightarrow OMC}$, minimised the root-mean-square error (RMSE) between each set of IMU-based kinematic signals (IMUs on harness, IMUs on skin) and the OMC system's raw signals (OMC on harness) as reference. A second implementation, REFRAME$_{RMS}$, minimised the root-mean-square (RMS) of abduction/adduction and external/internal rotation of each of the three signal sets (IMUs on harness, IMUs on skin, and OMC on harness) independently. Note that since frame transformations applied by REFRAME were constant across the entire activity cycle, the relative motion between limb segments actually remained the same (it was just illustrated differently). This self-contained implementation additionally minimised the absolute value of flexion/extension at the first timepoint (i.e., 0%) of the cycle. This combination of objective criteria would minimise cross-talk effects, while still allowing for signal convergence with an independent methodology. For both REFRAME$_{IMU \rightarrow OMC}$ and RE-FRAME$_{RMS}$, optimisations were formulated to hinder femoral frame transformations consisting of rotations around the femoral X-axis, thus preventing unrealistic changes in the pitch of the femoral and tibial segment frames that could impair the clinical interpretability of the optimised signals. Finally, the RMSEs for each individual gait cycle of the pairwise comparisons between the IMUs (IMUs on harness or IMUs on skin) and the OMC on harness were calculated for each gait cycle before vs. after each REFRAME implementation. Furthermore, the mean RMSEs ± standard deviation across all knees and cycles, and the mean RMSEs ± standard deviation across all cycles of each individual knee were calculated as well.

2.5. Statistical analysis

To evaluate the statistical significance of the mean RMSE differences for each knee before (raw) vs. after REFRAME (REFRAME$_{IMU \rightarrow OMC}$ or REFRAME$_{RMS}$), a two-tailed paired t-test with a significance level of $\alpha = 0.05$ was performed after each of the two REFRAME implementations independently. Given the considered sample size of 40 knees, testing for normality was not necessary (normality assumption can be violated for $n > 30$ [32]. To account for the possible effects of multiple comparisons, the significance threshold was adapted from 0.05 to 0.004 (2 sensor configurations * 2 RE-FRAME implementations * 3 planes; therefore, n = 12) using a Bonferroni correction [33].

3. Results

For the mean across all knees and cycles, minor differences between the raw kinematic signals (Figure 2, left column) from the IMUs on harness (purple) were observed versus the raw signals from OMC on harness (blue), in the frontal and transverse planes especially. Mean RMSEs between the two systems were 3.8° ± 2.6°, 3.0° ± 2.1°, and 5.1° ± 2.7°, for flexion/extension, abduction/adduction and external/internal rotation, respectively (Table 2). Visibly larger differences could be observed between the IMUs on skin (green) and OMC on harness (blue) (also particularly for abduction/adduction and external/internal rotation) than between the IMUs on harness (purple) and OMC on harness (blue). Mean RMSEs between raw OMC on harness signals and raw IMUs on skin signals were 4.8° ± 2.8°, 3.9° ± 2.1°, and 6.5° ± 2.5°, for flexion/extension, abduction/adduction, and external/internal rotation, respectively (Table 2). Analogous differences were more pronounced in participant-specific results (Figure 3, left column), where mean values were affected by much smaller standard deviations (Table 3). Furthermore, OMC on harness kinematic signals showed clear fluctuations upon heel strike for several knees (e.g., Figure 3; for more examples see Supplementary Materials). These fluctuations appeared highly repeatable, as demonstrated by the relatively small standard deviation across the trials (e.g., Table 3; for more examples see Supplementary Materials).
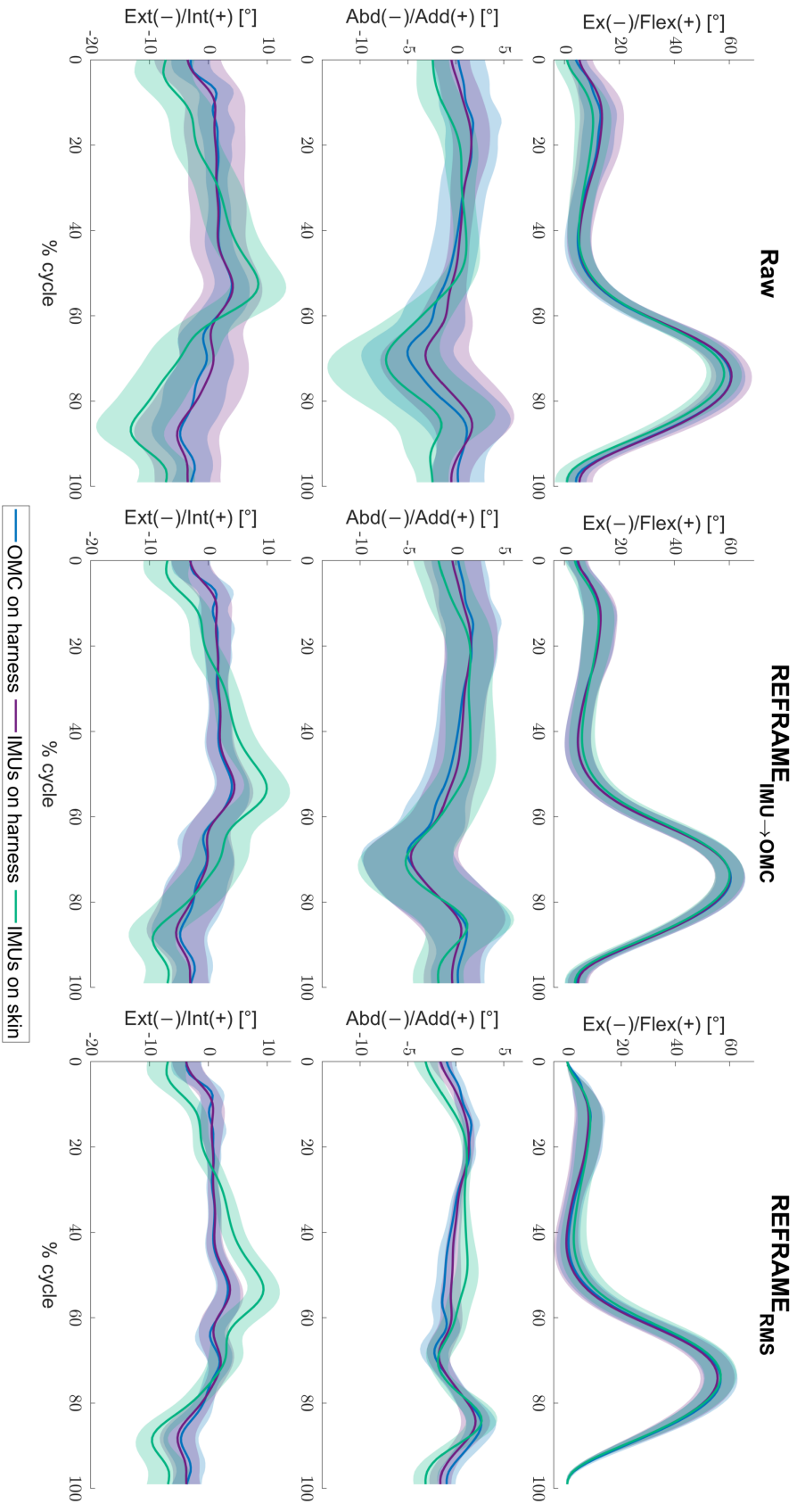
Figure 2. Mean tibiofemoral joint angles (solid lines) ± standard deviation (shaded areas), in degrees, as estimated by inertial measurement units (IMUs) on harness (purple), IMUs on skin (green), and optical motion capture (OMC) on harness (blue), averaged over all knees and cycles. Note that flexion angles have been illustrated as positive (despite representing a negative rotation around the laterally directed X-axis) for easier comparisons against other studies. Angles are shown as a percentage of the gait cycle under three conditions: (1) raw, i.e., in the absence of post-processing methods to correct reference frame orientation differences (left), (2) after implementation of $\text{REFRAME}_{IMU\rightarrow OMC}$ (middle), and (3) after implementation of REFRAME_{RMS} (right).
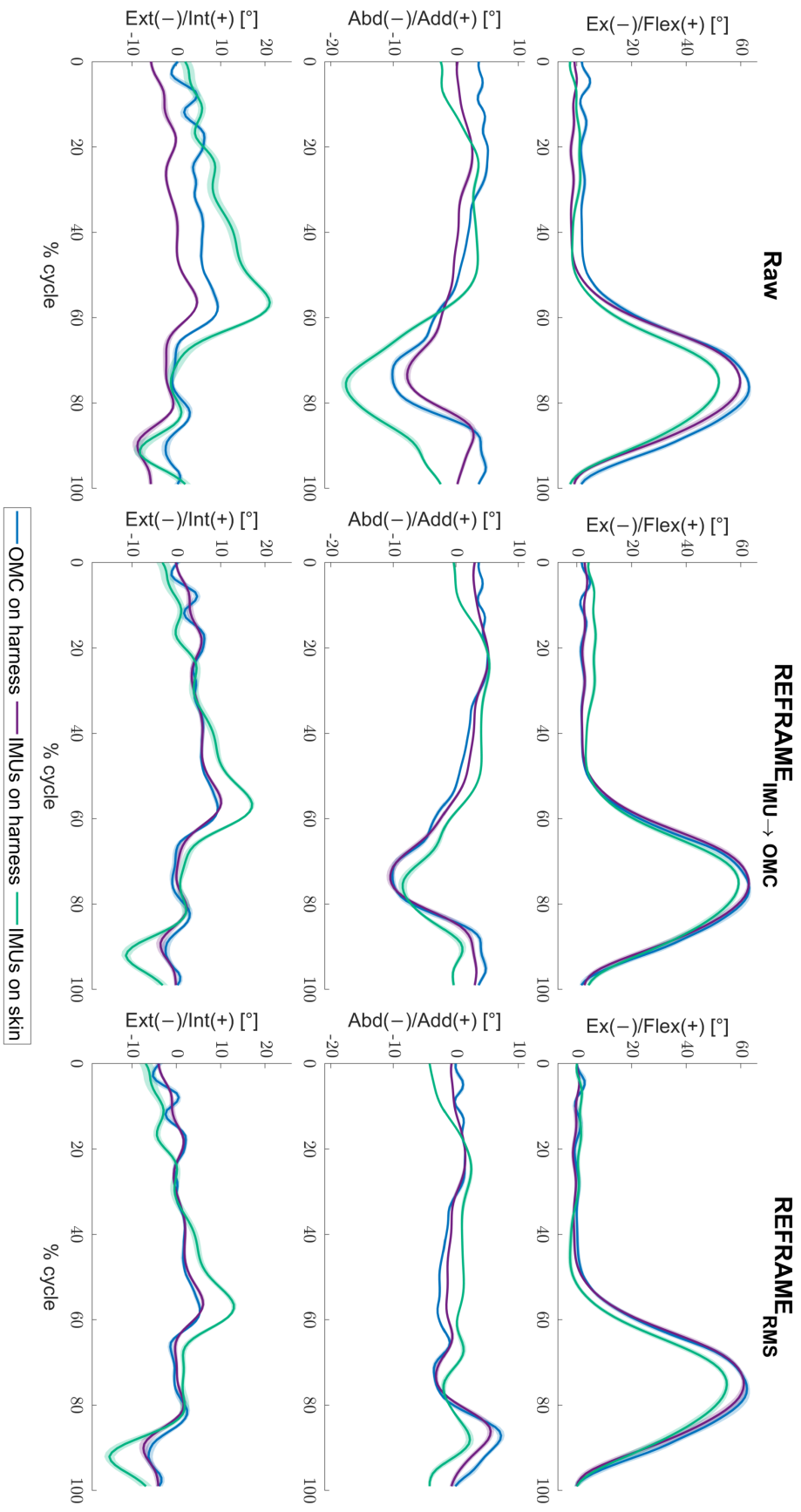
Figure 3. Mean tibiofemoral joint angles (solid lines) ± standard deviation (shaded areas), in degrees, as estimated by inertial measurement units (IMUs) on harness (purple), IMUs on skin (green), and optical motion capture (OMC) on harness (blue), averaged over all cycles for knee 17. Note that flexion angles have been illustrated as positive (despite representing a negative rotation around the laterally directed X-axis) for easier comparisons against other studies. Angles are shown as a percentage of the gait cycle under three conditions: (1) raw, i.e., in the absence of post-processing methods to correct reference frame orientation differences (left), (2) after implementation of REFRAME$_{\text{IMU}\to\text{OMC}}$ (middle), and (3) after implementation of REFRAME$_{\text{RMS}}$ (right).

Table 2. Mean ± standard deviation (in degrees) root-mean-square errors between tibiofemoral joint rotations estimated by the IMU-based systems and the optical reference on harness, calculated across all knees and cycles.

	Raw		REFRAME$_{IMU \to OMC}$		REFRAME$_{RMS}$	
	IMUs on harness	IMUs on skin	IMUs on harness	IMUs on skin	IMUs on harness	IMUs on skin
Flexion/extension	3.8 ± 2.6	4.8 ± 2.8	1.1 ± 0.5	1.9 ± 0.6	1.5 ± 0.5	2.7 ± 1.2
Abduction/adduction	3.0 ± 2.1	3.9 ± 2.1	0.6 ± 0.3	1.5 ± 0.6	0.7 ± 0.3	1.7 ± 0.7
External/internal rotation	5.1 ± 2.7	6.5 ± 2.5	0.9 ± 0.3	4.1 ± 1.2	0.9 ± 0.3	4.0 ± 1.1

Table 3. Mean ± standard deviation (in degrees) root-mean-square errors between tibiofemoral joint rotations estimated by the IMU-based systems and the optical reference on harness, calculated across all cycles of an exemplary knee (knee 17).

	Raw		REFRAME$_{IMU \to OMC}$		REFRAME$_{RMS}$	
	IMUs on harness	IMUs on skin	IMUs on harness	IMUs on skin	IMUs on harness	IMUs on skin
Flexion/extension	4.1 ± 0.1	6.9 ± 0.1	1.7 ± 0.2	3.2 ± 0.1	2.0 ± 0.2	4.6 ± 0.2
Abduction/adduction	2.4 ± 0.1	5.7 ± 0.1	0.8 ± 0.0	2.8 ± 0.1	1.0 ± 0.0	3.2 ± 0.1
External/internal rotation	5.3 ± 0.2	5.6 ± 0.3	1.0 ± 0.1	4.3 ± 0.2	1.0 ± 0.1	4.2 ± 0.2

The application of REFRAME$_{IMU \to OMC}$ (Figure 2, middle column) resulted in a decrease in mean RMSEs between the OMC on harness (blue) and the IMUs on harness (purple) from 3.8° to 1.1° for flexion/extension, from 3.0° to 0.6° for abduction/adduction, and from 5.1° to 0.9° for external/internal rotation (Table 2). However, mean RMSEs between OMC on harness (blue) and IMUs on skin (green) after the application of REFRAME$_{IMU \to OMC}$ resulted in a comparably smaller decrease from 4.8° to 1.9° for flexion/extension, from 3.9° to 1.5° for abduction/adduction, and from 6.5° to 4.1° for external/internal rotation (Figure 4). On average, the frame transformations executed under REFRAME$_{IMU \to OMC}$ consisted of rotating the local segment frames of the IMUs on harness by no more than 3° around any of the three axes (Table 4). In contrast, the average frame transformations resulting from REFRAME$_{IMU \to OMC}$ for the local segment frames of the IMUs on skin were comparably larger, in some cases exceeding 5°. Notably, the large magnitude of standard deviations affecting these average transformations (Table 5) was not present for participant-specific averages, where mean transformations were affected by much smaller standard deviations (Supplementary Materials, e.g., Tables S25, S43, and S76).

Table 4. Mean ± standard deviation (in degrees) of the rotational transformations (Rx: rotation around X, Ry: rotation around Y, Rz: rotation around Z) applied to the femoral and tibial segment frames as part of REFRAME$_{IMU \rightarrow OMC}$, calculated across all knees and cycles.

	Femur		Tibia	
	IMUs on harness	IMUs on skin	IMUs on harness	IMUs on skin
Rot X [°]	0.0 ± 0.0	0.0 ± 0.0	0.5 ± 4.3	-1.9 ± 4.7
Rot Y [°]	0.1 ± 2.8	-5.8 ± 4.9	0.7 ± 3.0	-5.5 ± 4.9
Rot Z [°]	-2.4 ± 6.4	5.0 ± 7.9	-2.0 ± 8.4	5.0 ± 7.9

Table 5. Mean ± standard deviation (in degrees) of the rotational transformations (Rx: rotation around X, Ry: rotation around Y, Rz: rotation around Z) applied to the femoral and tibial segment frames as part of REFRAME$_{IMU \rightarrow OMC}$, calculated across all cycles of an exemplary knee (knee 17).

	Femur		Tibia	
	IMUs on harness	IMUs on skin	IMUs on harness	IMUs on skin
Rot X [°]	0.0 ± 0.0	0.0 ± 0.0	-3.7 ± 0.1	-6.7 ± 0.2
Rot Y [°]	-0.5 ± 0.2	-4.7 ± 1.0	2.2 ± 0.2	-3.2 ± 1.0
Rot Z [°]	-6.0 ± 0.2	11.3 ± 0.4	-0.4 ± 0.2	6.1 ± 0.3

Analogously, the implementation of REFRAME$_{RMS}$ (Figure 2, right column) resulted in a decrease in mean RMSEs between OMC on harness (blue) and the IMUs on harness (purple) from 3.8° to 1.5° for flexion/extension, from 3.0° to 0.7° for abduction/adduction, and from 5.1° to 0.9° for external/internal rotation (Table 2). Application of REFRAME$_{RMS}$ also led to a relatively smaller decrease in mean RMSEs between OMC on harness (blue) and the IMUs on skin (green), from 4.8° to 2.7° for flexion/extension, from 3.9° to 1.7° for abduction/adduction, and from 6.5° to 4.0° for external/internal rotation. Notably, all changes in mean RMSEs were found to be statistically significant even after Bonferroni correction (Figure 4; Supplementary Materials Tables S121 and S122). Similar results were once again more evident for knee-specific averages (Figure 3, right column; Table 3). The transformations executed under REFRAME$_{RMS}$ were lowest for OMC on harness and IMUs on harness, compared to those applied to IMUs on skin (Table 6). Once again, participant-specific transformations demonstrated much smaller standard deviations (e.g., Table 7, Supplementary Materials Tables S26, S35, and S101) than inter-participant averages.

Table 6. Mean ± standard deviation (in degrees) of the rotational transformations (Rx: rotation around X, Ry: rotation around Y, Rz: rotation around Z) applied to the femoral and tibial segment frames as part of REFRAME$_{RMS}$, calculated across all knees and cycles.

	Femur			Tibia		
	OMC on harness	IMUs on harness	IMUs on skin	OMC on harness	IMUs on harness	IMUs on skin
Rot X [°]	0.0 ± 0.0	0.0 ± 0.0	0.0 ± 0.0	4.3 ±3.9	5.5 ± 5.2	2.1 ± 5.0
Rot Y [°]	-0.4 ± 5.3	-0.3 ± 5.6	-4.2 ± 7.0	-1.4 ± 4.3	-1.1 ± 5.4	-4.6 ± 6.8
Rot Z [°]	5.1 ± 6.4	2.8 ± 4.7	9.3 ± 7.1	4.5 ± 6.7	2.5 ± 7.1	9.7 ± 6.5

Table 7: Mean ± standard deviation (in degrees) of the rotational transformations (Rx: rotation around X, Ry: rotation around Y, Rz: rotation around Z) applied to the femoral and tibial segment frames as part of REFRAME$_{RMS}$, calculated across all cycles of an exemplary knee (knee 17).

	Femur			Tibia		
	OMC on harness	IMUs on harness	IMUs on skin	OMC on harness	IMUs on harness	IMUs on skin
Rot X [°]	0.0 ± 0.0	0.0 ± 0.0	0.0 ± 0.0	1.8 ± 0.6	-0.9 ± 0.5	-1.0 ± 0.6
Rot Y [°]	1.7 ± 0.5	2.0 ± 0.5	-3.2 ± 1.5	-2.0 ± 0.5	1.0 ± 0.4	-4.6 ± 1.5
Rot Z [°]	11.1 ± 0.3	5.3 ± 0.3	22.6 ± 0.5	7.0 ± 0.3	7.0 ± 0.3	13.9 ± 0.3
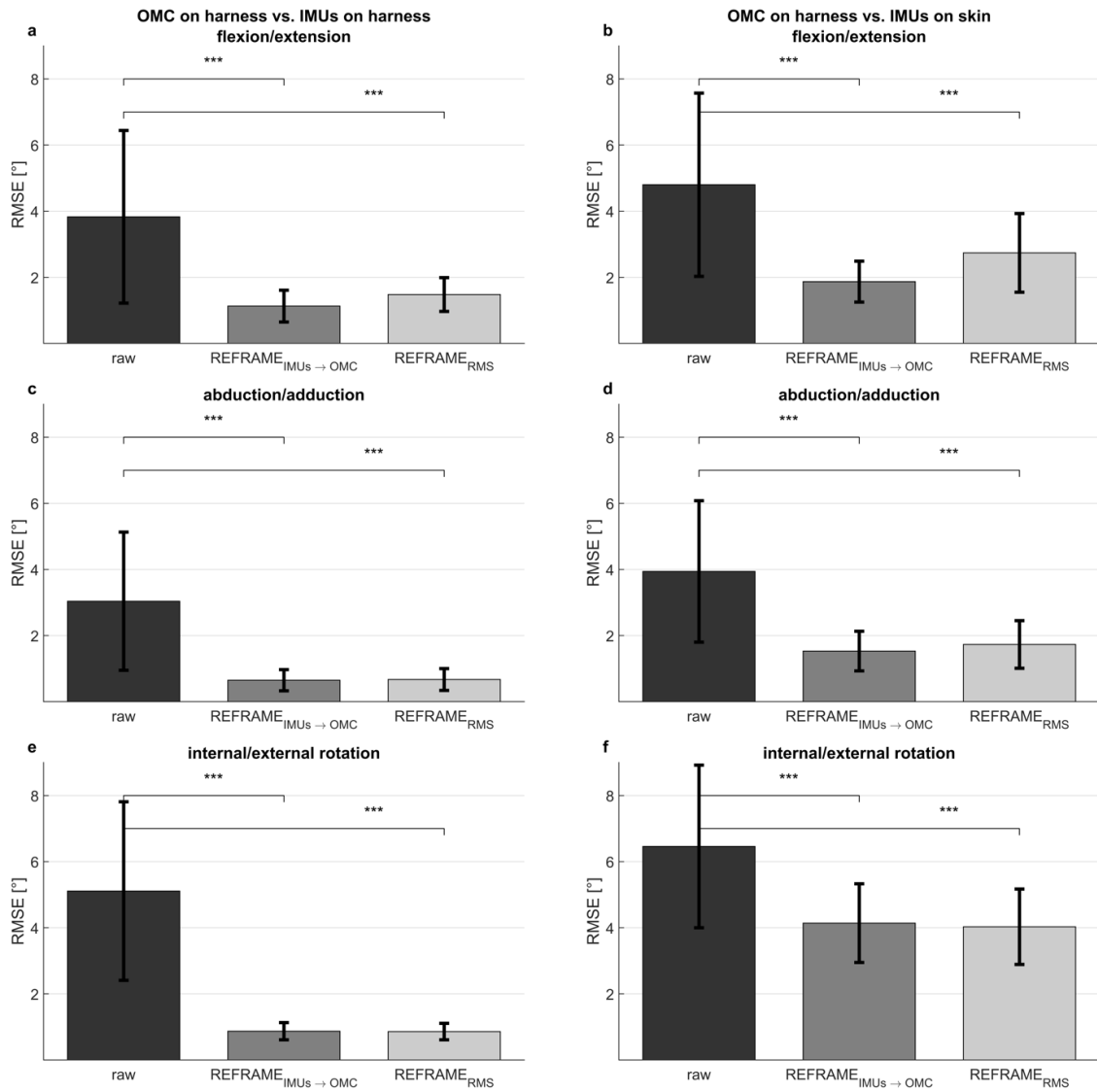
Figure 4: Mean ± standard deviation of root-mean-square errors (RMSEs, in degrees) between the optical reference system on a harness and the inertial measurement units on the harness (left), as well as between the optical reference system on a harness and the inertial measurement units on the skin (right). Shown for flexion/extension (a,b), abduction/adduction (c,d), and external/internal rotation (e,f). Significant changes in RMSEs after implementation of REFRAME$_{IMU \rightarrow OMC}$ and of REFRAME$_{RMS}$, as determined by paired t-tests, are shown ($p < 0.004$ indicated by ***; full p-values are available in Supplementary Materials Tables S121 and S122).

4. Discussion

Despite showing promising results [3-5, 31, 34], further validation of IMU-based motion capture systems is needed before they are widely used in clinics. Previously [9], a sensor fusion algorithm based on Rauch-Tung-Striebel smoothing [17] was assessed under ideal conditions (i.e., in the absence of STA) using a robotic simulator. In this study, we tested the same IMU-based system *in vivo*, under the presence of STA, against an optical harness-based reference system.

Both IMU- and optical marker-based motion capture systems aim to characterise the relative motion of the underlying bony segments. To achieve this non-invasively, the systems track (optical or inertial) sensors attached (non-rigidly) to the relevant segments. Any displacement of the sensors relative to the underlying bones therefore results in motion artefacts, which in this context referred not only to STA caused by the movement of skin, muscle, etc., but also displacements of the sensor fixation device (e.g., harness). Here, the IMU system was tested in two distinct configurations (attached to a rigid harness or, alternatively, to the skin using elastic hook-and-loop straps; Figure 1), and differences between the resulting knee kinematic signals were evaluated against a harness-based optical reference system.

A preliminary assessment of the raw tibiofemoral kinematic signals obtained using each IMU configuration revealed visible differences against the optical reference. These differences could stem from a number of sources, especially STA and/or cross-talk effects. In the previous study [9], the IMU-based system characterised rotational knee kinematics during simulated level walking with less than 1° of error in the absence of STA. Given our cohort's normal average BMI of 23.7 kgm2, STA magnitudes could reasonably be expected to reach 5° [35, 36]. Although average RMSE values between IMUs on skin and the optical reference were roughly within that range, peak RMSEs clearly exceeded these values (>10°, Supplementary Materials; Tables S1 and S2), indicating that error sources beyond STA could be present. For IMUs on harness vs. OMC on harness, motion artefacts between systems could even be excluded, as both inertial sensors and optical markers were fixed to the same rigid brace, so peak RMSEs over 10° suggested that cross-talk effects were likely also present.

As described by Hagemeister et al., the optical reference system leveraged joint axes that involved some level of functional calibration, but were still largely dependent on the manual identification of the 3D coordinates of key anatomical landmarks in a laboratory reference frame [15]. On the other hand, the joint axes implemented by the IMU-based system were based only on the available gyroscope and accelerometer data (as the position/orientation of bony points relative to the sensor positions/orientations were not directly measured) and were thus entirely functional [3, 9, 17]. The joint axes estimated by the different systems were therefore likely similar, but not perfectly coincident [37, 38]. Previous work has demonstrated that even very minor differences in joint axis definition leads to considerable artefacts on kinematic signals [18, 37-39]. We therefore re-assessed signal differences after two distinct implementations of a REference FRame Alignment MEthod (REFRAME) [19] to address such discrepancies in joint axis definition.

In order to address differences in joint axis orientations, REFRAME$_{IMU \to OMC}$ was applied to the set of kinematic signals stemming from each of the two IMU configurations (on harness and on skin) in turn. The underlying goal of this first REFRAME implementation was to re-align the IMU-based local segment reference frames to minimise the RMSE between IMU-based joint angles against the optical reference. The required transformations ranged from as little as 0.0° to as much as 31.0° (Supplementary Table S1). In addition to a visible improvement in signal convergence, average RMSEs decreased

to well below 2° for the IMUs on harness (Table 2). The level of agreement observed after optimisation suggested the underlying motion captured by both systems was highly comparable. Both the optical markers and the IMU sensors on the harness were effectively rigid relative to each other, so after frame alignment, the resulting signals were highly similar. However, average RMSEs between OMC on harness and IMUs on skin after REFRAME$_{IMU \to OMC}$ were higher (up to 5°; Table 2), and clear disagreement remained between signals from the harness-mounted configurations and the skin-mounted IMU set up (Figure 2, middle column; Figure 3, middle column). The remaining differences could not plausibly stem from differences in frame alignment, so alternative sources of error, such as noise and/or measurement error, but especially differences in STA behaviour, were suspected. The differences in these kinematic signals therefore indicated that tibiofemoral motion, as characterised by a harness-based system, was inherently different to that captured by a system using skin-mounted sensors. In contrast to the IMUs on harness, the IMUs on skin quantified the motion of the elastic hook-and-loop bands wrapped tightly around the limb segments (rather than the motion of the harness). Since the harness likely moved relative to the elastic hook-and-loop bands, even after reference frame alignment, the IMUs on skin and IMUs on harness did not quantify the same underlying movement pattern, and so those signals remained visibly different.

Even though the implementation of REFRAME$_{IMU \to OMC}$ revealed valuable new insights by characterising the frame transformations needed to achieve maximum signal convergence, it inherently targeted the local frame orientations used by the OMC system, which we knew to also be error-prone (due to inaccurate palpation, marker placement, etc.). For example, in some cases, the OMC-based abduction/adduction signals were clearly dependent on flexion angle, a strong indicator of cross-talk (c.f. knees 10, 29, and 32 in Supplementary Materials; Figure S10, S28, and S31, middle). Moreover, this REFRAME configuration was not independent. In order to optimise one signal set, it relied on information contained within the other set. Consequently, we then implemented REFRAME$_{RMS}$, seeking to achieve a similar level of signal convergence using a strictly self-contained method. Mean RMSEs between OMC on harness and the IMUs on harness decreased after REFRAME$_{RMS}$, as did RMSEs between the OMC on harness and the IMUs on skin, although the latter did so to a lesser extent. Moreover, frame transformations implemented as part of REFRAME$_{RMS}$ ranged from 0.0° to 32.7° (Supplementary Table S2). The results of this second REFRAME implementation therefore corroborated our previous findings; inconsistencies in reference frame orientations could account for most, but not all, differences between systems, especially between IMUs on skin and the optical reference on harness.

Even after REFRAME implementation, certain differences between signals remained, most obviously between external/internal rotation signals (as reflected by RMSE values) of IMUs on skin and OMC on harness (and IMUs on harness as well) (c.f. knee 11 in Supplementary Materials; Figure S11). A tendency to estimate larger ranges of axial rotation with the IMUs on skin was observed, although it remained unclear whether this reflected an overestimation of external/internal rotation by the IMUs on skin vs. an underestimation of this rotation by the harness-mounted sensors. Moreover, signals from harness-mounted systems often displayed characteristic fluctuations, sometimes throughout the entire cycle (c.f. knee 22 in Supplementary Materials, Figure S21), or specifically upon heel strike for the OMC system (c.f. knee 17 in Figure 3). Association with heel strike led us to hypothesise that the observed fluctuations could be due to the added mass of the harness, which interestingly was originally intended to reduce such artefacts [14]. From a simplified spring–mass system perspective, heel strike can be thought of as representing a transformation of kinetic energy into spring potential, resulting in vibration of the harness, much like a mass on a spring. A larger mass would logically lead to a larger relative displacement, plausibly explaining the differences in relative motion between sensors on skin and sensors on harness. Notably, although the general movement patterns after REFRAME were

essentially the same for both harness-mounted systems, heel-strike-related fluctuations were visible mostly on OMC on harness signals only (and not on IMUs on harness signals). We hypothesised that this effect was likely associated with the use of Rauch–Tung–Striebel smoothing to estimate the knee joint angles from inertial data. As this method considered the levels of uncertainty associated with state variables at different timepoints, it was likely able to "reject" sensor measurements pointing to non-physiological movement patterns. Nevertheless, it remained unclear whether this smoothing effect could inadvertently discard real, relevant information (e.g., the presence of tremors in Parkinson's patients).

The added mass of the harness was not the only concern associated with the OMC system. The brace was designed to act as a femoral "clamp", where the lateral femoral attachment was meant to fit between the iliotibial band and the biceps femoralis tendon [14]. This not only led to difficulties related to harness placement in some of the more athletic participants (for example, due to muscle size obstructing this "groove"), but also to reported participant discomfort during dynamic activities and therefore possible gait alterations of natural movement patterns [40]. Although the system was only tested on a healthy population within this study, these effects would likely be exacerbated in a patient population displaying pathological patterns of gait. Notably, the technician supervising data collection mentioned noticing a visible reduction in flexion/extension range of motion between treadmill familiarisation trials without the brace and data collection trials with the brace for several participants. We hypothesised that this could be associated with the lateral femoral attachment of the brace obstructing the motion of the iliotibial band, which would otherwise naturally move from being anterior to the lateral femoral epicondyle in full knee extension, to being posterior of the epicondyle with flexion [41]. Moreover, the optical marker-based system used in this study required the use of a treadmill for level walking to ensure that all markers stayed within the cameras' field of view during the entire activity. Although this did allow for controlling of gait speed, it was nevertheless yet another limitation of the optical system that could be tackled using inertial sensors. The optical system also specifically instructed users to walk on the treadmill with socks for "better visualisation", which could be considered by some to be suboptimal (vs. walking in athletic shoes or barefoot).

In addition to participant discomfort arising from the use of the rigid harness and other usability-related issues that could clearly be improved, further limitations were identified. In a recent study, we established post-processing methods to ensure that consistent reference frame poses would ideally achieve three objectives: (1) clinical interpretability, (2) consistent reference frame orientation and position regardless of initial frame choice, and (3) method independence [11]. We concluded, however, that achieving all three was extremely challenging. REFRAME$_{RMS}$ prioritised method independence to fulfil objective #3. In order to achieve a similar level of convergence as with REFRAME$_{IMU \to OMC}$ (and therefore attempt to fulfil objective #2), it was necessary to additionally target a common starting flexion angle of 0°. The comparably higher RMSE achieved in flexion/extension after REFRAME$_{RMS}$ vs. REFRAME$_{IMU \to OMC}$, however, suggested that this objective was only partially fulfilled. Moreover, the target of 0° flexion at heel strike was chosen arbitrarily and was kept consistent across trials and participants for convenience. Fulfilling the remaining goal of clinical interpretability (objective #1) would naturally require targeting a clinically accurate value instead, determined based on, e.g., a sagittal view standing X-ray (assuming that knee flexion angle at heel strike was consistent with knee flexion angle during neutral standing). Likewise, the minimisation of abduction/adduction RMS as part of REFRAME$_{RMS}$ favoured a zero mean for that signal, possibly leading to the loss of information regarding, e.g., static varus/valgus alignment. Importantly, while our study systematically analysed agreement between the optical and inertial systems, establishing which of the systems most accurately captured the true motion of the underlying knee joints was considered a philosophical question beyond the scope of

this investigation. The present comparison against the harness-based optical marker system was meant strictly to put the IMU-based estimates into context, by comparing against an established system that is currently used by experts for gait analysis [21-23]. It was certainly not meant to be an assessment of objective accuracy of the IMU-based system, as that would have required the use of, e.g., fluoroscopy to obtain soft-tissue-artefact-free kinematic measurements.

In conclusion, the negligible magnitude of the differences between the harness-mounted IMUs and the optical system after REFRAME conclusively demonstrated that the inertial-based system was capable of capturing the same underlying motion pattern as the optical-based system. On the other hand, the visible differences that remained between the skin-mounted IMUs and the optical reference indicated that the movement profile captured by the sensors on the harness was fundamentally different to that captured by IMUs on the skin, even after accounting for differences due to reference frame misalignment. This difference, however, did not conclusively indicate that the IMUs attached to the skin were subject to greater soft tissue artefact. In fact, the small fluctuations observed in the kinematic signals obtained from both the optical and inertial sensors that were fixed to the harness were suggestive of vibrations undergone by the rigid device upon heel strike, likely due to inertial effects resulting from its additional mass. Our study results propose that (1) the use of optical markers and camera systems can be successfully replaced by more cost-effective IMUs with similar accuracy (although further testing should more thoroughly assess performance in characterising more complex activities and, e.g., pathological gait patterns), while (2) further investigation (especially in vivo and upon heel strike) against moving videofluoroscopy is recommended. Further testing should enable us to not only conclusively validate IMU-based knee kinematics, but also establish exactly how the kinematics captured using a rigid brace compare to the actual relative movement of the underlying bone segments.

Author contributions

Conceptualisation: J.G.W., A.O.-V., I.D., M.U., A.M. and T.M.G.; Methodology: J.G.W., A.O.-V., I.D., A.M. and T.M.G.; Software: J.G.W., A.O.-V. and A.S.; Formal analysis: J.G.W., A.O.-V. and A.S.; Investigation: J.G.W. and A.O.-V.; Resources: I.D., M.U., A.M. and T.M.G.; Data curation: J.G.W., A.O.-V., A.S. and M.U.; Writing—original draft: J.G.W. and A.O.-V.; Writing—review and editing: J.G.W., A.O.-V., A.S., I.D., M.U., A.M. and T.M.G.; Supervision: A.O.-V., A.S., I.D., A.M. and T.M.G.; Project administration: A.O.-V., I.D., M.U., A.M. and T.M.G.; Funding acquisition: I.D., A.M. and T.M.G. All authors have read and agreed to the published version of the manuscript.

Funding

Data availability

The raw data supporting the conclusions of this article will be made available by the authors on reasonable request.

Ethics declarations

This study was approved by the ethics committee of the Ludwig Maximilians University Munich, Germany (approval 22-0232, 19 July 2022), and carried out in accordance with relevant guidelines and regulations. Informed consent was obtained from all subjects involved in the study.

Competing interests

J.G.W., A.O.-V., A.S., I.D., M.U., A.M. and T.M.G. are/were employees of B. Braun Aesculap AG, Tuttlingen, Germany.

References

1. Carse, B., Meadows, B., Bowers, R., and Rowe, P., *Affordable clinical gait analysis: an assessment of the marker tracking accuracy of a new low-cost optical 3D motion analysis system.* Physiotherapy, 2013. **99**(4): p. 347-351.
2. Simon, S.R., *Quantification of human motion: gait analysis—benefits and limitations to its application to clinical problems.* Journal of Biomechanics, 2004. **37**(12): p. 1869-1880.
3. Seel, T., Raisch, J., and Schauer, T., *IMU-based joint angle measurement for gait analysis.* Sensors, 2014. **14**(4): p. 6891-6909.
4. Zhao, H., Wang, Z., Qiu, S., Shen, Y., and Wang, J. *IMU-based gait analysis for rehabilitation assessment of patients with gait disorders.* in *2017 4th International Conference on Systems and Informatics (ICSAI).* 2017.
5. Zhou, L., Tunca, C., Fischer, E., Brahms, C.M., Ersoy, C., Granacher, U., and Arnrich, B. *Validation of an IMU Gait Analysis Algorithm for Gait Monitoring in Daily Life Situations.* in *2020 42nd Annual International Conference of the IEEE Engineering in Medicine & Biology Society (EMBC).* 2020.
6. Benson, L.C., Räisänen, A.M., Clermont, C.A., and Ferber, R., *Is This the Real Life, or Is This Just Laboratory? A Scoping Review of IMU-Based Running Gait Analysis.* Sensors, 2022. **22**(5): p. 1722.
7. Yang, S. and Li, Q., *Inertial Sensor-Based Methods in Walking Speed Estimation: A Systematic Review.* Sensors, 2012. **12**(5): p. 6102-6116.
8. Goldsack, J.C., Coravos, A., Bakker, J.P., Bent, B., Dowling, A.V., Fitzer-Attas, C., Godfrey, A., Godino, J.G., Gujar, N., and Izmailova, E., *Verification, analytical validation, and clinical validation (V3): the foundation of determining fit-for-purpose for Biometric Monitoring Technologies (BioMeTs).* npj Digital Medicine, 2020. **3**(1): p. 55.
9. Ortigas-Vásquez, A., Maas, A., List, R., Schütz, P., Taylor, W.R., and Grupp, T.M., *A Framework for Analytical Validation of Inertial-Sensor-Based Knee Kinematics Using a Six-Degrees-of-Freedom Joint Simulator.* Sensors, 2022. **23**(1).
10. Schütz, P., Postolka, B., Gerber, H., Ferguson, S.J., Taylor, W.R., and List, R., *Knee implant kinematics are task-dependent.* Journal of the Royal Society Interface, 2019. **16**(151): p. 20180678.
11. Sagasser, S., Sauer, A., Thorwächter, C., Weber, J.G., Maas, A., Woiczinski, M., Grupp, T.M., and Ortigas-Vásquez, A., *Validation of Inertial-Measurement-Unit-Based Ex Vivo Knee Kinematics during a Loaded Squat before and after Reference-Frame-Orientation Optimisation.* Sensors, 2024. **24**(11): p. 3324.
12. Taylor, W.R., Ehrig, R.M., Duda, G.N., Schell, H., Seebeck, P., and Heller, M.O., *On the influence of soft tissue coverage in the determination of bone kinematics using skin markers.* Journal of Orthopaedic Research, 2005. **23**(4): p. 726-734.
13. Peters, A., Galna, B., Sangeux, M., Morris, M., and Baker, R., *Quantification of soft tissue artifact in lower limb human motion analysis: a systematic review.* Gait & Posture, 2010. **31**(1): p. 1-8.
14. Sati, M., De Guise, J.A., Larouche, S., and Drouin, G., *Improving in vivo knee kinematic measurements: application to prosthetic ligament analysis.* The Knee, 1996. **3**(4): p. 179-190.

15. Hagemeister, N., Parent, G., Van De Putte, M., St-Onge, N., Duval, N., and De Guise, J., *A reproducible method for studying three-dimensional knee kinematics.* Journal of Biomechanics, 2005. **38**(9): p. 1926-1931.

16. Clément, J., De Guise, J.A., Fuentes, A., and Hagemeister, N., *Comparison of soft tissue artifact and its effects on knee kinematics between non-obese and obese subjects performing a squatting activity recorded using an exoskeleton.* Gait & Posture, 2018. **61**: p. 197-203.

17. Versteyhe, M., De Vroey, H., Debrouwere, F., Hallez, H., and Claeys, K., *A Novel Method to Estimate the Full Knee Joint Kinematics Using Low Cost IMU Sensors for Easy to Implement Low Cost Diagnostics.* Sensors, 2020. **20**(6).

18. Ortigas-Vásquez, A., Taylor, W.R., Maas, A., Woiczinski, M., Grupp, T.M., and Sauer, A., *A frame orientation optimisation method for consistent interpretation of kinematic signals.* Scientific Reports, 2023. **13**(1): p. 9632.

19. Ortigas-Vásquez, A., Taylor, W.R., Postolka, B., Schütz, P., Maas, A., Woiczinski, M., Grupp, T.M., and Sauer, A., *A Reproducible and Robust Representation of Tibiofemoral Kinematics of the Healthy Knee Joint during Stair Descent using REFRAME – Part I: REFRAME Foundations and Validation.* 2024: Preprint on Research Square.

20. Lustig, S., Magnussen, R.A., Cheze, L., and Neyret, P., *The KneeKG system: a review of the literature.* Knee Surgery, Sports Traumatology, Arthroscopy, 2012. **20**(4): p. 633-638.

21. Bytyqi, D., Shabani, B., Lustig, S., Cheze, L., Karahoda Gjurgjeala, N., and Neyret, P., *Gait knee kinematic alterations in medial osteoarthritis: three dimensional assessment.* International Orthopaedics, 2014. **38**(6): p. 1191-1198.

22. Cagnin, A., Choinière, M., Bureau, N.J., Durand, M., Mezghani, N., Gaudreault, N., and Hagemeister, N., *A multi-arm cluster randomized clinical trial of the use of knee kinesiography in the management of osteoarthritis patients in a primary care setting.* Postgraduate Medicine, 2020. **132**(1): p. 91-101.

23. Gasparutto, X., Bonnefoy-Mazure, A., Attias, M., Dumas, R., Armand, S., and Miozzari, H., *Comparison between passive knee kinematics during surgery and active knee kinematics during walking: A preliminary study.* PLOS One, 2023. **18**(3): p. e0282517.

24. Northon, S., Boivin, K., Laurencelle, L., Hagemeister, N., and De Guise, J.A., *Quantification of joint alignment and stability during a single leg stance task in a knee osteoarthritis cohort.* The Knee, 2018. **25**(6): p. 1040-1050.

25. Rauch, H.E., Tung, F., and Striebel, C.T., *Maximum likelihood estimates of linear dynamic systems.* AIAA journal, 1965. **3**(8): p. 1445-1450.

26. Zeighami, A., Aissaoui, R., and Dumas, R., *Knee medial and lateral contact forces in a musculoskeletal model with subject-specific contact point trajectories.* Journal of Biomechanics, 2018. **69**: p. 138-145.

27. Zeighami, A., Dumas, R., and Aissaoui, R., *Knee loading in OA subjects is correlated to flexion and adduction moments and to contact point locations.* Scientific Reports, 2021. **11**(1): p. 8594.

28. Aissaoui, R., Husse, S., Mecheri, H., Parent, G., and De Guise, J.A. *Automatic filtering techniques for three-dimensional kinematics data using 3D motion capture system.* in *2006 IEEE International Symposium on Industrial Electronics*. 2006. IEEE.

29. Grood, E.S. and Suntay, W.J., *A joint coordinate system for the clinical description of three-dimensional motions: application to the knee.* Journal of Biomechanical Engineering, 1983. **105**(2): p. 136-144.

30. Macwilliams, B.A. and Davis, R.B., *Addressing some misperceptions of the joint coordinate system.* Journal of Biomechanical Engineering, 2013. **135**(5): p. 54506.

31.	Catalfamo, P., Ghoussayni, S., and Ewins, D., *Gait Event Detection on Level Ground and Incline Walking Using a Rate Gyroscope.* Sensors, 2010. **10**(6): p. 5683-5702.

32.	Frey, B.B., *The SAGE Encyclopedia of Research Design.* 2022: Thousand Oaks,, California.

33.	Bonferroni, C.E., *Teoria statistica delle classi e calcolo delle probabilità.* 1936: Seeber.

34.	Gujarathi, T. and Bhole, K. *Gait analysis using IMU sensor.* in *Proceedings of the 2019 10th International Conference on Computing, Communication and Networking Technologies (ICCCNT).* 2019.

35.	Reinschmidt, C., Van Den Bogert, A.J., Lundberg, A., Nigg, B.M., Murphy, N., Stacoff, A., and Stano, A., *Tibiofemoral and tibiocalcaneal motion during walking: external vs. skeletal markers.* Gait & Posture, 1997. **6**(2): p. 98-109.

36.	Benoit, D.L., Ramsey, D.K., Lamontagne, M., Xu, L., Wretenberg, P., and Renström, P., *Effect of skin movement artifact on knee kinematics during gait and cutting motions measured in vivo.* Gait & Posture, 2006. **24**(2): p. 152-164.

37.	Most, E., Axe, J., Rubash, H., and Li, G., *Sensitivity of the knee joint kinematics calculation to selection of flexion axes.* Journal of Biomechanics, 2004. **37**(11): p. 1743-1748.

38.	Walker, P.S., Heller, Y., Yildirim, G., and Immerman, I., *Reference axes for comparing the motion of knee replacements with the anatomic knee.* The Knee, 2011. **18**(5): p. 312-316.

39.	Postolka, B., Taylor, W.R., Datwyler, K., Heller, M.O., List, R., and Schütz, P., *Interpretation of natural tibio-femoral kinematics critically depends upon the kinematic analysis approach: A survey and comparison of methodologies.* Journal of Biomechanics, 2022. **144**: p. 111306.

40.	Lu, Z., Sun, D., Xu, D., Li, X., Baker, J.S., and Gu, Y., *Gait Characteristics and Fatigue Profiles When Standing on Surfaces with Different Hardness: Gait Analysis and Machine Learning Algorithms.* Biology, 2021. **10**(11): p. 1083.

41.	Jelsing, E.J., Finnoff, J.T., Cheville, A.L., Levy, B.A., and Smith, J., *Sonographic Evaluation of the Iliotibial Band at the Lateral Femoral Epicondyle.* Journal of Ultrasound in Medicine, 2013. **32**(7): p. 1199-1206.

5. Supplementary Material

A full copy of the supplementary material for this article is available online and can be downloaded from the following link:

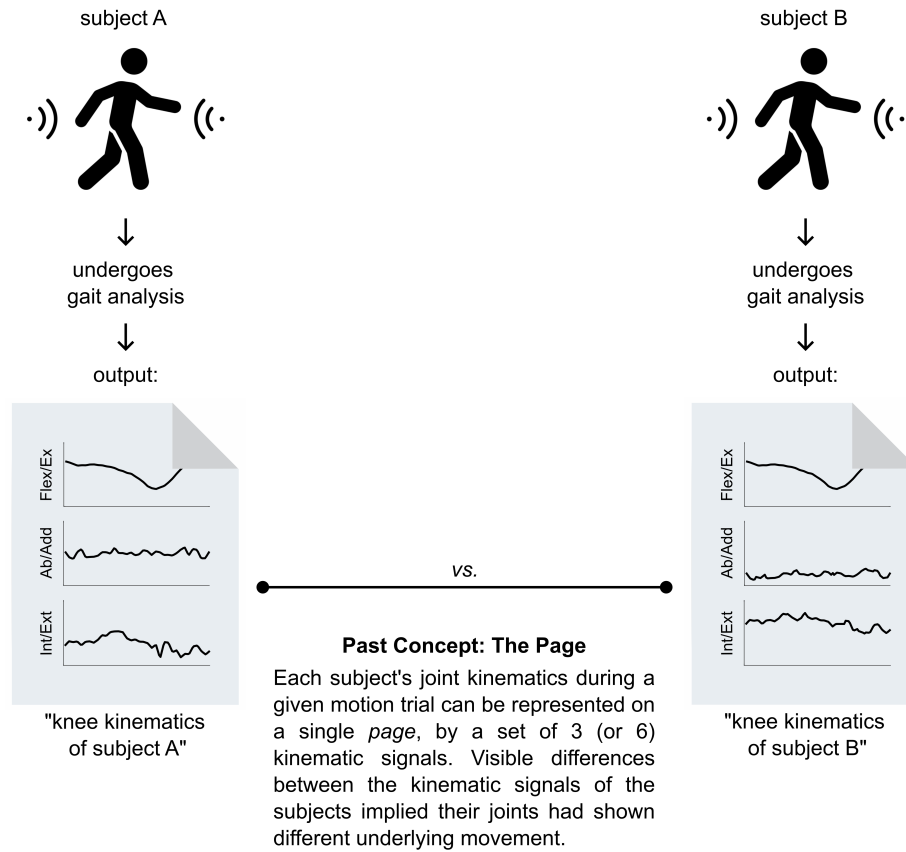https://www.mdpi.com/article/10.3390/bioengineering11100976/s1

Appendix A: The Book Analogy

The detailed analyses performed as part of this dissertation to explore the relationship between the pose (i.e. orientations and positions) of local segment reference frames and the resulting kinematics signals led to an important re-conceptualisation of joint kinematics, especially in the context of comparisons. To clearly portray this conceptual shift, we found it useful to rely on what we called "The Book Analogy". The Book Analogy juxtaposes our previous (flawed) impression of how kinematic data could be compared (a.k.a. "The Page") against our more recent, improved understanding of how truly robust comparisons of sets of kinematic signals should be approached (a.k.a. "The Book").

First, we consider a hypothetical scenario in which we aim to compare the tibiofemoral rotations of subject A's right knee during one cycle of level walking against those of subject B's right knee. We could have subject A come into our institution's gait laboratory and have them undergo marker-based optical motion capture to record the motion of their tibial and femoral joint segments as they perform this activity. The optical system would store the 3D coordinates of the entire marker set, where each marker would have been strategically placed to represent a key anatomical landmark on the subject's musculoskeletal system. 3D Cartesian coordinate systems would then be defined based on the marker data and the chosen joint axis approaches to establish a local reference frame for each of the joint's relevant segments (here, femur and tibia). Subject A's rotational knee kinematics over one trial would then be illustrated by the estimated joint angles from start to end (0% to 100%) of a gait cycle; essentially by three (or six, if we include translations) 2D line graphs fitting on a single page (Figure 1; "knee kinematics of subject A"). By following the same methodology to record, estimate and graph the rotational knee kinematics of subject B, one could then visually assess both "kinematic reports" (i.e. each subject's "page") and (misguidedly) conclude that the presence of obvious differences between the shape and magnitude of the two sets of kinematic signals are a reliable indication that the underlying joint motion pattern displayed by each subject was, by extension, inherently different as well.

The crucial problem with "The Page" stems from the complex relationship between local segment reference frame poses and the corresponding kinematic signals. Specifically, while the plots on "The Page" are indeed a mathematically valid representation of the joint motion pattern captured during the gait trial, they are *one of many possible representations*. In fact, if we take Subject A's first trial, keep everything else the same except for the exact orientation of the local femoral reference frame (even for a very small difference, e.g. 1° of clockwise rotation around the femoral x-axis) the kinematic signals resulting from that same trial would be visibly different from our original "page", *even though the underlying joint motion and raw data for that trial clearly did not change.* This fundamental flaw in approaching the comparison of kinematic signals with a framework like the one presented in "The Page" then led us to developing a new, more robust approach, which we labelled "The Book".

Past Concept: The Page

Each subject's joint kinematics during a given motion trial can be represented on a single *page*, by a set of 3 (or 6) kinematic signals. Visible differences between the kinematic signals of the subjects implied their joints had shown different underlying movement.

Figure 1. The Page: Graphical illustration of how we used to approach the comparison of two (or more) sets of joint kinematic signals.

The assumption that comparing the joint motion of two subjects is as simple as assessing the standard plots of joint angles/displacements to identify visible differences between subjects is clearly deficient. Consequently, "The Book" approach (Figure 2) instead incorporates what we now grasp to be the effect of local reference frame poses on kinematic signals. The set of three (or six) plots obtained from processing the motion data captured in the previously described scenario is indeed one valid representation of the joint motion during that trial. Nevertheless, the use of slightly differently orientated (and/or positioned) local reference frames would have resulted in a different set of plots, i.e. a different "page". The same underlying joint motion pattern can thus be graphically represented by different sets of kinematic signals or, to fit our analogy, a *collection of pages*; in other words, a "book". "The Book" perspective captures the fact that when we derive a set of kinematic signals from a trial, we have essentially found one page in the book of that recorded motion pattern. Because of inherent uncertainties such as marker placement errors, we cannot guarantee that our analysis of a second subject will arrive precisely at the same page of their book. Moreover, comparing, e.g., page 7 of subject A's book against page 5 of subject B's book would obviously not be a robust assessment, as the signals on those pages would appear different *even if the underlying joint motion pattern were exactly the same for both*. Instead, it becomes clear we need to ensure both our subjects' books are turned to the same page (i.e. we have consistent local reference frame poses) prior to reaching a conclusion. This is essentially what the REFRAME approach does. The choice of objective criteria effectively dictates which page within each book we are targeting, and by subjecting every dataset to the same criteria, we ensure all our books are ultimately turned to the same page.

subject A

undergoes
gait analysis

output:

Flex/Ex

Ab/Add

Int/Ext

"one representation of
subject A's knee
kinematics"

pg.7

New Concept: The Book
The *book* is the collection of pages containing all possible sets of kinematic signals representing the same single underlying joint movement pattern. The conventional set of 3 (or 6) kinematic signals obtained from a gait analysis trial is *one possible representation* of each subject's joint motion, specific to the exact combination of local reference frame orientations (and/or positions) used to process that trial, i.e. it is *one page within the book*. A slightly different set of reference frames would lead to a different page within the book. Note: even though the pages within a book look different, they all represent the same underlying motion pattern.

Problem
Data processing may ouput pg. 7 of subject A's book, but pg. 5 of subject B's book. Referring to different isolated pages of each subject's book may lead to inadequate conclusions about the similarity/difference in the joint motion of subject A vs. B. (Signals could look different even if they represent the same motion.)

subject B

undergoes
gait analysis

output:

Flex/Ex

Ab/Add

Int/Ext

"one representation of
subject B's knee
kinematics"

pg.5

pg.7

REFRAME
By ensuring consistency in the orientations (and/or positions) of reference frames, we essentially make sure the books being compared are all turned to the same page. Any visible differences between kinematic signals with the same underlying local reference frames are now a much more robust indication of actual differences in joint motion.

Figure 2. The Book: Graphical illustration of our newly developed, more robust approach for the comparison of two (or more) sets of joint kinematic signals, whereby REFRAME is used to ensure the consistent orientations and/or positions of the underlying local segment reference frames.

Appendix B: REFRAME Tool

REFRAME Tool User Guide

Basic Executable Version

REFRAME (REference FRame Alignment MEthod) is an approach to standardise the orientation and position of local joint segment frames, in order to facilitate the consistent interpretation and comparison of kinematic signals [1]. With the REFRAME Helper Tool, users can input "raw" kinematic signals and specify their choice of objective function for optimisation. The REFRAME Helper Tool will then output an "optimised" (also referred to as "REFRAMEd") set of kinematic signals, as well as the transformations (rotations + translations) that were performed on the raw segment frames to obtain the modified segment frames associated with these output signals.

I.   Underlying Conventions

> › All coordinate systems are right-handed.
> › Rotations are expressed in degrees.
> › Translations are expressed in millimetres.
> › Base rotations:

$$R_x(\alpha) = \begin{bmatrix} 1 & 0 & 0 \\ 0 & \cos\alpha & -\sin\alpha \\ 0 & \sin\alpha & \cos\alpha \end{bmatrix}$$

$$R_y(\beta) = \begin{bmatrix} \cos\beta & 0 & \sin\beta \\ 0 & 1 & 0 \\ -\sin\beta & 0 & \cos\beta \end{bmatrix}$$

$$R_z(\gamma) = \begin{bmatrix} \cos\gamma & -\sin\gamma & 0 \\ \sin\gamma & \cos\gamma & 0 \\ 0 & 0 & 1 \end{bmatrix}$$

> › Implemented for a RIGHT knee (Figure 1)
>   - o X-axis: Mediolateral (lateral +/medial -)
>   - o Y-axis: Anteroposterior (anterior +/posterior -)
>   - o Z-axis: Proximodistal (proximal +/distal -)
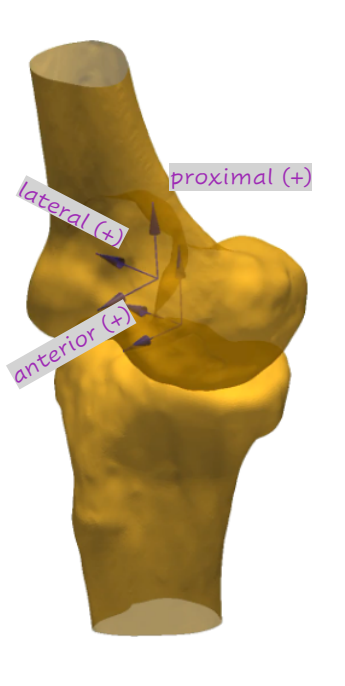
Figure 7. *Illustration of the axes directions used in REFRAME script. Axes were defined with a right knee (tibiofemoral) joint in mind. (See also Figure S1 in [1])*

II.   Quick Start Guide for Beginners

Step-by-Step

1. While a licensed copy of MATLAB (The Mathworks Inc., Natick, Massachusetts, USA) is not necessary to run this application, it does require the correct version of MATLAB Runtime to be installed. Download and unzip the REFRAME zip file. To run the REFRAME tool:

   On Windows

   a. Download and install MATLAB Runtime version R2023a (9.14) separately from the following link before running REFRAME: https://de.math-works.com/products/compiler/matlab-runtime.html

   b. You can now run REFRAME by navigating to the "**for_redistribution_files_only**" folder and double clicking on the file "**REFRAME.exe**"

   On Mac

   a. Navigate to the "**for_redistribution**" folder and run "**MyAppInstaller_web**". Installing REFRAME in this way will verify whether the correct required version of MATLAB Runtime has already been installed in the system. If it has not been installed, this will attempt to download and install it from the web automatically. Once installation is complete, you can run the newly installed REFRAME application.

      Note 1 – If the automatic MATLAB Runtime installation failed:

      i. Download and install MATLAB Runtime version R2023a (9.14) separately from the following link before running REFRAME: https://de.mathworks.com/products/compiler/matlab-runtime.html

      ii. You can then run REFRAME by navigating to the "**for_redistribution_files_only**" folder and double clicking on the file "**REFRAME**".

      Note 2 – If you have a MacBook with an M Chip:

      i. After installation of the REFRAME application via "**MyAppInstaller_web**", open the terminal and go to the directory where the file "**run_REFRAME.sh**" has been saved, for example, by running:

         cd /Applications/REFRAME/application

      ii. Then type

         ./run_REFRAME.sh /Applications/MATLAB/MATLAB_Runtime/R2023a

         and press **Enter**.

      iii. Now you can run REFRAME by double-clicking on the "**REFRAME**" file within the **application** folder.

2. The application can take quite a bit of time to load, even if it has been run successfully (especially the very first time you run it). It can take anywhere from 30 seconds up to a couple of minutes (if you know how we can improve this please reach out!). If the terminal pops-up, this is a good indication that REFRAME is running successfully; it just needs some time to load. Once it has finished loading, the following GUI should appear:
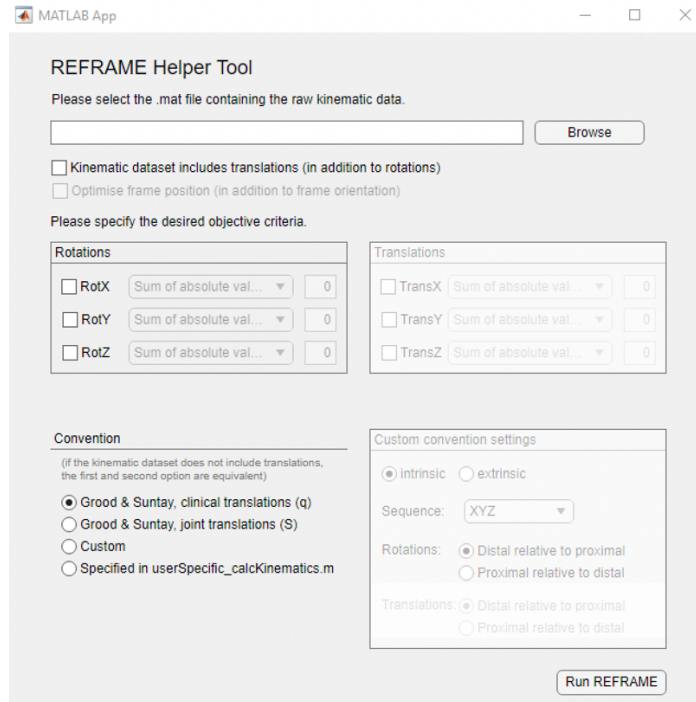
Figure 2. *Screen capture of the REFRAME Helper Tool's graphical user interface.*

3. Click on **Browse** (Figure 2) to select the input file that contains the raw kinematic signals you would like to process with REFRAME. An ideal input file will be in **.mat** format, with six columns (or three, if you are only dealing with rotational signals), and 101 rows (i.e. signals are normalised to 100% of an activity cycle) (Figure 3).
4. Use the GUI to provide your individual specifications for the REFRAME implementation.[1,2]
5. Verify your choices and click on **Run REFRAME**.
6. Select appropriate paths to save the output files **Transformations.csv** and **OptKin.csv**.

---

[1] The "Grood & Suntay" options are meant to follow the **_exact_** definitions given in the original paper [2] (implemented for a <u>right</u> knee: flexion (+), abduction (+), external (+) tibial rotation). We *strongly* recommend reviewing the equations in the original article before selecting this option.

[2] The use of custom parameters or root-mean-square error (RMSE) vs. a reference curve within the objective function are recommended only for advanced users and require access to additional MATLAB files and a MATLAB license. For more information, please contact us.

Rot X   Rot Y   Rot Z   Trans X   Trans Y   Trans Z

0%
1%
2%

99%
100%

Figure 3. *Structure of input .mat file. This is the transpose of matrix $\mathbf{K}^0$, described in [1]. For datasets not including joint translations, the last three columns would be omitted.*[3]

Output

After running REFRAME, you will receive three main outputs:

1) **Output Figure 1**
   <u>If your dataset contains rotations only:</u>
   Output Figure 1 shows three subplots displaying the rotational kinematic signals (in degrees) in the sagittal, frontal and transverse planes, in turn. Raw signals are given by the dashed blue lines; REFRAMEd signals are solid red. Signals are plotted over 100% of the activity cycle.

Figure 4. *Example of figure output by the REFRAME Helper Tool for a dataset containing joint rotations only.*

---

[3] The clinical meaning of positive values will vary depending on your chosen convention. E.g., for Grood and Suntay: flexion, abduction and external tibial rotation should be positive. (Where Adduction = β - 90°. For the orientation of the distal relative to the proximal frame following an XYZ intrinsic rotation sequence: extension, adduction and internal tibial rotation should be positive. Please ensure you follow these conventions correctly.

Output Figure 1 shows six subplots displaying the rotational kinematic signals in degrees (first column of subplots) and the translational kinematic signals in millimetres (second column of subplots). Raw signals are given by the dashed blue lines; REFRAMEd signals are solid red. Signals are plotted over 100% of the activity cycle.
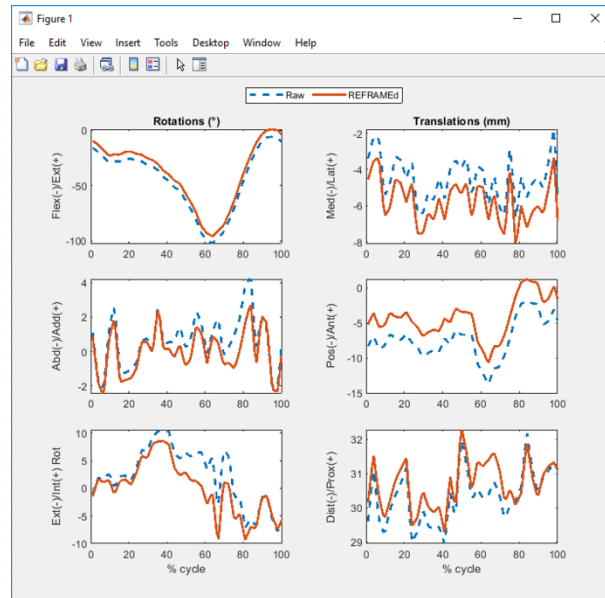
Figure 5. *Example of figure output by the REFRAME Helper Tool for a dataset containing joint rotations and translations.*

Note on y-axis labels:

The y-axis labels shown in Figures 4-5 are correct for a right tibiofemoral joint (Figure 3). <u>These labels automatically update to account for the user's chosen convention, but may require adaptation when applying REFRAME to another body joint.</u>

2) **Transformations.csv**

6x2 array with rotations and translations applied to raw frames to transform them into optimised frames. These are expressed in our convention of XYZ intrinsic Cardan sequence (see Figure 1 for axis directions). Rows 1 and 4 are always around/along the X-axis; Rows 2 and 5 around/along the Y-axis; Rows 3 and 7 around/along the Z-axis.

Figure 6. *Example of the contents of the Transformations.csv file. In this example, the orientation of the optimised proximal segment results from rotating the raw proximal segment frame with an intrinsic rotation sequence of 0.0050° around X, 2.3240° degrees around Y, and -3.9235° around Z. Similarly, the position of the optimised proximal segment frame origin is 13.9809 mm along X, -1.7344 mm along Y, and -1.3471 mm along Z, relative to the raw proximal segment frame origin (along the raw proximal segment frame axes).*

3) OptKin.csv

101x6 array with "optimised"/"modified"/"REFRAMEd" kinematics; same structure as input file (Figure 3).

Figure 7. *Example contents of the first five rows of the OptKin.csv file.*

Sample files

We have additionally provided the following three files:

1) imu_mat.mat
2) OptKin.csv
3) Transformations.csv

As a validity check, feel free to upload imu_mat.mat to the REFRAME tool and run RE-FRAME with the following configuration:

Figure 8. *Example REFRAME configuration to optimise imu_mat.mat.*

Save the resulting OptKin and Trasnformations. Values should coincide (at least to the third decimal place!) with those given in the provided sample OptKin.csv and Transformations.csv files.

III.   References

1.   Ortigas-Vásquez et al. *In review.* 2024.
2.   Grood and Suntay. *J Biomech Eng*. 1983.

IV.   Note from the Authors

REFRAME scripts and this accompanying user guide are meant to be an ongoing, collaborative effort. While we have done our best to comb through the code and run basic tests to validate the REFRAME Helper Tool, we are not computer programmers. It is certainly possible that we overlooked something. If you suspect you have identified an error, or have suggestions for future improvement, please do reach out to us. We will be happy to take a closer look and continue to improve REFRAME.

We hope you find our work helpful!

All the best,

The REFRAME Team (reframe@aesculap.de)

Acknowledgements

This work would not have been possible without the support of multiple people.

Among my supervisors, advisors and colleagues, I especially would like to thank the following:
- Thomas, for always finding time in his impossibly busy schedule to listen to me, challenge me and encourage me to look far ahead.
- Allan, for being an awesome boss, giving me the space and tools to become more independent (and for many rides to/from the office!)
- Michael, for believing in us, laughing with us, and saving us on multiple occasions.
- Bill,
    - ... for countless hours of editing and discussing manuscripts, honouring me with what at one point felt like the highest possible compliment one could strive to hear from him regarding a piece of scientific writing: "That's actually not too bad,"
    - ... for challenging me, mentoring me, sometimes down-right arguing with me, all the while teaching me to be ambitious and aim high,
    - ... for bringing up the topic of cross-talk in the first place,
    - ... and for believing in our work, and encouraging me to believe in myself.
- and Adrian,
    - ... for reminding me of the importance of work-life balance,
    - ... for inspiring me, pushing me, annoying me, advising me, helping me, teaching me, questioning me, arguing with me, understanding me, challenging me, supporting me, and laughing with me,
    - ... for making work fun and something I looked forward to every day,
    - ... for being the best colleague I could have asked for, best research partner, and friend,
    - ... for always saying yes to so many "Do you have a minute for a quick question?" messages that 90% of the time actually meant "Do you have 2-3 hours to discuss something with me, and get off topic, and figure out our individual futures, and talk about life and family and happiness, and then at some point (maybe) get back on track and get some actual work done?"
    - ... and finally, for breaking knee kinematics with me, and for going through the emotional rollercoaster that was our journey of trying to put it back together. You once described it best: Somehow, when we work together, the result is *so much more* than just the sum of what each of us would have achieved individually. This dissertation would not be what it is without you.

I am also extremely grateful to Renate, Pascal, and Barbara for their vital contributions to this dissertation and their ongoing guidance, as well as to Jana and Svenja for their valuable support.

I would also like to thank my family, especially:
- My partner, Max,
    - ... for building me a three-metre-long desk (of which I used every centimetre) on which to work on throughout my entire PhD,

... for respecting how much I love my work and how important it is to me, without ever making me feel guilty about how much of my time and effort it takes up,

... for cooking for us, cleaning for us, driving us, and planning vacations for us when I had too much work to get done and could not always do my share,

... for taking care of me when I was too focused on work to fully take care of myself,

... and for cheering me on, reminding me of my worth, and being proud of me.

- My parents and my older brother,

  ... for literally *always* being there for me, and for selflessly encouraging me to leave home and go wherever I could develop myself the most, learn the most, and grow the most, even if it was halfway across the world,

  ... for teaching me that education is one of the most valuable gifts one can possibly give,

  ... and for sacrificing so much of their own lives to be able to grant me that gift in the best possible way they could.

I dedicate this work to my parents.